Fundamental Principles of Cloud and Aerosol Physics

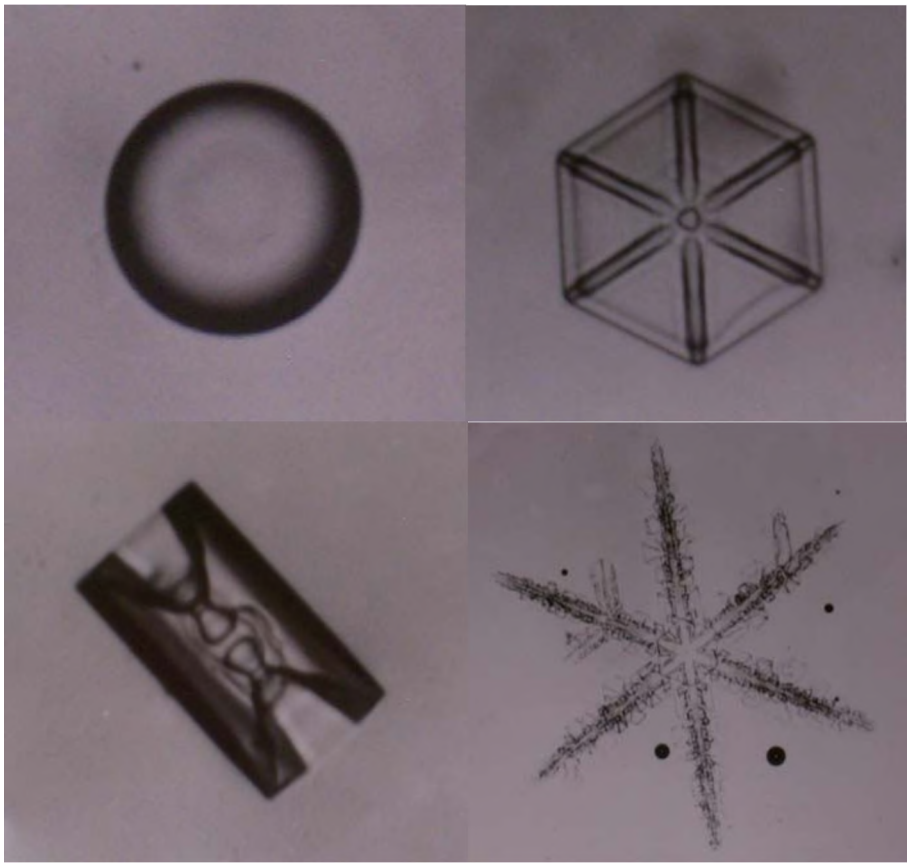

Norihiko Fukuta

Fundamental Principles of Cloud and Aerosol Physics by Professor Norihiko Fukuta lays a sophisticated foundation in Cloud Physics through an illustration of theoretical principles and experimental results. The treatment starts from a general discussion of the relevant thermodynamic and kinetic principles at macroscopic and molecular scales. It moves on to discuss mechanisms for the nucleation, growth and precipitation of cloud droplets and ice crystals. The text concludes with a discussion of interactions between microphysics and dynamics in clouds.

Professor Fukuta was one of the world's leading cloud physicists who continued to make significant advances in his field up until his death in May of 2010 at the age of 78. He received his B.S. in Chemistry (1954) and M.S. (1956) and Ph.D. (1959) in Physical Chemistry from Nagoya University, Japan. Following graduation, he served in several public and private-sector teaching and research positions at institutions around the world including Imperial College, London (under the direction of Sir B. J. Mason); C.S.I.R.O., Sydney, Australia, Meteorology Research Inc., Altadena, CA; and the University of Denver. He became a Professor in the University of Utah Department of Meteorology (now Atmospheric Sciences) in 1977 and Professor Emeritus in 2001. Professor Fukuta supervised 20 graduate students during his tenure at the University of Utah and published more than 100 journal articles. He authored the Japanese Meteorological Society book Weather Engineering –- New Approach to Weather Modification, and served as editor for Nucleation and Atmospheric Aerosols. He was named a fellow of the American Meteorology Society in 1998.

Professor Fukuta's unique talent was his ability to approach difficult physical problems by combining his deep knowledge of theory and experimental techniques to yield novel insights into droplet and ice crystal nucleation and growth. This book's cover shows photographs of cloud particles grown in a world-class diffusion chamber at the University of Utah, aimed at elucidating ice crystal growth mechanisms. Professor Fukuta demonstrated the important effect of electricity on the coalescence and orientation of plate and column crystals, and he underscored the importance of non-equilibrium thermodynamics for understanding the early stages of droplet formation. Much of the material described in Advanced Cloud Physics reflects advances in the field of Cloud Physics that were made by Professor Fukuta himself.

TABLE OF CONTENTS

LIST OF SYMBOLS

a	a constant, radius, lattice parameter
A	a constant, Cunningham's constant, area
b	a constant
B	a constant, second virial coefficient, buoyancy factor
c	a constant, specific heat
C	molar heat capacity, electrostatic capacitance, third virial coefficient, a constant
d	a constant, diameter
D	diffusivity
e	eccentricity, vapor pressure
E	electric field vector, efficiency, collection efficiency, energy
f	relative humidity, ventilation factor, fog factor, normalization factor
f( )	function of
F	Helmholtz free energy, flux, force
g	specific Gibb's free energy, acceleration of gravity, thermal gradient, $(1 - 2mx + x^2)^{1/2}$
G	molar Gibbs free energy
h	specific Helmholtz free energy, Planck's constant, height
H	molar Helmholtz free energy, collection kernel based on volumetric expression
i	van't Hoff's factor
I	ice
j	degrees of freedom
J	joule, nucleation rate
k	Boltzmann's constant
K	thermal conductivity, collection kernel based on size expression, a constant, Knudsen number, eddy diffusivity
ℓ	mean free path distance, jump distance
L	specific latent heat, liquid phase
m	mass, mass of a water molecule, $\cos\theta$
M	molecular weight
n	number of moles, number concentration, number of atoms in a molecule, normal distance
N	Avogadro's number, number of droplets, number of state, total number of molecules

p	pressure
P	probability
q	heat per unit mass, specific humidity
Q	heat per mole, electrostatic charge, magnitude of property
r	radius
r	radial distance
R	specific gas constant, radius of collector drop, rain water mixing ratio
Re	Reynolds number
s	specific entropy
S	entropy per mole, saturation ratio, solid phase
t	time
T	absolute temperature
T_e, T_s, T_v, T_w	equivalent temperature, temperature at particle surface, virtual temperature, wet bulb temperature
$T_o, T_{s,w}$	melting temperature of ice, adiabatic wet bulb temperature
T', T_Δ, T_∞	ambient temperature, temperature at about mean free path above particle surface, in environment
u	velocity in x-direction, specific internal energy
U	internal energy per mole
v	velocity in y-direction, molecular volume
V	volume, molar volume, electrostatic potential, vapor phase
w	velocity in z-direction, mixing ratio, work per unit mass
W	liquid water content per unit volume of air
x	coordinate distance in x-direction, r_n/r^*, a variable, axial ratio between major and minor axes of spheroids, separation of droplet center from fall line of collector drop center
y	coordinate distance in y-direction
z	coordinate distance in z-direction

GREEK LETTERS

α	angle, thermal accommodation coefficient, specific volume
α'	$= 2\alpha/(2 - \alpha)$ representative thermal accommodation coefficient
β	condensation coefficient
β'	$= 2\beta/(2 - \beta)$ representative condensation coefficient
γ	deposition coefficient, ambient lapse rate, edge free energy
γ'	$= 2\gamma/(2 - \gamma)$ representative deposition coefficient
Γ	dry adiabatic lapse rate
Γ_s	pseudo-adiabatic lapse rate
δ	lattice misfit
Δ	difference
ϵ	$= M/M_a$, strain
η	dynamic viscosity
θ	angle, potential temperature, fraction, contact angle
θ_v	characteristic temperature for vibrational modes
θ_e, θ_w	equivalent potential temperature, wet bulb potential temperature
κ	$= R/c_p$, thermal diffusivity
μ	chemical potential, dipole moment
ν	kinematic viscosity
ρ	density, density of water vapor
σ	surface free energy
ϕ	specific angle
Φ, ψ	angle
χ	adiabatic liquid water content of air
ω	solid angle

SUBSCRIPTS

a	air
adiab	adiabatic
B	basal plane
c	cubic, condensation, condensate, crystal
C	crystal
d	dry air, deposition
D	drag
DK	diffusion kinetic
f	flat surface, freezing, fog
G	gas
h	heat, homogeneous, hexagonal
i	ice, inside, incoming
L	liquid
m,melt	melting
max	maximum
msl	mean sea level
M	Maxwellian
n,N	nucleus
o	standard state, outside, outgoing
p	particle, polydisperse
P	photophoresis, prism plane
Q	property Q
R	resistance
s	saturation, surface
sat	saturation
S	solid
T	thermophoresis
u	unit area
v,V	vapor
w	water, water vapor

x,y,z	components corresponding to coordinate axes
α	thermal accommodation
β	condensation
γ	deposition
Δ	mean free path

SUPERSCRIPTS

$'$	ambient, solute, representative
$''$	with solute and curvature effects
$-$	average
$\rightarrow$	forward
$\leftarrow$	backward
$*$	critical state, molar property

INTRODUCTION

Cloud physics is a field of atmospheric sciences in which aerosols, clouds and precipitation processes are exclusively studied. Cloud microphysics covers the non-dynamical aspects of clouds and precipitations consisting of condensed phases of water substance dispersed in air. So, they are sometimes called an "aerodisperse system." This dispersed system, unlike some stable colloids, is basically unstable; and the rate processes involved in development of precipitation may be considered as a cancellation course of the dispersed state. Such changes, including formation of the dispersed systems and their cancellation or precipitation development, occur under the conditions of Earth's atmosphere in motions and affect transfer processes of energy, mass, and momentum. In this regard, cloud physics and cloud microphysics border many other fields of atmospheric sciences. The intention of this class is, therefore, to describe the central concepts and processes of cloud microphysics quantitatively, based on clear scientific principles, while explaining the bordering areas in a descriptive manner.

CHAPTER 1. THERMODYNAMICS OF AIR AND WATER VAPOR

1.1 Origin and Evolution of the Earth's Atmosphere

The Earth's atmosphere, which accommodates the cloud processes of our interest, is believed to have originated in a relatively short geological time, less than 1 billion years after the formation of the Earth some 4.6 billion years ago. Evidences suggest that the Earth formed due to collision of planetesimals, and the resultant heating that led to degassing of CO_2, NH_3, H_2O, etc, under the influence of the so-called "dark sun" which gave an estimated brightness of only about 70% of the present level. The molten rocks thus formed partially absorbed H_2O vapor and others to become magma. The temperature and pressure of CO_2-H_2O rich proto-atmosphere were about 1,200°C and 100 atm at the magma surface. The OH radical formed by photo-chemical decomposition of H_2O vapor oxidized gases, like CO and NH_3, into CO_2 and N_2. As the flux of falling planetesimals and the resultant heating rate at the Earth's surface reduced, magma solidified to release the dissolved gases. Further cooling led to condensation of water vapor, and the rain, though hot, fell to form the proto-ocean. The remaining CO_2-N_2 rich proto-atmosphere provided a greenhouse effect and trapped the weak solar radiation to maintain the liquid state of the ocean. CO_2 gas then slowly deposited into carbonate rocks. Under this primitive atmosphere without oxygen, life appeared (chemical era). After life had originated, the atmospheric composition further evolved, and as photosynthesizing green-plant developed, the atmospheric oxygen accumulated eventually to the present level (microbial era). After this, the essentially modern atmosphere has been controlled by geological and biological processes that have not changed significantly in nature for perhaps 2 billion years (geological era) (Matthews et al., 1989; Walker, 1977).

1.2 Contemporary Atmosphere, Air, and Water Vapor

Contemporary Earth's atmosphere is outlined as follows:

Total mass is 5 x 10^{18} kg, 10^{-6} of the Earth's mass.
95% of the mass is below 20 km.
Up to 100 km above the sea level, the composition is uniform, due to turbulence and convection.
Above 100 km msl, lighter gas molecule concentration increases.
Temperature profile is given in Fig. 1.1. There are two minima, one at above the tropopause and the other at above the mesopause, the latter being colder.
Tropopause altitude is about 8 km at a pole and about 18 km at the equator. Below the tropopause, or in the troposphere, most meteorological phenomena take place, and the temperature normally drops with altitude.

Some gaseous components are variable:
H_2O; 0 - 7% (in various forms; vapor, liquid, and solid)
CO_2; 0.02 - 0.05%. Recent anthropogenic activities keep the CO_2 concentration rapidly increasing.
Composition of dry air is shown in Table 1.1. O_3, SO_2, NO_x (NO_2), CO, etc.
Aerosol particles of various compositions are found in air. They may be water-soluble, water-insoluble, organic, inorganic, liquid, solid, mixed, crystalline, or noncrystalline.

The composition of the contemporary Earth's atmosphere is unique, telltaling the extraordinary history of its development. Atmospheres of earth-like inner plants (Venus and Mars) consist primarily of CO_2, while those of the outer giant planets (Jupiter, Saturn, Uranus, and Neptune) are based on light gases such as H_2, CH_4, NH_3, and He, H being the most abundant element in the universe.

Water exists largely in the form of liquid or ocean covering 72% of the Earth's surface. 1/4950 of the Earth's mass is water, and the average depth of the hydrosphere is 2.3 km.

1.3 Outline of Thermodynamics

Thermodynamics deals with macroscopic phenomena of a thermal nature. It only provides conditions of thermal equilibrium, as well as the relationships between equilibria before and after changes. So, the rate or the time-dependent processes are essentially beyond its scope. However, there has been a phenomenological development of thermodynamics in order to describe irreversible processes, such as Fourier's law of heat conduction, which we shall look into in later chapters. The latter is called phenomenological irreversible thermodynamics.[1]

Thermodynamics is often substantiated by statistical mechanics that

---

[1] There has been a new development in non-phenomenological irreversible thermodynamics (see Sections 1.3.2 and 1.3.3).

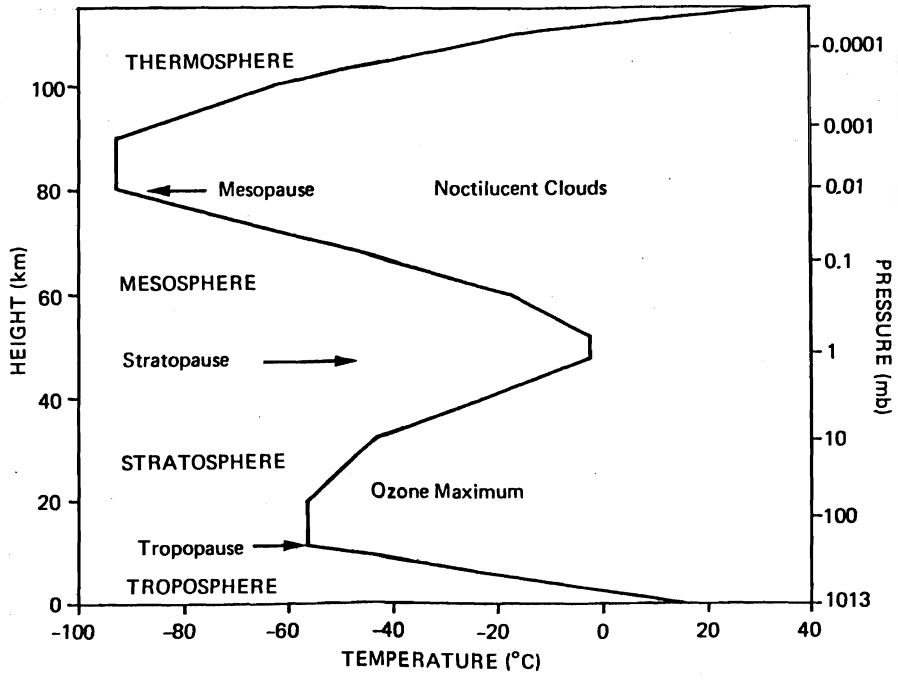

Fig. 1.1 The generalized vertical distribution of temperature and pressure up to about 110 km. Note the tropopause and the zone of maximum ozone concentration with the warm layer above it (Barry and Chorley, 1970).

Table 1.1 Composition of dry air (Tverskoi, 1962).

Gases	Molecular weight	Content (percents by volume)	Density		Critical temperature* T*(°C)
			absolute (g/m^3) at 1013 mb 0°C	relative to dry air	
Nitrogen	28.016	78.084 ± 0.004	1250	0.967	-147.2 (33.5)
Oxygen	32.000	20.946 ± 0.002	1429	1.105	-118.9 (49.7)
Argon	39.944	0.934 ± 0.001	1786	1.379	-122.0 (48.7)
Carbon dioxide	44.010	0.033 ± 0.001	1977	1.529	31.0 (73.0)
Neon	20.183	$(18.18 \pm 0.04)10^{-4}$	900	0.695	-228.0 (26.0)
Ozone	48.000	Highly variable; $(0\text{-}0.07)10^{-4}$ near surface, $(1\text{-}3)10^{-4}$ at height of 20-30 km	2140	1.624	5 (92.3)
Dry air	28.966	100	1293	1.000	-140.7 (37.2)

* In the last column the number in brackets indicates the pressure (in atmospheres) corresponding to the given temperature.

describes phenomena from the microscopic or atomic and molecular standpoints in a statistical manner. Statistical mechanics that specifically treats thermodynamic phenomena, is called statistical thermodynamics, and statistical mechanics that deals with quantum mechanical processes is called quantum statistical mechanics. Nevertheless, caution must be exercised with their application since hidden misconceptions exist.[2]

1.3.1 The definition of thermodynamic system

In thermodynamics, which is an energetics and successful particularly in phase equilibria, there are only two energies involved in exchange, i.e., heat and work. Heat has been identified as the energy associated with random motions of atoms and molecules and is shown to correspond to mechanical energy as

$$1 \text{ calorie } (\text{cal}_{IT}) = 4.1868 \text{ joul (J)}$$
$$1 \text{ J} = 10^7 \text{ ergs.}$$

For a given material without phase change, as we shall see later, the amount of heat given is proportional to the increase of temperature (T) of the material. T is thus equivalent to the height of the water column, if the total amount of water is considered the same as the heat energy.

Work is also a form of energy that is transferred against the resisting force, and is given by the product between the resistance force acted and the displacement induced.

A homogeneous system or a part of a homogeneous system is called phase. There are two categories of thermodynamic properties. An extensive property is any property whose value for the whole system is the sum of the value of its parts (for example, mass and volume). Whereas, an intensive property is any property whose value is constant throughout the system and independent of the amount of phase (for example, density, pressure, and temperature).

In thermodynamics, changes are defined as follows:

Natural changes occur towards equilibrium.

Unnatural changes are those which take place away from equilibrium.

Under equilibrium, no change takes place.

A reversible process consists of a continuous series of equilibrium states, and they do not actually occur in nature.

1.3.2 The first law of thermodynamics

Thermodynamics consists of two major laws, i.e., the first and the second. The first law describes conservation of energies: Total amount of heat added to a gas (or a system), dQ, is equal to the sum of the increased internal energy, dU, and the work done by the gas to outside (loss of work to outside), dW, or

---

[2] Corrections are planned in publication.

$$dQ \equiv dU + dW \tag{1.1}$$

The internal energy includes kinetic energies of all motions of atoms and molecules and potential energy by molecular binding forces.

For a unit mass of gas

$$dq \equiv du + dw, \tag{1.2}$$

where small letters express corresponding properties per unit mass.

Since the work is the product between the resisting force, f, and the displacement, dn, due to the force, and the pressure, p, is related to the force as

$$p = f/A, \tag{1.3}$$

where A is the area the force is acting upon, and since the increase of volume is given as (see Fig. 1.2),

$$dV = Adn, \tag{1.4}$$

dn being the displacement in the direction of the force, from Eqs. (1.3) and (1.4),

$$dW \equiv p_r dV, \tag{1.5}$$

where subscript r stands for resisting. Describing V for unit mass of the gas, Eq. (1.5) becomes

$$dw \equiv p_r d\alpha, \tag{1.6}$$

where α is the specific volume of the gas. Then, an expansion from α_1 to α_2 against the external resisting force, while adding heat to the gas

$$\int dw = \int_{\alpha_1}^{\alpha_2} p_r d\alpha \tag{1.7}$$[3]

gives the total amount of work done against the pressure.

If the expansion is followed by a compression to come back to the original state or a cyclic process (see Fig. 1.3), the contour integral,

$$\int_c dw = \int p_o d\alpha - \int p_i d\alpha, \tag{1.8}$$

where subscripts o and i stand for outside and inside, respectively, gives the net work done to the outside by the gas. Whereas, integral of an exact (total) differential, such as

---

[3] If this is a natural change, the pressure of the gas in question should be higher than the external pressure which is p_r.

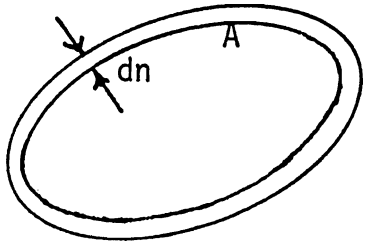

Fig. 1.2 Work by volume expansion.

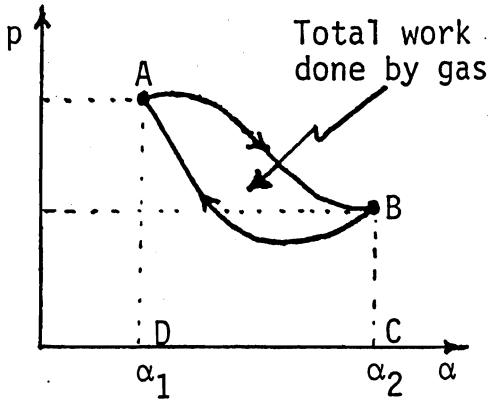

Fig. 1.3 The contour integral.

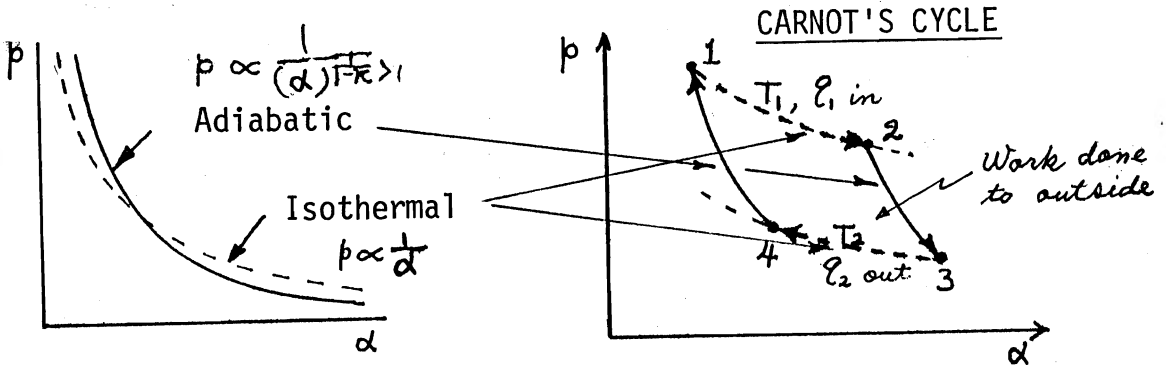

Fig. 1.4 The Carnot cycle.

$$d(p\alpha) = \frac{\partial(p\alpha)}{\partial p}dp + \frac{\partial(p\alpha)}{\partial \alpha}d\alpha = \alpha dp + pd\alpha, \tag{1.9}$$

over any closed contour becomes zero (see Fig. 1.3).

1.3.3 The second law of thermodynamics and entropy

In the above section, it was shown that the first law of thermodynamics concerns only conservation of energy and does not state the direction of change. In nature, there are many irreversible processes, and the second law gives conditions to determine if a change in question is irreversible. All natural changes are irreversible. We shall briefly look into the second law below, first using the Carnot cycle.

N.L. Sadi Carnot devised an idealized cyclic process to examine the efficiency of the thermal engine. The cyclic process consists of quasistatic (infinitesimal deviation from equilibrium and reversible) adiabatic and isothermal processes, so that each state of change is in equilibrium. Some heat is absorbed during the latter and eventually converted into mechanical work.

As we shall see in the following section, the heat exchange in an isothermal reversible process may be expressed as

$$\Delta q = RT \ln\left[\frac{\alpha}{\alpha_o}\right], \tag{1.10}$$

where α and α_o are the final and the initial specific volumes, respectively, R the specific gas constant, and an adiabatic reversible process as

$$\left[\frac{T}{T_0}\right] = \left[\frac{p}{p_o}\right]^{\kappa}, \text{ (Poisson's equation)}, \tag{1.11}$$

where T_0 and p_0 are the temperature and pressure of the initial condition and κ Poisson's constant. Combining Eq. (1.11) with the ideal gas law

$$p\alpha = RT, \tag{1.12}$$

we have, for adiabatic process,

$$p \propto \frac{1}{\alpha^{\frac{1}{1-\kappa}}}. \tag{1.13}$$

For an isothermal process of an ideal gas, Eq. (1.12) gives

$$p \propto \frac{1}{\alpha}. \tag{1.14}$$

In Fig. 1.4, the following express the changes:

From 1 to 2; isothermal, Eq. (1.10), $q_1 = \int_1^2 pd\alpha = RT_1 \ell n \frac{\alpha_2}{\alpha_1}$ (1.15)

From 2 to 3; adiabatic, Eq. (1.11) + ($p\alpha$=RT), $$\left(\frac{T_2}{T_1}\right)^{1-\kappa} = \left(\frac{\alpha_3}{\alpha_2}\right)^{-\kappa} \tag{1.16}$$

From 3 to 4; isothermal, Eq. (1.10), $$q_2 = \int_4^3 p\,d\alpha = RT_2 \ell n \frac{\alpha_3}{\alpha_4} \tag{1.17}$$

From 4 to 1; adiabatic, Eq. (1.11) + ($p\alpha$=RT), $$\left(\frac{T_2}{T_1}\right)^{1-\kappa} = \left(\frac{\alpha_4}{\alpha_1}\right)^{-\kappa} \tag{1.18}$$

Equations (1.16) and (1.18) yield

$$\frac{\alpha_3}{\alpha_2} = \frac{\alpha_4}{\alpha_1} \quad \text{or} \quad \frac{\alpha_2}{\alpha_1} = \frac{\alpha_3}{\alpha_4}. \tag{1.19}$$

From Eqs. (1.15), (1.17), and (1.19), we obtain

$$\frac{q_1}{q_2} = \frac{T_1 \ell n \frac{\alpha_2}{\alpha_1}}{T_2 \ell n \frac{\alpha_3}{\alpha_4}} = \frac{T_1}{T_2}. \tag{1.20}$$

Thus, in a reversible cyclic process, only by transferring heat from a higher to a lower temperature, heat is converted into work. All the reversible engines have the same and the <u>highest efficiency</u>.[4] From Eq. (1.20), the efficiency η may be derived as

$$\eta = \frac{q_1 - q_2}{q_1} = \frac{T_1 - T_2}{T_1}. \tag{1.21}$$

Then,

$$\left.\begin{aligned} \frac{q_1}{T_1} - \frac{q_2}{T_2} = \sum_i \frac{q_i}{T_i} = \oint \frac{dq}{T} &= 0 \text{ (reversible cycle) } (p_i = p_o) \\ &< 0 \text{ (irreversible cycle) } (p_i > p_o), \end{aligned}\right\} \tag{1.22}$$

where s = q/T is specific <u>entropy</u>, and S = Q/T is entropy, and <u>entropy is always defined for the reversible route of the process</u>.

S or s is a state function for a reversible process. To apply the entropy concept thus defined only for the reversible process, if the process is irreversible, one must find a reversible route to estimate the entropy difference.

In an <u>isolated system</u> where neither energy nor mass is exchanged with the outside,

---

[4] The reason is that the hypertrophy change is zero in a reversible process, and as we shall see below, the hypertrophy is responsible for non-work change.

$$\left.\begin{array}{ll} ds = (dq)_{rev}/T, & \text{(defined for reversible process)} \\ \Delta s = 0, & \text{(reversible process)} \\ \Delta s > 0, & \text{(irreversible, natural process)} \\ \Delta s < 0. & \text{(unnatural process)} \end{array}\right\} \tag{1.23}$$

In this generalized treatment of entropy, applicable to both reversible and irreversible processes, there exists missing information which describes the pressure p_r that provides the resisting force for the work transfer. "Work energy is transferred only against the resisting force." Out of the following three possible cases;

$$\left.\begin{array}{ll} \text{(a)} \quad p_r = p_i < p_o & \\ \text{(b)} \quad p_r = p_i = p_o & dw = p_i d\alpha \\ \text{(c)} \quad p_r = p_o < p_i & dw = p_o d\alpha \end{array}\right\} \tag{1.24}$$

cases (a) and (b) allow the variables of the system in question, which carry subscript i, to describe the changes. However, case (c) does require information which does not belong to the system, i.e., p_o, but describes an important work-irreversibility. In (c) of an irreversible process,

$$p_i d\alpha = \underbrace{(p_i - p_o)d\alpha}_{\text{(non-work)}} + \underbrace{p_o d\alpha}_{\text{(work transferred)}}. \qquad (p_r = p_o) \tag{1.25}$$

When $p_i = p_o$ or the process is reversible, $p_o d\alpha = p_r d\alpha = dw$ becomes the largest, explaining the nature of the Carnot cycle. The relationship

$$p_r = p_o < p_i, \tag{1.26}$$

is the missing link in non-phenomenological irreversible thermodynamics.[5] When applied to the work irreversible process with the condition of Eq. (1.26), in the present treatment of "reversible process-defined" entropy, there appears a term arising from the non-work terms of Eq. (1.25), which is termed "hypertrophy."[5] Hypertrophy, B, describes the concentration change without energy transfer, together with calorimetric entropy which describes energy transfer. Ordinary entropy thus consists of the sum of calorimetric entropy and hypertrophy as

$$dS = dS_c + dB. \tag{1.27}$$

Then, it is clear that while the second law is often stated as "a mere transfer of heat from a colder to a hotter body, without assistance from some other process, is not possible" (Clausius), it is not sufficient. An additional expression, "And a mere transfer of molecules or particles from a system of low concentration to that of high concentration without assistance from some other process, is also not possible" has to be added for completion. With this information, the thermodynamics, structured both in reversible and irreversible processes, is complete, because it now describes all the possible cases.

For the irreversible process, a determining operation

---

[5] Fukuta, to be published.

$$p_i d\alpha \rightarrow \underset{\text{(non-work)}}{(p_i - p_o)d\alpha} + \underset{\text{(work)}}{p_o d\alpha} \tag{1.28}$$

may be introduced in the ordinary thermodynamic functions, starting from Eq. (1.27), to see what portion is controlled by energy (S_c) and the rest by the concentration (B), and to define the meaning and proportion of terms in the characteristic function of thermodynamics to be described below.

From Expression (1.23) and Eq. (1.2), for natural change we obtain

$$du - Tds \leq - dw. \quad (< \text{ sign is for irreversible processes}) \tag{1.29}$$

Note that when operation (1.28) is applied, some of the above terms become partly or wholly non-energy and reduce the reversible work term ($p_i d\alpha$).

Absolute temperature

From Eqs. (1.2) and (1.6), the first law may be expressed as

$$dq = du + pd\alpha. \tag{1.30}$$

Using Eqs. (1.30) and (1.23) for the reversible process, we may define the absolute temperature

$$T = \left(\frac{\partial u}{\partial s}\right)_\alpha. \tag{1.31}$$

1.4 Thermodynamic Functions and Equilibrium

Adiabatic change

From Eq. (1.2) applied to the irreversible or natural process, with dq = 0, and Eq. (1.29)

$$ds \geq 0. \tag{1.32}$$

This is to say that in adiabatic change, entropy increases unless the process is reversible. Thus, entropy will reach a maximum value (the equilibrium condition in adiabatic process).

Isothermal and isochoric change and Helmholtz free energy

For isothermal natural change, Eq. (1.29) may be written as

$$d(u - Ts) \leq - dw, \tag{1.33}$$

and the quantities in the parenthesis are state variables. So we express them as

$$f = u - Ts \quad \text{or} \quad F = U - TS, \tag{1.34}$$

where f and F are specific and molar Helmholtz free energies, respectively. Then, Eq. (1.33) reduces to

$$df \leq - dw = -pd\alpha. \tag{1.35}$$

This is to say that the amount of f increase is smaller than the actual work added to the system. For an isothermal change, the maximum work the system can do to the outside is -df; and d(Ts) = Tds remains in the system.

Under isothermal and isochoric condition ($d\alpha = 0$, $dw = 0$), Eq. (1.35) becomes

$$df \leq 0. \tag{1.36}$$

This suggests that for isothermal and isochoric conditions, the change always takes place in the direction of f reduction, and the system takes f minimum under equilibrium. Only for the reversible process, f remains constant.

Isothermal and isobaric change and Gibbs' free energy

Under isothermal and isobaric conditions, Eqs. (1.29) and (1.6) lead to

$$d(u - Ts + p\alpha) \leq 0. \tag{1.37}$$

Here, again, we define the quantity in the parenthesis as

$$g = u - Ts + p\alpha \quad \text{or} \quad G = U - TS + pV, \tag{1.38}$$

where g and G are specific and molar Gibbs' free energies, respectively. Then, for natural change, Eq. (1.37) becomes

$$dg \leq 0. \tag{1.39}$$

This implies that, under isothermal and isobaric conditions, unless reversible, the natural change is towards a decrease in Gibbs' free energy.

Isobaric change and enthalpy

For reversible change under isobaric condition, Eq. (1.30) may be written as

$$dq = d(u + p\alpha). \tag{1.40}$$

So we define the quantity in the parenthesis as

$$h = u + p\alpha \quad \text{or} \quad H = U + pV, \tag{1.41}$$

where h and H are specific and molar enthalpies, respectively. Then, from Eqs. (1.29), (1.40), and (1.41) under isobaric condition

$$Tds = dh \quad \text{or} \quad ds \geq 0 \text{ for } dh = dq + \alpha dp \geq 0. \tag{1.42}$$

Characteristic functions

Considering the first law relationship given in Eqs. (1.23) and (1.30), and taking total (exact) differentials, Eqs. (1.30), (1.34), (1.38), and (1.41) may

be expressed as

$$du = Tds - pd\alpha, \tag{1.43}$$

$$df = -sdT - pd\alpha, \tag{1.44}$$

$$dg = -sdT + \alpha dp, \tag{1.45}$$

$$dh = Tds + \alpha dp, \tag{1.46}$$

Among these characteristic functions, f and g decrease under the conditions respectively assigned above when natural changes take place. We shall see application of some of these functions later.

Chemical potential (open system)

The properties of characteristic functions we have seen above may be transferred with the mass. The mass transfer is rather common in chemical systems where reactions cause the shift of mass and development of the chemical potential concept.

For Gibbs' free energy, for example, using Eq. (1.45), we can write

$$dG = -SdT + Vdp + \left(\frac{\partial G}{\partial m}\right)dm, \tag{1.47}$$

where dm is the mass added to the system and

$$\left(\frac{\partial G}{\partial m}\right)_{p,T} = \mu = g, \tag{1.48}$$

where μ is the chemical potential defined for unit mass.[6]

Since all the characteristic functions express energy in different forms, their increases due to the mass addition are all the same if the conditions of their own definition are taken:

$$\mu = \left(\frac{\partial U}{\partial m}\right)_{S,V} = \left(\frac{\partial F}{\partial m}\right)_{T,V} = \left(\frac{\partial G}{\partial m}\right)_{p,T} = \left(\frac{\partial H}{\partial m}\right)_{S,p}. \tag{1.49}$$

For the system involving the number of phases, i, Eq. (1.47) becomes

$$dG = -SdT + Vdp + \sum_i \mu_i dm_i. \tag{1.50}$$

Partial quantities

---

[6] Chemical potential can also be defined for a mole or for a molecule. Chemical potential is in essence hypertropy-derived potential, and as the latter clearly describes the mechanical nature of energy (or non-energy) transfer, direct use of the latter is more advantageous.

In the system with T, p, and m_i as independent variables, we can define partial quantities for extensive properties. The partial properties thus derived are now intensive properties.

Example:

$$u_i = \frac{\partial U}{\partial m_i}, \tag{1.51}$$

$$U = \sum m_i u_i. \tag{1.52}$$

Phase equilibrium

For two phase equilibria consisting of a single substance,

$$G = m_1 g_1 + m_2 g_2, \tag{1.53}$$

where subscripts 1 and 2 stand for phases 1 and 2, respectively. Under equilibrium and dT = 0 and dp = 0, transfer of dm from phase 1 to phase 2 results in dG = 0 or

$$(g_1 - g_2)dm = 0 \quad \text{or}$$
$$g_1 = g_2. \tag{1.54}$$

1.5 Thermodynamics of Air and Water Vapor

Air and water molecules

Table 1.2 Main components of dry atmospheric air.

Gas	Molecular weight*	Molar (or volume) fraction	Mass fraction	Specific gas constant ($J\ kg^{-1}\ K^{-1}$)	$m_i R_i/m$ ($J\ kg^{-1}\ K^{-1}$)
Nitrogen (N_2)	28.013	0.7809	0.7552	296.80	224.15
Oxygen (O_2)	31.999	0.2095	0.2315	259.83	60.15
Argon (Ar)	39.948	0.0093	0.0128	208.13	2.66
Carbon dioxide (CO_2)	44.010	0.0003	0.0005	188.92	0.09
		1.0000	1.0000	$\frac{\sum m_i R_i}{m}$ =	287.05

*Based on 12.000 for C^{12} (Iribarne and Godson, 1981).

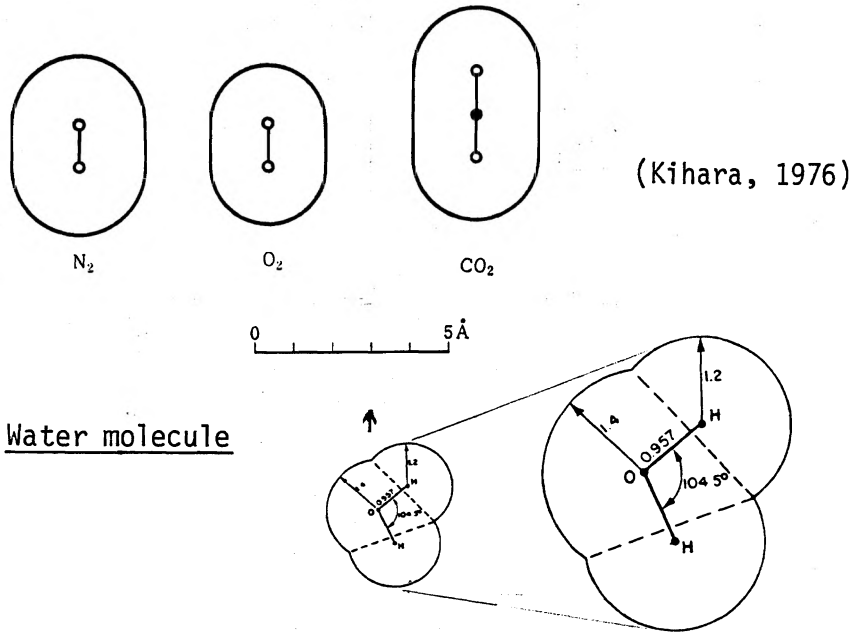

Fig. 1.5 Two dimensional geometry of a single water molecule. The O–H distance (in 10^{-8} cm) and the H–O–H angle are indicated, as are radii of the hydrogen and oxygen atoms (Pruppacher and Klett, 1978).

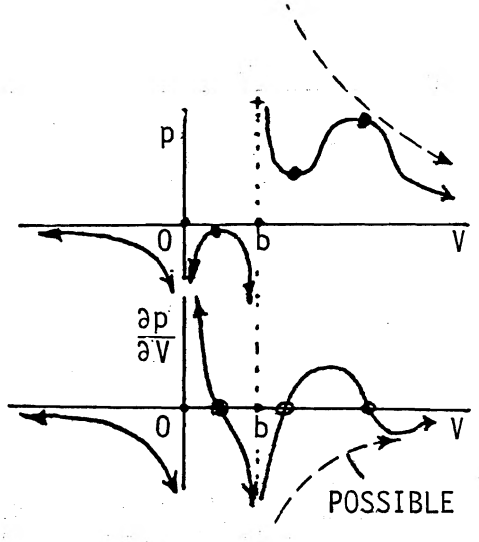

Fig. 1.6 Behavior of van der Waals equation.

Water molecule

Molecular weight; 18.015
Exact O–H distance; 0.95718 Å, H–O–H angle; 104.523° (tetrahedron; 109°28′)
Dipole moment; $\mu = 1.834 \times 10^{-18}$ e.s.u.-cm (Debye)
Critical point; 374.2°C, 218 atm.
Dielectric constant; 81 (18°C)
VERY HIGH LATENT AND SPECIFIC HEATS; (only in condensed phases) due to hydrogen-bonding.
Polar nature ---- dissolve and dissociate various salts
→ Conduction of electric current

Equations of state: ideal and real gases

Ideal gas law (Perfect gas law or Boyle-Charles' law)

The empirical relationship between p and V under constant T or Boyle's law and that between V and T under constant p or Charles' law or Gay-Lusac's law lead to a combined relationship known as ideal gas law or Boyle-Charles' law;

$$pV = nR^*T, \tag{1.55}$$

where n is the number of moles of the gas and R* the molar (universal) gas constant.

$$R^* = 8.31441 \times 10^7 \text{ erg mol}^{-1} \text{ K}^{-1} = 8.3144 \text{ J mol}^{-1} \text{ K}^{-1}$$
$$= 1.9858 \text{ cal}_{IT} \text{ mol}^{-1} \text{ K}^{-1}.$$

Standard volume of ideal gas
$V_0 = 2.24136 \times 10^{-2} \text{ m}^3 \text{ mol}^{-1}$ (at 273.15 K, 1 atm)

Ideal gas: molecules are assumed to have no volume and no molecular interaction. Real gas will approach to ideal gas at low pressure and high temperature.

Real (imperfect) gas law: van der Waals' equation

Real gas

Real gas molecules have finite sizes so that actual space volume for the molecules to fly is smaller than the total space volume. In addition, intermolecular forces pull molecules back which are colliding with the wall to exert pressure. The pull is proportional to the density of molecules near the wall and to the density of molecules inside, or

$$\rho \propto 1/V \text{ or } \rho^2 \propto 1/V^2.$$

Therefore, the true pressure can be expressed as $p + a/V^2$. Then, Eq. (1.55) becomes

$$\left(p + \frac{a}{V^2}\right)(V - b) = nR^*T, \tag{1.56}$$

which is called Van der Waals' equation of state (1873), and is one of the earliest of its kind.

There are other equations of state for real gas. Equation (1.55) may be written as (for n = 1)

$$\begin{aligned} V(p/R^*T) &= 1 - a/VR^*T + b(p/R^*T) + ab/V^2R^*T \\ &= 1 + (1/V)\left(b - \frac{a}{R^*T}\right) + \frac{b^2}{V^2} + \text{----------}, \\ &= 1 + B/V + C/V^2 + \text{----------}, \end{aligned} \tag{1.57}$$

B; second virial coefficient,
C; third virial coefficient (virial; force).
Values of B, C, --- give clues for intermolecular forces

By rearranging Eq. (1.56) in the form

$$p = \frac{R^*T}{V - b} - \frac{a}{V^2}, \tag{1.56}'$$

and differentiating it with V under constant temperature, we obtain

$$\frac{\partial p}{\partial V} = \frac{-R^*TV^3 + 2a(V - b)^2}{(V - b)^2V^3}. \tag{1.58}$$

Equation (1.58) is a cubic function for V > b (see Fig. 1.5). A cubic function has at most 3 roots and at least 1 root, but one of the three in Eq. (1.58) always appears at V = ∞. The remaining two correspond to a minimum and a maximum in Eq. (1.56). These two extrema lead to instability of phase and phase change. Thus, the van deer Waals equation describes condensation phenomena.

Air and water vapor as ideal gases (Dufour and Defay, 1963)

Setting Eq. (1.55) for one mole air, with the deviation from the ideal gas in C_1, we write

$$pV = C_1R^*T. \tag{1.59}$$

$C_1 = 1$ is for the ideal gas.

Table 1.3 Correction coefficient C_1 to the perfect gas law for dry air.

t(°C)	p_1(mb)		
	0	500	1000
−100	1	0.9958	0.9917
−50	1	0.9992	0.9984
0	1	0.9997	0.9994
+50	1	0.9999	0.9999

Similarly, for water vapor, we have

$$pV = C_2R^*T. \tag{1.60}$$

$C_2 = 1$ is for the ideal gas.

Table 1.4 Correction coefficient C_2 to the perfect gas law for pure water vapor.

t(°C)	p_2(mb)	
	0	Saturation
−100	1	1.0000
−50	1	1.0000
0	1	0.9995
+50	1	0.9961

Air and water vapor deviate from ideal gas law by less than 1%, and the ideal gas law is a good approximation for them under atmospheric conditions.

Main temperature points of phase change for water substance are:
Melting point of ice under 1 atm. = 0°C = 273.15 K
Boiling point of water under 1 atm. = 100°C = 373.15 K
Triple Point = 0.01°C = 273.16 K
(6.107 mb = 6.107 hPa)

The liquid (L) - solid (S) line tilting to the left in Fig. 1.8 is due to volume increase during freezing, which is rather unusual (due to hydrogen bonding). The L-S lines for most substances tilt to the right due to shrinkage when they solidify.

Clausius-Clapeyron equation

For two phases under equilibrium [water vapor (1) vs. liquid water or ice (2)], we apply Eq. (1.45) for each phase, for p,T change (reversible).

$$dg_1 = -s_1 dT + \alpha_1 dp \quad \text{and} \quad dg_2 = -s_2 dT + \alpha_2 dp. \qquad \text{(own vapor)}$$

Now, as long as the equilibrium between the two phases is maintained according to Eq. (1.54), the deviations dg_1 and dg_2 in respective phases from an equilibrium point with $g_1 = g_2$ must also be the same, or

$$dg_1 = dg_2.$$

Consequently,

$$\frac{dp}{dT} = \frac{de_s}{dT} = \frac{(s_1 - s_2)}{(\alpha_1 - \alpha_2)}, \tag{1.61}$$

where e_s is the saturation vapor pressure. Equation (1.61) is called the Clausius-Clapeyron equation. Since

$$s_1 - s_2 = \frac{\Delta q}{T} = \frac{L}{T}, \tag{1.62}$$

where L is the specific latent heat of the phase change (see Fig. 1.9), and

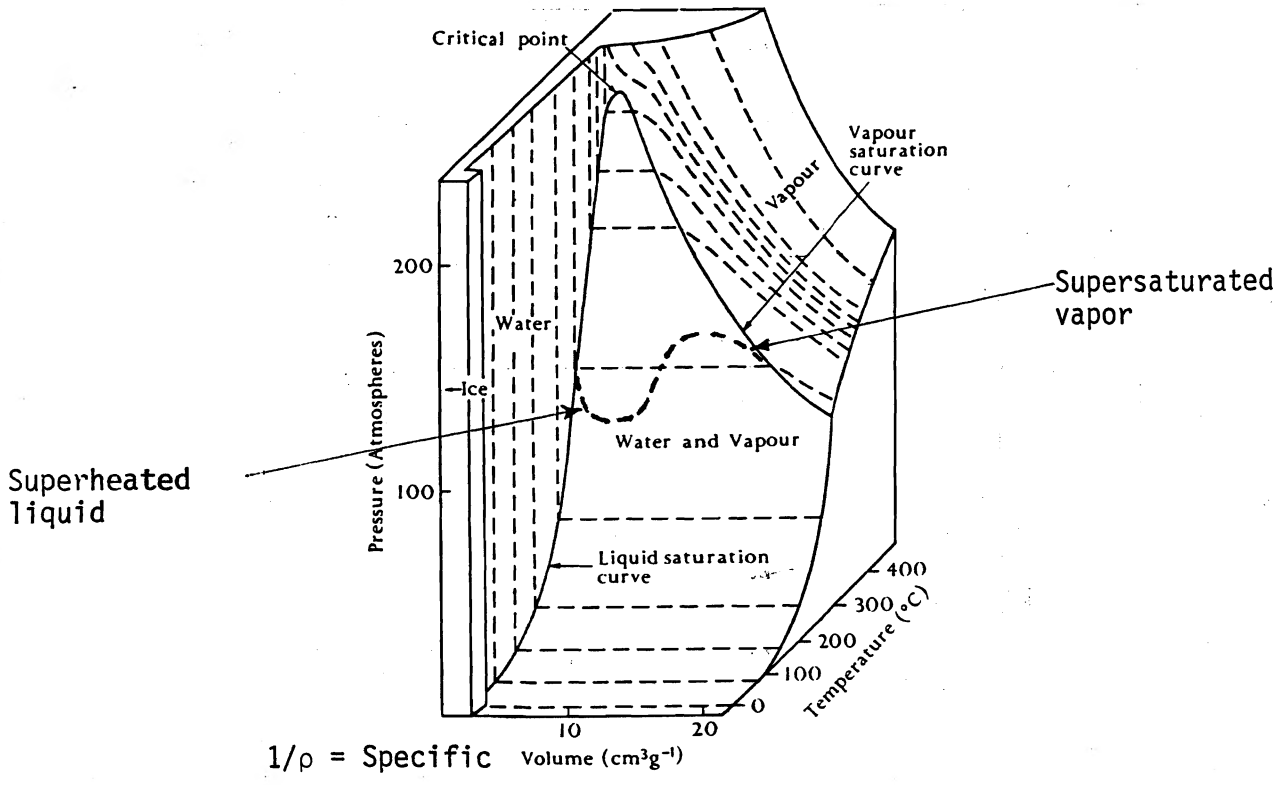

Fig. 1.7 *P-V-T* surface for H_2O. (The dashed lines are isotherms.) Adopted with changes from Slater (1939).

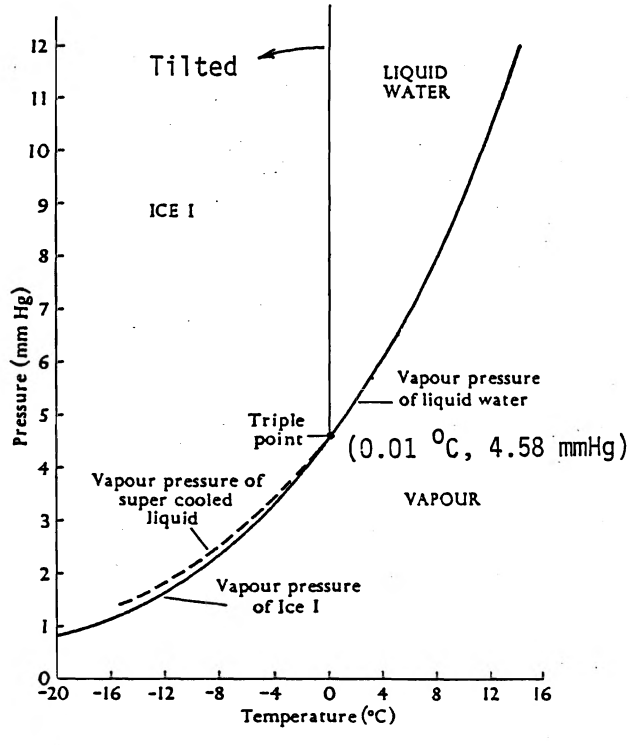

Fig. 1.8 *P-T* diagram for H_2O in the region of the triple point.

$$\alpha_1 \gg \alpha_2, \quad \text{(low p)}$$

using the ideal gas law,

$$\alpha_1 = \frac{R_v T}{e_s},$$

where R_v (=R*/M, M the molecular weight of water) is the specific gas constant for water vapor, we have

$$\frac{de_s}{dT} = \frac{Le_s}{R_v T^2}. \tag{1.62'}$$

Integration of Eq. (1.62') yields a useful formula for the Clausius-Clapeyron equation

$$\ln\left(\frac{e_s}{e_{so}}\right) = \frac{\bar{L}}{R_v}\left(\frac{1}{T_0} - \frac{1}{T}\right), \tag{1.62''}$$

where e_{so} is the saturation vapor pressure at temperature T_o, and $\bar{L}$ is the specific latent heat of phase change (condensation or deposition) averaged over the temperature range in question.

Kirchhoff's equation

The specific latent heat L is a function of T, although very mild. Here, we obtain the temperature dependency.

By differentiating Eq. (1.62) with T

$$\frac{1}{T}\frac{dL}{dT} - \frac{L}{T^2} = \left[\left(\frac{\partial s_1}{\partial T}\right)_p + \left(\frac{\partial s_1}{\partial p}\right)_T \frac{dp}{dT}\right] - \left[\left(\frac{\partial s_2}{\partial T}\right)_p + \left(\frac{\partial s_2}{\partial p}\right)_T \frac{dp}{dT}\right]. \tag{1.63}$$

Under p = const, (1.46) gives

$$\left(\frac{\partial q}{\partial T}\right)_p = c_p = T\left(\frac{\partial s}{\partial T}\right)_p = \left(\frac{\partial h}{\partial T}\right)_p, \tag{1.64}$$

where c_p is the specific heat at constant pressure; and from Eq. (1.45),

$$s = -\left(\frac{\partial g}{\partial T}\right)_p,$$

and by differentiating under T-const with respect to p,

$$\left(\frac{\partial s}{\partial p}\right)_T = -\frac{\partial}{\partial p}\left(\frac{\partial g}{\partial T}\right)_p = -\frac{\partial}{\partial T}\left(\frac{\partial g}{\partial p}\right)_T = -\left(\frac{\partial \alpha}{\partial T}\right)_p. \tag{1.65}$$

Inserting Eqs. (1.64) and (1.65) into Eq. (1.63) and using Eq. (1.61) and the ideal gas law, we obtain

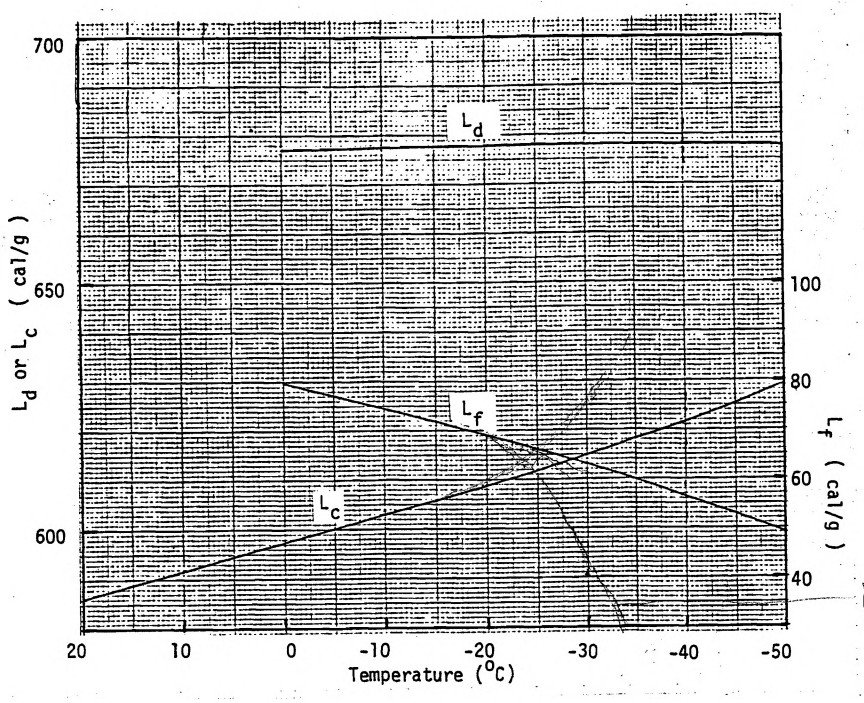

Fig. 1.9. Specific latent heats of phase change for water substance.
L_c; specific latent heat of condensation (heat per unit mass)
L_d; specific latent heat of deposition
$L_f = L_d - L_c$; specific latent heat of fusion

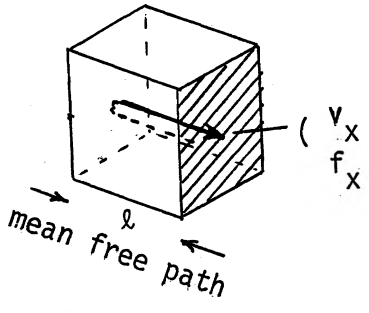

Fig. 1.10. A gas molecule in the "mean free path" box.

$$c_{p1} - c_{p2} = \frac{dL}{dT}, \tag{1.66}$$

which is called Kirchhoff's law and describes the temperature dependency of the latent heats of phase changes.

The specific heat at constant volume can also be defined as [cf. (1.64)]

$$\left(\frac{\partial q}{\partial T}\right)_v = c_v = \left(\frac{\partial u}{\partial T}\right)_v = T\left(\frac{\partial s}{\partial T}\right)_v. \tag{1.67}$$

Thermodynamic relationship between c_v and c_p

Equation (1.30) (the first law) under the condition of Eq. (1.67) yields

$$dq = c_v dT + p d\alpha. \tag{1.68}$$

Further insertion of the differential form of the ideal gas law into Eq. (1.68) results in

$$dq = (c_v + R)dT - \alpha dp,$$

which, under the condition of Eq. (1.64), reduces to

$$c_p = c_v + R, \tag{1.69}$$

or

$$dq = c_p dT - \alpha dp. \tag{1.70}$$

Thermodynamics does not provide further information about the absolute value of c_v or c_p (p=const), and we have to resort to atomic and molecular processes.

Specific heats: molecular aspects

In the above section, specific heats of gases are thermodynamically defined, but detailed knowledge cannot be obtained by thermodynamics alone. Here, we look into micromechanisms that contribute storage of heat energy in gaseous molecules.

Kinetic energy and temperature of a gas molecule

First of all, from the viewpoint of gas kinetics, we derive the relationship between the kinetic energy and thermal energy of a gas molecule.

A molecule in the mean free path box, colliding with a wall which is perpendicular to the direction of flight x, communicates its momemtum with the wall (see Fig. 1.10).

$$f_x t = 2mv_x, \tag{1.71}$$

where f_x is the force exerted to the molecule, t the time, m the molecular mass, and v_x the velocity component in the x direction.

If n_x represents the number of collisions the molecule makes with the wall per second,

$$t = 1/n_x = 2\ell/v_x. \tag{1.72}$$

Then, from Eqs. (2.46) and (2.47),

$$f_x = 2mv_x\left(\frac{v_x}{2\ell}\right) = \frac{mv_x^2}{\ell}. \tag{1.73}$$

Since

$$v_x^2 + v_y^2 + v_z^2 = \bar{v}^2, \tag{1.74}$$

where v_y and v_z are y and z components of the molecular velocity v, and

$$v_x = v_y = v_z. \tag{1.75}$$

Equation (1.74) reduces to

$$v_x^2 = \frac{1}{3}(\bar{v}^2). \tag{1.76}$$

Then, the pressure p on the wall, using Eqs. (1.73) and (1.76), may be expressed as

$$p = \frac{f_x}{\ell^2} = \frac{1}{3}\, m\, \frac{\bar{v}^2}{\ell^3}. \tag{1.77}$$

From the ideal gas law for 1 mole of gas and $V = N\ell^3$, where N is Avogadro's number,

$$N = 6.022045 \times 10^{23}\ \text{mol}^{-1},$$

$$pV = \frac{1}{3} m \frac{\bar{v}^2}{\ell^3} N\ell^3 = R^*T \quad \text{or}$$

$$\frac{1}{2}m\bar{v}^2 = \frac{3}{2}kT, \tag{1.78}$$

and where k is Boltzmann's constant;

$$k = 1.380662 \times 10^{-23}\ \text{J K}^{-1} = 1.3807 \times 10^{-16}\ \text{erg K}^{-1}\ (=R^*/N).$$

From Eqs. (1.76) and (1.78),

$$\frac{1}{2}mv_x^2 = \frac{1}{2}kT. \tag{1.79}$$

This is to say that the kinetic energy of a molecule in one direction corresponds

to ½kT of thermal energy and explains the relationship between the molecular kinetic energy and the temperature. (A more rigorous treatment produces the same result) (see Chapman and Cowling, 1970).

When a gas molecule reflects from the wall upon collision, an energy shock (temporary transfer), $2 \times \frac{1}{2}m\overline{v_x^2} = kT$, is given to the wall at least temporarily (e.g. billiard ball collision). Physically, this kT, instead of ½kT, seems to activate microkinetic processes, such as nucleations. However, derivation of the term involving kT does not physically state the molecular mechanism.

Specific heats of gases

Here, we shall examine how heat energy is stored in molecular motions.

A monatomic gas, has no motions other than the translational (flying). So, under α = const, du = dq, and the total kinetic energy, i.e., Eq. (1.78), becomes the internal energy for heat storage, i.e.,

$$u = \frac{3}{2}kT\,\frac{N}{M} = \frac{3}{2}RT, \tag{1.80}$$

where M is the molecular weight of the gas, or under the condition of Eq. (1.67),

$$c_v = \frac{3}{2}R. \quad \text{(monatomic gases)} \tag{1.81}$$

Since c_p is larger than c_v by R, Eq. (1.81) gives

$$c_p = \frac{5}{2}R. \quad \text{(monatomic gases)} \tag{1.82}$$

For polyatomic gases, three kinds of motion normally contribute to specific heats:

(1) translational
The motion is not quantized.

(2) rotational
Below characteristic temperature, the motion is quantized, and above the temperature, equipartition of energy applies. No gas molecules are quantized under atmospheric temperature.

(3) vibrational
Below characteristic temperature, θ_v, quantized and above it, equipartition of energy applies. Most of the gases under room temperature are quantized, and equipartition of energy does not apply.

Quantization of molecular and atomic motions restricts the motions and reduces the number of motions and energies involved. In order for quantization to occur, atoms in motion must be under restoring forces. A restoring force is the reason for wave development, and quantum mechanics is a wave mechanics under the restriction of the wave behavior.

Equipartition of energy;

Total energy is equally divided among each degree of freedom (of motion), and each component of energy is ½kT (equipartition principle of energy, only applicable to simple molecules). If the number of degrees of freedom is defined as the number of coordinates which is necessary to describe the motion, the number of degrees of freedom or the number of independent motions for a gas molecule in three different motions are:

	Number of independent motions	
Translational:	3	(maximum)
Rotational:	3#	(maximum)
Vibrational:	3 n(trans) − 3 − 3#	(maximum) (liquid and solid)

(n: number of atoms in the molecule. # for linear molecules, use 2 instead.)

Dry air:

$$c_p = 1005 \text{ J kg}^{-1} \text{K}^{-1} = 0.24 \text{ cal g}^{-1} \text{K}^{-1} \left(=\frac{7}{2}R\right)$$
$$c_v = 718 \text{ J kg}^{-1} \text{K}^{-1} = 0.171 \text{ cal g}^{-1} \text{K}^{-1} \left(=\frac{5}{2}R\right)$$

Water vapor:

$$c_p = 1850 \text{ J kg}^{-1} \text{K}^{-1} = 0.443 \text{ cal g}^{-1} \text{K}^{-1} \left(=\frac{8}{2}R_v\right)$$
$$c_v = 1390 \text{ J kg}^{-1} \text{K}^{-1} = 0.332 \text{ cal g}^{-1} \text{K}^{-1} \left(=\frac{6}{2}R_v\right)$$

Rotational and vibrational motions receive quantum mechanical restrictions and reduce their energy contribution at low temperatures. The equipartition principle applies only to simple molecules and as the molecular size increases, the principle should be eventually overtaken by the Dulong-Petit's law (solid at high temperature; 3kT/atm).

Table 1.5 Molecular properties of atmospheric gases.

Gas	Degrees of Freedom			J g^{-1} K^{-1}				
	trans.	rot.	vib.	R R*/M=J/gK	c_p	c_v	$c_p c_v$ (obs., 18-25°C)[a]	θ_v (K)
Monatomic gases								
Helium (He)	3			2.076	5.226	3.148	1.63	
Argon (Ar)	3			0.2081	0.531	0.318	1.648	
Diatomic gases								
Hydrogen (H_2)	3	2	+	4.124	14.058	9.970	1.407	6140
Nitrogen (N_2)	3	2		0.2967	1.004	0.746	1.401	3180
Oxygen (O_2)	3	2		0.2598	1.05	0.750	1.396	2260
Triatomic gases								
Water vapor (H_2O)	3	3	3*	0.4617	1.912	1.450	[1.32]	
Carbon dioxide (CO_2)	3	2	4*	0.1889	0.822	0.632	1.293	
Ozone (O_3)	3	3		0.1732				
Dry air				0.2870			1.402	

[a] J. D'ans and E. Lax, "Taschenbuch fur Chemiker und Physiker." Springer, Berlin, p. 1052, 1943.
*quantized. * less than ½kT for each freedom. + lowest energy.

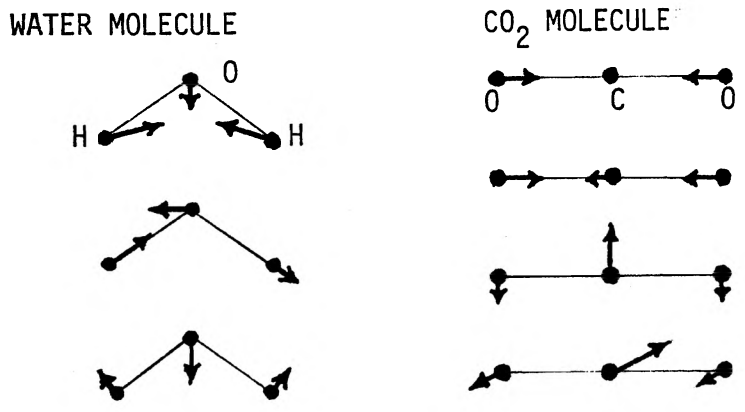

Fig. 1.11 Vibrational modes of H_2O and CO_2 molecules.

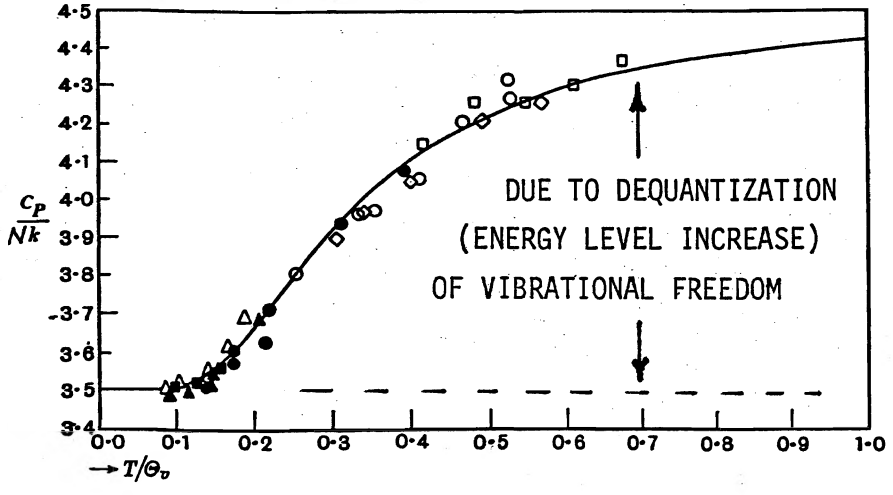

Fig. 1.12 Molecular heat capacities of diatomic gases; quantum mechanical effect.

The specific heat of dry air at constant pressure, c_p, varies less than 0.4% for the ranges p; 0 - 1,100 mb and T; −40 - +30°C. For more confined ranges of p; 300 ~ 1,100 mb and T; −30 - +30°C, the deviation reduces to less than 0.3% (Smithsonian Meteor. Table).

Thermodynamics of gases

There are two forms of the first law commonly applied to gases;

$$dq = c_v dT + p d\alpha, \tag{1.68}$$

and

$$dq = c_p dT - \alpha dp. \tag{1.70}$$

We proceed from these.

Special processes may be described as

(a) Isobaric processes: $dp = 0$

$$(1.70) \rightarrow dq = c_p dT = \frac{c_p}{c_v} du. \tag{1.83}$$

(b) Isothermal processes: $dT = 0$

$$\begin{aligned} &(1.70) \rightarrow dq = -\alpha dp, \\ &(1.68) \rightarrow dq = pd\alpha. \quad (=dw) \end{aligned} \tag{1.84}$$

(c) Isochoric processes: $d\alpha = 0$

$$(1.68) \rightarrow dq = c_v dT = du. \tag{1.85}$$

(d) Adiabatic processes: $dq = 0$

$$(1.70) \rightarrow c_p dT = \alpha dp, \tag{1.86}$$

$$(1.68) \rightarrow c_v dT = -pd\alpha. \tag{1.87}$$

Adiabatic processes

Adiabatic processes often occur under meteorological conditions.

From Eq. (1.86) and the ideal gas law,

$$c_p dT = RT\frac{dp}{p}. \tag{1.88}$$

By integration, Eq. (1.88) yields

$$\frac{c_p}{R}(\ln T - \ln T_o) = \ln p - \ln p_o,$$

or

$$\left(\frac{T}{T_o}\right) = \left(\frac{p}{p_o}\right)^{R/c_p} = \left(\frac{p}{p_o}\right)^{\kappa}. \tag{1.89}$$

Equation (1.89) is called Poisson's equation for adiabatic process.

$$\kappa = \frac{c_p - c_v}{c_p}. \quad (= 0.286 = 2/7 \text{ for dry air})$$

Potential temperature

For the purpose of describing atmospheric processes, we introduce a standardized temperature called potential temperature θ. From Eq. (1.89)

$$\frac{T}{\theta} = \left(\frac{p}{10^5\ Pa}\right)^{\kappa} = \left(\frac{p}{1000\ mb}\right)^{\kappa},$$

or

$$\theta = T\left(\frac{1000\ mb}{p}\right)^{\kappa}. \tag{1.90}$$

The potential temperature is a temperature which a parcel of air would have at 1000 mb or 10^5 Pa through adiabatic process. Thus, when entropy change is zero, potential temperature remains constant.

Entropy

When the potential temperature changes, entropy change also happens through heat exchange. From Eqs. (1.70), (1.23), and the ideal gas law,

$$ds = \frac{1}{T}(c_p dT - \alpha dp) = c_p\frac{dT}{T} - R\frac{dp}{p} = c_p\frac{d\theta}{\theta}. \tag{1.91}^7$$

By integration, (1.91) gives

$$s = c_p \ln\theta + \text{const.} \tag{1.92}$$

For reversible adiabatic process (dq=0 or ds=0), potential temperature and entropy remain unchanged (isentropic process).[8]

Moist air

In meteorology, moist air is considered to be a mixture of dry air and water vapor. When we deal with moist air, the subscript, a, will be used. Similarly, d is used for dry air and v for water vapor.

(a) Mixing ratio: w

Under varying temperature, pressure, and volume in the atmosphere, the condition of water vapor can be described relative to dry air:

$$w = \frac{\text{mass of water vapor}}{\text{mass of dry air}} = \frac{\rho_v}{\rho_d} = \frac{m_v}{m_d}. \tag{1.93}$$

---

[7] Exact differential of Eq. (1.90) yields

$$d\theta = \frac{\partial\theta}{\partial T}dT + \frac{\partial\theta}{\partial p}dp = \frac{T}{T}\left(\frac{10^5\ p_a}{p}\right)^{\kappa}dT - \kappa T\left(\frac{10^5\ p_a}{p}\right)^{\kappa}\frac{dp}{p},$$

which combines with Eq. (1.90) and $\kappa = R/c_p$ to yield

$$c_p\frac{d\theta}{\theta} = c_p\frac{dT}{T} - R\frac{dp}{p}.$$

[8] The isentropic process used here is strictly for $ds_c = 0$ and not necessarily ds = 0 as long as dq is a real heat exchanged instead of reversible heat (see Eq. 1.27).

From the ideal gas law,

$$\rho_v = \frac{e}{R_v T}, \quad \text{and} \quad \rho_d = \frac{(p - e)}{R_a T},$$

where R_a is the specific gas constant for dry air and p the total pressure. R_a is also used for moist air unless there is a specific need to express the effect of moisture. Then,

$$w = \frac{R_a}{R_v} \frac{e}{p - e} \simeq \epsilon \frac{e}{p}, \tag{1.94}$$

where

$$\epsilon = \frac{R_a}{R_v} = \frac{M_w}{M_a} = 0.622. \tag{1.95}$$

(b) Specific humidity: q

A slightly different definition can be used to describe the moist air: specific humidity = mass of water vapor per unit mass of moist air.

$$q = \frac{\rho_v}{\rho_a} = \frac{\rho_v}{\rho_d + \rho_v} = \frac{\epsilon e}{p - e + \epsilon e} \simeq \frac{\epsilon e}{p} \ (\simeq w). \tag{1.96}$$

The saturation mixing ratio w_s and the saturation specific humidity q_s are defined by Eqs. (1.94) and (1.96), with $e \to e_s$. Since $e_s = f(T)$, then w_s and q_s are functions of T and p only and do not depend on the vapor content of air.

(c) Relative humidity, RH

Relative humidity RH is expressed as the ratio of the mixing ratio to its saturation value in %:

$$RH = 100 \frac{w}{w_s} \simeq 100 \frac{e}{e_s}. \tag{1.97}$$

Effects of moisture on dry air characteristics

The moisture content in the air affects the air characteristics; and when accuracy is needed, corrections as a function of w have to be given.

(a) Gas constant

For air of volume V, total pressure p and water vapor pressure e,

$$p = p_d + e = \rho_d \frac{R^*}{M_a} T + \rho_v \frac{R^* T}{M_w} = \frac{R^* T}{V}\left(\frac{m_d}{M_a} + \frac{m_v}{M_w}\right)$$

$$= \rho_a \frac{R^* T}{M_a}\left(\frac{m_d}{M_a} + \frac{m_v}{M_w}\right)\frac{M_a}{m_d + m_v} = \rho_a R_a T\left(\frac{1 + w/\epsilon}{1 + w}\right). \tag{1.98}$$

From Eq. (1.98), one can write

$$p\alpha = R_m T, \tag{1.99}$$

where R_m is the specific gas constant for moist air; and

$$R_m = R_a(1 + 0.6w). \tag{1.100}$$

(b) Specific heats

Suppose we have a system consisting of 1 g of dry air and w g of water vapor, under the constant volume,

$$(1 + w)dq = c_v dT + w c_{vv} dT,$$

where c_v is for dry air and c_{vv} is c_v for water vapor. Then,

$$c_{vm} = \frac{dq}{dT} = c_v\left(\frac{1 + wr}{1 + w}\right), \tag{1.101}$$

where c_{vm} is c_v for moist air and

$$r = \frac{c_{vv}}{c_v} \simeq 1.9. \tag{1.102}$$

Thus,

$$c_{vm} \simeq c_v(1 + 1.9w - w) = c_v(1 + 0.9w). \tag{1.103}$$

Similarly, one can obtain

$$c_{pm} \simeq c_p(1 + 0.8w). \tag{1.104}$$

Using the relationship in exponent of the Poisson equation, Eq. (1.89),

$$\frac{R_a}{c_p} = \kappa \rightarrow \frac{R_m}{c_{pm}} = \kappa_m = \frac{R_a(1 + 0.6w)}{c_p(1 + 0.8w)} = \kappa(1 - 0.2w). \tag{1.105}$$

(c) Viritual temperature, T_v

The virtual temperature is defined to account for the effect of moisture in the air buoyancy. It is the temperature of dry air having the same density as the air in question under the same pressure.

From the equation of state given in (1.98),

$$T_v = T\left(\frac{1 + w/\epsilon}{1 + w}\right) \simeq T(1 + 0.6w). \tag{1.106}$$

Because w is often of the order of 10^{-2} or less, the correction factors in Eqs. (1.100) through (1.106) can be neglected.

Meteorological temperatures

Temperature is almost always a great concern in meteorology. A variety of temperatures are defined under different conditions such as isothermal or adiabatic.

Pseudoadiabatic ($\simeq$ saturated adiabatic) process

We have already seen the behavior of air that undergoes an adiabatic change without involving any phase change [Eqs. (1.89) through (1.92)]. When a phase change such as condensation or evaporation takes place, heat generation or absorption accompanies; and the air condition changes. When a cloud parcel is cooled adiabatically due to lifting, water condenses out of it. The latent heat released during the process slows the adiabatic cooling of the parcel. It is a common practice to assume that after the water condensation, heat is generated; but water is removed out of the system.

Suppose we have 1 g of dry air mixed with w_s g of water vapor (in cloud condition), and it undergoes a change of dp, dT, and dw_s. Applying the first law, Eq. (1.70), we have

$$\underbrace{\frac{dT}{T} = \kappa\frac{dp}{p}}_{\text{dry adiabatic}} - \frac{L}{Tc_p}dw_s. \tag{1.107}$$

With this in mind, we now examine temperatures of meteorological interest.

(a) Dew point temperature: T_d

Frost point temperature: T_f

At these temperatures, saturation, with respect to liquid water (T_d) and that with respect to ice (T_f), is reached when cooled under constant p and w. Since p is held constant,

$$w_s = w(T_d).$$

(b) Equivalent temperature: T_e (two definitions)

Equivalent potential temperature: θ_e

Isobaric definition: the temperature which an air parcel would attain if entire moisture were condensed out under constant pressure.

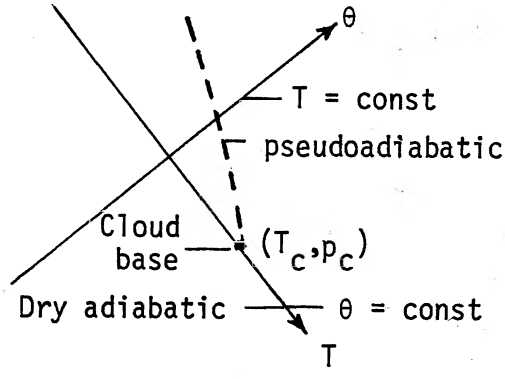

Pseudoadiabatic process[9] is warmer than the dry adiabatic process.

Fig. 1.13 Cloud processes on tephigram.

Suppose 1 g of dry air mixed with w g of water vapor experiences heating due to condensation of dw g of water. From Eq. (1.104),

$$dq = c_{pm}dT \simeq c_p dT, \quad \text{and} \quad (1 + w)dq = - Ldw,$$

we have

$$c_p dT = - Ldw. \tag{1.108}$$

After integration from (T, w) to (T_e, 0),

$$T_e = T + \frac{Lw}{c_p}. \tag{1.109}$$

Adiabatic definition

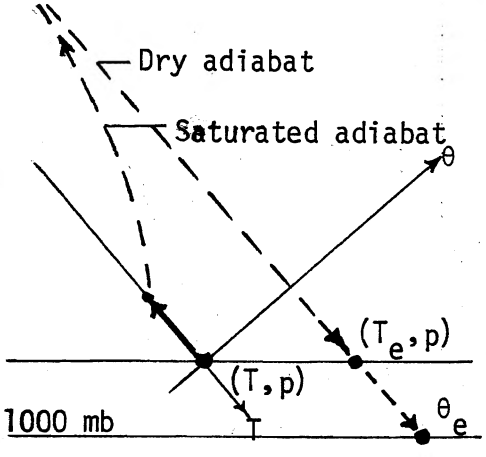

In this definition, T_e is the temperature an air mass reaches when it is cooled to a very low temperature saturated adiabatically to precipitate all the moisture out and returns to the original pressure.

For equivalent potential temperature, θ_e, the air mass should be brought to 1000 mb level.

Fig. 1.14 Adiabatic definition of equivalent temperature.

[9] Condensed water is assumed to be precipitated.

(c) Isentropic condensation temperature: T_c

This is the temperature at which saturation is reached when moist air is cooled adiabatically with w = const. Since it is adiabatic, θ remains constant until the saturation value of the given w is reached. It is the temperature of cloud condensation for adiabatic lifting of moist air.

(d) Wet bulb temperature: T_w (thermodynamic and kinetic definitions)

Adiabatic (Pseudo) wet bulb temperature: T_{sw}

Wet bulb potential temperature: θ_w

T_w in thermodynamic definition is the temperature to which air is cooled by evaporation of water at constant pressure until the saturation is reached. Since w is not held constant,

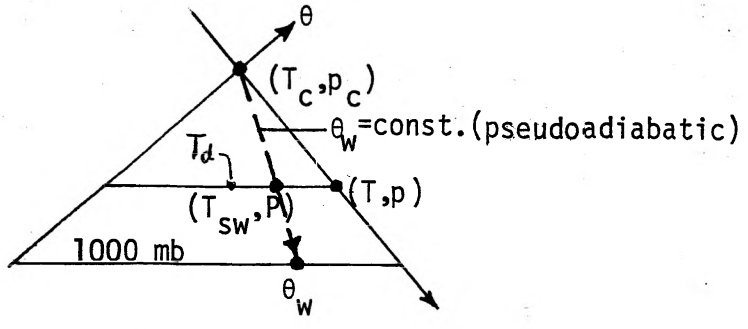

Fig. 1.15 Wet bulb temperatures.

$T_d \neq T_w$ and $T_w > T_d$.

Integration of Eq. (1.108) yields

$$\frac{T - T_w}{w_s - w} = \frac{L}{c_p}. \qquad (1.110)$$

Therefore,

$$T_w = f(T,w).$$

Among the non-potential temperature we have the following inequality relations:

$$T_s < T_d < T_{aw} < T_{iw} < T < T_v < T_{ie} < T_{ae}.$$

Dry temperatures

T_v = virtual temperature
$T_e = T_{ie}$ = (isobaric) equivalent temperature
T_{ae} = adiabatic equivalent, or pseudo-equivalent, temperature

Saturation temperatures

T_d = dew point temperature
T_f = frost point temperature
$T_w = T_{iw}$ = (isobaric) wet-bulb temperature
T_{aw} = adiabatic wet-bulb, or pseudo-wet-bulb, temperature
T_s = saturation temperature

Potential temperatures

θ = potential temperature
θ_v = virtual potential temperature
$\theta_e = \theta_{ie}$ = (isobaric) equivalent potential temperature*
θ_{ae} = adiabatic equivalent, or pseudo-equivalent, potential temperature
$\theta_w = \theta_{iw}$ = (isobaric) wet-bulb potential temperature*
θ_{aw} = adiabatic wet-bulb, or pseudo-wet-bulb, potential temperature

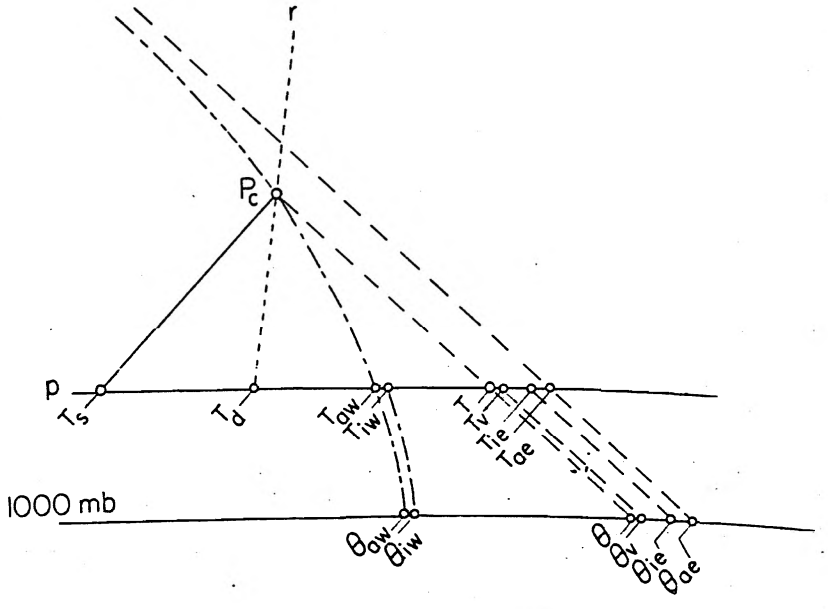

Fig. 1.16 Summary of temperature humidity parameters (Iribarne and Godson, 1981).

*Defined in a similar way to the corresponding pseudo-potential temperature.

T_w in the kinetic definition (see the section for Maxwellian droplet growth theory) is

$$\frac{T - T_w}{w_s - w} = \frac{D}{\kappa}\frac{L}{c_p}. \tag{1.111}$$

The difference between the thermodynamic definition and the kinetic one is D/κ (κ: the thermal diffusivity, see Section 2.4). $D/\kappa \simeq 1.19$ at $-10°C$.

T_{sw} is defined as the temperature which air attains after being cooled dry-adiabatically to (T_c, p_c) and then warmed pseudoadiabatically until the initial pressure is reached. T_{sw} is within 0.5°C of T_w and $T_{sw} < T_w$ (see Fig. 1.16).

θ_{sw} is the temperature if the pressure were brought to 1000 mb level.

1.6 Thermodynamics of Atmosphere

In sections above, we have seen the basic thermodynamic behaviors of air

and water vapor as gases. In this section, we look into their behaviors as components of our atmosphere.

Thermodynamic diagrams

(a) Stübe diagram [adiabatic chart based on Eq. (1.90)]
$T - p^{\kappa}$ diagram, having θ as the parameter.

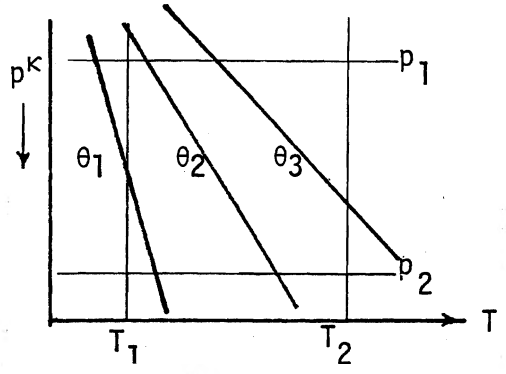

Fig. 1.17 Stübe diagram.

(b) Emagram

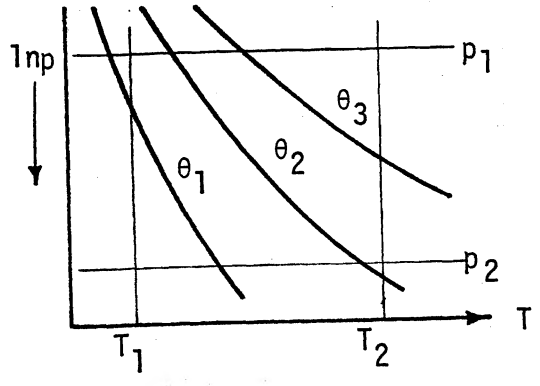

Fig. 1.18 Emagram.

ln p vs. T with θ as the parameter. From the differential form of ideal gas law

$$dw = pd\alpha = R_a dT - \alpha dp.$$

For cyclic process,

$$\int_c dw = \int_c R_a dT - \int_c \frac{R_a T}{p} dp.$$
$$= -R_a \int_c T d\ln p. \qquad (1.112)$$

R_a is the specific gas constant for air (moist).

The product of T and ln p has the property of work.

(c) Tephigram

$T - \phi$ diagram ($\phi \propto c_p \ln\theta$, ϕ is often used for entropy)

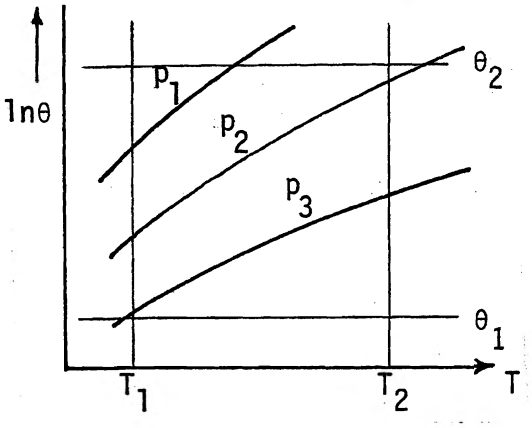

Fig. 1.19 Tephigram.

From the definition of entropy Eqs. (1.23) and (1.91)

$$\int_c dq = \int_c Tds = c_p \int_c T d\ln\theta. \qquad (1.113)$$

Normally the tephigram is rotated so that isobars end up more or less horizontal with pressure decreasing upwards.

CHAPTER 2 KINETIC THEORY OF GASES AND TRANSPORT PHENOMENA

In the preceding chapter, we have examined characteristics of air and water vapor thermodynamically and macroscopically. In this chapter, we shall look into their microscopic or gas kinetic behaviors and try to understand the basic transport processes of various thermodynamic properties.

2.1 Intermolecular Potentials

The van der Waal equation showed that vapor molecules may condense due to intermolecular attractive forces when the temperature becomes sufficiently low. Condensation occurs when the kinetic energy of vapor molecules is lost normally in the form of heat in the potential well consisting of long range attractive and short range repulsive forces. The molecules which lost a part of the kinetic energy in the condensed phase still maintain their thermal motions in the potential well, and their escaping from the well due to the thermal motion constitutes the vapor pressure of the condensed phase.

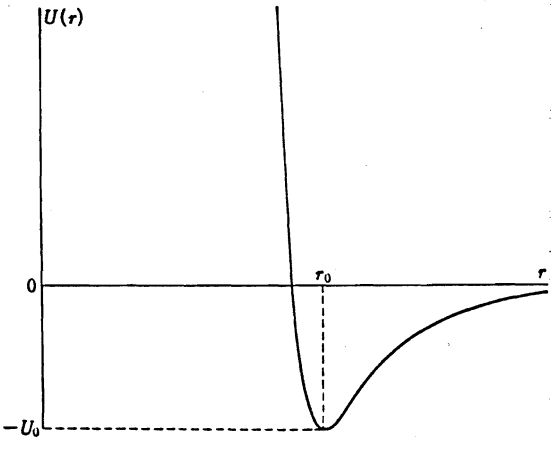

Fig. 2.1 Intermolecular potential for a rare gas $U(r)=U_0[(r_0/r)^{12}-2(r_0/r)^6]$.

The intermolecular potential is due to an attraction force of various origins and a repulsive force. Attractive force is caused by interactions among permanent and induced electric charges, dipoles, quadrapoles, etc. Whereas, repulsive force comes from overlapping of outer electron orbits of molecules. An example is the Lenard-Jones potential (see Fig. 2.1), and for this particular potential, the range of interaction is about a few molecular diameters. Potential that develops among electric charges reaches deeper.

For complex molecules, the potential depends on the orientation of molecules and the additivity does not necessarily hold. For application to water molecules, potential proposed by Stillinger and Rahman is known.

2.2 Property Distribution under Thermal Equilibrium

Heat is a random form of energy, and under thermal equilibrium, thermodynamic quantities of seemingly uniform value actually deviate in molecular scale in space and time. Only the average of the molecular distribution corresponds to a thermodynamic value.

Historically, J.C. Maxwell (1859) first obtained the velocity distribution of gas. Later, L. Boltzmann (1868) generalized it to the probability distribution of molecular states under thermal equilibrium. Let us call it thermal ensemble.[1]

The distribution of energy (kinetic only) in an ideal gas is given by (see Appendix A),

$$\frac{dn}{N} = \frac{2\epsilon^{1/2}}{\sqrt{\pi}(kT)^{3/2}} e^{-\epsilon/kT}\, d\epsilon, \tag{A.8}$$

where dn is the number of gas molecules whose momenta are between p_x and p_x+dp_x, p_y and p_y+dp_y, and p_z and p_z+dp_z or energies between ϵ and $\epsilon+d\epsilon$ and N the total number of molecules. This is known as Boltzmann's distribution of energy. For molecular velocity,

$$\frac{dn}{N} = \left(\frac{2}{\pi}\right)^{1/2} \left(\frac{m}{kT}\right)^{3/2} e^{-\frac{1}{2}\frac{mv^2}{kT}} v^2\, dv, \tag{A.12}$$

where m is the molecular mass and v the velocity. It is called Maxwell's law of velocity distribution.

If a unit volume is taken for the system, n and N correspond to concentration or density. Then, the probability of finding molecules with energy ϵ_i is

$$\frac{n_i}{N} = \frac{\epsilon_i^{1/2} e^{-\epsilon_i/kT}}{\sum \epsilon_i^{1/2} e^{-\epsilon_i/kT}} = \frac{\epsilon_i^{1/2} e^{-\epsilon_i/kT}}{f}, \tag{2.0}$$

where n_i and ϵ_i are the number and the energy of i identical molecules and f the partition function (this is a new partition function and different from the conventional one). This is to say that the probability of finding a microscopic state of molecules is solely determined by its energy level and temperature. The probability is proportional to the factor, $\epsilon_i^{1/2}\exp(-\epsilon_i/kT)$,[1'] instead of the commonly practiced Boltzmann factor, $\exp(-\epsilon_i/kT)$.

2.3 Mean Free Path

The distance a molecule flies between two consecutive collisions is called the free path, and its average value plays a role in a simple theory of molecular transport processes. Therefore, we shall estimate it in a simplified manner below. The concept involved in the collision process will apply, with some refinements, to coagulation of aerosols, collision-coalescence of cloud droplets, and ice crystal riming and aggregation.

Suppose molecules of identical mass and size flying at an average speed of v. A molecular collision will occur when a molecule comes within 2r distance

---

[1] A term called canonical ensemble, said to be due to Gibbs, has been commonly used, but it contains a historical and fundamental misconception. The grand canonical ensemble concept, also due to Gibbs, describes only systems without surfaces and it cannot apply to the cluster system. So, we refrain from using them here.

[1'] Due to momentum distribution interpreted as a function of energy in three dimensions.

from the line of flight of another molecule, where r is the radius of the molecules. In time t, the molecule flies a distance vt. During the time, it sweeps a collision volume of $4\pi r^2 vt$. Denoting the number concentration of the molecules by n, the total number of molecules in the collision volume is expressed as $4\pi r^2 vtn$. Hence, the mean free path

$$\ell = \frac{vt}{(4\pi r^2 vtn)} = \frac{1}{4\pi r^2 n}. \tag{2.1}$$

However, Eq. (2.1) overestimates the length of the mean free path by assuming that all the molecules but one in question (the one flying) are at rest. In real gas, the moving molecule in question is hit from the side, front, and rear, making the ℓ value smaller. A more rigorous treatment gives (Chapman and Cowling, 1970)

$$\ell = \frac{1}{4\sqrt{2}\pi r^2 n}. \tag{2.2}$$

For a binary gas mixture of species 1 and 2, the mean free path of the species 1 is given as (Chapman and Cowling, 1970)

$$\ell_1 = \left[4\sqrt{2}\pi n_1 r_1^2 + 4\pi n_2 (r_1 + r_2)^2 \left[1 + \frac{m_1}{m_2} \right]^{1/2} \right]^{-1}. \tag{2.3}$$

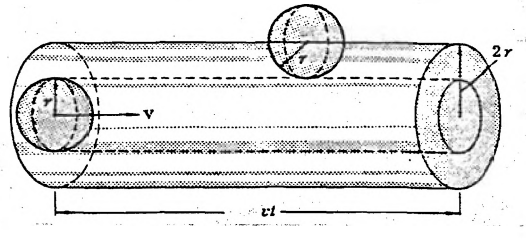

Fig. 2.2 Sweeping volume of a flying molecule.

2.4 Transport Processes and Transport Constants

Consider a system consisting of molecules carrying an average characteristic property Q. The characteristic property can be mass, momemtum, or kinetic energy. The flying molecules carry the property in the x-direction

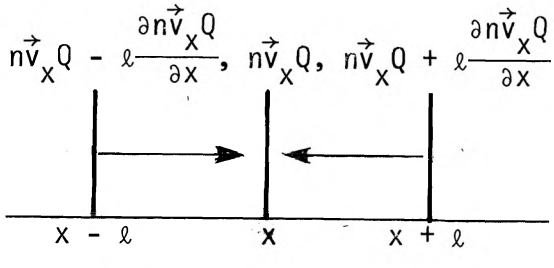

Fig. 2.3 Distribution of the $n\vec{v}_x Q$ and the transport through the distance ℓ.

across a unit area. Since both $\vec{v}_x$ component and $\overleftarrow{v}_x$ component of velocity are assigned to n molecules, they both carry the property Q, where $\vec{v}_x$ is the average molecular velocity in positive x-direction and $\overleftarrow{v}_x$ in the negative x-direction.

Hence, Q transportation from left to right is

$$n\vec{v}_x Q - \ell \frac{\partial n\vec{v}_x Q}{\partial x},$$

and from right to left,

$$n\overleftarrow{v}_x Q + \ell \frac{\partial n\overleftarrow{v}_x Q}{\partial x}.$$

Observing that $\overleftarrow{v}_x = -\vec{v}_x$, the net rate of Q transport toward right is

$$F_Q = -2\ell \frac{\partial n\vec{v}_x Q}{\partial x} = -\frac{1}{2}\ell \nabla n\bar{v}Q, \qquad (2.4)^2$$

where $\vec{v}_x = \frac{1}{4}\bar{v}$ (Eq. A.24), and

$$\nabla = i\frac{\partial}{\partial x} + j\frac{\partial}{\partial y} + k\frac{\partial}{\partial z}, \qquad (2.5)$$

and i,j,k being respective unit vectors. This case, $\nabla = i\frac{\partial}{\partial x}$.

Note the relationships among various velocities are (see Appendix A);

$(\bar{v}^2)^{1/2} = \sqrt{\frac{3kT}{m}}$ (1.78), $\bar{v} = \sqrt{\frac{8kT}{\pi m}}$ (A.16), $v_x = \sqrt{\frac{2kT}{\pi m}}$ (A.22),

$\vec{v}_x = \sqrt{\frac{kT}{2\pi m}}$ (A.23), and $\bar{v} = 2\bar{v}_x = 4\vec{v}_x$ (A.24).

($\vec{v}_x$ includes the effect of number concentration and this is why $\bar{v}_x = 2\vec{v}_x$.)

We now estimate fluxes of quantities basic to the cloud physical processes below.

Flux densities for ideal gas

Mass flux density: Q = m

The mass flux density may be obtained by replacing Q in Eq. (2.4) with m

---

[2] Note a factor ⅛ is sometimes used erroneously instead of ½ (Moelwyn Hughes, 1957). This view is also supported by Chapman and Cowling (1970).

$$F_m = -2\ell\nabla(nm\vec{v}_x) \quad \text{(general expression)}$$
$$= -\tfrac{1}{2}\ell\bar{v}(\nabla\rho + \tfrac{1}{2}\rho\nabla\ln T). \qquad (2.6)^3$$

From Eq. (2.6), it is clear that the mass flux results, not only from the density gradient, but from the temperature gradient, the latter involving so-called "Soret effect" (Soret, 1879-1881).

Momentum flux density: $Q = m\bar{v}$

The momentum flux density which describes the momentum transfer, or viscous effect, may be obtained by replacing Q with $m\bar{v}$

$$F_{mv} = -\tfrac{1}{2}\ell\nabla(nm\bar{v}^2)$$
$$= -\tfrac{3}{2}\ell\nabla p. \qquad (2.7)^4$$

The momentum flux is thus proportional to pressure gradient.

Internal energy flux density (heat): $Q = \tfrac{1}{2}jkT = \tfrac{j}{6}m\bar{v}^2$

Under steady heat conduction through the air, due to no continuing volume expansion, the heat flow carries the internal energy. The heat flux density may therefore be expressed by replacing Q in Eq. (2.4) with the internal energy

$$F_q = -\tfrac{1}{2}\ell\nabla\left(nm\bar{v}\cdot\tfrac{j}{6}\bar{v}^2\right) \quad (j;\ \text{number of degrees of freedom})$$
$$= -\tfrac{j}{8}\ell\bar{v}R\rho(\nabla T + 2T\nabla\ln p). \qquad (2.8)^5$$

The heat flux is thus a function of gradients of pressure p and temperature T, the former involving "diffusion thermoeffect" or "Dufour effect" (Dufour, 1873).

---

3 $nm = \rho,\ \bar{v} = \sqrt{\frac{8kT}{\pi m}}$ (A.16)

$$\nabla(nm\bar{v}) = \sqrt{\frac{8k}{\pi m}}\nabla\rho\sqrt{T} = \sqrt{\frac{8k}{\pi m}}\sqrt{T}\nabla\rho + \sqrt{\frac{8k}{\pi m}}\rho\nabla\sqrt{T} = \bar{v}\nabla\rho + \frac{\bar{v}\rho}{2}\nabla\ell nT$$

$$\left(\sqrt{\frac{8k}{\pi m}}\sqrt{T} = \bar{v} \ \text{ and } \ \nabla\sqrt{T} = \frac{1}{2}\cdot\frac{1}{\sqrt{T}}\cdot\nabla T = \frac{\sqrt{T}}{2T}\nabla T = \frac{\sqrt{T}}{2}\nabla\ell nT\right)$$

4 $\tfrac{1}{2}m\bar{v}^2 = \tfrac{3}{2}kT \qquad \bar{v}^2 = \frac{3kT}{m} = 3RT \qquad nm\bar{v}^2 = 3\rho RT = 3p \qquad (nm=\rho)$

5 $-\tfrac{1}{2}\ell\nabla\left(nm\bar{v}\cdot\tfrac{j}{6}\bar{v}^2\right) = -\tfrac{1}{12}\ell j\nabla(nm\bar{v}\bar{v}^2) \qquad \bar{v} = \sqrt{\frac{8k}{\pi m}}\sqrt{T},\ \bar{v}^2 = \frac{3kT}{m} = 3RT$

$$= -\tfrac{1}{12}\ell j\nabla\frac{p}{RT}\sqrt{\frac{8k}{\pi m}}\sqrt{T}\cdot 3RT = -\tfrac{1}{4}\ell j\sqrt{\frac{8k}{\pi m}}\nabla p\sqrt{T} = -\tfrac{1}{4}\ell j\sqrt{\frac{8k}{\pi m}}\left(p\frac{1}{2\sqrt{T}}\nabla T + \sqrt{T}\nabla p\right)$$

$$= -\tfrac{1}{4}\ell j\sqrt{\frac{8k}{\pi m}}\frac{\sqrt{T}p}{2T}\left(\nabla T + \frac{2T}{p}\nabla p\right) = -\tfrac{1}{8}\ell j\rho R\bar{v}(\nabla T + 2T\nabla\ell np)$$

$$\left(\sqrt{\frac{8k}{\pi m}}\sqrt{T} = \bar{v} \ \text{ and } \ \frac{p}{T} = \rho R\right)$$

Heat conduction and thermal conductivity

We now proceed to estimate the heat flux under no mass flux, i.e., Eq. (2.6) = 0, or converting ln ρ to ln p using $p = \rho RT$

$$\nabla(\ln p) = \tfrac{1}{2}\nabla(\ln T). \tag{2.9}$$

Using Eq. (2.9) in Eq. (2.8) to eliminate ∇ (ln p), i.e.,

$$F_q = -\tfrac{1}{4} j \ell \bar{v} R \rho \nabla T$$

and recalling that

$$c_v = \tfrac{1}{2} jR$$

one obtains

$$F_q = -\tfrac{1}{2} \ell \bar{v} \rho c_v \nabla T. \tag{2.10}$$

Since the ratio of heat flux density to the temperature gradient defines the thermal conductivity, K, under no mass flux (Fourier's law of heat conduction)

$$F_q = -K \nabla T, \tag{2.11}$$

and from Eq. (2.10), we have

$$K = \tfrac{1}{2} \ell \bar{v} \rho c_v, \tag{2.12}$$

or using Eq. (2.2)

$$K = \frac{m c_v \bar{v}}{8\sqrt{2}\pi r^2}. \tag{2.13}^{6}$$

Thermal conductivity of air, Sutherland's formula

From Eq. (2.13), the thermal conductivity $K \propto \bar{v}/r^2$. Since $\bar{v} \propto \sqrt{T}$ and the effective radius varies according to the empirical relation,

$$r^2 = r_\infty^2 \left[1 + \frac{C}{T}\right],$$

where r_∞ is r at $T = \infty$, and C a constant,

$$\frac{K}{K_o} = \frac{T_o + C}{T + C} \left(\frac{T}{T_o}\right)^{1\frac{1}{2}}, \quad \text{(Sutherland's formula)} \tag{2.14}$$

is C = 398 K for air, and K_o is K at T = 273.15 K. It is important to note that $K = f(T) \neq f(p)$. Unit of K is J/(m s K).

For air in the temperature range between −20 and +40°C, $K \propto T^{1.80}$.

---

[6] For rigid spheres, $K \propto T^{1/2}$ due to $\bar{v} \propto T^{1/2}$.

Shear stress and dynamic viscosity

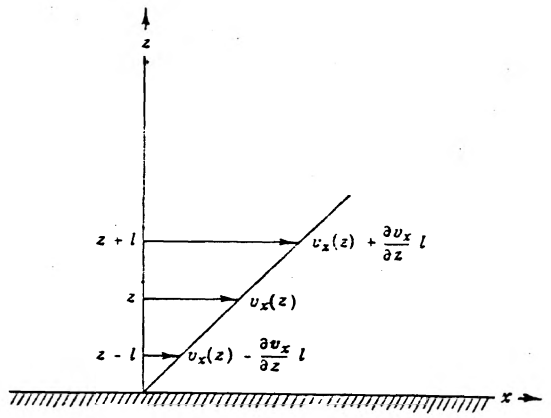

Under vertical shear of x-component of velocity (linearly varying, see the Fig. 2.4), the time rate change of x-component of momentum or force per unit area may be expressed by Eq. (2.4) with mv_x

Fig. 2.4 Velocity profile $[v_x(z)]$ for the case of linear shear.

$$F_{(mv_x)_z} = -\frac{1}{2} nm\bar{v}\ell \frac{\partial v_x}{\partial z}$$
$$= -\frac{1}{2}\rho\bar{v}\ell \frac{\partial v_x}{\partial z}. \qquad (2.15)$$

On the other hand, viscosity is defined in relation with viscous force as

$$F_{(mv_x)_z} = -\eta \frac{\partial v_x}{\partial z}, \qquad (2.16)$$

where η is called viscosity coefficient or (dynamic) viscosity.

Equating Eq. (2.15) with Eq. (2.16) and replacing Eq. (A.16), we obtain

$$\eta = \frac{1}{2}\rho\bar{v}\ell = \frac{1}{4\pi r^2}\left(\frac{mkT}{\pi}\right)^{1/2}. \qquad (2.17)$$

Thus, for the same reason as K, $\eta \neq f(p)$; and the temperature dependency of η is given by an equation similar to Eq. (2.14)

Unit of η; poise = 1 dyne s/cm^2 = 1 g (cm s)$^{-1}$ = 10^{-1} kg (m s)$^{-1}$

Diffusion and diffusivity (diffusion coefficient)

The diffusion of water molecules always takes place when cloud droplets and ice crystals grow or evaporate in the air environment. We first look into the self diffusion process, i.e., diffusion of water molecules through themselves.

Diffusion flux density of water vapor may be expressed by Eq. (2.6)

$$F_v = -\frac{1}{2}\ell\bar{v}\left[\nabla\rho + \frac{1}{2}\rho\nabla(\ln T)\right] \quad (\ell, \bar{v}, \rho \text{ for water vapor})$$
$$= -\frac{1}{2}\frac{\ell_v\bar{v}_v}{R_vT}\left[\nabla e - \frac{1}{2}e\nabla(\ln T)\right], \qquad (2.18)$$

where the subscript v stands for water vapor. The second term of Eq. (2.18) amounts 2-3% of the first term for saturated vapor (Soret effect).[7]

Since the diffusivity of water vapor is defined by Fick's first law of diffusion,

$$F_v = - D\nabla\rho_v, \tag{2.19}$$

where D is the self-diffusion coefficient (diffusivity) of water vapor. Then, from Eq. (2.18) under constant temperature and Eq. (2.19), we have

$$D = \tfrac{1}{2}\ell_v\bar{v}_v. \tag{2.20}$$

Equation Eq. (2.20) is a self-diffusion equation. Using Eq. (2.2) and $\bar{v}$ expression in Appendix A

$$D = \frac{1}{4\pi r^2 n}\left(\frac{kT}{\pi m}\right)^{1/2}, \tag{2.21}$$

and for gases in general, since $n = \rho/m$ and $\rho = p/RT$ and $D \propto f(T)/p$. Thus, D increases as the pressure drops. In reality, the power of T is larger than 1.5 due to r^2 term contribution. D unit is cm^2/s or m^2/s

Mutual diffusivity of air and water vapor

For air-water vapor system, assuming that molecules are rigid elastic spheres, the mutual diffusion coefficient may be expressed as (Chapman and Cowling, 1970)

$$D_{1,2} = \frac{3}{8}\frac{k}{d_{1,2}^2}\left(\frac{R_a + R_w}{2\pi}\right)^{1/2}\frac{T^{1.5}}{p}, \tag{2.22}$$

where $d_{1,2} = (d_1 + d_2)/2$. $D_{1,2} \propto T^{1.94}$ (Pruppacher and Klett, 1978).

Relationship among transport constants (single component gas)

Using Eqs. (2.12) and (2.17),

$$K = \eta c_v. \tag{2.23}$$

From Eqs. (2.17) and (2.20),

$$D\rho = \eta. \tag{2.24}$$

---

7 $\dfrac{\nabla e}{\frac{1}{2}e\nabla(\ell nT)} = \dfrac{de}{\frac{1}{2}ed(\ell nT)}$. From Eq. (1.63), since in cloud physics, T and e are coupled at droplet surface,

$$\frac{de_s}{dT} = \frac{L}{T\alpha} = \frac{e_s L}{R_w T^2}\left[\times 1/\left(\frac{e_s}{2T}\right)\right] \rightarrow \frac{de_s}{\frac{1}{2}e_s d\ell nT} = \frac{2L}{R_w T}.$$

At 20°C for water, the ratio is 1/0.0276; -30°C ice, it is 1/0.0198.

Hence,

$$D = K/\rho c_v. \tag{2.25}$$

D may be compared with the thermal diffusivity

$$\kappa = K/\rho c_p, \tag{2.31}$$

to give

$$D/\kappa = c_p/c_v. \tag{2.26}$$

κ applied to transient or non-steady state process of heat conduction where air continues to expand due to the increased temperature under the given pressure.

Equations (2.23), (2.24) and (2.25) are applicable for low pressure gases and deviate when the pressure is high.

Molecular diffusion and heat conduction equations

Continuity equation

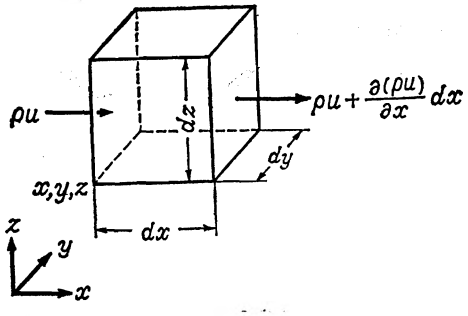

Fig. 2.5 Mass flow economy in the x-direction of the elementary volume, dx dy dz.

The accumulation of mass due to the flow of density ρ in the x-direction is

$$\rho u dydz - \left[\rho u + \frac{\partial(\rho u)}{\partial x}dx\right]dydz = -\frac{\partial(\rho u)}{\partial x}dxdydz.$$

Considering the accumulation in y- and z-direction flows, we have

$$\frac{\partial \rho}{\partial t}dxdydz = -\left[\frac{\partial(\rho u)}{\partial x} + \frac{\partial(\rho v)}{\partial y} + \frac{\partial(\rho w)}{\partial z}\right]dxdydz,$$

or the continuity equation

$$\frac{\partial \rho}{\partial t} + \frac{\partial(\rho u)}{\partial x} + \frac{\partial(\rho v)}{\partial y} + \frac{\partial(\rho w)}{\partial z} = 0. \tag{2.26'}$$

For incompressible fluid,

$$\frac{\partial u}{\partial x} + \frac{\partial v}{\partial y} + \frac{\partial w}{\partial z} = 0. \tag{2.26''}$$

Transport of conservative property

When F_Q alone is responsible for the time variation of conservative property Q in a unit volume of open system,

$$\frac{\partial(nQ)}{\partial t} = -\nabla \cdot F_Q. \tag{2.27}^8$$

For a closed system, since n remains constant,

$$n\frac{\partial Q}{\partial t} = -\nabla \cdot F_Q. \tag{2.28}$$

Convective transport

If convective motion of air further carries F_Q, a term

---

8 $\nabla \cdot F_Q$ is the scalar product of ∇ and a vector F_Q or $\partial F_{Qx}/\partial x + \partial F_{Qy}/\partial y + \partial F_{Qz}/\partial z$.

$$-\left(u\frac{\partial nQ}{\partial x} + v\frac{\partial nQ}{\partial y} + w\frac{\partial nQ}{\partial z}\right)$$

where u, v, and w are x, y, and z components of velocity, can be added to Eq. (2.27) or Eq. (2.28). Such an equation may be called a convective diffusion (or conduction) equation.

For water vapor diffusion without simultaneous heat conduction, $nQ = \rho_v$; and using Eq. (2.19) in Eq. (2.27), we have

$$\frac{\partial \rho_v}{\partial t} = \nabla\cdot(D\nabla\rho_v)(+ \text{ sources or sinks, if they exist}).$$

For isotropic diffusion without sources and sinks,

$$\frac{\partial \rho_v}{\partial t} = D\nabla^2\rho_v$$

where

$$\left[\nabla^2 = \frac{\partial^2}{\partial x^2} + \frac{\partial^2}{\partial y^2} + \frac{\partial^2}{\partial z^2}\right] \text{(Laplacian)}.^9 \tag{2.29}$$

For non-steady heat conduction under constant pressure, expansion of air accompanies (see Fig 2.5). Then, from Eq. (1.46), $dh = dq = c_p dT$. Then, inserting $mc_pT = Q$ into Eq. (2.28) with Eq. (2.11),

$$\frac{\partial T}{\partial t} = \frac{K}{\rho_a c_p}\nabla^2 T, \tag{2.30}$$

where

$$\frac{K}{\rho_a c_p} = \kappa \tag{2.31}$$

is the thermal diffusivity[10], with dimension of m^2/s, and plays an identical role as D in the diffusion of mass. κ is thus involved in transient (non-steady state) phenomena.

Under steady state, since the property involved in the transportation at an arbitrary space point does not change with time, Eqs. (2.29) and (2.30) become

$$\nabla^2 T = \nabla^2 \rho = 0. \tag{2.32}$$

Transport processes in free molecule regime

When the distance involved in the transport process is much shorter than the mean free path, the molecular transfer process takes place without collisions, and the process is said to be in the free molecule regime.

Applying a concept similar to that described above, the free molecular flux density of mass may be expressed as (1, left; and 2, right)

---

[9] For the spherical coordinate, see Appendix B.

[10] Diffusivity was used by Kelvin and thermometric conductivity by Maxwell (Carslaw and Jaeger, 1959).

$$F_{fm} = n_1 m_1 \vec{v}_x + n_2 m_2 \overleftarrow{v}_x = -\sqrt{\frac{R_v T}{2\pi}}(\rho_2 - \rho_1). \tag{2.33}$$

Similarly, the free molecular flux density of heat without mass transfer may be expressed as

$$\begin{aligned} F_{fq} &= n\vec{v}_x\left(\tfrac{1}{2}jkT_1\right) + n\overleftarrow{v}_x\left(\tfrac{1}{2}jkT_2\right) \\ &= -\frac{c_v p(T_2 - T_1)}{(2\pi R_a T)^{1/2}}. \end{aligned} \tag{2.34}$$

It is said that because of a larger contribution from faster and hotter molecules, instead of c_v, $(c_v + \frac{1}{2}R_a)$ describes the process better.

2.5 Accommodation coefficients

When properties, such as mass, momentum, or heat are to be transferred across the boundaries between the gaseous phase and walls or condensed phases, inefficiencies normally appear.

Momentum accommodation and slip flow (Chapman and Cowling, 1970)

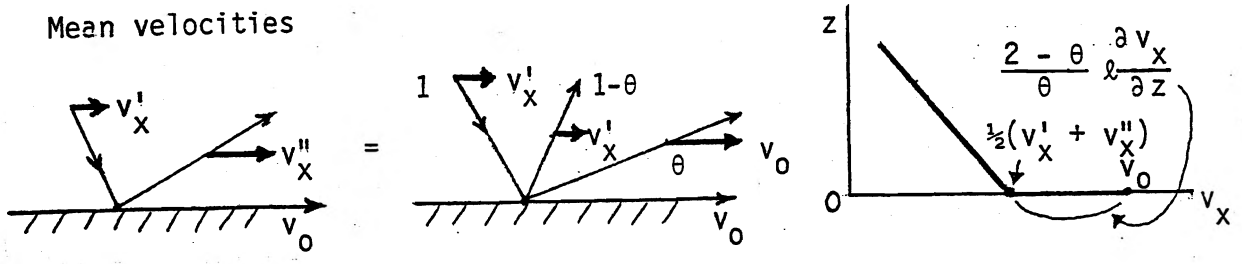

Let v_x' and v_x'' denote the mean x-velocites of molecules before striking and just after leaving the wall that is moving with the velocity v_o. Then, the average x-velocity of the gas at the wall is $\frac{1}{2}(v_x' + v_x'')$. This can be interpreted as some of the molecules hitting the moving wall, leave (θ proportion) it with the velocity of the wall, and the mean x-velocity is equal to the wall velocity v_o. The remainder $(1 - \theta)$ is reflected elastically. Therefore, v_x'' (leaving) is given by the weighted sum of v_x' and v_o, i.e.,

$$v_x'' = (1 - \theta)\, v_x' + \theta v_o. \tag{2.35}$$

Then the difference between v_x' at the mean free path distance away from the wall and the average at the wall $\frac{1}{2}(v_x' + v_x'')$ is given as

$$v_x' - \tfrac{1}{2}(v_x' + v_x'') = \ell(\partial v_x/\partial z). \tag{2.36}$$

From Eqs. (2.35) and (2.36)

$$\tfrac{1}{2}(v_x' + v_x'') = v_o + \frac{2-\theta}{\theta}\,\ell\,\frac{\partial v_x}{\partial z}. \qquad (2.37)^{11}$$

(Thermal) accommodation coefficient, α

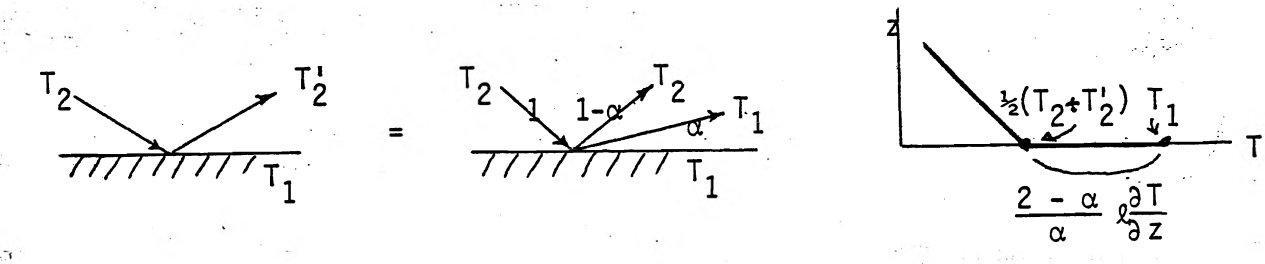

Similarly to what applied above,

$$T_2' = (1-\alpha)T_2 + \alpha T_1 \quad \text{or} \quad \alpha = \frac{T_2 - T_2'}{T_2 - T_1}. \qquad (2.38)$$

Condensation coefficient, β[12] and deposition coefficient, γ

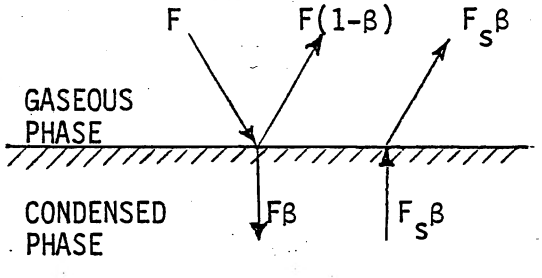

$F = F_s$: equilibrium

$F > F_s$: condensation

$F < F_s$: evaporation

Suppose a vapor flux condenses across the interface between the air and the condensed phase. Under equilibrium, the condensing flux $F\beta$ matches the evaporating flux $F_s\beta$, where β is the condensation coefficient. Under that

---

[11] Setting $v_x' + v_x'' = x$,

$$\left.\begin{aligned}(2.35) &\rightarrow x - v_x' = (1-\theta)v_x' + \theta v_o \\ (2.36) &\rightarrow v_x' = \tfrac{1}{2}x + \ell\frac{\partial v_x}{\partial z}\end{aligned}\right\} \xrightarrow[v_x]{\text{eliminating}} \tfrac{1}{2}x = \frac{(2-\theta)}{\theta}\,\ell\,\frac{\partial v_x}{\partial z} + v_o \text{----(2.37)}$$

[12] Just above the surface, the average water vapor density

$\frac{1}{2}x = \frac{1}{2}[\rho + \rho(1-\beta) + \rho_s\beta]$. Then,

$\rho - \frac{1}{2}x = \ell\frac{\partial \rho}{\partial z}$ (incoming).

Eliminating ρ from these equations, $\frac{1}{2}x - \rho_s = \frac{(2-\beta)}{\beta}\,\ell\,\frac{\partial \rho}{\partial z}$.

condition, the flux F arriving at the interface from the gaseous phase equals the saturation vapor flux (pressure) of the condensed phase F_s. Whenever the condition shifts from equilibrium, $(F - F_s)\beta$ controls the net flux instead of $(F - F_s)$.

Table 2.1 Condensation coefficient for water (Pruppacher and Klett, 1978).

(a)

Evaporation From A Quasi-Quiescent Water Surface

OBSERVER	TEMPERATURE (°C)	β
Alty (1931)	18 to 60	0.006 to 0.016
Alty and Nicholl (1931)	18 to 60	0.01 to 0.02
Alty (1933)	−8 to +4	0.04
Alty and Mackay (1935)	15	0.036
Baramaev (1939)	–	0.033
Pruger (1940	100	0.02
Yamamoto and Miura (1949)	–	0.023
Hammeke and Kappler (1953)	20	0.045
Delaney *et al.* (1964)	0 to 43	0.0415
Kiriukhin and Plaude (1965)	7	0.019
Chodes *et al.* (1974)	20	0.033
Rogers and Squires (1974)	–	0.065
Narusawa and Springer (1975)	18 to 27	0.038
Sinarwalla *et al.* (1975)	22.5 to 25.7	0.026

Table 2.1 Continued.

(b)

Evaporation From A Rapidly Renewing Water Surface

OBSERVER	TEMPERATURE (°C)	β
Hickman (1954)	0	0.42
Berman (1961)	–	1.0
Nabavian and Bromley (1963)	10 to 50	0.35 to 1.0
Jamieson (1965)	0 to 70	0.35
Mills and Seban (1967)	7 to 10	0.45 to 1.0
Tamir and Hasson (1971)	50	0.20
Narusawa and Springer (1975)	18 to 27	0.18

Deposition coefficient, γ, is the same as condensation coefficient, except that the solid phase is involved instead of liquid phase. γ is the result of integral effect of all the surface processes involved in the vapor transfer, such as landing, migration, two-dimensional nucleation, and leaving the surface.

Table 2.2 Deposition coefficient for ice (Pruppacher and Klett, 1978).

Observer	Temperature (°C)	γ
Delaney *et al.* (1964)	−2 to −13	0.014
Vulfson and Levin (1965)	−6 to −7	0.04
Vulfson and Levin (1965)	−10 to −11	0.7
Fukuta and Armstrong (1974)	−25	0.12
Davy and Somorjai (1971)	−45	0.36
Kramers and Stemerding (1951)	−40 to −60	0.93
Tschudin (1945)	−60 to −85	0.94
Davy and Somorjai (1971)	−85	1.0
Koros *et al.* (1966)	−115 to −140	0.83

2.6 Relaxation of Transient Processes

In many material phenomena, against a sudden change the response takes place towards an equilibrium or a steady state. If the time rate of change of a property Q is proportional to the property difference in the form

$$\frac{dQ}{dt} = A - BQ, \tag{2.39}$$

where A and B are constants and $Q = 0$ at time $t = 0$, the solution of this differential equation may be readily obtained by the method of separation of variables as

$$Q = \frac{A}{B}\left(1 - e^{-Bt}\right), \tag{2.40}$$

where

$$\tau = 1/B, \tag{2.41}$$

is called the relaxation time. Then, the ratio of the Q difference at $t = \tau$ and that at $t = 0$ may be obtained as

$$\frac{Q_\infty - Q_\tau}{Q_\infty} = e^{-t/\tau} = 1/e = 0.368, \tag{2.42}$$

where Q_τ is Q at $t = \tau$. This is to say that in the period τ, the difference in Q becomes e^{-1} of the initial value. Half of the initial value is reached more quickly at $t = 0.693\tau$.

In a transport phenomenon such as heat conduction without involving advective or radiative transfer, source or sink,

$$\frac{\partial T}{\partial t} = \kappa \nabla^2 T. \tag{2.30}$$

If a sudden conduction takes place from the surface of a semi-infinite body into the quiescent, isotropic medium of uniform temperature in contact under an initial temperature difference $(\Delta T)_0$,

$$\frac{(\Delta T)_0 - (\Delta T)}{(\Delta T)_0} = \text{erfc}\left[\frac{x}{2\sqrt{\kappa t}}\right], \tag{2.43}$$

(Carslaw and Jaeger, 1959), where subscript 0 stands for t = 0, erfc the complimentary error function, and x the distance from the surface. Then, one can define another relaxation time for this transport process

$$\tau_T = \frac{x^2}{\kappa}. \tag{2.44}$$

At $t = \tau_T$, the above equation gives

$$\frac{(\Delta T)_0 - (\Delta T)}{(\Delta T)_0} = \text{erfc}\,(1/2) = 0.480,$$

which is close to the half value. The true half value corresponds to $t = 0.954\ \tau_T$.

2.7 Radiative Heat Transfer

Thermal radiation continuously leaves the surface of a body as long as it is warmer than 0 K. In relation with the incident radiative energy, the fraction that reflects is called reflectivity ρ, the one that is absorbed is called absorptivity α, and the one that passes through is called transmissivity τ. So

$$\rho + \alpha + \tau = 1.$$

For non-transparent body, $\tau = 0$ or

$$\rho + \alpha = 1.$$

The ratio between the emitted energy and the incident one is called emissivity ϵ and $\epsilon = \alpha$. Since shiny metals reflect radiation, their emissivities are low. For most of the non-metallic materials, $\epsilon \simeq 0.8$. For water and ice, ϵ is probably around 0.95 in the range of atmospheric temperatures.

Stefan-Boltzmann's law

The radiation flux density emitted by a blackbody is given by Stefan-Boltzmann's law

$$F = \sigma T^4, \tag{2.45}$$

where σ is the Stefan-Boltzmann constant; and

$$\sigma = 5.67032 \times 10^{-8}\ \text{J s}^{-1}\text{m}^{-2}\text{K}^{-4}.$$

For heat transfer from a surface, in addition to considering the above factors, both incident and reflected energies on all the surfaces involved, the solid angles and angles from the surfaces have to be considered. For the intensity of radiation energy coming out of a flat surface, the Lambert cosine law applies for blackbody ($\epsilon = \alpha = 1$)

$$I_\theta = I_n \cos\theta, \tag{2.46}$$

where I_θ and I_n are radiation intensities at an angle θ (from the normal line) and on the normal line, respectively.

CHAPTER 3 MOTIONS OF ATMOSPHERIC PARTICLES

One of the outstanding features of the aerodisperse system is the large density difference between the air medium and the dispersed particles, which leads to their relative motions under the existing gravitional field. Particles interact with each other under the moving or quiescent air medium. In this chapter, we look into fundamental processes that describe motions of atmospheric particles.

3.1 Knudsen Number

When the size of atmospheric particles reaches the length of the mean free path, the dynamic behaviors of the particles change. The extent of this effect is a function of the Knudsen number:

$$K_n = \ell/r, \tag{3.1}$$

where ℓ is the mean free path length of the air molecules and r the radius of the particle.

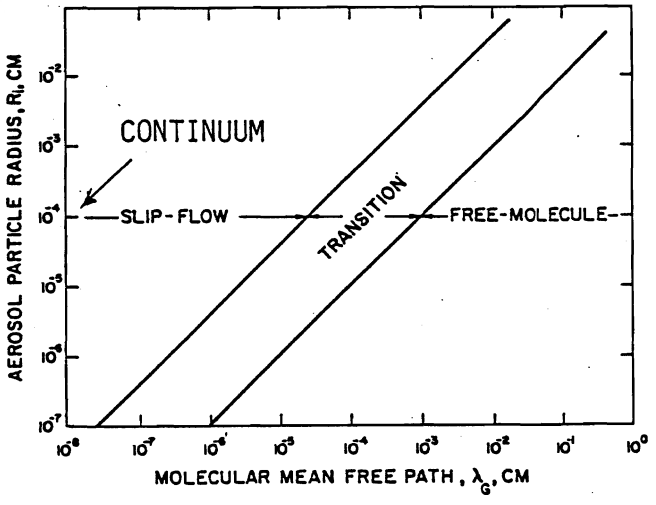

Fig. 3.1 Ranges of gas dynamic behavior for aerosol particles in terms of radius and mean free path (Hidy and Brock, 1970).

3.2 The Navier-Stokes Equation

The motion of fluid medium, e.g., the air flow around a falling particle, can be derived from Newton's second law: the product of mass and acceleration is equal to the sum of external forces. Considering the fluid in an elementary volume of dxdydz, the products in x, y, and z direction are, respectively,

$$\rho_a \frac{Du}{Dt} dxdydz, \quad \rho_a \frac{Dv}{Dt} dxdydz, \quad \text{and} \quad \rho_a \frac{Dw}{Dt} dxdydz,$$

where

$$\frac{D}{Dt} = \frac{\partial}{\partial t} + u\frac{\partial}{\partial x} + v\frac{\partial}{\partial y} + w\frac{\partial}{\partial z}. \tag{3.2}$$

The operation of Eq. (3.2) is called Lagrangian differentiation.

For external forces acting, the force proportional to the fluid mass and that which acts at the fluid boundary normally have to be considered. The former may be expressed as

$$\rho_a f_x dxdydz, \quad \rho_a f_y dxdydz, \quad \text{and} \quad \rho_a f_z dxdydz,$$

where f_x, f_y, and f_z are x, y, and z components of acceleration based on the force acting on the fluid. The force acting on dydz plane in the x-direction is $\left(\frac{\partial p_x}{\partial x}dx\right)dydz$. Considering also y and z directions, the force acting at the fluid boundary may be expressed as

$$\left(\frac{\partial p_x}{\partial x} + \frac{\partial p_y}{\partial y} + \frac{\partial p_z}{\partial z}\right)dxdydz.$$

For the Newtonian fluid, Eq. (2.16) of incompressible nature and constant viscosity, the term in this bracket is expressed as

$$\frac{\partial p_x}{\partial x} = -\frac{\partial p}{\partial x} + \eta\nabla^2 u, \quad ---, \quad ---,$$

where p is the static pressure.

Combining all these terms, we have the Navier-Stokes equation (in x-direction)

$$\frac{Du}{Dt} = f_x - \frac{\nabla p}{\rho_a} + \nu\nabla^2 u, \tag{3.3}$$

where $\nu = \eta/\rho_a$ is the kinematic viscosity, and f_z (in z-direction) corresponds to g under the gravitational force only. For the steady state, $\partial u/\partial t = 0$ should apply to Du/Dt. Furthermore, it is the normal procedure to ignore f_x unless there exist specific reasons for it. Then, Eq. (3.3) becomes

$$u\nabla u = -\frac{\nabla p}{\rho_a} + \nu\nabla^2 u. \tag{3.4}$$

3.3 Flow Around a Sphere

In Eq. (3.4), the convective acceleration term on the left-hand side and the linear viscous acceleration term, the second on the right, are of relative importance as far as the flow around a sphere is concerned. Since the former is on the order of w_∞^2/d, where d is the diameter, and the latter $\nu w_\infty/d^2$, the ratio,

$$\frac{w_\infty^2/d}{|\nu\nabla^2 w_\infty|} \simeq \frac{w_\infty d}{\nu} = Re, \tag{3.5}$$

is called the Reynolds number. The smaller the diameter of the sphere is, the smaller the Reynolds number.

Stokes approximation

When Re is small, it is immediately apparent that the term on the left-hand side of Eq. (3.4) can be ignored, which is called the Stokes approximation. Solution of the Navier-Stokes equation under this approximation gives the drag force

$$D = 6\pi\eta r w_\infty, \tag{3.6}$$

where r is the radius of the sphere (see Appendix C).

Since the non-dimensional drag coefficient is defined by the ratio of the drag to the product of cross section and dynamic pressure,

$$C_D = D/(\tfrac{1}{2}\rho_a w_\infty^2 \cdot A), \tag{3.7}$$

for a sphere of the Stokes drag,

$$C_D = \frac{24}{Re}. \tag{3.8}$$

For $Re \leq 1$, Eq. (3.8) holds well.

Oseen's approximation

The Stokes approximation creates a problem at large distance from the surface. To ease this difficulty, Oseen introduced the following approximation,

$$w\nabla w \simeq w_\infty \nabla w. \tag{3.9}$$

This approximation results in

$$C_D = \frac{24}{Re}\left[1 + \frac{3}{16}Re - \frac{19}{1280}Re^2 + \text{---}\right]. \tag{3.10}$$

Equation (3.10) describes the observed data well if $Re \leq 3$.

3.4 Settling

When a particle is at its terminal velocity of settling, the viscous resistance force is balancing with the gravitational force. Then, we have

$$w = \frac{2g(\rho_p - \rho_a)r^2}{9\eta}, \tag{3.11}$$

which is called the Stokes equation of particle settling. It is applicable where the Stokes approximation is valid.

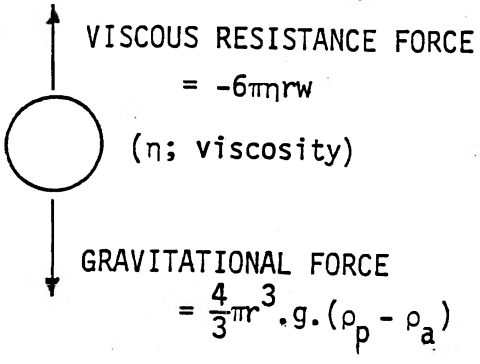

Fig. 3.2 Force balance within a particle falling at the terminal velocity.

For particles whose radii are comparable to the mean free path length, the medium is no longer considered to be continuous, and particles accelerate between collisions. Due to this "slip," w value becomes larger than that predicted by Eq. (3.11). Cunningham (1910) introduced an empirical correction for the effect so that Eq. (3.11) writes

$$w = \frac{2}{9}\frac{g(\rho_p - \rho_a)r^2}{\eta}\left[1 + \frac{A\ell}{r}\right], \qquad (3.12)$$

where A is a numerical factor near unity and called Cunningham's constant, and ρ_p the density of particle. This is, therefore, called the Stokes-Cunningham equation.

3.5 Coagulation

Particles, small relative to the mean free path, move randomly due to unbalanced molecular bombardments. This phenomenon is called the Brownian motion. The mean displacement x is expressed as

$$x^2 = 2Dt, \qquad (3.13)^1$$

where D is the diffusion coefficient of the particle. Considering the effect of small particle size or large K_n (Einstein, 1905, 1906, 1907 and Stokes-Cunningham),

$$D = kT\left[1 + \frac{A\ell}{r}\right]/6\pi\eta r. \qquad (3.14)^2$$

Due to collision caused by the Brownian motion, particles tend to coagulate.

For uniform size particles, the rate of decrease in the number concentration n, since it is doubly proportional to concentrations of both particles in collision, is expressed as

---

[1] See Appendix D.

[2] See Appendix D.

$$-\frac{dn}{dt} = Kn^2, \tag{3.15}$$

where K is the coagulation constant.[3] Upon integration, it yields

$$\frac{1}{n} - \frac{1}{n_o} = Kt, \tag{3.16}$$

where n_o is n at t = 0.

There is another way to describe the coagulation rate based on the diffusion flux of aerosol particles. Since the total flux of particles to the surface of other aerosol particle is $4\pi D(2r)(n - n_s)$,[4] where $n_s = 0$ is the particle number concentration at the aerosol particle surface and 2 r the radius of the sphere of influence, we have

$$-\frac{dn}{dt} = 4\pi D(2r)n^2. \tag{3.17}$$

For small particles, the Cunningham correction factor $(1 + AK_n)$ is needed for D.

For <u>different size particles</u>, similar to Eq. (3.17),

$$-\frac{dn_2}{dt} = 2\pi(D_1 + D_2)(r_1 + r_2)n_1n_2. \tag{3.18}$$

For D_1 and D_2, Eq. (3.14) may be applied. $2D = D_1 + D_2$.

K value varies with the nature and slightly with the weight concentration of aerosol particles. For NH_4Cl smoke, $K = 7 \times 10^{-10}$ cm^3s^{-1}; and for coagulation of Aitken nuclei, $K = 1.4 \times 10^{-9}$ cm^3s^{-1}. As can be seen from Eq. (3.14), small particles coagulate rapidly.

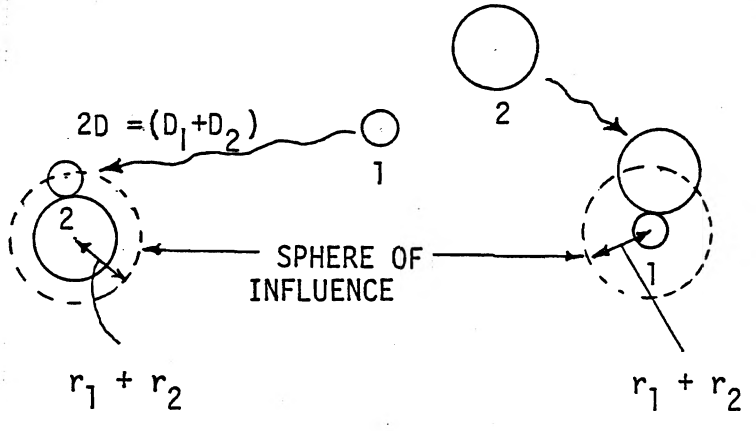

Fig. 3.3 Particle coagulation.

---

[3] Also known as coagulation kernel.

[4] See Section 5.3.

Table 3.1 Terminal velocities, w_p, and diffusion coefficients of rigid spheres of unit density in air, D, at 1013 hP_a pressure and 20°C (Green and Lane, 1964).

Diameter μm	w_p cm/s	D cm^2/s
0•1	$8•71 \times 10^{-5}$	$6•84 \times 10^{-6}$
0•2	$2•27 \times 10^{-4}$	$2•02 \times 10^{-6}$
0•4	$6•85 \times 10^{-4}$	$8•42 \times 10^{-7}$
1•0	$3•49 \times 10^{-3}$	$2•76 \times 10^{-7}$
2	$1•29 \times 10^{-2}$	$1•28 \times 10^{-7}$
4	$5•00 \times 10^{-2}$	$6•16 \times 10^{-8}$
10	$3•03 \times 10^{-1}$	$2•41 \times 10^{-8}$
20	1•20	--
40	4•71	--
100	24•7	--

3.6 Phoretic processes

Small aerosol particles move under influences of thermal and vapor density gradients and under irradiation of light. They are called thermophoresis, diffusiophoresis, and photophoresis, respectively.

Photophoresis

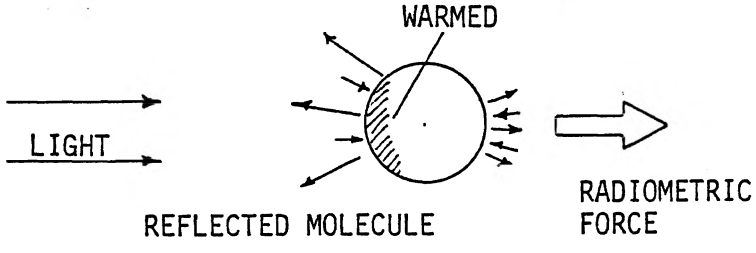

Fig. 3.4 Photophoresis.

Photophoresis is due to the gas molecules rebounding from the hotter, illuminated side of the particle with greater velocities than from the unilluminated side. The photophoretic force is

$$f_p = -\frac{\pi r^3 \alpha p}{3T}\left(\frac{dT}{dx}\right)_i, \tag{3.19}$$

where α is the thermal accommodation coefficient, and i stands for inside (Fuchs, 1964).

Thermophoresis

An aerosol particle, when placed under a temperature gradient of the gaseous medium is known to move toward the colder region like the inner wall of a fireplace. This phenomenon is called "thermophoresis." The origin of the force may be understood from the following simple treatment:

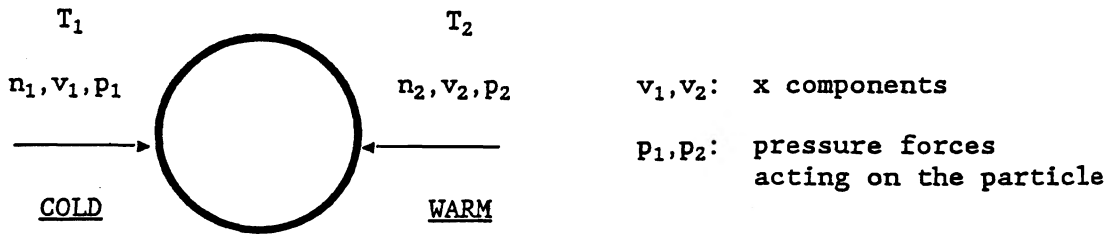

Fig. 3.5 Origin of thermophoretic force.

Since

(1) $T_1 < T_2$ and $\frac{1}{2}mv_x^2 = \frac{1}{2}kT$, $v_1 < v_2$
(2) $n_1v_1 = n_2v_2$ (no net flow of gas), and
(3) $p = nkT = nmv_x^2$,

we have

$$\frac{p_1}{p_2} = \frac{n_1mv_1^2}{n_2mv_2^2} = \frac{v_1}{v_2} < 1, \text{ or the net force is toward } T_1.$$

The general expressions for thermophoretic force and velocity in the slip-flow regime are obtained by Brock (1962):

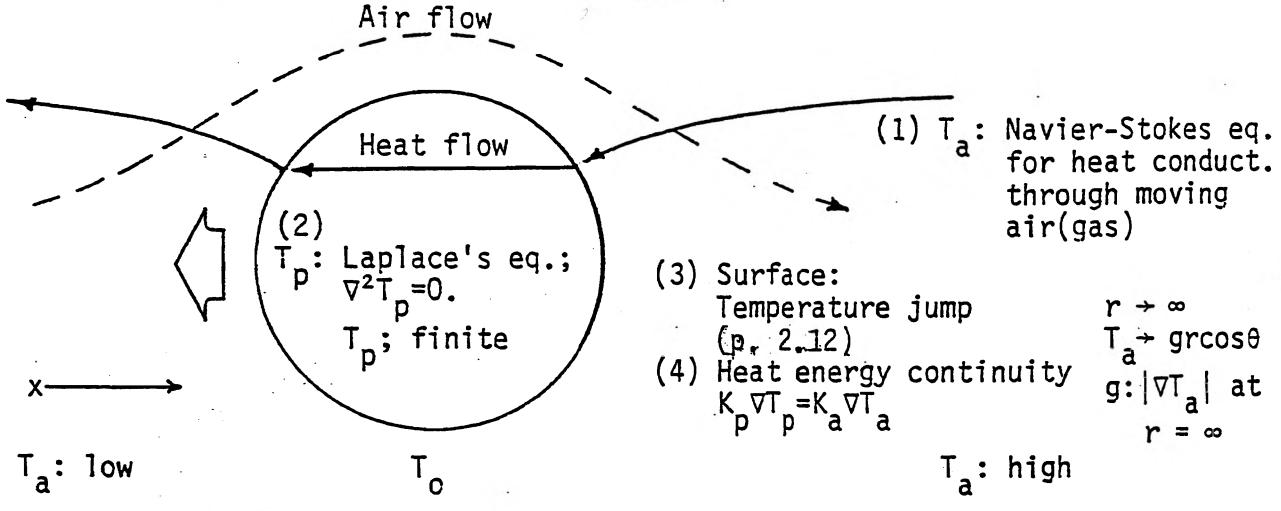

(5) $\nabla^2\vec{v} = \frac{1}{\eta}\nabla p$ (viscous resistance force balances with pressure grad.)
(6) $\nabla\vec{v} = 0$ (momentum conservation)

Fig. 3.6 Thermophoretic system.

Solving the temperature jump and integrating x-component of force due to the temperature difference over the particle surface, thermophoretic force is

$$f_T = \frac{-12\pi\eta\nu r C_s (K_a/K_p + C_t K_n)(g/T_o)}{(1 + 3C_m K_n)(1 + 2K_a/K_p + 2C_t K_n)}, \quad (0 < K_n < 0.2) \tag{3.20}$$

where $\nu = \eta/\rho_a$ is the kinematic viscosity of air, C_s, C_m, and C_t are numerical factors of order unity obtainable from kinetic theory, and $K_n = \ell/r$ is the Knudsen number, or

$$v_T = \frac{-2C_s \nu (K_a/K_p + C_t K_n)(g/T_o)}{(1 + 2C_m K_n)(1 + 2K_a/K_p + 2C_t K_n)}. \quad (0 < K_n < 0.2) \tag{3.21}$$

For the <u>continuum flow regime</u>, $K_n \to 0$ or $\ell \ll r$ (large particle)

$$f_T = \frac{-9\pi\eta\nu r g}{T_o} \frac{K_a/K_p}{(1 + 2K_a/K_p)}, \text{ (Epstein's equation, 1929)} \tag{3.22}$$

where $C_s = 3/4$ is taken; and K_a and K_p are thermal conductivities of air and particle, respectively.

For the <u>free molecule regime</u>, $K_n \to \infty$ or $\ell \gg r$, particles are small; and the force is (Waldmann, 1959)

$$f_T = -4pr^2 g/T_o. \tag{3.23}$$

The thermal force expressed by Eq. (3.22) for the continuum regime and that expressed by Eq. (3.23) for the free molecule regime may also be equated with the respective drag forces to obtain the steady thermophoretic velocity of aerosol particles:

$$f_D = 6\pi\eta r v, \quad \text{(Stokes drag, continuum regime)} \tag{3.24}$$

$$f_D = \frac{8}{3} r^2 p \left(\frac{2\pi}{R_a T}\right)^{1/2} \left(1 + \frac{\pi\alpha_m}{8}\right) v, \text{ (free molecule regime)} \tag{3.25}$$

where α_m is the momentum accommodation coefficient.

Epstein's equation (3.22) has been widely referenced, but the theory failed to account for the case of thermally conducting spheres like NaCl or metal. The observed force was a few tens times larger than what the theory predicts. In this regard, Eq. (3.21) obtained from Eq. (3.20), can account for the discrepancy better, although it still underestimates the thermophoretic velocity of particle for $K_n \geq 0.2$. An expression that is made to fit experimental data for aerosol particles with high thermal conductivity is available (Hidy and Brock, 1970).

In all the treatments of thermophoresis, there appears to be violation of all the first law of thermodynamics![5]

Diffusiophoresis

When an aerosol particle is placed in a concentration gradient of gaseous mixture, the particle moves. This phenomenon is called diffusiophoresis. Unlike thermophoresis, two effects contribute to the process: one is the mass-average hydrodynamic flow of diffusing gas (vapor) called Stefan flow and the other the impaction of molecules of different masses in the concentration gradient. The former produces a force that acts in the direction of vapor diffusion through a stagnant gas and the latter in the direction of diffusion of the heavy component of gas mixture.

Stefan's flow (Fuchs, 1964)

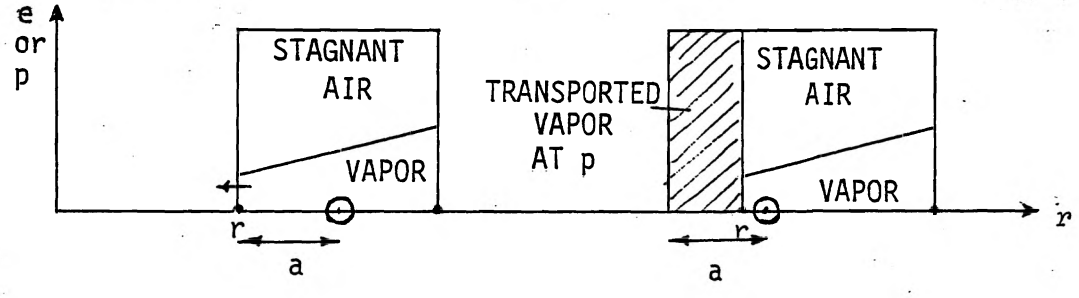

Fig. 3.7 Stefan's flow.

Stefan flow of water vapor in air is then

$$v = -\frac{1}{\epsilon\rho_a} D\nabla\rho = -\frac{1}{\epsilon\rho_a} D\frac{d\rho}{dr}, \tag{3.26}$$

where $\frac{1}{\epsilon\rho_a}$ is the specific volume of vapor at p and r the radial distance. At around a growing droplet of radius r,

$$v = \frac{D(\rho_\Delta - \rho_\infty)r}{\epsilon\rho_a r^2}, \tag{3.27}$$

where ρ_Δ and ρ_∞ are the vapor pressure just above the droplet surface and in the environment, respectively (see Chapter 5). Stefan flow is responsible for a large particle movement in a diffusing gas mixture.

Diffusion molecular impact effect

This effect is similar to that of thermophoresis. A simple treatment is given as follows.

---

[5] In the thermophoretic theories, continuity of thermal flux is assumed on the particle surface, which is the sole source of driving force for the process. The thermal force is then assumed to balance with the (viscous) resistance force in which particle kinetic energy dissipates away from the particle. Thus, the dissipating energy appears from nowhere, a clear violation of the energy conservation law. The culprit is the continuity assumption. However, in our atmospheric environment, the error is negligible (Fukuta, 1984).

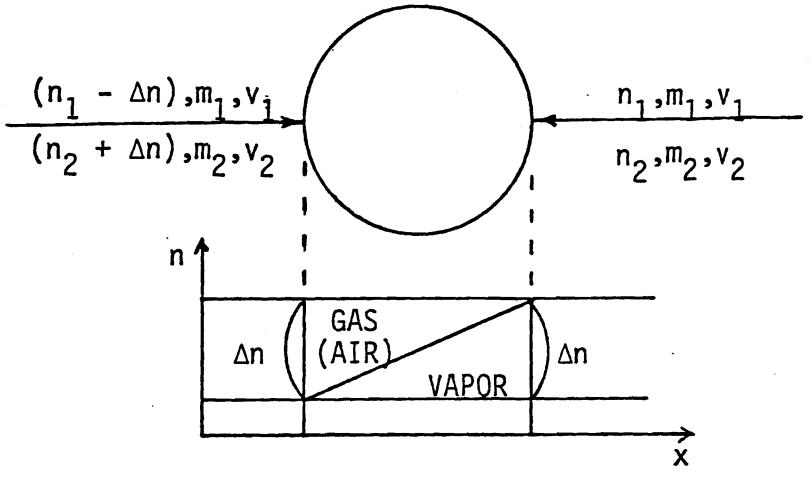

Fig. 3.8 Diffusion molecular impact effect.

(1) $m_1 < m_2$
(2) $n_1 + n_2 = \text{const}$
(n: number concentration)
(3) In x direction, using Eq. (1.79)

$$\tfrac{1}{2}m_1v_1^2 = \tfrac{1}{2}kT = \tfrac{1}{2}m_2v_2^2 \rightarrow \sqrt{\frac{m_1}{m_2}} = \frac{v_2}{v_1}. \tag{3.28}$$

From (2), the difference of force acting in unit time is

$$\begin{aligned} &2\left[(n_1 - \Delta n)m_1v_1 + (n_2 + \Delta n)m_2v_2\right] - 2(n_1m_1v_1 + n_2m_2v_2) \\ &= 2\Delta n(m_2v_2 - m_1v_1) \\ &= 2\Delta n m_2v_2\left(1 - \sqrt{m_1/m_2}\right) > 0 \quad \text{when } m_2 > m_1. \end{aligned}$$

Therefore, the force is in the direction of diffusion of heavy molecules.

The diffusiophoretic force, considering both the Stefan flow and the diffusion molecular impact effect for slip flow regime, may be taken from Waldmann and Schmitt (1967) as

$$f_D = -6\pi\eta r(1 + \sigma_{va}X_a)\frac{D}{X_a}(\nabla X_v)_\infty, \quad (0 \le K_n \le 0.25) \tag{3.29}$$

where $\sigma_{va} = -0.26$ (Pruppacher and Klett, 1978) and X_a and X_v are the mole fraction of air molecules and of vapor molecules, respectively.

For the free molecule regime (Hidy and Brock, 1970),

$$f_D = -\frac{8}{3}r^2p\left(\frac{2\pi}{R_vT}\right)^{1/2}\left[1 + \frac{\alpha_{mv}\pi}{8}\right]\frac{D}{X_a}\nabla X_v, \tag{3.30}$$

where α_{mv} is the momentum accommodation coefficient of vapor on the aerosol particle surface.

The diffusiophoretic force may be combined with the drag force to obtain the diffusiophoretic velocity of aerosol particles.

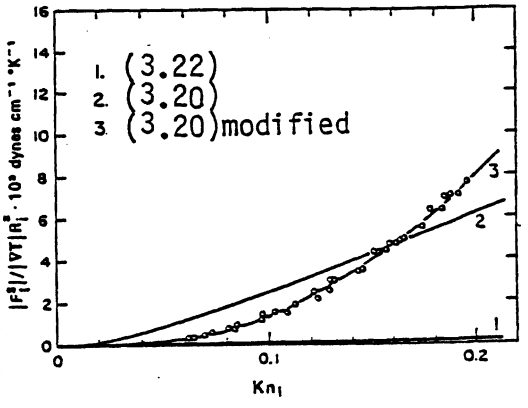

Fig. 3.9 Theory and experiments for the thermal force in the slip flow region (Jacobsen and Brock, 1965).

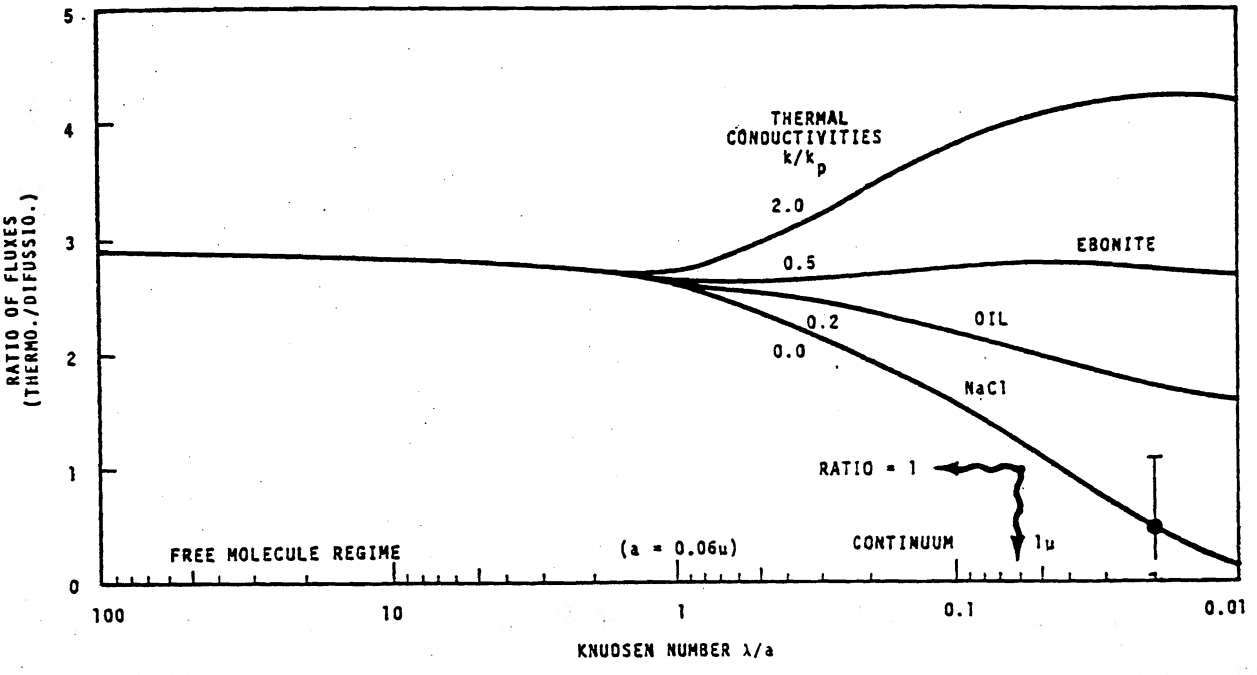

Fig. 3.10 Phoretic flux ratio as a function of Knudsen number (Slinn and Hales, 1971).

Diffusiophoresis occurs towards lower vapor density such as toward the surface of the growing droplet. However, from the growing droplet, heat flows out; and this thermophoretic effect appears to dominate the diffusiophoretic effect, at least for aerosol particles with a radius smaller than a few microns. As a result, under the growing condition, the chance of particle coagulation to the droplets reduces. On the other hand, evaporating cloud elements, including melting, attract small particles on them (Fuchs, 1964).

CHAPTER 4 SURFACE AND DISPERSE SYSTEMS

The aerodisperse system involves a large area of the phase boundaries. Clarification of the surface structure and properties is essential to understand the system.

4.1. Surface Structure and Surface Energies

Surface is a place of space asymmetry. Due to this asymmetry, many unusual processes, such as adsorption and catalysis, take place. The surface structure may best be understood through its creation, i.e., by cutting the bulk of condensed phase with an infinite plane and letting the surface molecules settle down to an equilibrium position, or to the lowest (free) energy places.

The condensed phase is a state of lowered potential energy. Creation of the surface reduces this lowering or increases the potential energy, which is the reason for the appearance of surface energy. Adsorption of the molecule takes place so as to reduce this potential difference. Adsorbed molecules also receive forces in the directions tangential to the surface. With the help of thermal motions under the surface forces, the molecules are sometimes torn apart. If torn and activated molecules of other species exist, they may combine to form molecules of a new species which is called catalysis.

When one tries to expand the surface of the condensed phase in the tangential direction, a resisting force appears due to the unbalanced potential in the normal direction because the expansion requires transfer of molecules to the surface from the bulk or deep inside the phase to the surface against the

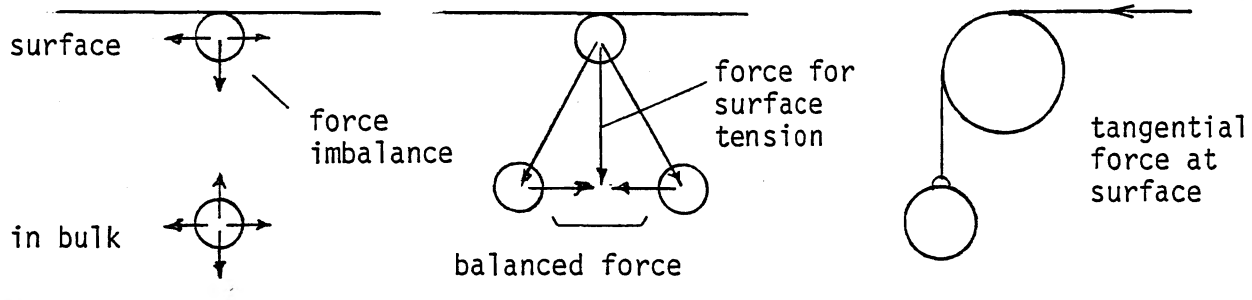

Fig. 4.1 Surface forces.

force in the normal direction. Increase of the potential energy in the tangential direction also exists. It is always balanced with another in a symmetrical position, so that it does not contribute to the force appearance against the surface expansion, although it does influence the non-directional energy balance or heat. The non-directional heat energy and the directional work energy are the only two that are exchanged with the system in question in thermodynamics. This is to say that the normal, unbalanced portion of the increase of surface energy acts against the surface expansion, and it is called (specific) surface free energy or surface tension. This and the tangential, balanced portion make up the total surface energy. If the surface reduces its area under constant temperature, this free energy portion that exerts the force against molecules coming from the bulk to the surface, increases the pressure p = nkT. This will be observed when the molecule reduces a portion of this surface

layer by leaving the surface in the form of increased number density in the gaseous phase at constant temperature. The surface is thus a layer in which imbalanced external force is acting on each molecule, and the commonly exercised method of estimating total potential lost due to surface formation for surface free energy is incorrect.

4.2 Variation of Surface Free Energy with Cluster Size

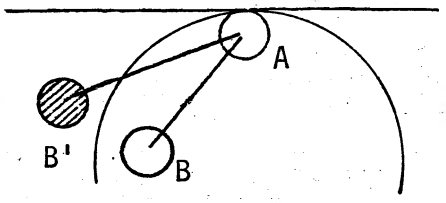

Fig. 4.2 Surface free energy, σ, of curved surface. The normal component of interaction AB′ disappears to cause σ reduction as the size decreases.

When the surface is highly curved, a portion of interaction (AB′) that existed in the flat surface will be lost, causing a reduction of surface free energy.[1]

Our recent study shows that the nearest neighbor interaction model for rigid, spherical molecules gives $\sigma_2/\sigma_\infty \simeq 0.07$, where σ is the surface free energy and subscripts 2 and ∞ stand for dimer and flat surface, respectively. For longer range and more realistic interactions, this ratio goes down as low as 0.05.

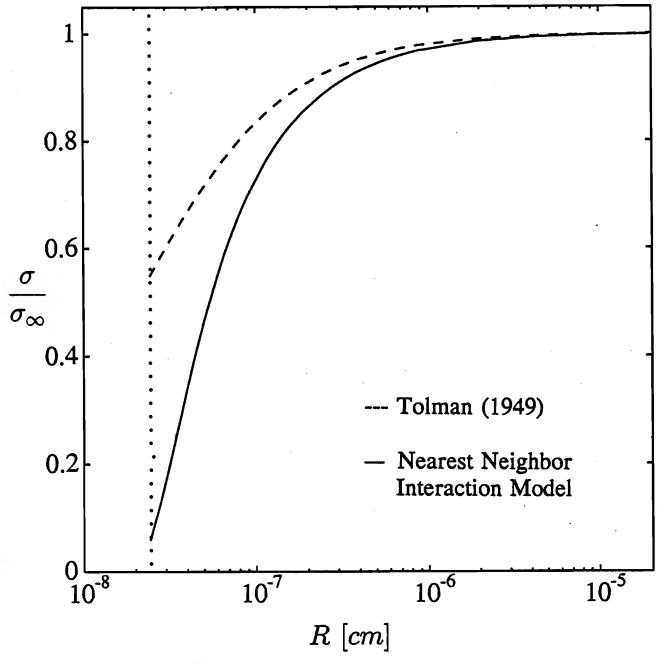

Fig. 4.3 Surface free energy ratio for the nearest neighbor interaction model. Dotted line indicates dimer position.

---

[1] The frequently quoted work for size dependency of surface free energy by Tolman (1949) is in error, because his treatment assumes no size dependence of σ in the total differential of σA (cf. Eqs. 4.3 and 4.5).

4.3 The Equation of (Young-) Laplace

When the radius of a sphere becomes smaller, the surface to volume ratio increases. The surface free energy acts to reduce the surface area. A sphere shows the smallest surface area for a given volume, and it is the shape of small drops for this reason.

A liquid surface carries energy. The free energy that exists in a unit area of the surface is called surface free energy or surface tension, with the unit of J/m^2, and expressed by σ.

Using ω for the solid angle,

$$\omega r^2 = A, \quad dA = 2\omega r dr, \tag{4.1}$$

and

$$\frac{\omega}{3} r^3 = V, \quad dV = \omega r^2 dr. \tag{4.2}$$

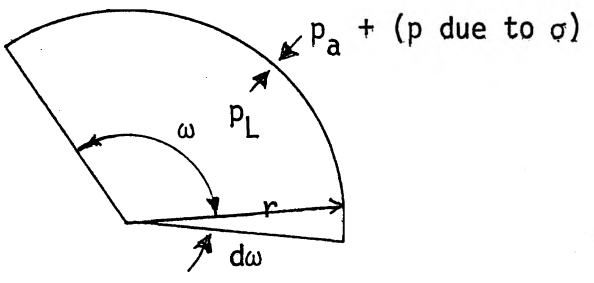

Fig. 4.4 Pressure force balance at curved surface.

If the volume increases against the external pressure caused by the surface free energy, the expended energy is converted into the increased free energy at the surface. Then, since

$$F_s/A = \sigma, \tag{4.3}$$

$$(dF)_T = -pdV = -dW \tag{4.4}$$

and

$$dF_s = \sigma dA + A d\sigma = (p_L - p_a)dV. \tag{4.5}^2$$

Using Eqs. (4.1) and (4.2) in Eq. (4.5), we obtain the generalized (Young-) Laplace equation,

$$(p_L - p_a) = \frac{2\sigma}{r} + \frac{\partial \sigma}{\partial r}. \tag{4.6}^3$$

For large particle, $\partial\sigma/\partial r \to 0$ and Eq. (4.6) becomes Laplace equation.

For a relatively large, non-spherical particle, ignoring $\frac{\partial \sigma}{\partial r}$ term,

$$\frac{2}{r} = \frac{1}{r_1} + \frac{1}{r_2}, \quad \text{(Theorem of Euler)} \tag{4.7}$$

---

[2] $pd\alpha$ is a work and αdp is not in thermodynamics. σdA corresponds to $pd\alpha$ and represents free energy increase by surface expansion under constant temperature, but unlike αdp, $Ad\sigma$ is also a free energy because σ itself is a free energy or a work potential per unit area (see Section 4.1).

[3] $\partial\sigma/\partial r$ is known as the Ono-Kondo factor (Ono and Kondo, 1960).

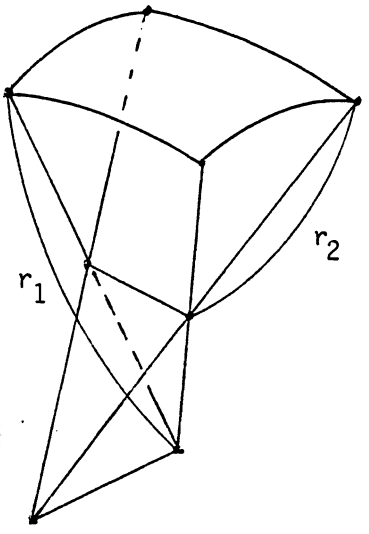

where r_1 is the principal radius of curvature, and r_2 the radius perpendicular to it may be used. Then the Laplace equation for non-spherical particle of relatively large size is expressed as

$$(p_L - p_a) = \sigma\left[\frac{1}{r_1} + \frac{1}{r_2}\right]. \qquad (4.8)$$

where $(p_L - p_a)$ is the net pressure due to surface free energy and can become very large when r becomes small.[4]

Fig. 4.5 Non-spherical surface.

4.4 The Kelvin Equation

We have seen above that increase in volume of small droplet requires relatively large energy. It is conceivable that when a molecule leaves from such a surface, it takes a relatively large energy away in terms of pressure under reversible change.

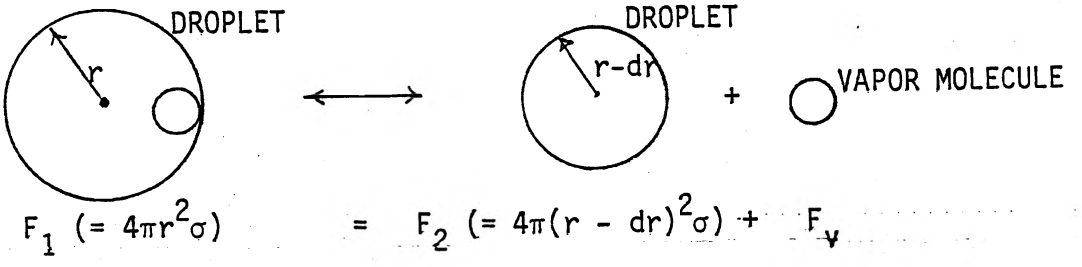

Fig. 4.6 Vapor equilibrium at the droplet surface.

The energy one molecule takes away, F_v, by evaporation from the droplet of radius, r, corresponds to the free energy loss at the surface;

$$F_v = F_1 - F_2 = (\text{free energy change per unit volume}) \times (\text{molecular volume})$$
$$= \left[\frac{\partial}{\partial V}(\sigma A)\right] v_L = \left[\sigma\frac{\partial A}{\partial V} + A\frac{\partial \sigma}{\partial V}\right] v_L = \left[\sigma\frac{8\pi r \partial r}{4\pi r^2 \partial r} + \frac{4\pi r^2 \partial \sigma}{4\pi r^2 \partial r}\right]$$
$$= \left[\frac{2\sigma}{r} + \frac{\partial \sigma}{\partial r}\right] v_L, \qquad (4.9)$$

where v_L is the molecular volume of liquid. When $r \to \infty$ or flat surface, $F_v = F_1 - F_2 \to 0$.

---

[4] $r = 10^{-8}$ m. $\sigma = 7.57\times10^{-2}$ J m^{-2} (0°C) for water. 1 atm = 1.014×10^5 J m^{-3}. $p_L - p_a = 7.57\times10^{-2} \times 2/10^{-8} = 1.51\times10^7$ J m^{-3} = 1.5×10^2 atm.

The process we are dealing with here is an isothermal change where for the ideal gas, $-pd\alpha = \alpha dp$. Then, the specific Helmholtz free energy change of Eq. (1.44) becomes

$$df = \alpha dp = R_v T d\ln p. \tag{4.10}$$

Upon integration from $r = \infty$, $p = e_\infty$, $f = f_\infty$, to $r = r$, $p = e$, and $f = f$,

$$f - f_\infty = R_v T \ln\left(\frac{e}{e_\infty}\right), \tag{4.11}$$

where subscript ∞ stands for flat surface.

Substitution of Eq. (4.11) into Eq. (4.9), with $M(f - f_\infty) = NF_v$ and $R_v = R^*/M$, results in

$$\ln \frac{e}{e_\infty} = \frac{V_L}{R^* T}\left(\frac{2\sigma}{r} + \frac{\partial \sigma}{\partial r}\right), \tag{4.12}$$

where V_L is the molar volume of liquid. Equation (4.12) is the <u>generalized Kelvin equation</u> valid down to very small sizes (see Fig. 4.7). For a relatively large particle where $\sigma \simeq \sigma_\infty$ holds,

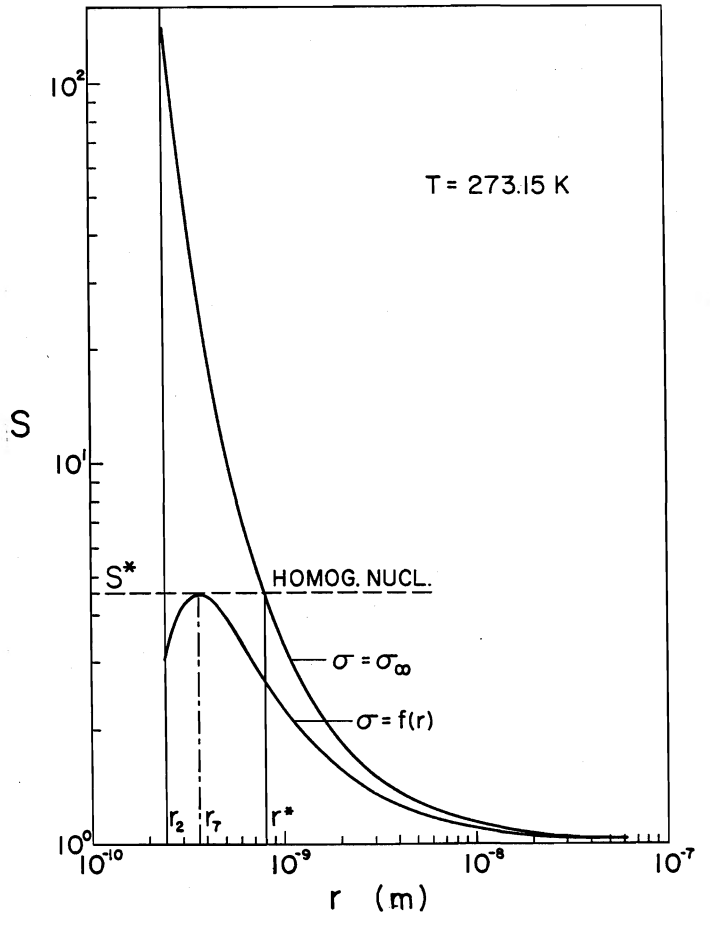

Fig. 4.7 The Kelvin equation ($\sigma = \sigma_\infty$) and the generalized form [$\sigma = f(r)$, the nearest neighbor interaction model] as a function of droplet radius. Note the maximum in saturation ratio, S, for $\sigma = f(r)$ curve.

$$\ln \frac{e}{e_\infty} = \frac{2\sigma_\infty V_L}{rR^*T} = \frac{2\sigma_\infty}{\rho_L r R_v T} = \frac{2\sigma_\infty v_L}{rkT}, \tag{4.13}$$

where V_L and v_L are the molar and molecular volume of liquid and ρ_L the density. Equation (4.13) is called the Kelvin equation.

From Eq. (4.13), it is apparent that small droplets have high vapor pressure.[5] As the particle size decreases towards molecular dimensions, the Kelvin equation begins to fail due to the fact that the surface free energy is the result of molecular interactions at the surface and the surface of tension takes different thickness. The different thickness of the surface is due to $\sigma = f(r)$, and the Ono-Kondo factor begins to play an important role resulting in a maximum (newly discovered) (cf. Fig. 4.2).

Equations (4.12) and (4.13) also apply to a surface outwardly concave or negatively curved ($r < 0$), such as a cavity or a contact point. In such a case, vapor molecules can condense below the saturation over the flat surface, and the process is called capillary condensation.

4.5 Adsorption

As we have seen above, the surface or the phase boundary is under the attractive force arising from the intermolecular potential, and molecules tend to transfer there to cause a phenomenon called adsorption and accumulate.

At constant temperature, terms involved in Gibbs free energy for a surface with area A is

$$G_S = \sigma A + \mu_1 n_1 + \mu_2 n_2, \tag{4.14}$$

where σ is the specific surface free energy, n the number of mole, and 1 and 2 the condensed and the gaseous phases for gaseous adsorption, respectively. Complete differential is therefore

$$dG_s = \sigma dA + A d\sigma + n_1 d\mu_1 + n_2 d\mu_2. \tag{4.15}$$

On a flat surface, adsorption occurs with $dA = 0$, and under equilibrium or $dG_s = 0$, Eq. (4.15) yields

$$A d\sigma = -n_1 d\mu_1 - n_2 d\mu_2. \tag{4.16}$$

If we choose the dividing surface of Gibbs, then $d\mu_1 = 0$, and we can write Eq. (4.16) as

$$d\sigma = -\Gamma_2 d\mu_2, \tag{4.17}$$

---

[5] Since $\ln \frac{e}{e_\infty} = \frac{2\sigma V_L}{rR^*T} = \frac{2x7.57x10^{-2}x18x10^{-6}}{rx8.31x273.1} = 1.20x10^{-3}\,\frac{1}{r}$ (r in μm)(0°C)

For $e/e_\infty = 2$, $\ln 2 = 0.6932$, then $r = 1.73x10^{-3}$ μm = 17.3Å

where Γ_2 is the concentration of component (2) adsorbed at the interface. The chemical potential of the species (2) changes due to transfer of the species under constant temperature and total pressure (Eq. 1.50). Then, from Eq. (1.45) with dT = 0 and the ideal gas law (Eq. 1.55), we have

$$d\sigma = -RT\ \Gamma_2\ d\ \ell n\ n_2, \tag{4.18}$$

where R is the specific gas constant of species (2). Equation (4.18) is Gibbs adsoprtion isotherm and expresses the adsorption process.

The concept of Gibbs dividing plane to represent a surface is useful so long as the surface is flat or only gently curved. When the surface is highly curved, the concept no longer applies in the manner same as Eq. (4.17).

There exist two main mechanisms of adsoprtion. The first is the physical adsorption in which a relatively small amount of energy is involved and the process is reversible. The process is similar to condensation, except that the vapor pressure of adsorbate (adsorbed molecules) is a function of the amount of adsorbed molecules. The other is chemisorption as a result of a stronger binding force, leading to formation of chemical compounds. The process is seldom reversible.

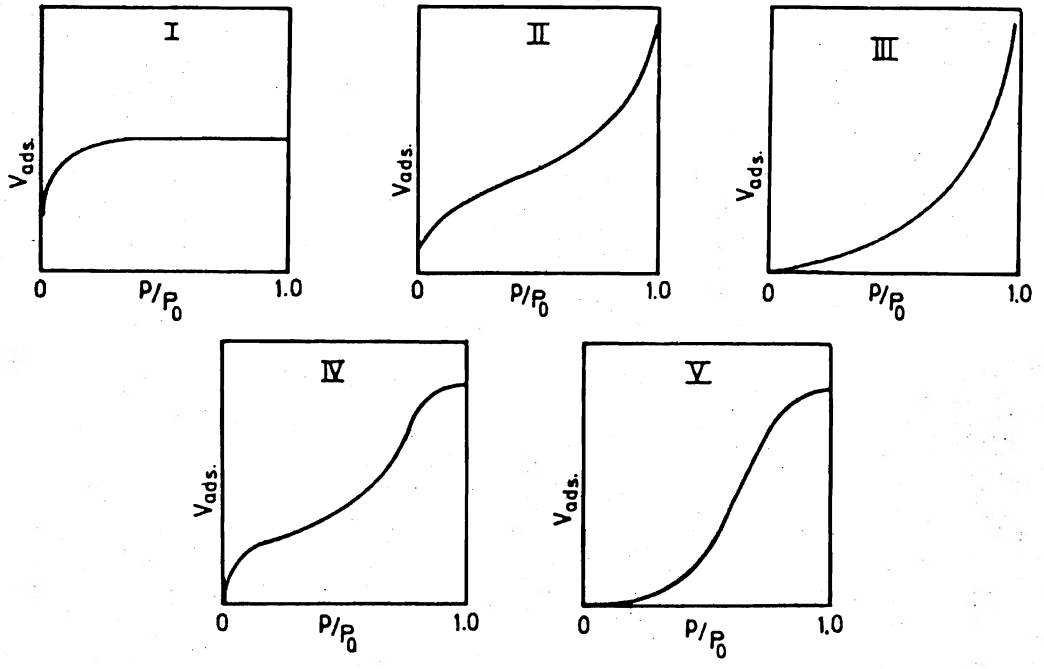

Fig. 4.8 Five types of adsorption isotherm (Brunauer et al., 1940).

CHAPTER 5 LIQUID PHASE MICRO CLOUD-PROCESSES AND AEROSOLS

Clouds form shortly after the water vapor pressure in air exceeds its saturation due to cooling by the air parcel lifting. Initiation of a new phase is called nucleation, and small droplets of the new phase continue to grow. This nucleation process is almost always assisted by a special kind of aerosol, the small particles existing in the atmosphere. Fog formation requires the same condition, although the process is often different from that of clouds. We shall look into these processes below, including precipitation formation by collision-coalescence mechanism.

5.1 Nucleation of Water Vapor Condensation

5.1.1 Thermodynamic conditions for condensation and fluctuation phenomena

Cloud and fog condensation

The ratio of vapor pressure e or vapor density ρ to their saturation e_s or ρ_s is defined as saturation ratio,

$$S = e/e_s = \rho/\rho_s. \tag{5.1}$$

Condensation or formation of clouds and fogs requires RH to exceed 100% or the S to exceed 1. There are two basic ways to do it. One is to increase the numerator of the saturation ratio by adding the vapor and the other to decrease the denominator by reducing the temperature.

In the atmosphere, these processes occur in mixed manners. Three of such processes are commonly observed:

(1) Adiabatic expansion, where cooling effect dominates the opposing effect of dilution to cause condensation,

(2) Mixing of warm moist and cold air masses.

(3) Radiative cooling of the ground which lowers the temperature of the air above. This process often and subsequently leads to Process (2).

When a change of phase is thermodynamically favored, small particles of new phase are thought to keep forming and disintegrating in the mother phase being indicated by appearance of opalescence. Phase change does not happen unless those small particles of new phase start growing spontaneously.

There are also some reports about lack of spontaneous growth. Under 1 atm, water was kept without boiling at 137°C (Donney). Similarly, water drops of 1 to 3 mm size were reportedly kept without boiling up to 178°C (Dufour). Liquid was reported to have been kept under negative pressure up to 10 atm or more without boiling.

The spontaneous growth process under the thermodynamic condition in favor of the phase change is termed as nucleation.

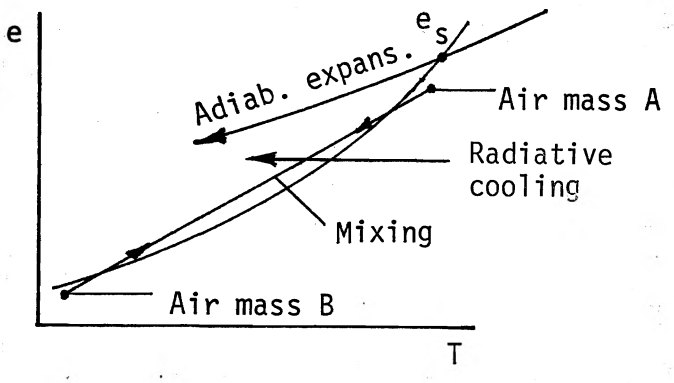

Fig. 5.1 Three common ways to exceed the saturation for cloud and fog formation.

Fluctuation phenomena

In a macroscopically uniform system, various thermodynamic properties, such as pressure, temperature, density, etc., are observed to deviate microscopically around the average macroscopic values. The fluctuation happens on the Brownian motion of colloid. Opalescence near the critical point of solution is the result of fluctuation. Fluctuations are also seen with atomic and molecular separations, free electron density, and various radioactivities.

5.1.2 Homogeneous nucleation of water vapor condensation

When the saturation ratio of the water vapor exceeds 1 or $S > 1$ under constant temperature and total pressure ($dS_c = 0$), the condition $\Delta B > 0$ appears for the vapor to change into the saturation value, or hypertrophy (one of the two entropy components) of the (closed) system to increase, the direction of natural change. The single molecules in the supersaturated environment will stick together one by one to create clusters which become droplets of visible size. This process or nucleation begins to take place when S exceeds a critical value.

$$\left.\begin{aligned} A_1 \quad + A_1 &\rightleftharpoons A_2 \\ A_2 \quad + A_1 &\rightleftharpoons A_3 \\ \text{----------} & \\ A_{i-1} + A_1 &\rightleftharpoons A_i \end{aligned}\right\}, \tag{5.2}$$

where subscript i stands for the number of molecules in the A_i cluster. Other routes such as $A_2 + A_2 \rightleftharpoons A_4$ are much less probable and do not significantly contribute to the nucleation (see Appendix E).

In the process of nucleation, a steady state current of clusters develops, and the current gives the nucleation rate only at the critical size or $i = i^*$.

$$J = A_i \cdot (\Delta nu)_i \cdot N_i, \tag{5.3}$$

(SURFACE AREA) x (NET NUMBER FLUX DENSITY) x (CLUSTER NUMBER CONCENTRATION)

where

$$A_i = 4\pi r^2, \tag{5.4}$$

$$(\Delta nu)_i = \frac{e\beta_{ic} - e_i\beta_{ie}}{\sqrt{2\pi mkT}}, \quad \text{(see p. E.4)} \tag{5.5}$$

$$e_i = e_\infty \exp\left[\frac{\partial \sigma A}{\partial V} \cdot v_L/kT\right], \quad \text{(cf. Eq. 4.12)} \tag{5.6}$$

and β_{ic} and β_{ie} the condensation and evaporation coefficients of water vapor and N_i the number concentration of the cluster consisting of i molecules (i-mer or i-cluster).

When i = 1, or for single molecule collision, Eq. (5.3) gives

$$\beta_1 \nu_3 \simeq \beta_1 \nu_2 \frac{d}{\ell}, \tag{5.7}$$

where ν_3 is the ternary collision rate of single molecules in a unit volume, ν_2 the binary one, d the molecular diameter and ℓ the mean free path length.

$$\nu_2 = \sqrt{2}\left(\frac{n}{2}\right)^2 \pi (2r)^2 \bar{u} \quad \text{(cf. Eqs. 2.1 and 2.2)}$$

$$= 2n^2 (2r)^2 \sqrt{\frac{\pi kT}{m}} \quad \text{(see p. 2.4)}, \tag{5.8}$$

where n is the number concentration of the monomers. The ternary collision is considered necessary in order to take the heat of condensation away or else the collision ends up as elastic and the collided molecules do not stay together. Condensation coefficient β for very small clusters including single molecule-single molecule collision may take a very small value and not be equal between the condensation and evaporation.

At 0°C, for the saturated water vapor

$\nu_2 \simeq 4.9 \times 10^{24}$ (cm^{-3} s^{-1})
$\nu_3 \simeq 2.8 \times 10^{20}$ (")
$n \simeq 1.6 \times 10^{17}$ (cm^{-3})
$\ell \simeq 0.05$ (μm) (H_2O-air molecule collision, 1 atm)

The nucleation is controlled by the critical embryo of the maximum vapor pressure (see Fig. 4.7). Then

$$J = A_c \cdot (\Delta nu)_c \cdot N_c, \tag{5.9}$$

where subscript c stands for critical. The nucleation starts at J = 0 and rapidly enhances as e exceeds e_i in $(\Delta nu)_c$. At around J = 0 of this thermodynamic nucleation current, the statistical mechanical fluctuation mentioned earlier provides a weak current to the nucleation.

The nucleation rate shown above should be exact, at least in concept, but it has not been sufficiently developed at this moment. Therefore, from here on, we shall follow the classical theory which contains a number of contradictions but has been shown to give an approximate match to experimental rate of nucleation. There exists an approximate, parallel relationship for free energy of embryo formation between the new and classical theories (space beteen S^* and curves in Fig. 4.7) which is likely the reason for the latter usefulness.

5.1.3 Heteromolecular homogeneous nucleation of vapor condensation

The homogeneous nucleation of vapor condensation we have seen above concerns single molecular species. It may, therefore, be called homomolecular homogeneous nucleation. When two or more molecular species are simultaneously involved in the nucleation, the process is called heteromolecular homogeneous nucleation, and such processes may take place in the atmosphere.

In the homomolecular nucleation, the vapor has to be supersaturated with respect to the species over the flat surface. Whereas, in the heteromolecular nucleation, due to the vapor pressure depression effect of a species in the solution droplets which are to be nucleated (see Section 5.1.6), the nucleation becomes possible even if the vapor is undersaturated with the species over the flat surface, as long as it is above the vapor pressure of the species in the solution droplets. The most common type of heteromolecular nucleation involves two different vapor species and accordingly it is called binary homogeneous nucleation. We look into this binary homogeneous nucleation process in the air below.

Suppose we have a solution droplet of two vapor species A and B with respective number of molecules in the droplet n_A and n_B. The free energy of embryo formation[1] is given as

$$\Delta G = -kT \frac{4\pi}{3} r^3 \left[n_A \ell n \frac{e_A}{e_{A,sol,\infty}} + n_B \ell n \frac{e_B}{e_{B,sol,\infty}} \right] + 4\pi r^2 \sigma_{sol}, \tag{5.10}$$

where e is the vapor pressure and subscripts A, B, sol and ∞ stand for species A and B, solution that has the droplet composition and flat surface, respectively (cf. Eq. E.4). The term in the bracket on the right-hand side of Eq. (5.10) shows a minimum with respect to variation of n of one species, and the whole ΔG gives a maximum with respect to the radius (Eq. E.8). This is to say that ΔG in Eq. (5.10) has a saddle point for free energy carrier of critical embryo formation.

In the contemporary binary homogeneous nucleation of vapors with $n_A \gg n_B$, the nucleation rate is constructed with respect to the saddle point, which gives $\Delta G = \Delta G^*$ as

$$J = \underbrace{4\pi r^{*2}}_{\substack{\text{SURFACE AREA OF} \\ \text{CRIT. EMBRYO}}} \cdot \underbrace{\frac{e_B}{\sqrt{2\pi m_B kT}}}_{\substack{\text{ARRIVAL RATE} \\ \text{OF SPECIES B}}} \cdot \underbrace{n_A \exp(-\Delta G^*/kT)}_{\substack{\text{\# OF CRITICAL EMBRYOS} \\ \text{PER UNIT VOL. IN THE} \\ \text{VAPOR PHASE}}}. \tag{5.11}$$

$H_2O - H_2SO_4$ system is an example of this binary homogeneous nucleation with A and B corresponding to water and H_2SO_4 vapors, respectively. The arrival rate of the species with lower number concentration (H_2SO_4) at the critical embryo surface determines the nucleation rate.

5.1.4 Heterogeneous nucleation of water vapor condensation - on ions

---

[1] The criticism of the contemporary theory given in Appendix E′ also applies here.

The two homogeneous condensation nucleation processes we have seen above occur unassisted by foreign particles. In the atmosphere, there are a variety of particles and ions which assist the nucleation of water condensation. Such a process is called heterogeneous nucleation of condensation. We shall look into several typical heterogeneous nucleation mechanisms of water condensation in this and the following few sections.

Ions are charged particles, and they are known to assist nucleation of water condensation. To examine condensation around the ions, we describe the electrostatic field around them. The electrostatic potential V, similar to T or ρ, as we shall see in later sections, is connected to the electrostatic field E as

$$\frac{dV}{dr} = E. \tag{5.12}$$

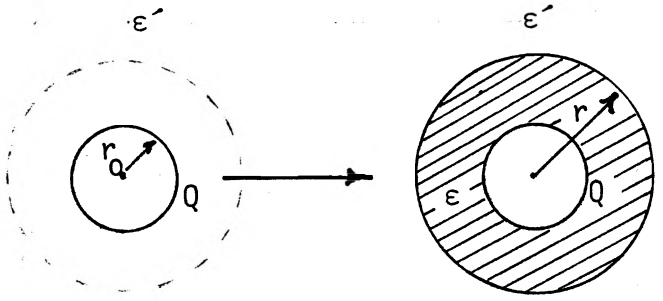

Fig. 5.2 Nucleation of water vapor condensation on an ion.

The work or energy of placing charge Q against electrostatic potential field is

$$W = \int_0^Q V dQ. \tag{5.13}$$

Whereas,

$$V = \int_r^\infty \frac{Q}{\epsilon r^2} dr, \tag{5.14}$$

where ϵ is the dielectric constant. Then from Eqs. (5.13) and (5.14), we obtain

$$W = \int_0^Q QdQ \int_r^\infty \frac{dr}{\epsilon r^2} = \frac{Q^2}{2}\left(\frac{1}{\epsilon r}\right). \tag{5.15}$$

Since FREE ENERGY OF FORMATION = G (FINAL) − G (INITIAL), we can write the free energy under the influence of the electrostatic field

$$\Delta G_e = \frac{Q^2}{2}\left[\frac{1}{\epsilon}\left(\frac{1}{r_o} - \frac{1}{r}\right) - \frac{1}{\epsilon'}\left(\frac{1}{r_o} - \frac{1}{r}\right)\right] = \frac{Q^2}{2}\left(\frac{1}{\epsilon'} - \frac{1}{\epsilon}\right)\left(\frac{1}{r} - \frac{1}{r_o}\right) < 0. \tag{5.16}$$

Then, the total free energy of embryo formation on the charged droplet (ion) is

$$\Delta G = -\frac{4}{3}\pi r^3 n_L kT \ln\left(\frac{e}{e_\infty}\right) + 4\pi r^2\sigma + \frac{Q^2}{2}\left(\frac{1}{\epsilon'} - \frac{1}{\epsilon}\right)\left(\frac{1}{r} - \frac{1}{r_o}\right), \tag{5.17}$$

which is due to J.J. Thomson. The critical embryo conditions can be obtained as before by differentiation or

$$\frac{\partial \Delta G}{\partial r} = 0. \quad \text{(see figure below)}$$

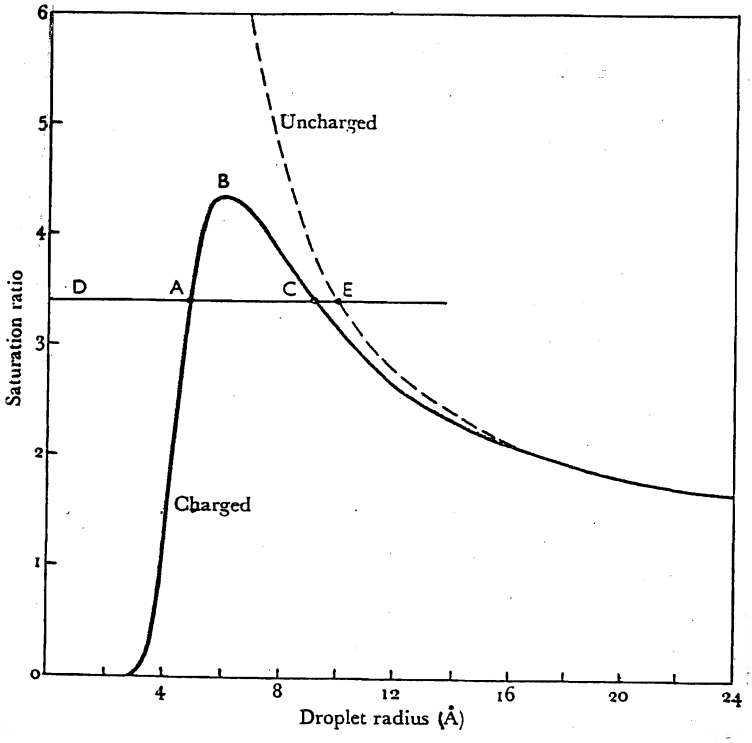

Fig. 5.3 Saturation ratio as a function of radius for charged and uncharged water droplets.

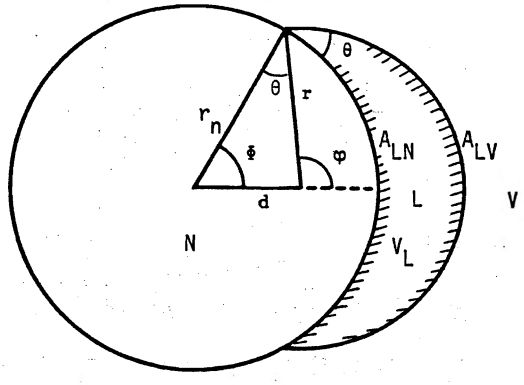

Fig. 5.4 The system of nucleating insoluble particle.

5.1.5 Heterogeneous nucleation of water vapor condensation - on insoluble particles

On particles

Insoluble particles can serve as the centers of condensation nucleation depending on their surface characteristics. The concept of this nucleation is also the backbone of ice nucleation and is largely due to Fletcher (1958 and 1960). In this treatment, there exists the same conceptual problem as discussed in Section 5.1.2.

As explained above

FREE ENERGY OF EMBRYO FORMATION ON AN INSOLUBLE PARTICLE = G (FINAL STATE) − G (INITIAL STATE).

Observing the right-hand side of Fig. 5.4, the free energy of embryo formation

$$\Delta G = \sigma_{LV}A_{LV} + \sigma_{LN}A_{LN} + (\mu_L - \mu_V)\frac{V_L}{v_L} - \sigma_{VN}A_{LN}. \qquad (5.18)^2$$

After a tedious derivation, one obtains

$$\Delta G^* = \Delta G_h^* \cdot f(m,x), \qquad (5.19)$$

where ΔG_h^* is the free energy of critical embryo formation for homogeneous process, and f(m,x) is the geometrical factor,

$$m = \cos\theta = (\sigma_{VN} - \sigma_{LN})/\sigma_{LV}, \qquad (5.20)$$

and

$$x = r_n/r^*, \qquad (5.21)$$

where r_n is the radius of the nucleus particle.

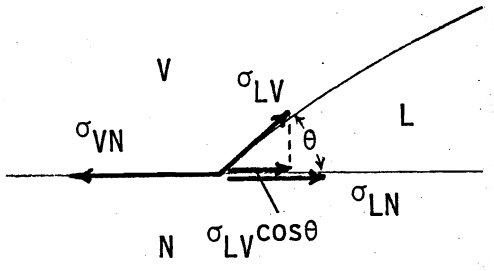

Fig. 5.5 Force balance at the vapor-liquid-nucleus interface.

Equation (5.20) is known as the Young-Dupré equation and is derived from the following relationship (see the figure)

$$\sigma_{VN} = \sigma_{LV}\cos\theta + \sigma_{LN}. \qquad (5.22)$$

Equation (5.19) suggests that the free energy of critical embryo formation on a nucleus particle surface can be expressed by the product between that for homogeneous process and f(m,x). The geometrical factor f(m,x) is given as

$$f(m,x) = \frac{1}{2}\left\{1 + \left(\frac{1-mx}{g}\right)^3 + x^3\left[2-3\left(\frac{x-m}{g}\right) + \left(\frac{x-m}{g}\right)^3\right] + 3mx^2\left(\frac{x-m}{g} - 1\right)\right\}, \qquad (5.23)$$

2

$A_{LV} = 2\pi r^2(1-\cos\phi)$, $\phi = \theta + \Phi$, $r_n\sin\Phi = r\sin\theta$, $r_n^2 - r_n^2\cos^2\Phi = r^2 - r^2\cos^2\phi$, $m = \cos\theta$,

$$A_{LV} = 2\pi r^2\left[1 - \frac{r - r_n m}{(r^2+r_n^2-2rr_n m)^{1/2}}\right],\quad A_{LN} = 2\pi r_n^2\left[1 - \frac{r_n - rm}{(r^2+r_n^2-2rr_n m)^{1/2}}\right],$$

$$V_L = \frac{\pi}{3}\left\{r^2\left[1 - \frac{r - r_n m}{(\quad)^{1/2}}\right]^2\left[3r - r\left(1 - \frac{r - r_n m}{(\quad)^{1/2}}\right)\right] - r_n^2\left[1 - \frac{r_n - rm}{(\quad)^{1/2}}\right]^2\left[3r_n - r_n\left(1 - \frac{r_n - rm}{(\quad)^{1/2}}\right)\right]\right\}$$

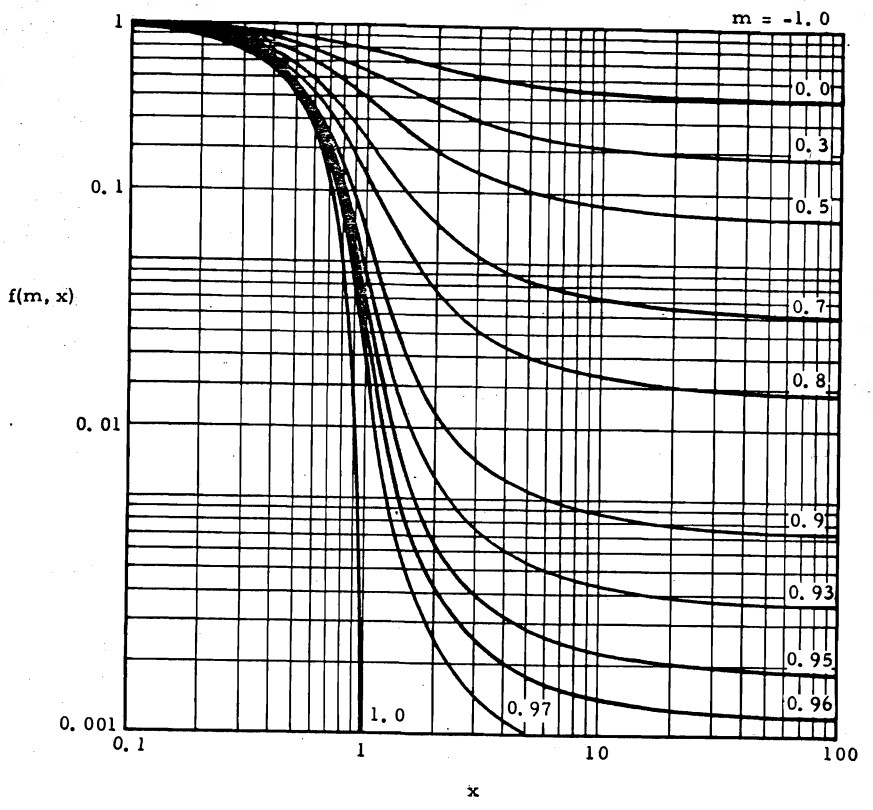

Fig. 5.6 The geometrical factor

where

$$g = (1 + x^2 - 2mx)^{1/2}. \tag{5.24}$$

On flat surface

On a flat surface, the geometry is different (see figures below); and the geometrical factor takes the form

$$f_f(m,x) = \frac{(2 + m)(1 - m)^2}{4}. \tag{5.25}$$

The rate of heterogeneous nucleation on a particle may, therefore, be written as

$$J = \underbrace{\frac{\beta e}{(2\pi mkT)^{1/2}}}_{\text{rate to receive molecules on critical embryo}} \cdot \underbrace{\pi r^{*2}}_{\text{\# of critical embryo on nucleus surface}} \cdot 4\pi r_n^2 \cdot n_a \exp(-\Delta G^*/kT), \quad (\#/s) \tag{5.26}$$

where n_a is the number of water molecules adsorbed on the unit area of nucleus surface. The pre-exponential term $\simeq 10^{25} \cdot 4\pi r_n^2$.

Main features of nucleation by insoluble particles

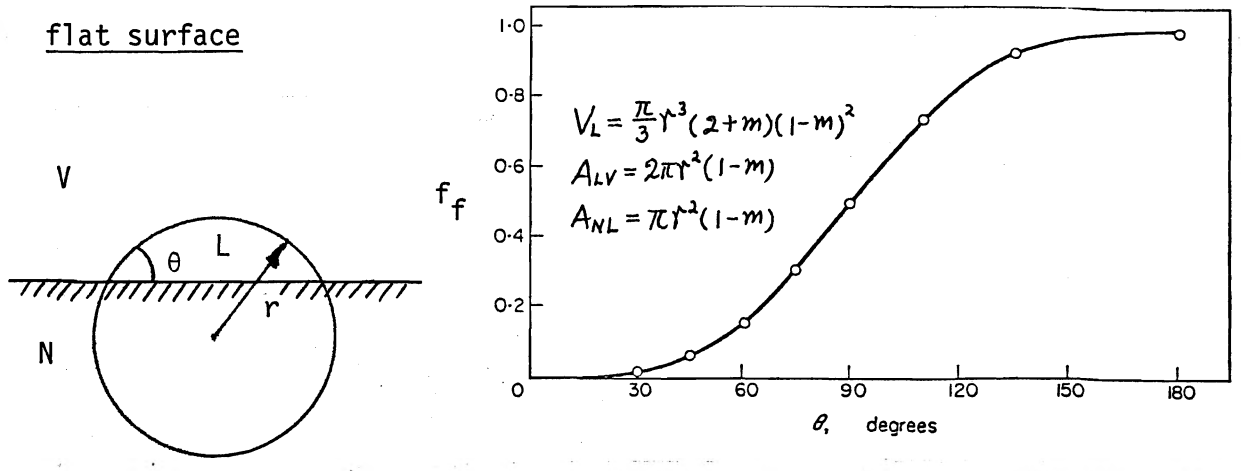

Fig. 5.7 Nucleation of water vapor condensation on a flat surface and the geometrical factor as a function of the contact angle.

The main features of condensation nucleation on insoluble particles are

(1) r^* of the liquid embryo on the nucleus surface is the same as that for homogeneous nucleation embryo, showing the same vapor pressure.

(2) ΔG_h^* is reduced by the factor f(m,x) so that a smaller amount of ΔG suffices to overcome the barrier of activation for nucleation, making the nucleation easier.

(3) A completely wettable nucleus nucleates best, and it becomes a Kelvin particle (same as water droplet). Whereas, with a completely non-wettable nucleus particle (m = −1), the nucleation becomes most difficult or the same as homogeneous nucleation because the nucleus surface provides no assistance to the nucleation.

5.1.6 Heterogeneous nucleation of water vapor condensation - on soluble particles

In this heterogeneous nucleation on soluble particles, there appears no conceptual problem as discussed in Section 5.1.2.

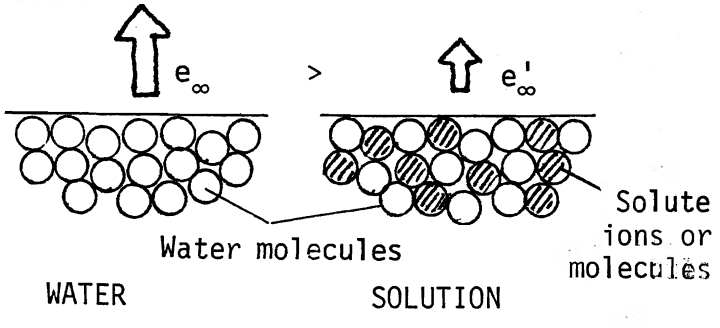

Fig. 5.8 Vapor pressure of solution.

Water soluble particles exist in the atmosphere. Since water soluble compounds attract water vapor, depending on their solubility in water, the particles consisting of such materials are capable of assisting the heterogeneous nucleation of water condensation. We shall begin here to examine the basic behaviors of water soluble compounds.

Raoult's law

Raoult's law states that the vapor pressure of solvent molecules (water) in the solution is proportional to the mole fraction of solvent, or

$$\frac{e'_\infty}{e_\infty} = \frac{n}{n + in'}, \tag{5.27}$$

where n and n′ are the number of mole of solvent (water) and of solute, respectively, and i the van't Hoff factor describing the effective dissociation rate of solute molecules in the case of electrolyte. For non-electrolyte, it is an efficiency factor.

Vapor pressure of solution droplets

In order to estimate the vapor pressure of solution droplets which determines the growth (or evaporation) behaviors with respect to the water vapor pressure in the environment, we take the following route considering the Kelvin effect of droplet curvature and the solute effect given by the Raoult law.

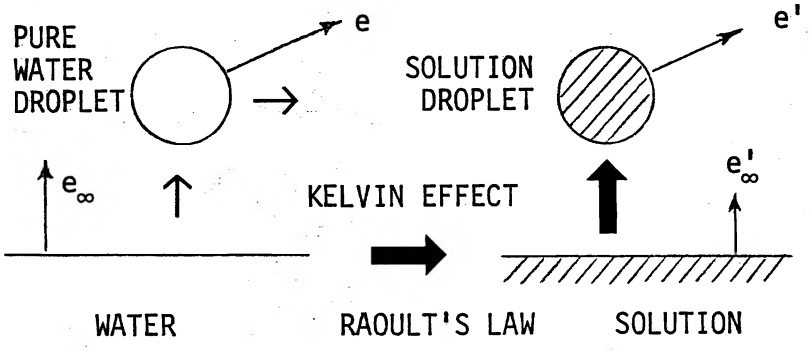

To estimate the vapor pressure of the solution droplet, there are two ways to do it, one passing through the pure water droplet and the other through the solution of flat surface. We take the latter here. Then

Fig. 5.9 Relationship between the vapor pressure of water over the flat surface and that of solution droplet.

$$\frac{e'}{e_\infty} = \frac{e'}{e'_\infty} \cdot \frac{e'_\infty}{e_\infty}, \tag{5.28}$$

where ′ means solution and the subscript ∞ stands for flat surface. Using the generalized Kelvin equation for the solution droplet, Eq. (5.28) writes

$$\frac{e'}{e_\infty} = \exp\left[\frac{v'_L}{kT}\left(\frac{2\sigma'}{r}\right)\right] \cdot \frac{e'_\infty}{e_\infty}, \tag{5.29}$$

where v'_L is the molecular volume of the solvent or water in the solution, and σ' the surface free energy of the solution, respectively. Frequently $v'_L < v_L$ due to hydration. Since the number of mole of solute is given as

$$n' = \frac{m'}{M'},$$

where m′ and M′ are the mass and the molecular weight of the solute,

$$n = \left(\frac{4\pi}{3} r^3 \rho_L' - m'\right)/M.$$

Inserting these relations into Eq. (5.27), we have

$$\frac{e_\infty'}{e_\infty} = \left(1 + \frac{in'}{n}\right)^{-1} = \left[1 + \frac{im'M}{M'\left(\frac{4\pi}{3} r^3 \rho_L' - m'\right)}\right]^{-1}. \tag{5.30}$$

Substitution of Eqs. (5.29) and (5.30) into Eq. (5.28) then yields

$$\frac{e'}{e_\infty} = \exp\left[\frac{1}{n_L' kT}\left(\frac{2\sigma'}{r}\right)\right]\left[1 + \frac{im'M}{M'\left(\frac{4\pi}{3} r^3 \rho_L' - m'\right)}\right]^{-1}, \tag{5.31}$$

which is the general form of the vapor pressure of solution droplet relative to that over a flat surface of pure water, and applicable to atmospheric conditions.

For <u>dilute solution</u>, by expanding Eq. (5.31) and taking the first three terms,

$$\frac{e'}{e_\infty} \simeq 1 + \left(\frac{2\sigma}{n_L kT}\right)\frac{1}{r} - \left(\frac{im'M}{M'\frac{4\pi}{3}\rho_L'}\right)\frac{1}{r^3}, \tag{5.32}$$

or

$$\frac{e'}{e_\infty} \simeq 1 + \frac{a}{r} - \frac{b}{r^3}, \tag{5.33}$$

where $a = 2\sigma/n_L kT$, expressing the Kelvin effect; and $b = im'M/\left(M'\frac{4\pi}{3}\rho_L'\right)$, expressing the solute effect. Their values may be taken as

$$a \simeq 3.3 \times 10^{-5}\ T^{-1} \quad \text{and} \quad b \simeq 4.3m'/M'. \quad (r \text{ in m})$$

The plot of Eq. (5.33), or the original expression, is called the <u>Köhler curve</u> (see below).

As can be seen in Fig. 5.10, there is a maximum in the curve; and if the environmental vapor pressure <u>exceeds</u> the maximum value of the curve, the droplet grows. To find the maximum, by differentiating Eq. (5.33) with r and setting $\partial(e'/e_\infty)/\partial r = 0$, we have

$$r^* = \sqrt{\frac{3b}{a}} \tag{5.34}$$

and

$$\left(\frac{e'}{e_\infty}\right)^* = 1 + \left(\frac{4a^3}{27b}\right)^{1/2}. \tag{5.34′}$$

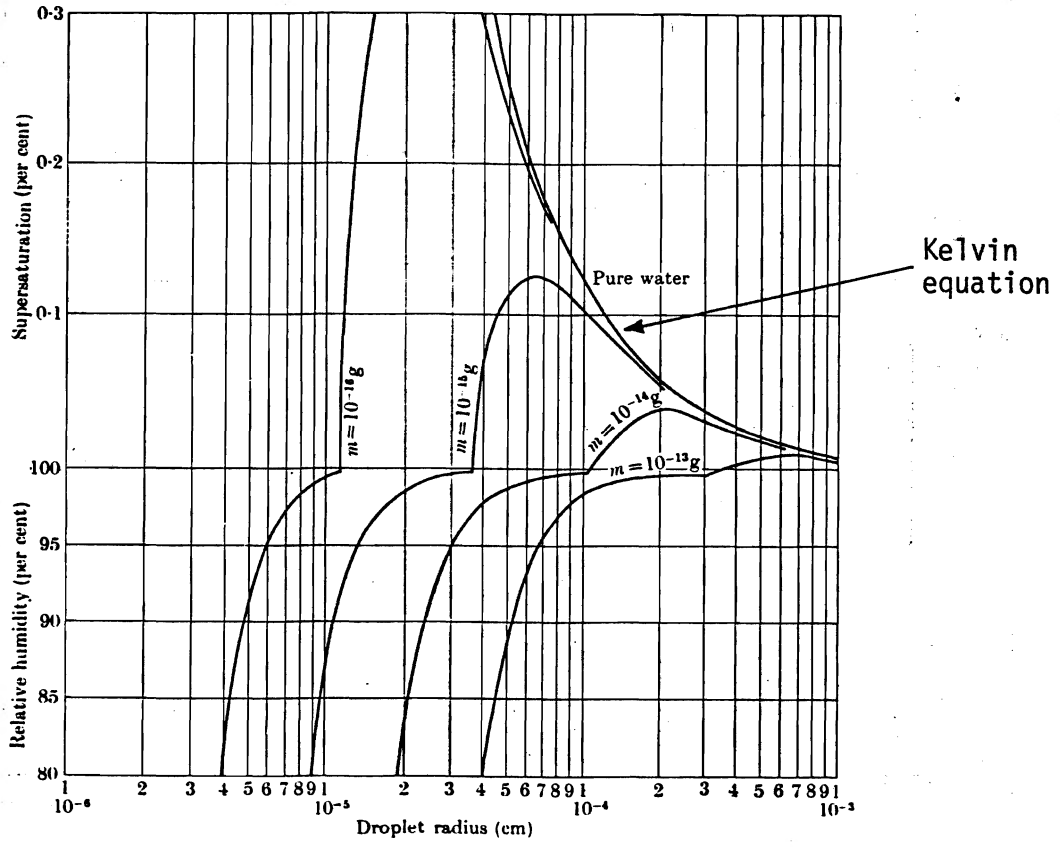

Fig. 5.10 The equilibrium relative humidity (or supersaturation) as a function of droplet radius for solution droplets containing the indicated masses of sodium chloride.

Number of nucleation in a unit volume

For heterogeneous condensation nucleation, the total number of nuclei activated in a unit volume, N, may be expressed as

$$N = \int_{r^*}^{\infty} \int_0^t J(r)\, n(r)\, dt\, dr, \tag{5.35}$$

where n(r) is the number of nuclei between r and r + dr in the unit volume, $r^* = f(S^*)$, and S^* the critical saturation ratio. For the water soluble nuclei, the nucleus population is given; and at a given supersaturation, the only time-dependent process is their swelling to the critical sizes. Therefore, if the condition were held constant, the activated nuclei will reach rapidly to a level. Thereafter, the number does not increase.

Table 5.1 Water activities and van't Hoff factors of electrolytes at 25C and 1 atm (Low, 1969).

	Sodium chloride $\nu = 2$		Ammonium sulfate $\nu = 3$		Magnesium sulfate $\nu = 2$		Calcium chloride $\nu = 3$	
Molality	a	i	a	i	a	i	a	i
0.1	0.9966	1.867	0.9959	2.306	0.9978	1.213	0.9954	2.568
0.2	0.9933	1.856	0.9921	2.202	0.9960	1.126	0.9907	2.598
0.3	0.9901	1.853	0.9886	2.133	0.9942	1.083	0.9859	2.647
0.4	0.9868	1.852	0.9852	2.086	0.9924	1.062	0.9809	2.708
0.5	0.9836	1.857	0.9819	2.050	0.9906	1.049	0.9755	2.785
0.6	0.9802	1.864	0.9786	2.023	0.9889	1.042	0.9700	2.863
0.7	0.9769	1.874	0.9754	1.999	0.9870	1.041	0.9642	2.942
0.8	0.9736	1.883	0.9722	1.984	0.9852	1.044	0.9582	3.028
0.9	0.9702	1.892	0.9691	1.969	0.9833	1.049	0.9517	3.128
1.2	0.9668	1.904	0.9660	1.954	0.9813	1.060	0.9450	3.228
1.1	0.9600	1.925	0.9598	1.935	0.9768	1.097	0.9307	3.443
1.4	0.9532	1.948	0.9536	1.930	0.9718	1.150	0.9152	3.673
1.6	0.9460	1.978	0.9475	1.923	0.9662	1.215	0.8986	3.917
1.8	0.9389	2.007	0.9412	1.927	0.9600	1.286	0.8808	4.174
2.0	0.9316	2.037	0.9349	1.933	0.9531	1.364	0.8618	4.451
2.5	0.9128	2.121	0.9189	1.960	0.9322	1.616	0.8091	5.239
3.0	0.8932	2.213	0.0922	2.006	0.9052	1.939	0.7494	6.186
3.5	0.8727	2.314	0.8848	2.065	--	--	0.6875	7.210
4.0	0.8514	2.422	0.8670	2.128	--	--	0.6239	8.364
4.5	0.8295	2.536	0.8490	2.194	--	--	0.5602	9.686
5.0	0.8068	2.659	0.8308	2.261	--	--	0.4988	11.155
5.5	0.7835	2.788	0.8124	2.331	--	--	0.4425	12.716
6.0	0.7598	2.926	--	--	--	--	0.3916	14.372

Table 5.2 Solubility of Inorganic Compounds in Water (Handbook of Chemistry and Physics, 1961).

The table shows the number of grams of the anhydrous substance indicated in the first column which can be dissolved in 100 grams of water at the temperature in degrees Centigrade given at the top. When the formula is preceded by a * the solubility is stated in grams of anhydrous substance in 100 grams of saturated solution; when preceded by ** the solubility is stated in grams of anhydrous substance in 100 c.c. of the saturated solution. The column headed with S.P. shows the solid phase hydrated form in equilibrium with the saturated solution.

Substance	S.P.	0°	10°	20°	30°	40°	50°	60°	70°	80°	90°	100°
AgI	--	--	--	--	$3x10^{-7}$	--	--	$3x10^{-5}$	--	--	--	--
CdI_2	--	79.8	83.2	86.2	89.7	93.8	97.4	--	--	--	--	127.6
$CO_2$760mm	--	0.3346	0.2318	0.1688	0.1257	0.0973	0.0761	0.0576	--	--	--	--
CuS	--	--	$3.3x10^{-5}$	at 18°	--	--	--	--	--	--	--	--
NaCl	--	35.7	35.8	36.0	36.3	36.6	37.0	37.3	37.3	38.4	39.0	39.8
$(NH_4)_2SO_4$	--	70.6	73.0	75.4	81.0	81.0	--	88.0	--	95.3	--	103.3
PbI_2	--	0.0442	--	0.068	0.125	0.125	0.164	0.197	--	0.302	--	0.436
$SO_2$760mm	--	22.83	16.21	11.29	5.41	5.41	4.5	--	--	--	--	--

Table 5.3 Critical radii and supersaturations for nuclei of various sizes (T = 273 K) (Mason, 1971).

(a) Hygroscopic nuclei of NaCl

log m(g)	−16	−15	−14	−13	−12	−11	−10	−9	−8
r(μm)at H = 78%	0.039	0.084	0.185	0.39	0.88	1.85	4.1	8.8	18.5
r_c(μm)†	0.20	0.62	0.62	6.2	20	62	200	620	2000
H_c−100 (=supersat.) %)‡	0.42	0.13	4.2×10^{-2}	1.3×10^{-2}	4.2×10^{-3}	1.3×10^{-3}	4.2×10^{-4}	1.3×10^{-4}	4.2×10^{-5}
r(of crystal) (μm)	0.022	0.048	0.103	0.22	0.48	1.03	2.2	4.8	10.3

r at H = 100% is approx. $r_c/\sqrt{c}$.

† For other nuclear substances of molecular weight W, multiple by $(58.5/W)^{1/2}$.

‡ For other nuclear substances of molecular weight W, multiple by $(w/58.5)^{1/2}$.

(b) Insoluble wettable nuclei (same as Kelvin, e.g. $\theta = 0°$)

log r (cm)	−7	−6	−5	−4	−3
$100p_r/p^\infty$	323	112.5	101.2	100.12	100.01

Table 5.4 Surface Tension of Inorganic Solutes in Water (Handbook of Chemistry and Physics, 1961).

% - Weight % of solute
σ = Surface tension in dynes/cm.

Solute	T°C	% σ							
HCl	20	%	1.78	3.52	6.78	12.81	16.97	23.74	35.29
		σ	72.55	72.45	72.25	71.85	71.75	70.55	65.75
HNO_3	20	%	4.21	8.64	14.99	34.87			
		σ	72.15	71.65	70.95	68.75			
H_2SO_4	25	%	4.11	8.26	12.18	17.66	21.88	29.07	33.63
		σ	72.21	72.55	72.80	73.36	73.91	74.80	75.29
NH_4OH	18	%	1.72	3.39	4.99	9.51	17.37	34.47	54.37
		σ	71.65	70.65	69.95	67.85	65.25	61.05	57.05
KCl	20	%	0.74	3.60	6.93	13.88	18.77	22.97	24.70
		σ	72.99	73.45	74.15	75.55	76.95	78.25	78.75
NaCl	20	%	0.58	2.84	5.43	10.46	14.92	22.62	25.92
		σ	72.92	73.75	74.39	76.05	77.65	80.95	82.55
$MgCl_2$	20	%	0.94	4.55	8.69	16.00	22.30	25.44	
		σ	73.07	74.00	75.75	79.15	82.95	85.75	
Na_2SO_4	20	%	2.76	6.63	12.44				
		σ	73.25	74.15	75.45				
$NaNO_3$	20	%	0.85	4.08	7.84	14.53	29.82	37.30	47.06
		σ	72.87	73.75	73.95	75.15	78.35	80.25	87.05

Table 5.5 Surface Tension of Organic Compounds in Water (Handbook of Chemistry and Physics, 1961).

% - Weight % of solute
σ = Surface tension in dynes/cm.

Solute	T°C	% σ							
Acetic acid	30	%	1.00	2.475	5.001	10.01	30.09	49.96	69.91
		σ	68.00	64.40	60.10	54.60	43.60	38.40	34.30
Acetone	25	%	5.00	10.00	20.00	50.00	75.00	95.00	100.00
		σ	55.50	48.90	41.10	30.40	26.80	24.20	23.00
p-Aminoben-zoic acid	25	%	12.35	22.36	30.45	37.44			
		σ	73.38	74.79	76.32	78.20			
n-Butanol	30	%	0.04	0.41	9.53	80.44	86.05	94.20	97.40
		σ	69.33	60.38	26.97	23.69	23.47	23.29	22.25
Glycerol	18	%	5.00	10.00	20.00	30.00	50.00	85.00	100.00
		σ	72.90	72.90	72.40	72.00	70.00	66.00	63.00
Phenol	20	%	0.024	0.047	0.118	0.417	0.941	3.76	5.62
		σ	72.60	72.20	71.30	66.50	61.10	46.00	42.30
n-Propanol	25	%	0.001	0.005	0.01	0.50	0.60	0.80	0.90
		σ	67.10	56.18	49.30	24.34	24.15	23.66	23.41
Sucrose	25	%	10.00	20.00	30.00	40.00	55.00		
		σ	72.50	73.00	73.40	74.10	75.70		

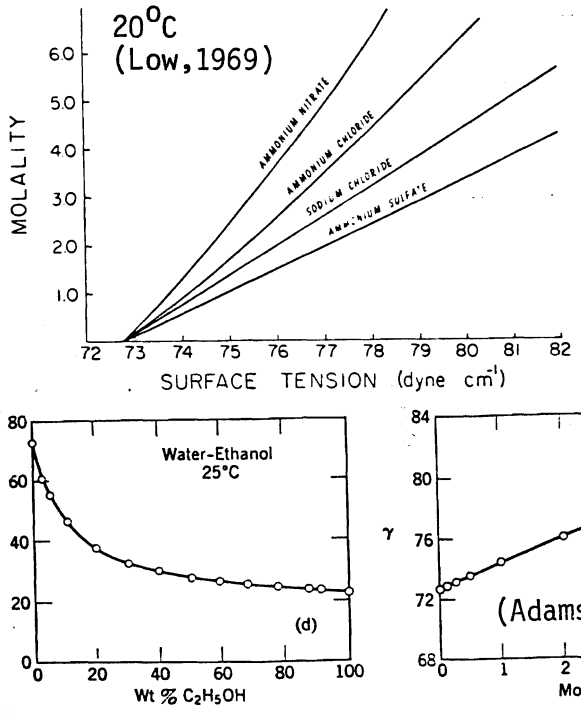

$$\frac{100\,m'}{\frac{4}{3}\pi r^3 \rho_L'} = C \quad \text{Weight \% of solute}$$

$$\frac{\partial \sigma'}{\partial C} = 0.38 \text{ (table)} \quad \boxed{NaCl}$$

$$\frac{\partial \sigma'}{\partial r} = \frac{\partial \sigma'}{\partial C} \cdot \frac{\partial C}{\partial r} = \frac{\partial \sigma'}{\partial C} C \frac{(-3)}{r}$$

C=26.5 at sat. 20°C

$\sigma' = 82.6$

$$\frac{\partial \sigma'}{\partial r} \Big/ \frac{2\sigma'}{r} = -3C \frac{\partial \sigma'}{\partial c} \frac{1}{2\sigma'} = \frac{-900\,m'}{8\pi\sigma' \rho_L'} \cdot \frac{\partial \sigma'}{\partial C} \cdot \frac{1}{r^3}$$

$= -0.18$ at saturation
[-0.22 for $(NH_4)_2SO_4$]

Fig. 5.11 Surface free energy of solutions as a function of the solute concentration.

Nucleation hysteresis

For water soluble nuclei, after being grown for some time, if they evaporate in a drier environment, they sometimes become supersaturated solution due to failure of solute crystal nucleation. This may induce a hysteresis effect in the behavior of the solution droplets.

5.2 The Nuclei of Atmospheric Condensation and Aerosols

As we have seen above, in the particle free air, condensation occurs only when supersaturation reaches several hundred percent. In the real atmosphere, particles serve as nuclei for condensation and prevent such a high supersaturation from being achieved. The environmental variables controlling the nuclei activation are the temperature and supersaturation which change depending on the vapor pressure and cooling rate. Whereas, the nucleus conditions also vary, such as the number concentration, size and distribution, and their nature, in terms of chemical and physical characteristics.

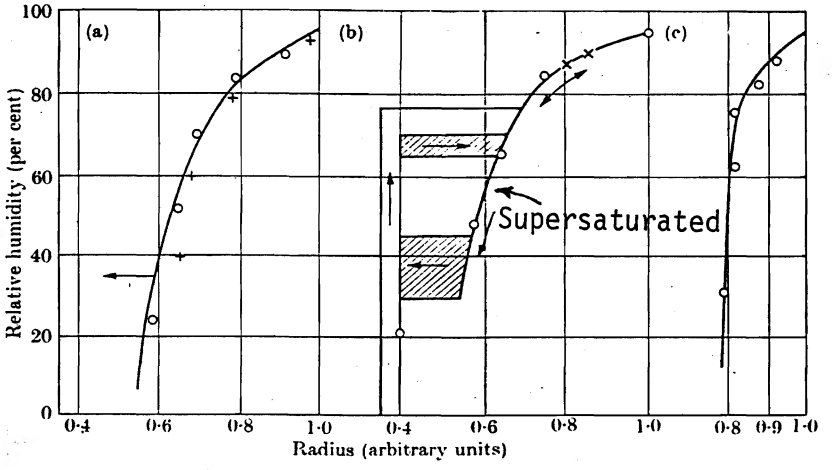

Fig. 5.12 Experimental values of the equilibrium radii of artificial nuclei as a function of relative humidity, and the corresponding theoretical curves: (a) a nucleus of pure $CaCl_2$ solution became supersaturated at $H > 35\%$. (b) A nucleus of pure NaCl--crystallization did not occur until humidity fell below 30%. The theoretical curve predicts that crystallization should have occurred at 78% relative humidity. (c) Artificial nucleus composed of mixture of $CaCl_2$ and $CaSO_4$ (From Junge, 1952).

Atmospheric nuclei are normally classified according to their sizes:

SIZE (μm)	NAME
$5x10^{-3} - 10^{-1}$	Aitken nuclei
0.1 - 1	large nuclei
r > 1	giant nuclei

Some of these terms bear the names of early workers (Coulier, 1875; Aitken, 1880-81).

5.2.1 Condensation nucleus measurement

Condensation nuclei are measured by actually activating them. Activation of Aitken nuclei requires high supersaturation, but for cloud condensation nuclei (CCN), the necessary supersaturation is rather low. Naturally, generation of supersaturation at high or low levels in a reproducible or stable manner features the methods of condensation nucleus measurement.

(a) Aitken nucleus measurement

Expansion-type counters are widely used, in which a saturated sample air is adiabatically expanded to a predetermined level to cool. Detection method of formed droplets varies. Some of the early methods let all droplets fall out, and the number concentration of nuclei or formed droplets was estimated from the number of droplets fallen on a unit area. Turbulence and non-uniform droplet distribution were common problems with this method.

One of the most successful counters for Aitken nuclei is the Nolan-Pollak counter. It uses a vertical tube with porous ceramic lining for humidification by wetting, and the top and bottom are made of glass. Allowing expansion from overpressure, supersaturation is rapidly established in which particles nucleate and grow at the same rate so that, at a given time after expansion, the light extinction is only a function of the number concentration of active nuclei. To establish the extinction-number concentration relationship, a calibration is needed with aerosol of known nucleus concentration. A counter developed by the General Electric Co., known as the Rich counter, allows the sample air to expand continuously instead of intermittently.

Expansion counters are known to be rather inaccurate for generation of low supersaturation.

(b) Cloud condensation nucleus measurement

Determination of the characteristics of condensation nuclei is a necessary step to understand the cloud formation process.

Thermal diffusion chambers are most widely used for counting CCN. The principle was originally developed by Langdorf (1936) for cosmic ray study. In the thermal-gradient version of the chamber, where the top and the bottom are covered with water, T and e profiles are linear with height z for low (S - 1) operation; but e_s is not, inducing supersaturation inside, as can be seen from the Clausius-Clapeyron equation (Fig. 5.15, Wieland, 1956). The relatively slight supersaturation held under steady state can easily be adjusted to that in the cloud. For high (S - 1) operation, T and e become non-linear and a proper kinetic treatment becomes necessary (see Section 2.4).

Detection of activated nuclei (droplets) may be photographic or photoelectric. The Univ. of Washington counter makes use of the first Mie scattering peak to estimate the total number of activated nuclei since, at that peak, the total scattering intensity is proportional to the number concentration only if the sampling volume is fixed. In this method, during sample introduction, transient supersaturation (high) often introduces a serious error.

There are continuous counters allowing sample air to continuously flow. Some use a single supersaturation and others a range of supersaturation (Fukuta-Saxena, 1979, see Figs. 5.16 and 5.17).

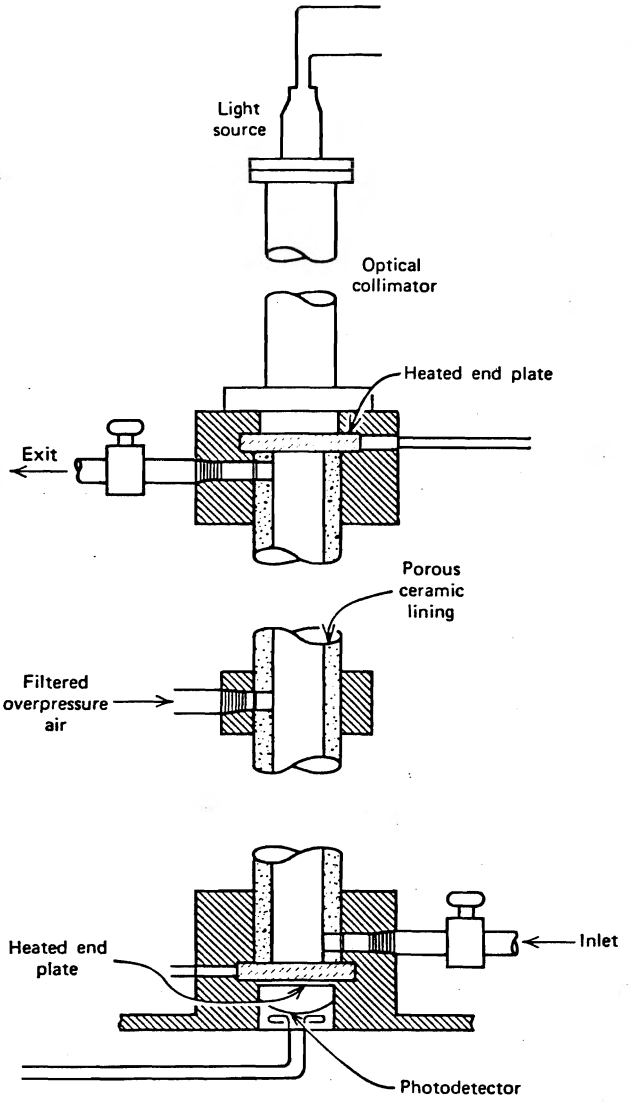

Fig. 5.13 Schematic diagram of condensation nuclei counter (Friedlander, 1977).

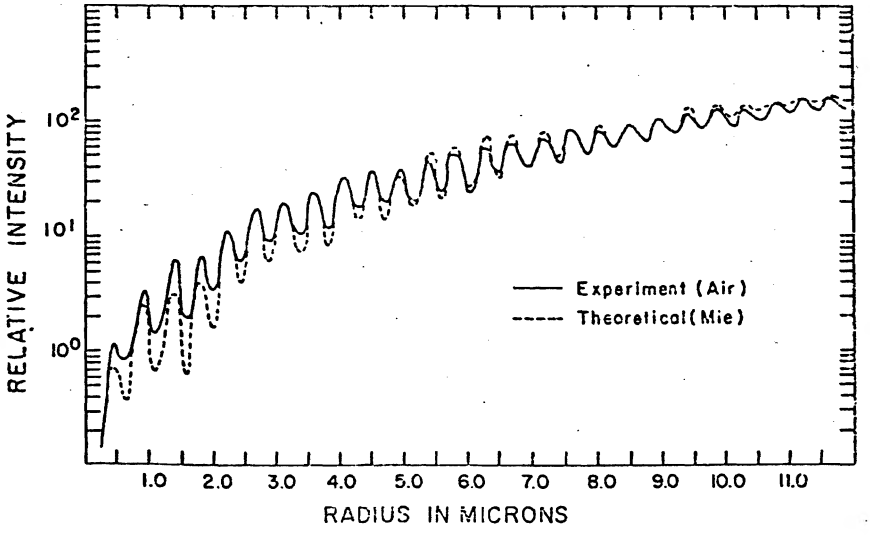

Fig. 5.14 Matching of experimentally and theoretically derived Mie peaks (after Vietti and Schuster, 1973). Wavelength of the scattering light is 632.8 A, and the angle is 30°.

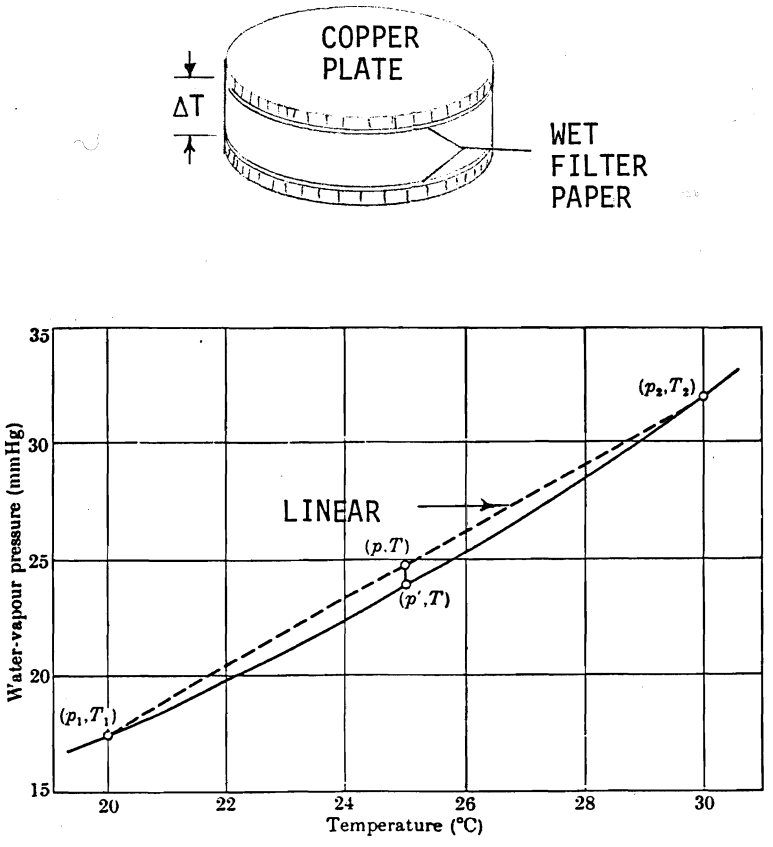

Fig. 5.15 The principle of the thermal gradient cloud chamber (Wieland, 1956).

A chemical gradient chamber was once applied using HCl solution on the bottom (Twomey), but possible sample change prevented it from being put to common use.

5.2.2 Particulate measurement

Atmospheric particulates can be measured directly while being suspended in air or by precipitating them.

(a) Direct observation methods

Diffusion and mobility measurements. For particles with radii smaller than 0.1 μm, the Brownian diffusion and ion mobility in an electric field are functions of the particle size under viscous resistance force with Cunningham's correction. Their motions can lead one to the corresponding sizes.

Ultramicroscope methods use dark field illumination of smoke particles under low magnification and are useful for size determination of particles larger than 0.1 μm in radius. The settling velocity measured gives the particle size through the Stokes-Cunningham equation.

Light scattering methods can apply to (1) whole cloud or (2) single particle. If monodispersed, scattering from whole cloud produces higher order Tyndall spectra (coloring). If particle size is close to the wavelength of light, the Mie scattering pattern can be observed, which may be used for particle size analysis (cf. Fig. 5.14).

Emission line method; N_a-D line in the hydrogen flame is an example of identifying Na-containing particles.

Laser cavity method is applied to determine aerosol particle size.

(b) Precipitation methods

Impaction techniques

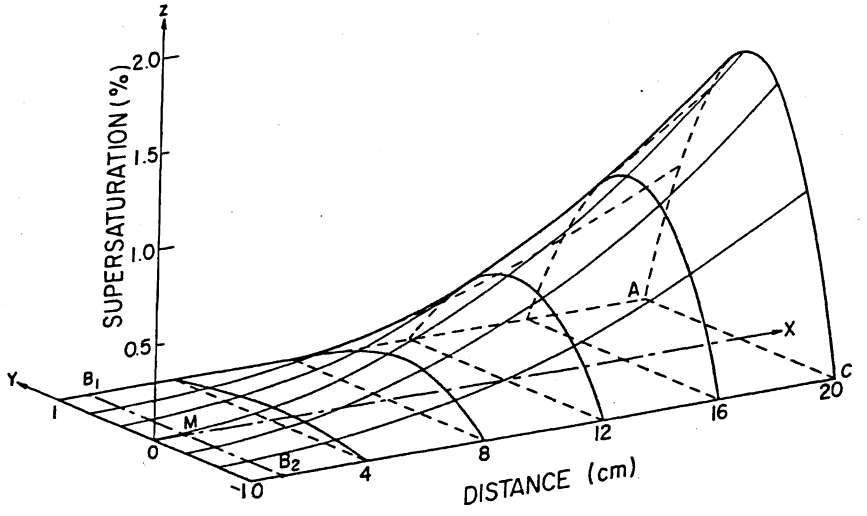

Fig. 5.16 An example of the supersaturation profile in the CCN spectrometer. Temperatures at A and C points are respectively 36 and 29°C. B_1 and B_2 positions shown here correspond to the case where a metal side wall with a finite thermal conductivity is used (Fukuta and Saxena, 1979).

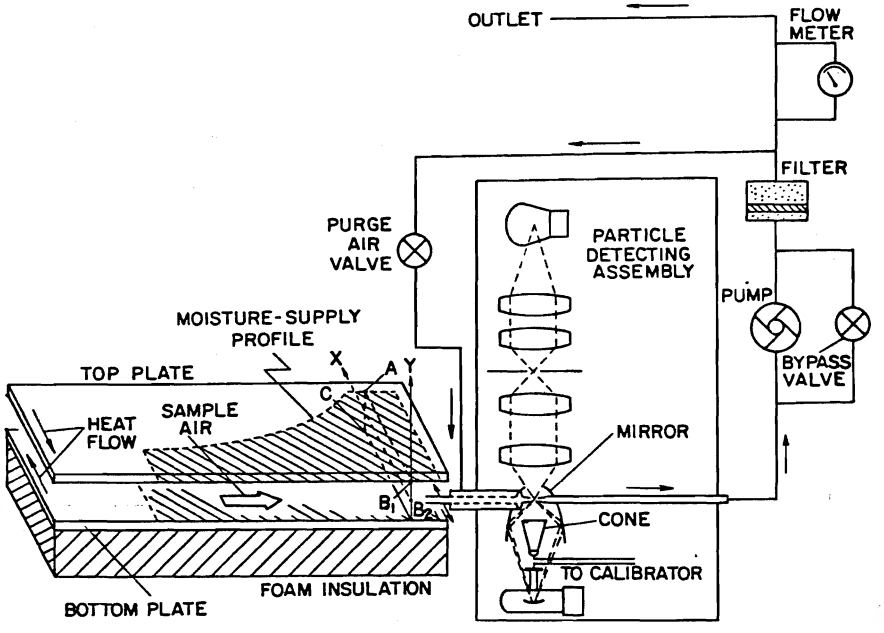

Fig. 5.17 Principle of the CCN spectrometer operation (Fukuta and Saxena, 1979).

Cascade impactor. The method is applicable to particles larger than 1 μm in diameter. The principle is to impact particles by air jets. Normally, sample air passes through a large orifice with slow speed and gradually to smaller orifices with faster air velocities. Example of air velocities: 2.2, 10.2, 27.5, and 77 m s^{-1}.

Centrifuge methods. Conifuge uses a range of centrifugal forces to settle the particles at correspondingly different positions. Two types exist: one uses flow of air to rotate and the other external force (motor) to rotate. Normally, 3000 RPM and 15 cm^3 s^{-1} are the sampling rates. For smaller particles, the Goetz spectrometer (Goetz and Preining, 1960) can be applied. It is a centrifuge of large RPM, up to 26,000 g acceleration. 0.03 - 3 μm can be separated. Dark-field illumination (ultramicroscope principle) can be applied for particle examination. Sampling rate is about 7.5 liter min^{-1}.

Rod and thread Thin silver rod or spider thread can be used in moving air to catch particles.

Thermal precipitation method

Thermophoretic force is used to precipitate particles. Sample air passes through a zone of high temperature gradient to precipitate on the colder surface. The temperature gradient is typically 50°C/0.05 cm with sample air flow rate of 7-500 cc min^{-1}. Particles above 0.05 μm in diameter deposit completely. Deposition of smaller particles is more difficult.

Filter methods

Millipore filters made of cellulose ester (acetate) membrane are frequently used to catch atmospheric particles. Hole diameter ranges from 0.1 to 1.5 μm. Air suction induces electric charge to attract particles to or near the pore surfaces so that particles smaller than pore size can

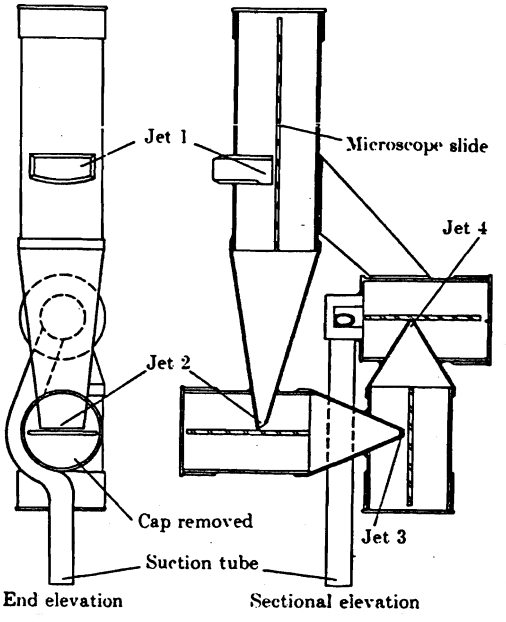

Fig. 5.18 Diagrammatic section of the cascade impactor (May, 1945).

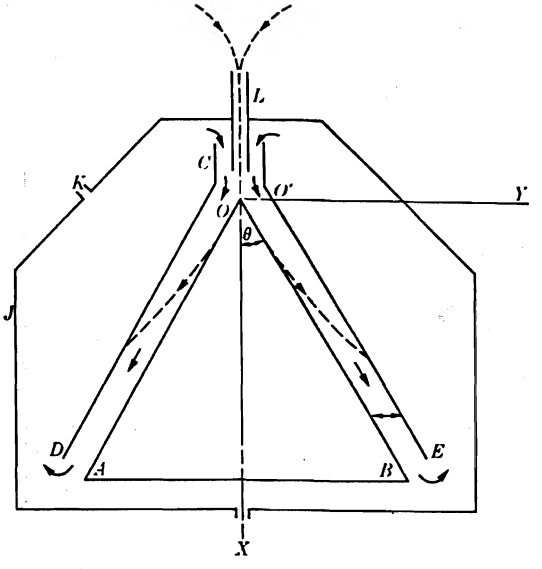

Fig. 5.19 Diagrammatic section of conifuge: —▸ clean air; --▸, particulate cloud (Sawyer and Walton, 1950).

actually be filtered. They become transparent in cedar-wood oil (refractive index: 1.54), which is convenient for microscopic observation. Millipore filters dissolve in acetone.

Nucleopore filters made of polycarbonate have uniform pore size and are advantageous for some studies.

Electron microscope can provide the shape and size of the aerosol sample held on thin plastic film. A Scanning electron microscope gives large depth of field. The electron diffraction method gives information about the sample crystal structure. An X-ray microanalyzer allows an electron beam to excite the aerosol sample (~ 1 μm diameter), and the resultant X-ray gives identification of elements in the aerosol particle.

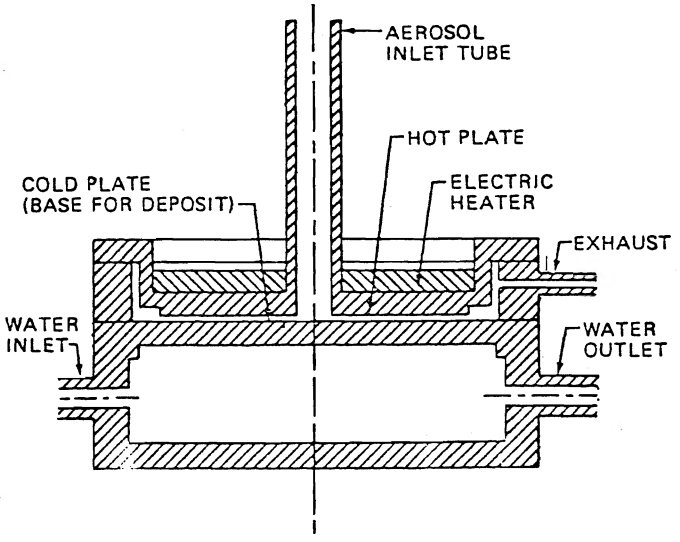

Fig. 5.20 Cross section of a plate-type thermal precipitator.

Microchemical analysis. Sometimes called the spot test. It utilizes specific chemical reaction to identify the chemical species. Example: $Cl^- + Hg_2SiF_6 \rightarrow Hg_2Cl_2\downarrow$ (Liesegang ring).

5.2.3 Nuclei in the atmosphere (see also p. 5.18)

(a) Aitken nucleus concentration

Aitken nucleus concentration varies depending on the location, in particular, the distance from the source.

Table 5.6 Nucleus contents of the atmosphere in different types of localities (Mason, 1970).

Locality	No. of places	No. of observations	Average concentrations	Average maximum	Average minimum	Average maximum	Average minimum
City	28	2500	147 000	379 000	49 000	4 000 000	35/00cm^3
Town	15	4700	34 300	114 000	5 900	400 000	620/cm^3
Country inland	25	3500	9 500	66 500	1 050	336 000	180/cm^3
Country seashore	21	2700	9 500	33 400	1 560	150 000	0
Mountain:							
500-1000 m	13	870	6 000	36 000	1 390	155 000	30
1000-2000 m	16	1000	2 130	9 830	450	37 000	0
2000 m	25	190	950	5 300	160	27 000	6
Islands	7	480	9 200	43 600	460	109 000	80
Ocean	21	600	940	4 860	840	39 800	2

The nuclei distribution also exists with altitude, but local air stability often leads to unevenness in the distribution.

Table 5.7 Average vertical distribution of nuclei from balloon ascents (Mason, 1970).

Altitude (m)	0-500	500-1000	1000-2000	2000-3000	3000-4000	4000-5000	>5000
Concentration (cm^{-3})	22 300	11 000	2500	780	340	170	80

Aitken nuclei distribution varies depending on the time of the day. In cities, a minimum is observed in the early morning before human activities start. After a maximum, the count decreases, probably due to enhanced upward transportation of air near the ground. As convective activities die down and vehicular activities increase towards late afternoon, an increase is observed, which is followed by a fall during the night (see pp. 5.34 and 5.35).

High humidity in the air seems to give low counts, presumably due to hygroscopic nuclei swell and coagulation of smaller Aitken nuclei on them. There is also the possibility of photochemical processes for particle production.

(b) Large and giant nuclei

According to Junge, the differential expression of the number concentration

$$n'(r) = \frac{dN}{d(\log r)} = \frac{A}{r^3}, \qquad (5.36)^*$$

$$= \frac{B}{m}, \qquad (5.37)$$

where N is the number of particles for the size r, A, and B constants, and m the mass (see Fig. 5.22).

Aitken nuclei, despite their large number, amount to only 20% of the aerosol mass. Aitken nuclei over the ocean seem to be independent of wind speed and height of waves.

5.2.4 Cloud condensation nuclei in the atmosphere

The active number of CCN depends on supersaturation, and the number concentration is often expressed as

$$N \simeq C(S - 1)^k, \qquad (5.38)$$

where C and k are constants. According to Twomey, the average of large numbers of observations results in $k \simeq \frac{1}{2}$ (see figures below).

In clean polar air mass, CCN concentration is as low as a few tens/cc, which is also the Aitken nuclei number concentration. In polluted air, the CCN count can be as high as 10^4/cc.

---

*$n(r) = \frac{dN}{dr} \propto r^{-4}$

The relationship between the CCN concentration and the cloud droplet concentration exists through the maximum supersaturation the cloud air parcel experiences. However, it is the result of interaction between the nucleation and the growth of nucleated droplets in the changing cloud environment; and its estimation requires proper consideration of the process and will be explained in a later chapter.

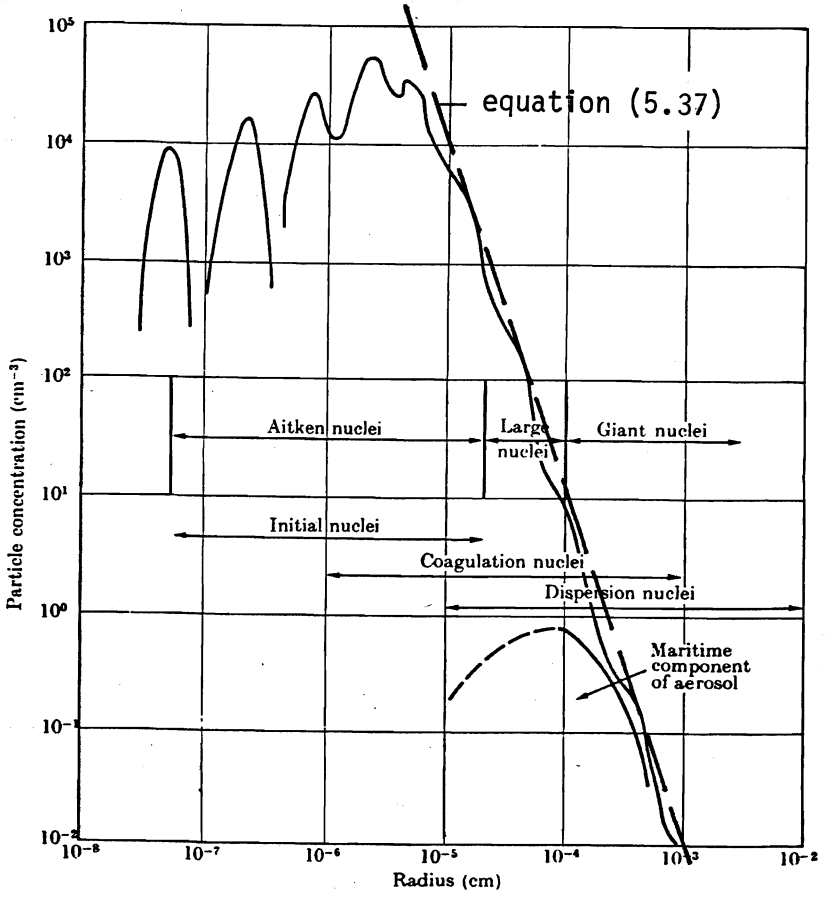

Fig. 5.21 A generalized representation of the size distribution of natural aerosols in heavily polluted air over land (Junge, 1952).

5.2.5 Chemical composition of atmospheric particles

Atmospheric particulates are physically (i) solid, (ii) liquid, or (iii) a mixture. Particles tend to swell as a function of humidity. Above 70% RH, the majority of mixed nuclei becomes droplets.

Aitken nuclei: the chemical composition is not well understood.

$(NH_4)_2SO_4 \leftarrow NH_3 + SO_2 + O_2$, mostly in large particles. Some contain excess H_2SO_4. Industrialized areas produce more nuclei of this sort, causing acid rain problems. Sulphur has a large marine origin in the forms of dimethylsulfide (DMS) and the derivatives emitted from marine phytoplanktons.

Cl^- exists in air mass of maritime origin and is mostly in giant nuclei.

NO_x (NO_3^-, NO_2, NO etc.) is another contributor to acid rain. Particulates in the form of NO_3 exist in photochemical air pollution involving automobile exhaust.

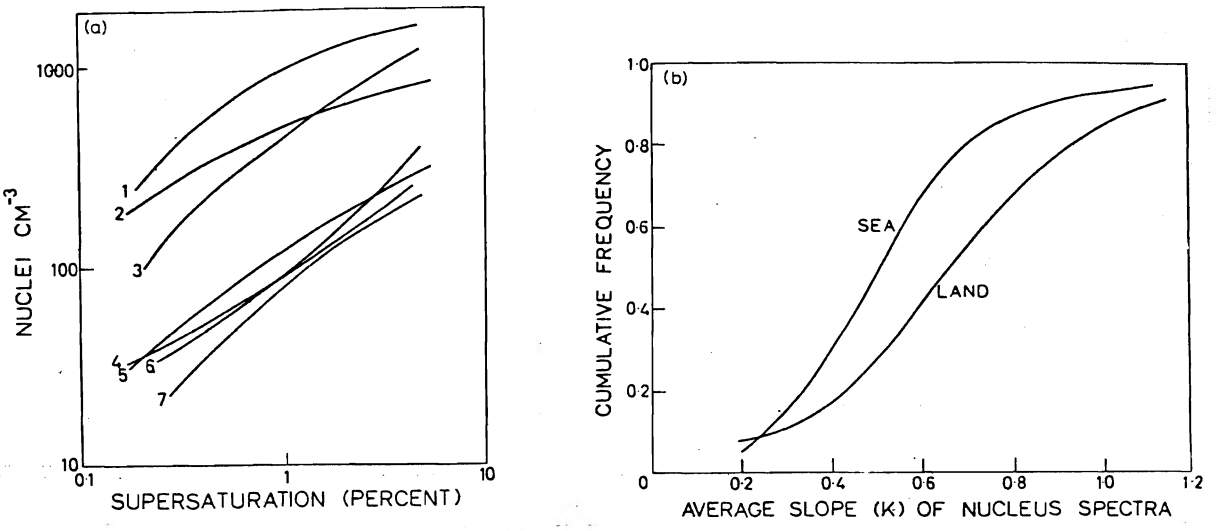

Fig. 5.22 (a) Experimentally measured supersaturation spectra from aircraft measurements in different geographic regions. Note the systematic difference between maritime and continental air. The numbers on these curves indicate the region, as follows: 1 = continental, Australia; 2 = continental, U.S.; 3 = continental, Africa; 4 = oceanic, South Pacific; 5 = oceanic, North Atlantic; 6 = oceanic, South Atlantic; 7 = oceanic, North Pacific. (b) Distribution of the slope parameter k among the data leading to the previous figure.

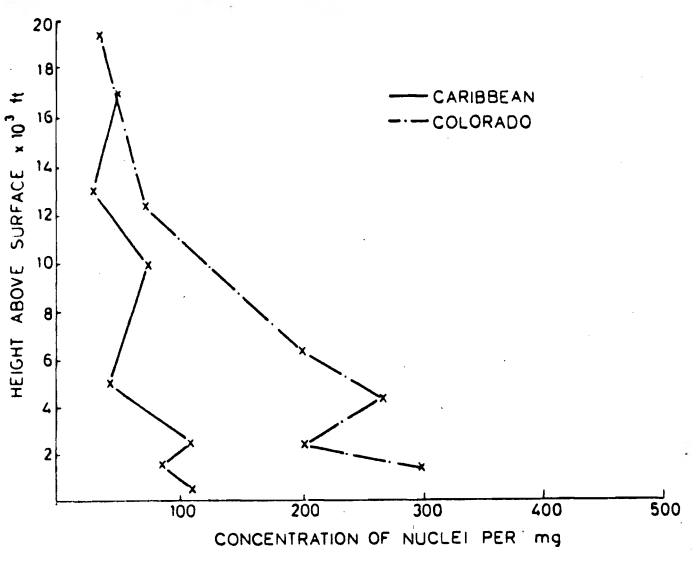

Fig. 5.23 Comparison of vertical profiles of cloud nuclei over Colorado and over the Caribbean Sea.

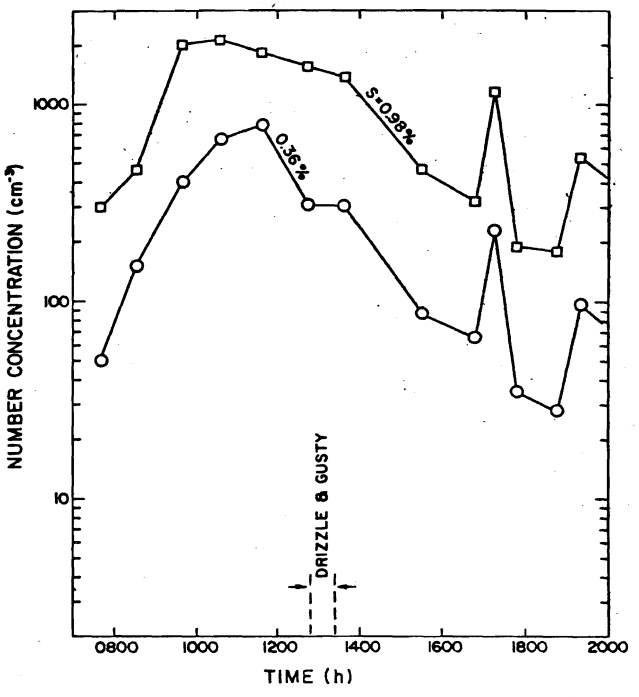

Fig. 5.24 CCN concentration obtained by the spectrometer on 9 August 1974 for the Denver aerosol (18.5 m above the ground).

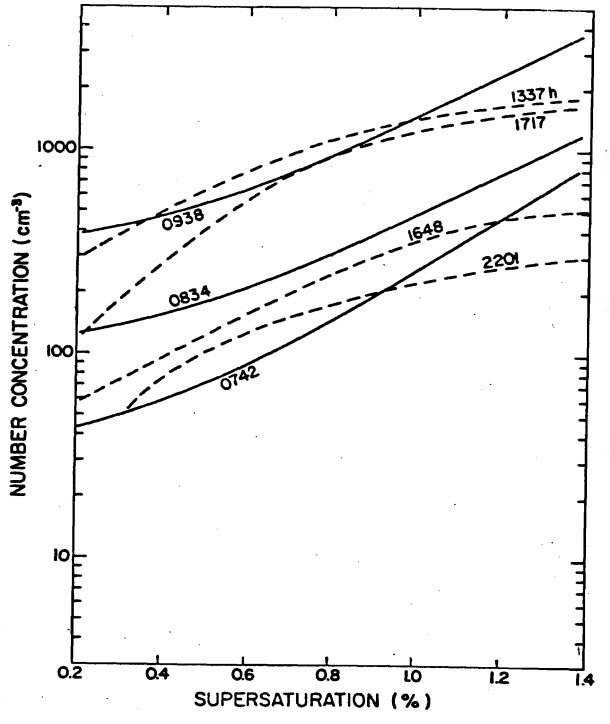

Fig. 5.25 CCN spectrum recorded at different times of the day on 9 August 1974 for the Denver aerosol (18.5 m above the ground).

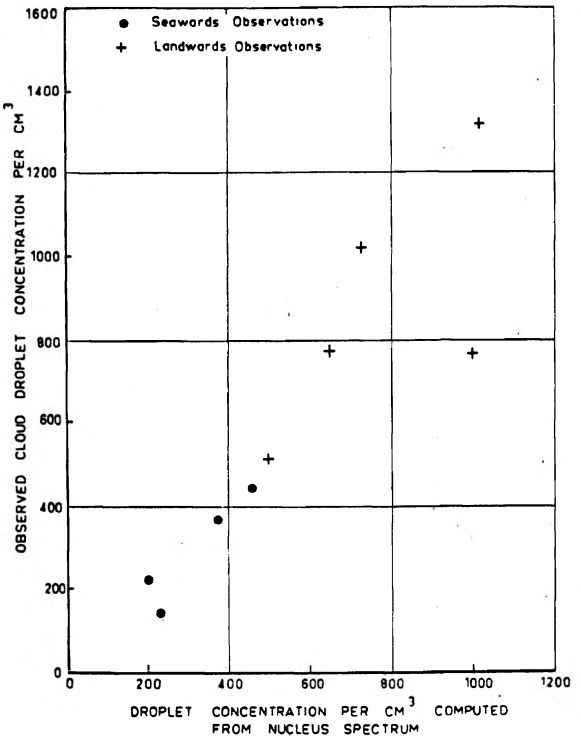

Fig. 5.26 Comparison of cloud drop concentration directly measured in the cloud with predicted from measurements of cloud nuclei in air below the cloud base. This diagram also shows an influence of man-made pollution: dots refer to samples in trade wind air before crossing the Queensland coast, crosses to air which had crossed the coast and been polluted by extensive cane fires.

Combustion products are very commonly found among all particulates.

Effect of location: In mid ocean areas, mostly water soluble particles are found and are large. In industrial areas, only 20% of particulate weight is water soluble, the remainder being soot, tar, ashes, and mineral dusts.

5.2.6 Production of natural aerosol particles

There are two basic mechanisms of particle production: (i) condensation and (ii) dispersion. The former involves nucleation of condensation (particle) and the latter mechanical breaking of existing condensed phase.

(a) Particle production by combustion and by chemical reaction (condensation)

Sulphur compounds

Gases for chemical reaction:

H_2S as well as DMS and the derivatives are major S-containing natural gases, and SO_2 is either their oxidation product or of anthropogenic origin.

Liquid:

H_2SO_4 forms by oxidation of SO_2 and other S-containing gases, and the reaction is fast in solution in cloud droplets. It tends to combine with NH_3 to form $(NH_4)_2SO_4$.

Solid:

$(NH_4)_2SO_4$ is an important CCN (for chemical constants, see p. 5.13).

Oxides of nitrogen

N_2O: very stable and inert

NO_2: forms by reactions

$NO + O_2 \rightarrow NO_2$ or $NO + O_3 \rightarrow NO_2 + O_2$.

NO_2 serves to form nitric acid (HNO_3) and its compounds.

HNO_3 in liquid form: $NO_2 + H_2O \rightarrow HNO_3 + NO\uparrow$.

NO_3^-: $HNO_3 + NaCl \rightarrow NaNO_3 + HCl\uparrow$. This may be one of the reasons for Cl/Na ratio reduction.

Ammonia, NH_3

Source: decaying organic matter (protein)

Sink: ocean, acidic soil and formation of $(NH_4)_2SO_4$

Chlorine

Gaseous form: the origin is probably HCl from industries and oceans -- $H_2SO_4 + NaCl \rightarrow Na_2SO_4 + HCl\uparrow$

Solid: NaCl

Sodium

Sodium exists in the form of NaCl. Others: Na_2SO_4 (or $NaHSO_4$), $NaNO_3$. Ratios K/Na and Mg/Na in aerosol particles increase with increasing distance from the coast. Smaller sea salt droplets are enriched with K and Mg during the spraying processes. They seem to be associated with organic compounds which adsorb at the surface.

The chemical reactions for aerosol formation can be assisted by ultraviolet light and ozone.

(b) Ocean contributions

Sea salt nuclei

Bursting bubbles are supplying sources of sea salt nuclei. Small bubbles (smaller than 0.2 mm) do not produce nuclei. Over the areas of breaking waves, the concentration can be 100 cm^{-3}, with a production rate of 10^3 $cm^{-2}s^{-1}$.

Derivatives of dimethylsulfide

Although these processes take place, the major contribution of ocean to aerosols and CCN appears to be DMS, a product of planktonic algae (phytoplankton) which subsequently forms sulfate aerosol after oxidation. Clouds appear to help formation of sulfate-based CCN from DMS.

(c) Production of nuclei over the continents

Over the land, primary production of aerosol particles depends on

combustion
chemical reactions involving trace gases, particularly in the presence of liquid water
raising of soil and dust particles, and
emission of pollen and volatile substances, such as H_2S, DMS, methanethiol (CH_3SH), CS_2, COS and others.

Anthropogenic production of nuclei is significant.

According to Squires, CCN active at 0.5% supersaturation,

Production rate over USA is	~500 cm^{-2} s^{-1}
Production rate over northern hemisphere	~200
Production rate over a city	~10^4
Aitken nuclei over a city	~10^5
Man-made CCN over USA	~14%
Man-made CCN over northern hemisphere	~ 5%

Mineral dusts are being transported from the land surface to ocean. Quartz particles deposited in the Pacific Ocean are between 0.5 and 15 μm in radius.

5.2.7 Removal of aerosol particles from the troposphere

The aerosol particles can be removed from the troposphere by the following four possible mechanisms.

(1) Fall out: effective for large particles of 10-20 μm in radius.

(2) Washout:

- CCN and IN (ice nuclei) into cloud and subsequent precipitation elements (cloud droplets, rain, snow, etc.) (nucleation scavenging)
- Attachment of aerosol particles to cloud elements; by
  Brownian motion
  diffusiophoresis
  thermophoresis.
- Dynamic impaction by falling cloud elements.

(3) Brownian coagulation of aerosol particles.

(4) Evaporation?

Particles in the size range between 1 and 0.1 μm do not easily coagulate and the efficiency of their removal by rain and snow is also low (Greenfield gap, further explanation in a later chapter). In this regard, the cloud formation (condensation) process which increases the particle size, drastically changes the particle removal rate of the size range. There also exists evidence that clouds help CCN generation and removal. When snow crystals grow, surrounding cloud droplets evaporate leaving the nucleus material behind. Although the crystals may collide with cloud droplets later, they are relatively free from the nucleus material. The reverse is effective with graupel and hail.

5.3 Condensation Growth and Evaporation of Cloud Droplets

The nucleation process of cloud droplets discussed in the preceding section is immediately followed by their growth in the supersaturated environment in which vapor diffusion towards the droplets and condensation result in generation of latent heat of the phase change.

5.3.1 The system involving a growing droplet

When a droplet is growing in the supersaturated environment, the water vapor arriving at the surface releases the latent heat of condensation. The system automatically establishes (a) a steady state balance[3] between the rate of heat generation and that of the removal by sensible heat conduction away from the surface (b) by satisfying the boundary conditions at its inner surface, i.e. droplet surface, and at its outer extreme, i.e. the environment.

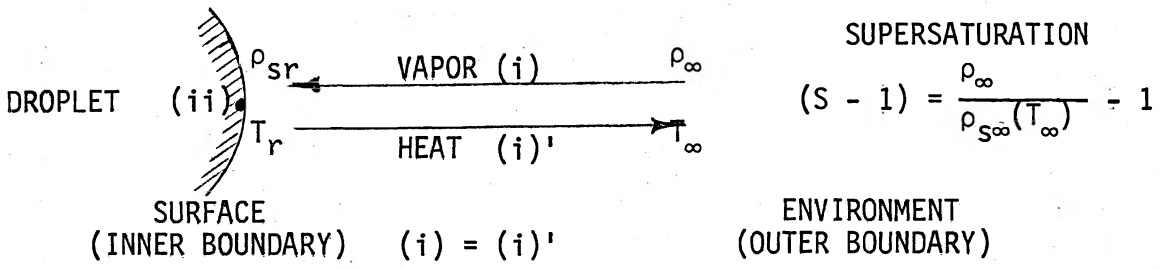

Fig. 5.27 Maxwellian system of growing droplet.

(a) Fick's law of diffusion (see Section 2.4)

The mass of water vapor m transported in the x direction in a unit time through an area A by molecular diffusion without temperature gradient is given by Fick's law

$$\frac{\vec{dm}}{dt} = -AD\frac{d\rho}{dx}, \qquad (5.39)^4$$

where ρ is the vapor density and D the diffusivity of water vapor in air. Equation (5.39) can be used to describe the vapor transportation process to the droplet.

(b) Fourier's law of heat conduction

---

[3] Strictly speaking, this is a quasisteady state balance because the condensing water vapor increases the droplet radius and advances the surface outward. The steady state processes survive better than time-dependent processes and often prevail in the atmosphere. In the steady state, the properties at an arbitrary point of space coordinate do not change with time, and its domination may be compared with that of the highest resistance process in a sequential phenomenon.

[4] Fuchs (1959) introduced an effect of the Stefan flow to alter the diffusional flux of vapor (see Section 3.6), and Clement (1985) and Seinfeld (1985) both appeared to have elaborated the effect. However, the effect has no physical foundation and is merely a result of misunderstanding the system involving the transport process.

Similar to the vapor diffusion, the heat energy transported in the x-direction in a unit time through an area A by conduction mechanism without simultaneous vapor transportation is given by Fourier's law

$$\frac{\vec{dQ}}{dt} = -AK\frac{dT}{dx}, \tag{5.40}$$

where Q is the amount of heat energy and K the thermal conductivity of air.

Although vapor diffusion and heat conduction are simultaneously taking place during the droplet growth process, under such slight gradients of heat and vapor density, their influences on the others are expected to be small. Therefore, such secondary terms are normally ignored for atmospheric droplet growth processes by vapor diffusion.

5.3.2 Droplet growth: Maxwellian theory

The simplest steady-state model of droplet growth, first applied by J.C. Maxwell, features the continuous vapor and temperature fields at the droplet surface. The theory is also applicable to the wet-bulb temperature on a quiescent thermometer (see Section 1.6).

Suppose a single droplet grows in an infinite quiescent and supersaturated environment and maintaining a quasi-steady state. The space surrounding the droplet allows diffusion of vapor towards and conduction of heat away from the surface. Since there is no source or sink of vapor and heat in the space and there is no density change, at all the space points due to the steady states, the continuity equation for vapor diffusion [Eq. (2.32)] leads to

$$\nabla^2\rho = 0. \tag{5.41}$$

An equation of this form is called Laplace's equation.

Similarly, the continuity equation for heat conduction leads to

$$\nabla^2 T = 0. \tag{5.42}$$

The solution of Laplace's equation around the droplet can be obtained from the form using the spherical coordinate (see Appendix B). Here, however, to make the physical process more visible, we use an intuitive approach considering the fluxes of water vapor and heat through the spherical surface concentric to a quiescent droplet.

(a) The vapor density field

Using Eq. (5.39), the mass arrival rate on the surface of a spherical droplet of radius r is

$$\frac{dm}{dt} = AD\frac{d\rho}{dr} = 4\pi r^2 D\frac{d\rho}{dr} = C_1, \quad \text{(under steady state)} \tag{5.43}$$

where C_1 is a constant. Integration of Eq. (5.43) yields the form

$$(\rho) = -\frac{C_1}{4\pi D}\left[\frac{1}{r}\right], \tag{5.44}$$

which, under the boundary conditions (r=r, $\rho=\rho_{sr}$) and ($r=\infty$, $\rho=\rho_\infty$) leads to[5]

$$\rho = \rho_\infty - (\rho_\infty - \rho_{sr})r\left[\frac{1}{r}\right], \tag{5.45}$$

where r and r are the droplet radius and the radial distance of the coordinate and ρ_{sr} and ρ_∞ the saturated vapor density at the droplet surface and that in the environment, respectively.

From Eq. (5.45) by differentiation, we have the vapor density gradient

$$\frac{d\rho}{dr} = \frac{(\rho_\infty - \rho_{sr})r}{r^2}. \tag{5.46}$$

(b) The temperature field

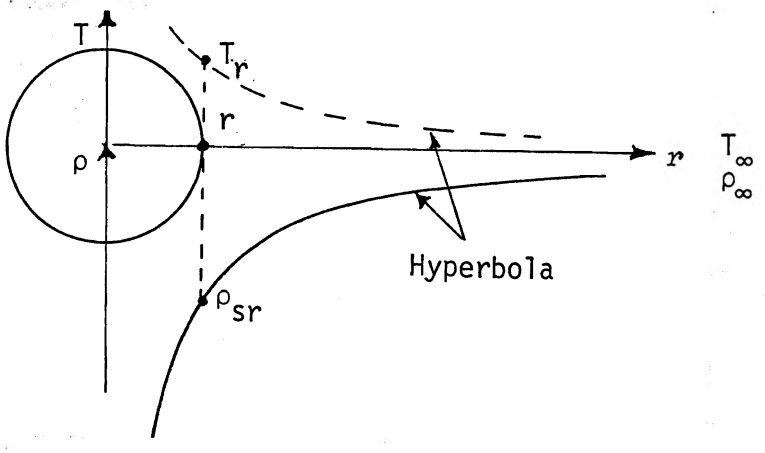

Fig. 5.28 Vapor density and temperature fields around a Maxwellian growing droplet.

The method of obtaining the temperature field is identical to that of vapor, except that the direction of the heat flow is opposite.

Treating Eq. (5.40) in a way similar to Eq. (5.45), we have

$$T = T_\infty - (T_\infty - T_r)\frac{r}{r}. \tag{5.47}$$

The temperature gradient can be obtained by differentiating Eq. (5.47) with r;

$$\frac{dT}{dr} = \frac{(T_\infty - T_r)r}{r^2}. \quad \text{(negative)} \tag{5.48}$$

(c) The restricting conditions for droplet growth

---

[5] $\rho - \rho_o = -\frac{C_1}{4\pi D}\left[\frac{1}{r} - \frac{1}{r_o}\right]$ where at $r = r_o$, $\rho = \rho_o$. When $r = \infty$, $\rho = \rho_\infty$, $\rho_\infty - \rho_o = \frac{C_1}{4\pi D r_o}$ or $-\rho_o = \frac{C_1}{4\pi D r_o} - \rho_\infty$. Then, $\rho - \rho_\infty = -\frac{C_1}{4\pi D}\frac{1}{r}$. Then $r = r$, $\rho = \rho_{sr}$, and $C_1 = 4\pi D(\rho_{sr} - \rho_\infty)r$. Hence $\rho = \rho_\infty - \frac{(\rho_\infty - \rho_{sr})r}{r}$.

The above equations contain two unknowns, ρ_{sr} and T_r. In order to solve them, two equations describing their connection are needed. They are

(i) the equation to describe the continuity (equivalence) of the vapor and the heat fluxes, and

(ii) flux connection at the droplet surface with the Clausius-Clapeyron equation.

Of course, both equations should satisfy the outer boundary condition.

Condition (i) is expressed as

$$L_c \frac{dm}{dt} = L_c \left(\frac{\vec{dm}}{dt}\right) = \left(\frac{\vec{dQ}}{dt}\right) \cdot \left(\frac{dm}{dt}; \text{ absolute}\right). \tag{5.49}$$

For condition (ii), or the Clausius-Clapeyron equation (1.62″), we use the linearized (truncated) form, including the present boundary conditions:[6]

$$\ln(e_{sr}/e_{s\infty}) = \frac{L_c}{R_v}\left(\frac{1}{T_\infty} - \frac{1}{T_r}\right) = (e_{sr}/e_{s\infty}) - 1. \tag{5.50}$$

(d) The derivation of growth equation

Using the above relationships, we shall first solve for ρ_{sr} and T_r and then obtain the gradient term of Eq. (5.39) to describe the growth rate. We now change Eq. (5.50) into the vapor density equation using the ideal gas law,

$$e = \rho R_v T, \tag{5.51}$$

that is, if T variation is not large, $T_r \simeq T_\infty$ and $e \propto \rho$ relationships may be applied to obtain

$$\frac{L_c(T_r - T_\infty)}{R_v T_\infty^2} = \frac{\rho_{sr}}{\rho_{s\infty}} - 1. \tag{5.52}$$

(A more accurate treatment of the e–ρ relationship will be given later.) From Eq. (5.49), with Eqs. (5.40), (5.43), (5.46), and (5.48), we have

---

[6] When $-1 < x \leq 1$, $\ln(1+x) = x - \frac{1}{2}x^2 + \frac{1}{3}x^3 - ---$. Setting $x = (e_{sr}/e_{s\infty}) - 1$,

$$\ln(e_{sr}/e_{s\infty}) = \left(\frac{e_{sr}}{e_{e\infty}} - 1\right) - \frac{1}{2}\left(\frac{e_{sr}}{e_{s\infty}} - 1\right)^2 + --- \approx \frac{e_{sr}}{e_{s\infty}} - 1.$$

$$-\frac{T_r - T_\infty}{\rho_{sr} - \rho_\infty} = \frac{DL_c}{K}. \qquad (5.53)^7$$

From Eqs. (5.52) and (5.53), we can now solve ρ_{sr} and T_r. Dividing Eq. (5.52) with Eq. (5.53),

$$\frac{DL_c^2 \rho_{s\infty}}{KR_v T_\infty^2} = \frac{-(\rho_\infty - \rho_{sr}) + (\rho_\infty - \rho_{s\infty})}{(\rho_\infty - \rho_{sr})},$$

or

$$\rho_{sr} = \rho_\infty - \frac{(S-1)}{\left(\frac{DL_c^2}{KR_v T_\infty^2} + \frac{1}{\rho_{s\infty}}\right)} = \rho_\infty - \frac{(S-1)}{\left(\frac{DL_c^2}{KR_v T_\infty^2} + \frac{R_v T_\infty}{e_{s\infty}}\right)}, \qquad (5.54)$$

where $S = \rho_\infty/\rho_{s\infty}$ is the saturation ratio in the environment. Replacement of Eq. (5.54) into Eq. (5.53) leads to

$$T_r = T_\infty + \frac{(S-1)}{\left(\frac{L_c}{R_v T_\infty^2} + \frac{K}{DL_c \rho_{s\infty}}\right)}. \qquad (5.55)$$

The droplet growth rate can, therefore, be obtained by inserting Eq. (5.54) into Eq. (5.46) and using Eq. (5.43).

$$\frac{dm}{dt} = \frac{4\pi r(S-1)}{\left(\frac{L_c^2}{KR_v T_\infty^2} + \frac{1}{D\rho_{s\infty}}\right)} = \frac{4\pi r(S-1)}{(a' + b')}, \qquad (5.56)$$

where $a' = f(T) = L_c^2/KR_v T_\infty^2$; and $b' = f(p,T) = 1/D\rho_{s\infty}$ are constants which depend on the environmental variables, p and T.

(e) The temperature correction (Mason, 1971)

The assumption $e \propto \rho$ is only valid under constant temperature; and if the temperature variation appears in its application, a correction is necessary.

---

[7] $T_r - T_\infty$ of Eq. (5.53) corresponds to the wet bulb temperature difference of kinetic definition, since from Eq. (2.31), Eq. (1.110) reads

$$-\frac{(T_r - T_\infty)}{(\rho_{sr} - \rho_\infty)} = \frac{\kappa L_c}{K} \quad (\kappa\text{: thermal diffusivity})(\text{Thermodynamic}),$$

which is in contrast to $\frac{DL_c}{K}$ (Kinetic).

Since $D > \kappa$, the latter is smaller than the former.

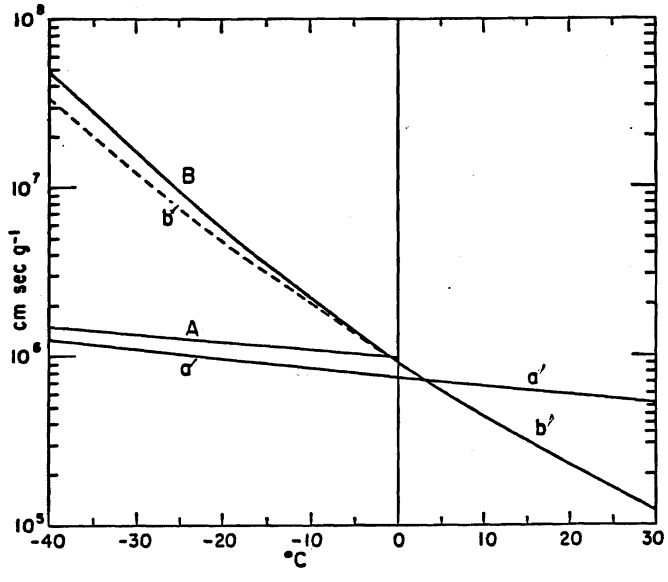

Fig. 5.29 Terms in denominator of Eqs. (5.56) (a', b') and (A,B) (for ice crystal growth) as function of temperature at a pressure (applicable to b' and B) of 1000 mb. At other pressures, B and b' would have p/1000ths of the given values (Byers, 1965).

From the ideal gas law,

$$d\ln e = d\ln\rho + d\ln T.$$

Using this in the Clausius-Clapeyron equation,

$$d\ln\rho_s + d\ln T = \frac{L_c dT}{R_v T^2},$$

which, after integration from (T_∞, $\rho_{s\infty}$) to (T_r, ρ_{sr}), results in

$$-\frac{L_c}{R_v}\left(\frac{1}{T_r}-\frac{1}{T_\infty}\right) = \ln\frac{\rho_{sr}}{\rho_{s\infty}} + \ln\frac{T_r}{T_\infty}.$$

Expanding the right-hand terms as shown on p. 5.35 and taking the first terms, we have

$$\frac{T_r - T_\infty}{T_\infty}\left(\frac{L_c}{R_v T_\infty} - 1\right) = \frac{\rho_{sr}}{\rho_{s\infty}} - 1. \qquad (5.57)$$

The use of $\left(\frac{L_c}{R_v T_\infty} - 1\right)$ in place of $\frac{L_c}{R_v T_\infty}$ will make the value smaller by 5%.

(f) Effects of the solute and the size of droplet: Maxwellian theory

In the Maxwellian theory, we have handled so far a pure water droplet without the surface curvature effect. If the droplet is very small and contains solute, the Kelvin effect and the Raoult law have to be included. The overall effect can be estimated in a way similar to that described in Section 5.1.6.

Expressing the vapor pressure of the droplet showing the Kelvin and Raoult effects by ρ'_{sr} in an isothermal system,

$$\frac{\rho'_{sr}}{\rho_{s\infty}} = \frac{\rho'_{sr}}{\rho'_{s\infty}}\frac{\rho'_{s\infty}}{\rho_{s\infty}} \simeq 1 + \frac{a}{r} - \frac{b}{r^3}, \qquad (5.33)$$

where ($'$) and the subscript ∞ stand for solution and flat surface, respectively. This vapor density change will also cause T shift in the flux balance equation (5.53), and the equation now takes T_r and ρ'_{sr} (see the schematic drawing below). Whereas, the second equation, i.e., the Clausius-Clapeyron equation (5.52), describes the relationship between the vapor pressure (density) of pure water

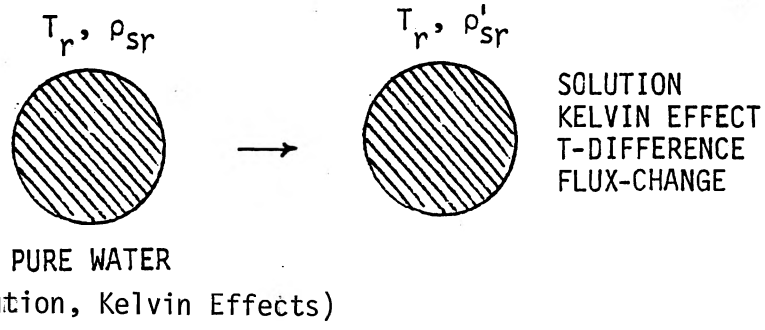

Fig. 5.30 Vapor pressure of a solution droplet with an elevated temperature T_r.

with flat surface and the temperature. Because of that, it takes T_r and $\rho_{s\infty}$. Since T_r is common, we can apply the same treatment which led to Eq. (5.54).

At the surface now, ρ_{sr} (Eq. 5.52) $= \rho'_{sr} \Big/ \left[1 + \frac{a}{r} - \frac{b}{r^3}\right]$, and setting ρ_{sr} (Eq. 5.52) $= \rho'_{sr}$ in Eq. (5.53), we have

$$\frac{DL_c^2 \rho_{s\infty}}{KR_v T_\infty^2} = \frac{-\left[\rho_\infty - \rho'_{sr} \Big/ \left[1 + \frac{a}{r} - \frac{b}{r^3}\right]\right] + (\rho_\infty - \rho_{s\infty})}{\rho_\infty - \rho'_{sr}}$$

$$= \frac{-(\rho_\infty - \rho'_{sr}) + \rho'_{sr}\left[-\frac{a}{r} + \frac{b}{r^3}\right] + (\rho_\infty - \rho_{s\infty})}{\rho_\infty - \rho'_{sr}},$$

which gives, with $\rho'_{sr} \simeq \rho_{s\infty}$,

$$\rho_\infty - \rho'_{sr} = \frac{S - 1 - \frac{a}{r} + \frac{b}{r^3}}{\left[\frac{DL_c^2}{KR_v T_\infty^2} + \frac{1}{\rho_{s\infty}}\right]}. \tag{5.58}$$

The growth rate is, therefore, from Eq. (5.43), with Eq. (5.58) substituted into Eq. (5.46) under ρ_{sr} (Eq. 5.52) $= \rho'_{sr}$,

$$\frac{dm}{dt} = \frac{4\pi r\left[S - 1 - \frac{a}{r} + \frac{b}{r^3}\right]}{\left[\frac{L_c^2}{KR_v T_\infty^2} + \frac{1}{D\rho_{s\infty}}\right]} = \frac{4\pi r\left[S - 1 - \frac{a}{r} + \frac{b}{r^3}\right]}{(a' + b')}. \tag{5.59}$$

(g) Time variation of mass and size for a growing droplet: constant supersaturation

To evaluate the time variation, we write Eq. (5.56) in the form

$$\frac{dm}{dt} = 4\pi r^2 \rho_w \frac{dr}{dt} = Cr, \quad (S: \text{ constant}) \tag{5.60}$$

where ρ_w is the density of liquid water and C is a constant. By rearranging, Eq. (5.60) gives

$$\frac{dr^2}{dt} = \text{constant.} \quad \text{(area increase rate)} \tag{5.61}$$

Integration of Eq. (5.60) results in

$$\frac{4\pi\rho_w}{C}\left(\frac{r^2}{2} - \frac{r_o^2}{2}\right) = t - t_o,$$

where r_o is r at t_o. If r_o is sufficiently small, taking t_o at the time origin,

$$\frac{2\pi\rho_w}{C} r^2 = t \quad \text{or} \quad \underline{r^2 \propto t}. \tag{5.62}$$

Inserting the mass $m = (4/3)\pi r^3 \rho_w$ into Eq. (5.62), we have

$$m = \frac{4\pi\rho_w}{3}\left(\frac{C}{2\pi\rho_w}\right)^{3/2} t^{3/2} \quad \text{or} \quad m \propto t^{3/2}. \tag{5.63}$$

This and Eq. (5.62) are the typical feature of Maxwellian droplet growth under constant supersaturation.

(h) Droplet growth under a supersaturation linearly changing with time

At slightly above the cloud base, there exists a zone of linear supersaturation change with time (details will be given in the chapter on Microphysics Dynamics Interaction). Setting

$$S - 1 = C't, \tag{5.64}$$

and using Eqs. (5.56), (5.60), and (5.64), we obtain

$$rdr = \frac{C''}{4\pi\rho_w} tdt, \quad \left[C'' = \frac{4\pi C'}{(a + b)}\right]$$

which, by integration, yields

$$r^2 - r_o^2 = \frac{C''}{4\pi\rho_w}(t^2 - t_o^2), \tag{5.65}$$

where $r = r_o$ at $t = t_o$, and C' and C'' are constants. When $r_o = t_o = 0$, $r \propto t$.

5.3.3 Droplet growth: Diffusion-kinetic theory
(Fukuta and Walter, 1970)

When mass or heat is being exchanged between gaseous and condensed phases, there normally exists inefficiency. The inefficiency is expressed by accommodation coefficients defined at respective interfaces (see Section 2.5). The effect of accommodation coefficients has to be included, and the theory which handles the effect is called the diffusion-kinetic theory. The droplet system, which deals with the effect, is shown below.

• Problem 1

Estimate size and mass of a droplet after 10 min growth under the following conditions: S-1=0.002 (0.2%), T=273.2 K (0°C), p=1 atm. $K=5.73 \times 10^{-5}$ cal cm^{-1} s^{-1} K^{-1}, $D=2.25 \times 10^{-1} cm^{-2}$ s^{-1}, $L_c=597.3$ cal g^{-1}, $R_v=R^*/M$, $R^*=8.314$ J mol^{-1} $K^{-1}=1.986$ cal mol^{-1} K^{-1}, $M=18.016$ g mol^{-1}, $\rho_{s\infty}=4.847 \times 10^{-6}$ g cm^{-3}, r=0 at t=0, $\rho_w=1.0$ g cm^{-3}.

$$C = \frac{4 \times 3.142 \times 0.002}{\left[\frac{18 \times (5.973 \times 10^2)^2}{5.73 \times 10^{-5} \times 1.986 \times (2.732 \times 10^2)^2} + \frac{1}{4.847 \times 10^{-6} \times 2.25 \times 10^{-1}}\right]} = \frac{2.514 \times 10^{-2}}{0.756 \times 10^6 + 0.9166 \times 10^6}$$

$$= 1.503 \times 10^{-8}.$$

Using Eq. (5.62)

$$r^2 = \frac{1.503 \times 10^{-8} \times 600}{2 \times 3.142 \times 1} = 1.435 \times 10^{-6} \qquad \underline{r = 11.97 \times 10^{-4} cm = 11.97\ \mu m}$$

$$m = \frac{4\pi\rho_w}{3}(r^2)^{3/2} = \frac{4 \times 3.142 \times 1}{3} \times (1.435 \times 10^{-6})^{3/2} = 4.1893 \times 1.719 \times 10^{-9} = \underline{7.20 \times 10^{-9} g}.$$

Dimensions, using Eq. (5.62)

$$r = \left(\frac{C}{2\pi\rho_w}\right)^{1/2} t^{1/2}$$

$$C = \frac{4\pi(S-1)}{\left(\frac{L_c^2}{KR_vT_\infty^2} + \frac{1}{D\rho_{s\infty}}\right)} = 1/\left[\frac{(cal/g)^2}{\frac{cal}{cm \cdot s \cdot K} \cdot \frac{cal}{g \cdot K} \cdot \frac{K^2}{1}} + \frac{1}{\frac{g}{cm^3} \cdot \frac{cm^2}{s}}\right]$$

$$= 1/\left[\frac{cm \cdot s}{g} + \frac{cm \cdot s}{g}\right] = \frac{g}{cm \cdot s}$$

$$cm = \left(\frac{g}{cm \cdot s} \cdot \frac{cm^3}{g}\right)^{1/2} (s)^{1/2} = cm.$$

• Problem 2

Using the droplet growth equation, show why the droplet size distribution narrows as the growth proceeds.

Using Eq. (5.62)

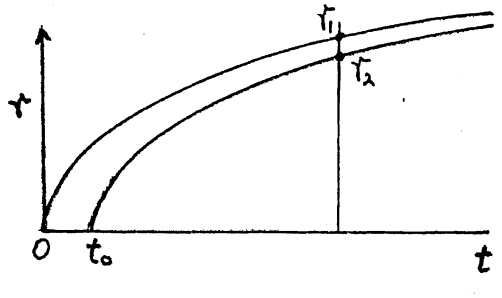

Fig. 5.31 Growth of Maxwellian droplets of two different sizes.

$$r = \left(\frac{C}{2\pi\rho_w}\right)^{1/2} t^{1/2}$$

$$\frac{r_1 - r_2}{r_1} = \frac{(\ )^{1/2} t^{1/2} - (\ )^{1/2}(t-t_o)^{1/2}}{(\ )^{1/2} t^{1/2}}$$

$$= 1 - \left(1 - \frac{t_o}{t}\right)^{1/2}$$

$$= 1 - \left[1 - \frac{1}{2}\frac{t_o}{t} + \frac{\frac{1}{2}\left(-\frac{1}{2}\right)}{2!}\left(\frac{t_o}{t}\right)^2 - \cdots\right]$$

$\to 0$ when $t \to \infty$.

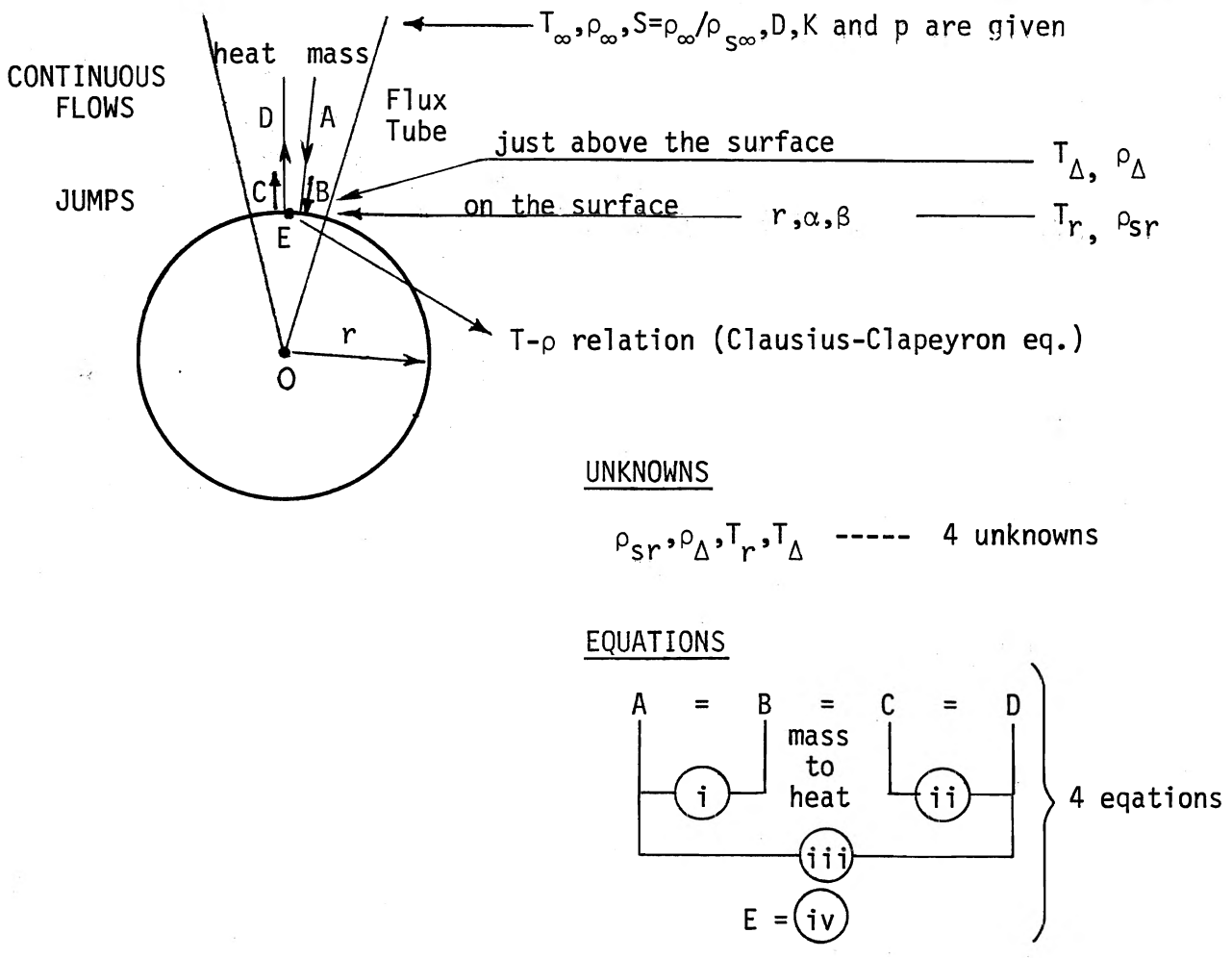

Fig. 5.32 The system of a growing droplet; diffusion-kinetic theory.

In the systems, there are four unknowns, i.e., T_r, T_Δ, ρ_{sr}, and ρ_Δ, where Δ stands for the free molecular fluxes (see Section 2.5). Against these four unknowns are five basic equations, A through E, which give four relationships to solve. We now examine below the basic equations for steady-state growth.

(a) Basic equations

Since the space where Process A is taking place is the same as that around the Maxwellian droplet, Eqs. (5.45) and (5.46) apply to the present system with $\rho_{sr} = \rho_\Delta$ replacement. Then, A defined for unit area is expressed from Eq. (5.46) at the droplet surface as

$$\left[\frac{dm}{dt}\right]_u = \frac{(\rho_\infty - \rho_\Delta)D}{r}. \tag{5.66}$$

Similarly, Process D may be expressed from Eq. (5.40) for unit area and Eq. (5.48) at the droplet surface, with $T_r = T_\Delta$ replacement:

$$\left(\frac{dQ}{dt}\right)_u = \frac{(T_\Delta - T_\infty)K}{r}. \tag{5.67}$$

The mass exchange by the free-molecular flow of water vapor at the droplet surface, Process B, may be expressed by an equation identical to (2.37). By making replacements, $\frac{1}{2}(v_x' + v_x'') = \rho_\Delta$, $v_o = \rho_{sr}$, $\theta = \beta$, $v_x = \rho$, and $z = r$ in Eq. (2.37), and using it in Eq. (5.43) for unit area, with $\bar{v} = (8kT/\pi m)^{1/2}$, [Eq. (A.16)] and Eq. (2.20), we have

$$\left(\frac{dm}{dt}\right)_u = D\left(\frac{d\rho}{dr}\right) = \left(\frac{R_v T_r}{2\pi}\right)^{1/2} \beta' (\rho_\Delta - \rho_{sr}), \tag{5.68}[8]$$

where

$$\beta' = \frac{2\beta}{2 - \beta}, \tag{5.69}$$

is the representative condensation coefficient and β the true condensation coefficient. When $\beta \ll 1$, $\beta' = \beta$.

For the free-molecular heat exchange, Process C, we can apply a treatment identical to Eq. (5.68). Using Eq. (2.37) with corresponding replacements in Eq. (5.40) for unit area,

$$\left(\frac{dQ}{dt}\right)_u = -K\left(\frac{dT}{dr}\right) = \frac{\alpha' p(c_v + \frac{1}{2}R_a)}{(2\pi R_a T_r)^{1/2}} (T_r - T_\Delta), \tag{5.70}[9]$$

where

$$\alpha' = \frac{2\alpha}{2 - \alpha} \tag{5.71}$$

is the representative thermal accommodation coefficient and α the true thermal accommodation coefficient. When $\alpha \ll 1$, $\alpha' = \alpha$. The $\frac{1}{2}R_a$ term is adjustment for high velocity (temperature) molecular contribution to the transport process. The use of representative coefficients can be justified as long as they are used for data analysis and application in the same equation.

---

[8] From (2.37), $\rho_\Delta - \rho_{sr} = \frac{2-\beta}{\beta}\ell\left(\frac{\partial\rho}{\partial r}\right)$. $\ell = 2D/\bar{v}$(2.20) and $\bar{v} = (8kT/\pi m)^{1/2}$(A.16). Then, $\ell = \frac{D}{2}\left(\frac{2\pi m}{kT}\right)^{1/2}$. $\rho_\Delta - \rho_{sr} = \frac{2-\beta}{\beta}\frac{1}{2}\left(\frac{2\pi}{R_v T}\right)^{1/2}\left(D\frac{d\rho}{dr}\right)$. $\left(\frac{dm}{dt}\right) = D\frac{d\rho}{dr} = \left(\frac{R_v T}{2\pi}\right)^{1/2}\frac{2\beta}{2-\beta}(\rho_\Delta - \rho_{sr})$.

[9] From (2.37), $\frac{dT}{dr} = (T_\Delta - T_r)\frac{1}{\ell}\frac{\alpha}{2-\alpha} = (\ )\frac{\bar{v}}{2D}\frac{\alpha}{2-\alpha} = (\ )\frac{\alpha}{2-\alpha}\frac{\rho c_v}{2K}\left(\frac{8kT}{\pi m}\right)^{1/2}$ $= (\ )\frac{\alpha}{2-\alpha}\frac{pc_v}{R_v T K}\left(\frac{2R_v T}{\pi}\right)^{1/2}$. Then, $-K\frac{dT}{dr} = (T_r - T_\Delta)\frac{2\alpha}{2-\alpha}\frac{pc_v}{(2\pi R_a T)^{1/2}}$.

The last basic equation is the Clausius-Clapeyron equation (E), with integration limits at $r = r, (T_r, \rho_{sr})$ and at $r = \infty, (T_\infty, \rho_{s\infty})$.

(b) Derivation of growth equation

We now obtain the four relationships necessary to solve the four unknowns which will give us the growth equation.

(i): (A) = (B)

Setting Eq. (5.66) = Eq. (5.68), we obtain

$$\frac{D(\rho_\infty - \rho_\Delta)}{r} = \left[\frac{R_v T_r}{2\pi}\right]^{1/2} \beta' (\rho_\Delta - \rho_{sr}). \tag{5.72}$$

Here, we introduce a normalization factor,

$$f_\beta = \frac{\rho_\infty - \rho_\Delta}{\rho_\infty - \rho_{sr}}, \tag{5.73}$$

whose meaning is apparent from Fig. 5.33. Inserting Eq. (5.73) into Eq. (5.72), we have

$$f_\beta = \frac{r}{r + \frac{D}{\beta'}\left[\frac{2\pi}{R_v T_r}\right]^{1/2}} = \frac{r}{r + \ell_\beta}, \tag{5.74}$$

where, with adjustment of $T_r \simeq T_\infty$,

$$\ell_\beta = \frac{D}{\beta'}\left[\frac{2\pi}{R_v T_\infty}\right]^{1/2}. \tag{5.75}$$

The behavior of f_β is

$$1 \geq f_\beta \geq 0. \quad \underline{f_\beta \to 1 \text{ when } r \to \infty, \text{ not when } \beta \to 1}.$$

(ii): (C) = (D)

Setting Eq. (5.67) = Eq. (5.70), we have

$$\frac{\alpha' p (c_v + \tfrac{1}{2}R_a)}{(2\pi R_a T_\infty)^{1/2}} (T_r - T_\Delta) = -\frac{(T_\infty - T_\Delta)K}{r}. \tag{5.76}$$

Here, we again introduce another normalization factor analogous to Eq. (5.73):

$$f_\alpha = \frac{T_\Delta - T_\infty}{T_r - T_\infty}, \tag{5.77}$$

and introduce it into Eq. (5.76), with $T_r = T_\infty$ replacement, to obtain

$$f_\alpha = \frac{r}{r + \dfrac{K(2\pi R_a T_\infty)^{1/2}}{\alpha' p(c_v + \frac{1}{2}R_a)}} = \frac{r}{r + \ell_\alpha}, \tag{5.78}$$

where

$$\ell_\alpha = \frac{K(2\pi R_a T_\infty)^{1/2}}{\alpha' p(c_v + \frac{1}{2}R_a)}. \tag{5.79}$$

Again,

$$1 \geq f_\alpha \geq 0. \quad \underline{f_\alpha \to 1, \text{ only when } r \to \infty}, \text{ and not when } \alpha \to 1.$$

<u>(iii): $L_c(A) = (D)$</u>

Applying Eq. (5.49) with Eqs. (5.66), (5.67), (5.73), and (5.77), we have

$$-\frac{f_\alpha(T_r - T_\infty)}{f_\beta(\rho_{sr} - \rho_\infty)} = \frac{DL_c}{K}, \tag{5.80}$$

which converges into Eq. (5.53) of the Maxwellian theory when $r \to \infty$.

<u>(iv): (E)</u>

We can use the linearized Clausius-Clapeyron equation (5.52).

From these four relationships, we now try to solve the four unknowns. Using Eqs. (5.52) and (5.80), we derive

$$\rho_{sr} = \rho_\infty - \frac{(S - 1)}{\left(\dfrac{f_\beta DL_c^2}{f_\alpha K R_v T_\infty^2} + \dfrac{1}{\rho_{s\infty}}\right)}, \tag{5.81}$$

which compares with Eq. (5.54).

Then replacement of Eq. (5.81) in Eq. (5.80) yields

$$T_r = T_\infty + \frac{(S - 1)}{\left(\dfrac{L_c}{R_v T_\infty^2} + \dfrac{f_\alpha K}{f_\beta DL_c \rho_{s\infty}}\right)}, \tag{5.82}$$

which corresponds to Eq. (5.55) in the Maxwellian theory.

Substitution of Eq. (5.81) in Eq. (5.73) results in

$$\rho_\Delta = \rho_\infty - \frac{(S-1)}{\left(\frac{DL_c^2}{f_\alpha K R_v T_\infty^2} + \frac{1}{f_\beta \rho_{s\infty}}\right)}. \tag{5.83}$$

Similarly, substitution of Eq. (5.82) in Eq. (5.77) leads to

$$T_\Delta = T_\infty + \frac{(S-1)}{\left(\frac{L_c}{f_\alpha R_v T_\infty^2} + \frac{K}{f_\beta D L_c \rho_{s\infty}}\right)}. \tag{5.84}$$

Using Eq. (5.66) with Eq. (5.83) over the entire droplet surface, the mass growth rate is obtained as

$$\frac{dm}{dt} = 4\pi r^2 \left(\frac{dm}{dt}\right)_u = \frac{4\pi r(S-1)}{\left(\frac{L_c^2}{f_\alpha K R_v T_\infty^2} + \frac{1}{f_\beta D \rho_{s\infty}}\right)} = \frac{4\pi r(S-1)}{\left(\frac{a'}{f_\alpha} + \frac{b'}{f_\beta}\right)}, \tag{5.85}$$

which corresponds to Eq. (5.56) of the Maxwellian theory.

The vapor and temperature fields in the space outside the droplet are identical to Eqs. (5.45) and (5.47), with $\rho_\Delta = \rho_{sr}$ and $T_\Delta = T_r$ replacements.

It should be pointed out that use of $r + \ell$, ℓ being the mean free path of the gas, taken in some other treatments in place of r is based on the erroneous perception of this process and introduces a large error when $r \leq \ell$.

(c) Effects of solute and size of droplet

The treatment is identical to that of the Maxwellian theory under Section 5.3.2 (f). The mass growth rate is

$$\frac{dm}{dt} = \frac{4\pi r\left(S - 1 - \frac{a}{r} + \frac{b}{r^3}\right)}{\left(\frac{L_c^2}{f_\alpha K R_v T_\infty^2} + \frac{1}{f_\beta D \rho_{s\infty}}\right)} = \frac{4\pi r\left(S - 1 - \frac{a}{r} + \frac{b}{r^3}\right)}{\left(\frac{a'}{f_\alpha} + \frac{b'}{f_\beta}\right)}. \tag{5.86}$$

(d) The behavior of the diffusion-kinetic theory

(i) Temperature and vapor fields

The discreteness of the fields is entirely due to f_α and f_β.

As can be seen in Fig. 5.37, the temperature of the droplet growing under the steady-state at 1000 mb pressure is warmer than the environment by about 0.1°C/1% supersaturation for the Maxwellian theory and lower for the DK theory.

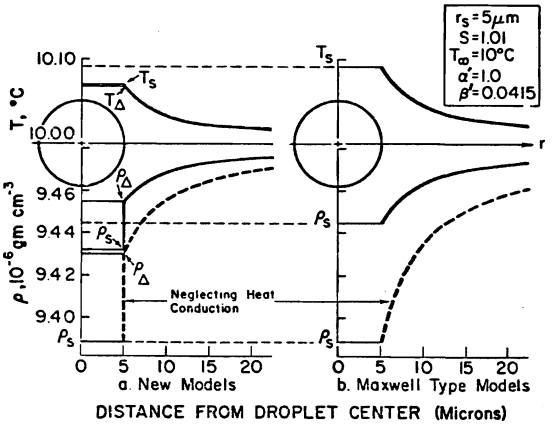

Fig. 5.33 Profiles of temperature and vapor density fields in the vicinity of the droplet for the diffusion kinetic and Maxwellian theories (Fukuta and Walter, 1970).

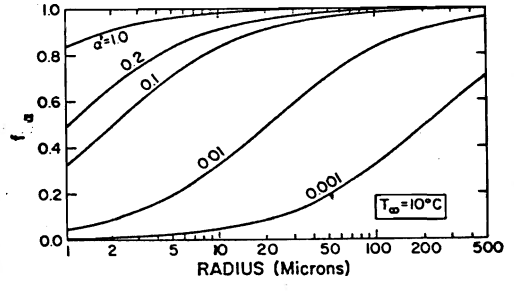

Fig. 5.34 Variation of f_α with droplet radius: T_∞ = 10°C, P = 1000 mb (Fukuta and Walter, 1970).

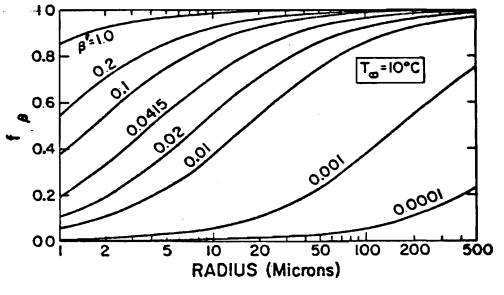

Fig. 5.35 Variation of f_β with droplet radius: T_∞ = 10°C, P = 1000 mb (Fukuta and Walter, 1970).

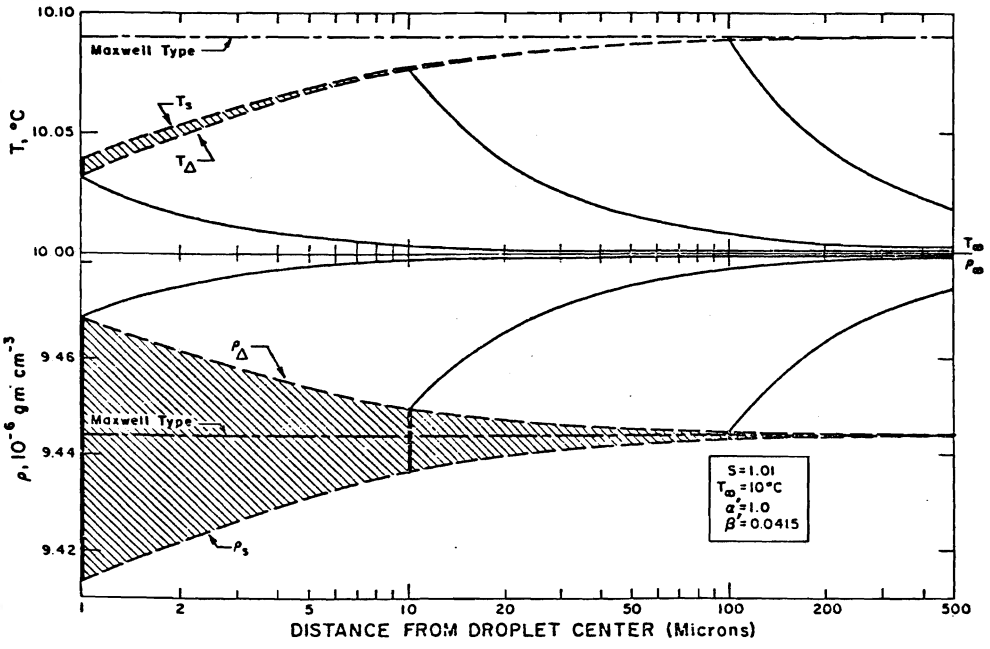

Fig. 5.36 Profiles of temperature and vapor fields: r_s = 1, 10, and 100 μm, p = 1000 mb (Fukuta and Walter, 1970).

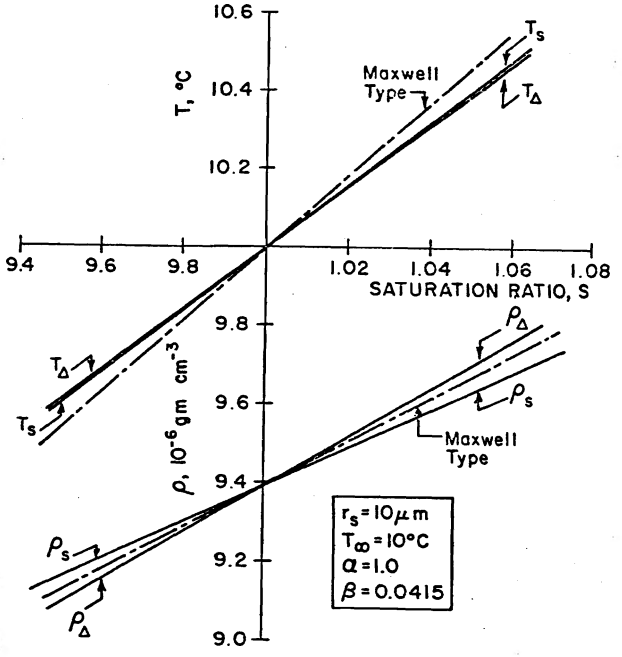

Fig. 5.37 Temperature and vapor density of droplet surface and boundary as a function of saturation ratio: p = 1000 mb (Fukuta and Walter, 1970).

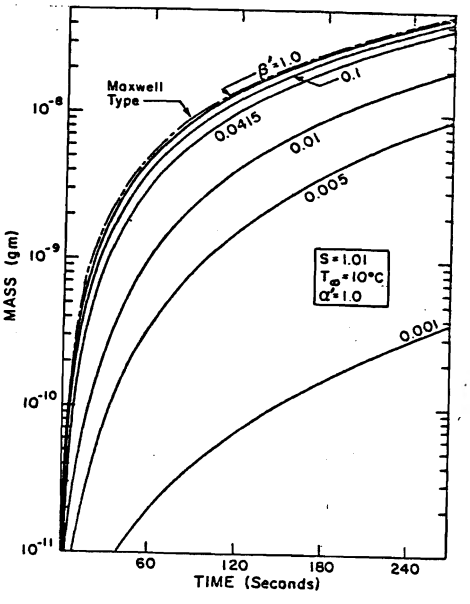

Fig. 5.38 Droplet mass as a function of time: p = 1000 mb, S = 1.01, with β as a variable (Fukuta and Walter, 1970).

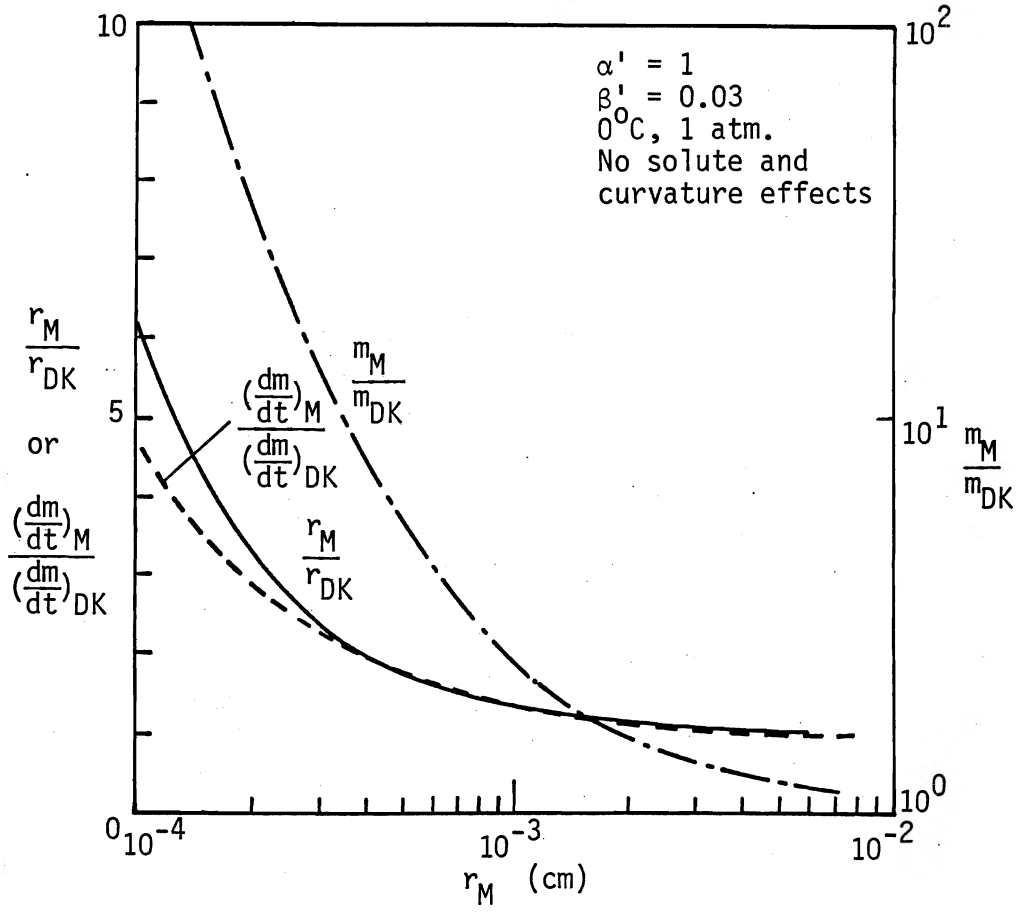

Fig. 5.39 Comparison between Maxwellian (M) and diffusion kinetic (DK) theories for m, dm/dt and r.

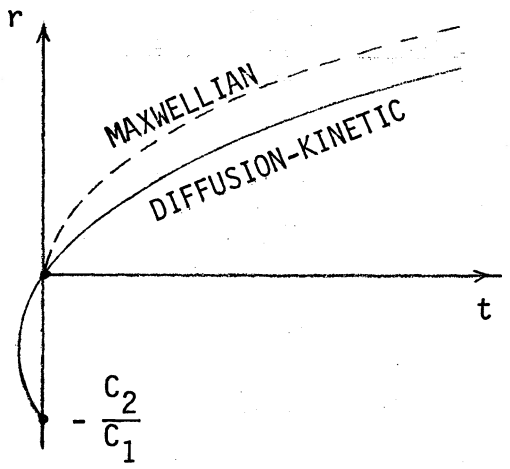

Fig. 5.40 Comparison between Maxwellian and diffusion kinetic theories in time dependence of the radius.

(ii) Variation of radius as a function of time (constant S)

Similar to Eq. (5.60), we can write Eq. (5.85), including Eqs. (5.74) and (5.78), as

$$4\pi r^2 \rho_w \frac{dr}{dt} = \frac{4\pi r(S-1)}{\left[\frac{L_c^2(r+\ell_\alpha)}{rKR_vT_\infty^2} + \frac{(r+\ell_\beta)}{rD\rho_{s\infty}}\right]},$$

which gives, by integration with $r = 0$ when $t = 0$,

$$\rho_w \left[\left(\frac{L_c^2}{KR_vT_\infty^2} + \frac{1}{D\rho_{s\infty}}\right)\frac{r^2}{2} + \left(\frac{L_c^2\ell_\alpha}{KR_vT_\infty^2} + \frac{\ell_\beta}{D\rho_{s\infty}}\right) r\right] = (S-1)t, \tag{5.87}$$

or

$$(C_1 r + C_2)r = t, \tag{5.87'}$$

(see Fig. 5.40).

(e) Relationship among growth equations (Special cases)

As we have seen above, the diffusion-kinetic theory is most general and takes two special cases:

(i) $r \to \infty$, $f_\alpha = f_\beta = 1$; it converges to the Maxwellian theory.

(ii) $r \to 0$, $r \ll \ell_\alpha$ or ℓ_β, or the free molecular flow processes become much slower than the continuum processes of heat and vapor transportation. Then from Eq. (5.85), with Eqs. (5.74) and (5.78),

$$\frac{dm}{dt} = \frac{4\pi r^2(S-1)}{\dfrac{L_c^2(2\pi R_a T_\infty)^{1/2}}{\alpha' p R_v T_\infty^2 (c_v + \frac{1}{2}R_a)} + \dfrac{1}{\beta' \rho_{s\infty}}\left(\dfrac{2\pi}{R_v T_\infty}\right)^{1/2}}. \tag{5.88}$$

Equation (5.88) described the mass growth rate of a very small droplet of $r \ll \ell_\alpha$ and ℓ_β, not $K_n \gg 1$, under the condition where the Kelvin and solute effects are still small. These effects can be incorporated starting from Eq. (5.86) instead of Eq. (5.85). Equation (5.88) is no longer a function of D and K. In addition, ignoring these two effects, we obtain

$$\frac{dm}{dt} \propto r^2, \text{ or} \tag{5.89}$$

$$r \propto t \quad \text{or} \quad m \propto t^3. \tag{5.89'}$$

General features of the diffusion-kinetic equation

The general features of the diffusion-kinetic equation are

(1) more accurate when r is smaller and slower in growth rate than the Maxwellian,
(2) includes the Maxwellian theory as the special case for large r and the free molecular growth theory for very small r,
(3) is sensitive to α and β values, and
(4) droplets tend to become more polydispersed after growth.

5.3.4 Competitive growth of cloud droplets

The above two theories of droplet growth assume a constant supersaturation and environmental conditions with the space unlimited. It is not the case of cloud droplet growth that occurs sometime after passing through the supersaturation maximum above the cloud base, and we now look into the problems that arise from the difference in conditions.

The cloud basically forms under two simultaneous processes, the adiabatic expansion of moist thermal lifting and the growth of nucleated droplets, in which

$$\frac{\partial T}{\partial t} = \kappa \nabla^2 T + C_1, \quad \frac{\partial \rho}{\partial t} = D\nabla^2 \rho + C_2,$$

where C_1 and C_2 are respective sinks created by the processes. Shortly after nucleation above the cloud base, due to still small expanse of the temperature and vapor fields established around the droplet and their short relaxation times, the cloud space does not feel the droplet growth effect and

$$\frac{\partial T}{\partial t} = C_1 \text{ or } \nabla^2 T = 0, \text{ and } \frac{\partial \rho}{\partial t} = C_2 \text{ or } \nabla^2 \rho = 0. \tag{5.41) (5.42}$$

In this stage, the cloud process is essentially dry adiabatic, and the supersaturation increases almost linearly with time free from droplet growth effect. The increasing supersaturation leads to nucleation of more droplets and their growth, and the two fields around the droplets continue to enlarge the expanse. The adjacent fields of droplets begin to interact; the fields deform to transfer the vapor and heat being made available by adiabatic expansion within the vicinity of each droplet, so that

$$\nabla^2 T = \text{const} \neq 0, \ \nabla^2 \rho = \text{const} \neq 0, \tag{5.90}$$

and come to following two major changes of the growth mode.

(1) the temperature and vapor fields become confined in the volume called cell occupied by each droplet, and

(2) the supersaturation in the environment reaches a maximum and thereafter begins to slowly decrease. The latter problem will be discussed in Section 7.1.

The temperature and vapor fields confined in the cell volume surrounding the droplet are finite compared with the infinitely stretching fields assumed in Sections 5.3.2 and 5.3.3. Within this cell volume, the vapor transfer to and heat transfer from the droplet take place. This should make some difference in the droplet growth kinetics, and we discuss the effect of the cell-boundary-controlled, steady-state kinetics below.

Consider a spherical surface placed at a position with radial distance r which lies between the droplet radius r and the radial distance of the cell boundary R. In a given period of time, the total amount of newly generated (S − 1) in the space between the spherical surface of radius r and that of radius R must be completely removed by the transfer of vapor to and heat from the spherical surface of radius r. Then, at the surface,

$$\frac{dm}{dt} = C_1 \left(\frac{4}{3}\pi R^3 - \frac{4}{3}\pi r^3 \right) = 4\pi r^2 D \frac{d\rho}{dr}, \tag{5.91}$$

where C_1 is a proportional constant. Here, the volume change due to an expansion by lifting is ignored. After integration with respect to r and inserting the boundary condition at the droplet surface, $r = r$, $\rho = \rho_{sr}$ and that at the cell boundary, $r = R$, $\rho = \rho_R$, Eq. (5.91) yields

$$\rho = \frac{-(\rho_R - \rho_{sr})r}{(R - r)[2R^2 - r(R + r)]} \left[\frac{2R^3}{r} + r^2 - 3R^2 \right] + \rho_R. \tag{5.92}$$

At $r = r$, from Eq. (5.92) we obtain

$$\frac{d\rho}{dr} = \frac{\rho_R - \rho_{sr}}{r} f_c, \tag{5.93}$$

where

$$f_c = \frac{2(1 + g + g^2)}{(2 - g - g^2)} \geq 1, \tag{5.94}$$

and

$$g = \frac{r}{R} \tag{5.95}$$

(see Fig. 5.41). $f_c \to 1$ when $g \to 0$ with $R \to \infty$, or the system converges into the condition without cell-boundary restriction.

Similarly, one may derive

$$T = -\frac{(T_R - T_r)r}{(R - r)[2R^2 - r(R + r)]}\left[\frac{2R^3}{r} + r^2 - 3R^2\right] + T_R, \tag{5.96}$$

where subscripts R and r stand for cell-boundary and droplet surface, respectively (see Fig. 5.42).

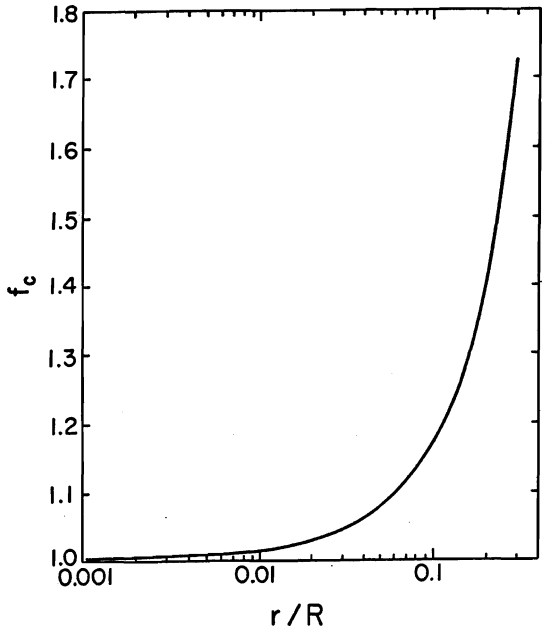

Fig. 5.41 f_c as a function of r/R.

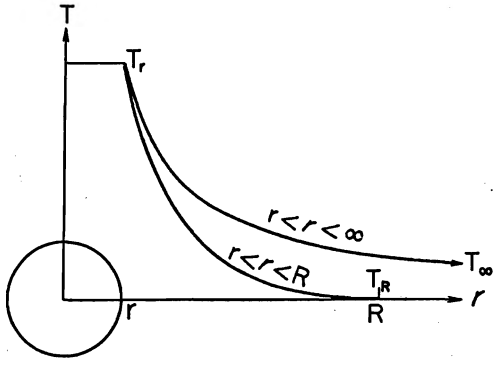

Fig. 5.42 Comparison of temperature field with (lower curve) and without (upper curve) cell-boundary restriction.

Equation (5.93) and the temperature gradient at the droplet surface derived from Eq. (5.96) may be combined through the latent and sensible heat flux balance equation (5.49). This equation, the linearized Clausius-Clapeyron equation (5.52), and Eq. (5.43) lead to

$$\frac{dm}{dt} = \frac{4\pi r(S_R - 1)}{\left[\frac{L^2}{KRT_R^2} + \frac{1}{D\rho_{sR}}\right]} \cdot f_c, \tag{5.97}$$

the Maxwellian growth rate of cell-boundary-controlled, steady state kinetics (see Fig. 5.43). Equation (5.97) shows that use of droplet growth equation without the cell-boundary restriction in the cell-boundary controlled growth tends to give f_c^{-1} of the realistic value, or an underestimation.

When accommodation coefficient effects are further considered, the diffusion-kinetic growth rate equation (5.85) modifies to

$$\frac{dm}{dt} = \frac{4\pi r(S_R - 1)}{\left[\frac{L^2}{KRT_R^2 f'_\alpha} + \frac{1}{\rho_{sR} D f'_\beta}\right]} \cdot f_c, \tag{5.98}$$

where

$$f'_\alpha = \frac{r}{r + \ell_\alpha f_c}, \tag{5.99}$$

and

$$f'_\beta = \frac{r}{r + \ell_\beta f_c}. \tag{5.99'}$$

Equation (5.98) converges to Eq. (5.85) when $r/R \to 0$.

If the cloud liquid water content is 1 g m^{-3} and droplet number concentration 10^3 cm^{-3}, g ~ 0.01 and the use of Maxwellian rate of infinite field expanse will result in an underestimation by about 1.5%. The error in the diffusion kinetic theory will be smaller due to the compensating effect of f_c in Eqs. (5.99) and (5.99').

5.3.5 Non-steady problem of droplet growth

If the condition of the environment surrounding a droplet or that of the environmental boundaries changes, the droplet can no longer maintain the steady state condition of growth, so that

$$\frac{\partial \rho}{\partial t} = D\nabla^2\rho \neq 0 \quad \text{and} \quad \frac{\partial T}{\partial t} = \kappa\nabla^2 T \neq 0. \tag{5.100}$$

Then, changes take place in the fields until the steady state is regained. There are two kinds of non-steady processes possible:

(1) 1st Kind: The condition of the outer boundary or surrounding environment changes suddenly.

(2) 2nd Kind: The inner boundary or droplet surface changes suddenly.

The latter can indeed happen when a supercooled droplet freezes, and that problem will be discussed in a later chapter.

For the non-steady state of the first kind, since the condition around the droplet was thought to be identical to that of the thermal field internally bounded by a sphere (Carslaw and Jaeger, 1959), an analogy was applied to obtain the vapor field,

$$\rho = \rho_\infty + (\rho_{sr} - \rho_\infty) \frac{r}{r} \left[1 - \text{erf}\left(\frac{r - r}{2\sqrt{Dt}}\right)\right], \tag{5.101}$$

where erf is the error function and

$$\text{erf } x = \frac{2}{\sqrt{\pi}} \int_0^x e^{-\xi^2} d\xi. \tag{5.102}$$

However, Eq. (5.101) assumes constant ρ_{sr} which actually changes, in the case of droplet growth under non-steady state, because of coupling with the surface temperature and ρ_{sr}, through the Clausius-Clapeyron equation and that between the surface temperature and the external temperature field. Nix and Fukuta (1973 and 1974) obtained a solution by considering the connection of Clausius-Clapeyron equation at the droplet surface with non-steady state Maxwellian fields and assuming the changing environmental conditions as

$$\frac{\partial \rho}{\partial t} = D\nabla^2\rho + A\exp(-\kappa t), \tag{5.103}$$

and

$$c_p\rho_a\frac{\partial T}{\partial t} = K\nabla^2 T + B\exp(-\kappa t), \tag{5.104}$$

where A and B are constants and κ is a constant describing the rate of change of the environmental conditions. The results are shown in Figs. 5.43 and 5.44. Note that use of steady state equation in a step-wise manner in the non-steady problem may cause a serious error due to the transient part in Fig. 5.43, if the time rate of change is large.

5.3.6 Evaporation of small drops

The droplet evaporation problem is identical to that of growth, as long as the signs for corresponding values are properly treated. Then, the equations derived above are all applicable to the evaporation problem within their limits.

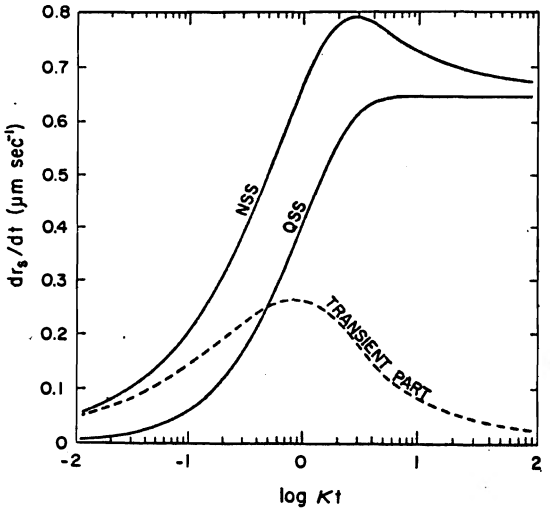

Fig. 5.43 Radial growth rates of a droplet 100 μm in radius during the cooling from 15 to 0°C under κ - 1000 s^{-1} (Nix and Fukuta, 1973).

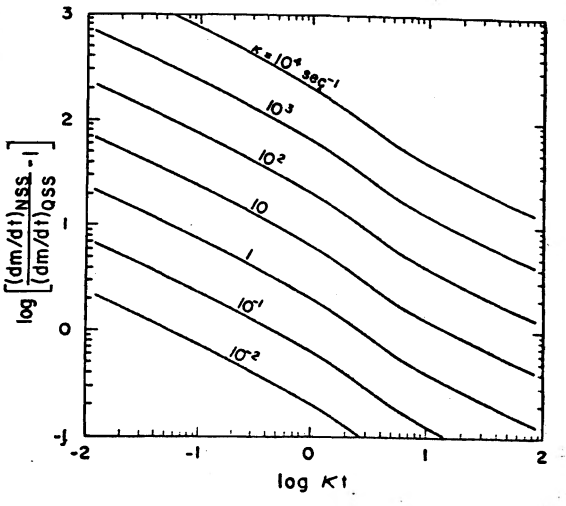

Fig. 5.44 Error in dm/dt vs κt with κ as the parameter (Nix and Fukuta, 1973).

5.4 Droplet Growth by Coalescence

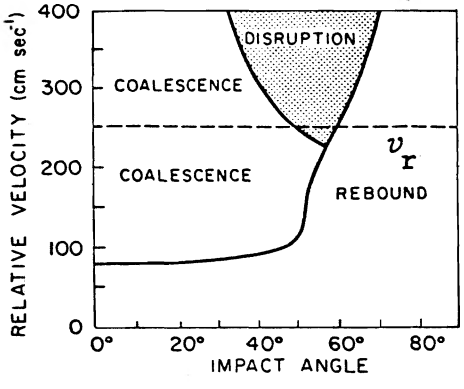

Fig. 5.45 Experimentally determined conditions or permanent coalescence (disruption) of water drops in air for various relative velocities imposed on the drops. (f) a_1=450 μm, a_2=150 μm. v_r is the difference in terminal velocity of the two interacting drops (From Park, 1970, with changes).

Cloud droplets nucleated and grown by diffusional mechanism can further grow by colliding with others and fusing together under influences of gravitational, electrical, acoustical, thermal, and aerodynamical fields. After mechanical collision with others, droplets

(i) coalesce and remain permanently fused,
(ii) rebound,
(iii) coalesce temporarily and then separate, retaining their original identities, and
(iv) coalesce first and then break up into a number of small droplets.

The total efficiency of droplets to fuse together after collision is called the collection efficiency.

COLLECTION EFFICIENCY = (COLLISION EFFICIENCY) x (COALESCENCE EFFICIENCY)
The latter is often assumed to be unity.

5.4.1 Liquid water content

The liquid water content W_L is defined as the total weight of condensed water in a unit volume:

$$W_L = \frac{4\pi\rho_w}{3}\int_0^\infty r^3 n(r)dr, \tag{5.105}$$

where n(r) is the number concentration (density) of droplets in the size range between r and r + dr.

The total number of droplets is
~200 cm^{-3} in continental clouds and
~several tens in maritime clouds (in Hawaii, as low as 10 cm^{-3})

The W_L value is
~0.5 gm^{-3}, with a maximum of 1 gm^{-3} in healthy cumulus.
~5 gm^{-3} is possible in cumulonimbi which approach the adiabatic value. The value is normally diluted by entrainment.

Bimodal distribution of n (Warner in cu) has been frequently reported with peaks at r = 6 and 12 μm.

5.4.2 Collision process

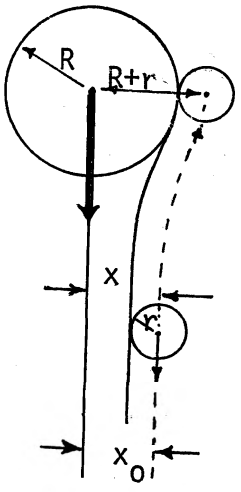

Fig. 5.46 Collision process of drops by fall.

The concept of droplet collision is identical to that of molecular collision (Section 2.3) or that of coagulation of particles (Section 3.5).

To understand the coalescence process quantitatively, we define the collision efficiency as

$$E' = \frac{x_o^2}{(R + r)^2}, \tag{5.106}$$

where x_o is the critical value of x within which a collision is certain to occur and outside of which a collision does not take place.

$$E' \leq 1.$$

There are other collision efficiencies, but Eq. (5.106) is most commonly used.

(a) Collision efficiency: Theoretical estimation

Collision efficiency can be estimated by the method of superposition, where each sphere is assumed to move in the flow field generated by the other sphere falling separately. Collision happens when the inertia force of a droplet resists against the change of the stream line due to approach of the second droplet and mutual contact is made. To obtain the flow behavior around a falling sphere, the Navier-Stokes equation [Eq. (3.4)], or its simplified version depending on the condition surrounding the sphere, has to be solved. The Stokes approximation is sufficient for $Re \leq 0.4$ or $r \leq 30$ μm.

For very small droplets whose radii are on the order of ten times the mean free path of air molecules or less, consideration of slip flow (momentum accommodation, Section 2.5) may be needed. However, for cloud droplet size range, it was found to be unnecessary (Pruppacher and Klett, 1978).

E′ decreases as the size of one of the droplets, or both, decreases. Whereas, E′ is nearly unity for $R \geq 40$ μm and $r \geq 15$ μm, unless $R \simeq r$, in which case $E' > 1$. There is generally good agreement between theory and experiment for drops of $R \leq 100$ μm falling in still air, and the shape distortions of interacting drops are insignificant.

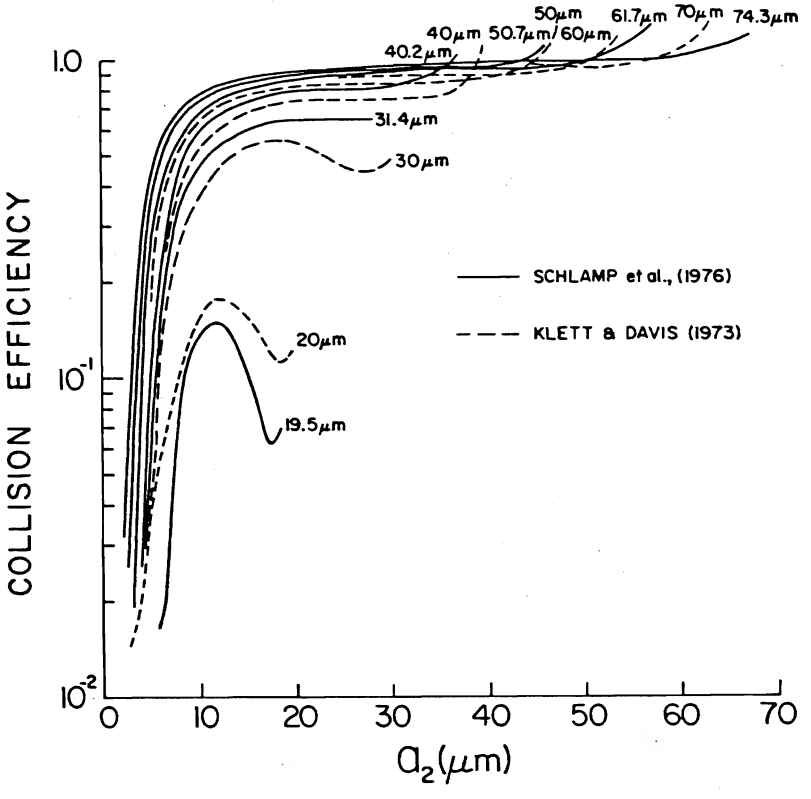

Fig. 5.47 Theoretical collision efficiencies of spherical water drops in calm air as a function of small drop radius and of large drop radius (given by label of each curve). —— Schlamp et al. (1976), ---- Klett and Davis (1973), -·-·- Lin and Lee (1975), ····· Jonas (1972) (Pruppacher and Klett, 1978).

(b) Drop coalescence behavior

A falling drop leaves wake behind, and the wake enhances collision efficiency. For large drops, complications appear due to wake oscillation, eddy shedding, and shape deformation.

When rebounding occurs, air film trapped between the drop surfaces plays an important role in coalescence. Its drainage or disruption is needed for coalescence to occur.

Drop break-up occurs following coalescence of two large drops. Bag-type, dumbbell-type, neck-type, sheet-type, and disk-type have been observed.

Turbulence is known to enhance the drop coalescence, in general, although one theoretical study indicates possible reduction under high turbulence.

5.4.3 Fall velocity of drops

Coalescence of droplets occurs primarily due to their fall velocity difference. So, we now examine the variation of drop fall velocity with respect to size and environmental conditions.

A drop falls due to the gravitational pull, and air surrounding the drop exerts resistance to it. When the resistance force balances with the gravita-

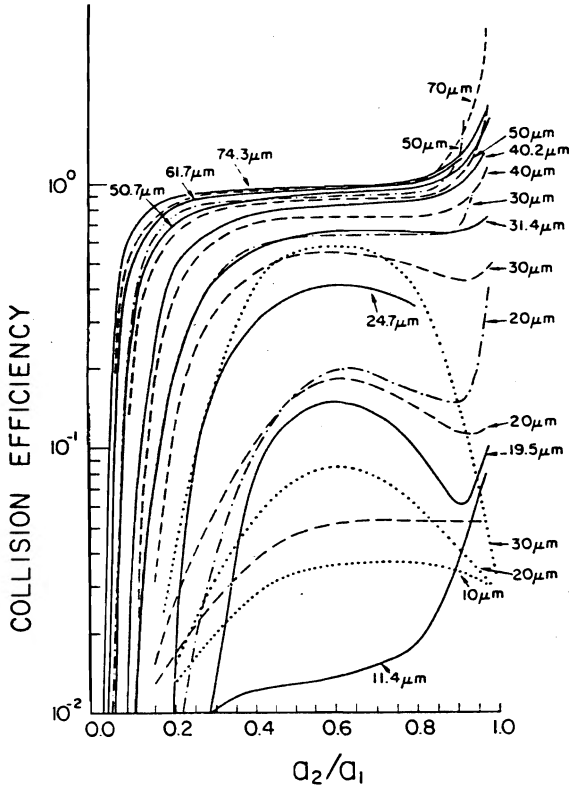

Fig. 5.48 Theoretical collision efficiencies of spherical water drops in calm air as a function of p-ratio and of collector drop radius (given by label of each curve); —— Schlamp et al. (1976), ---- Klett and Davis (1973), -·-·- Lin and Lee (1975), ····· Jonas (1972) (Pruppacher and Klett, 1978).

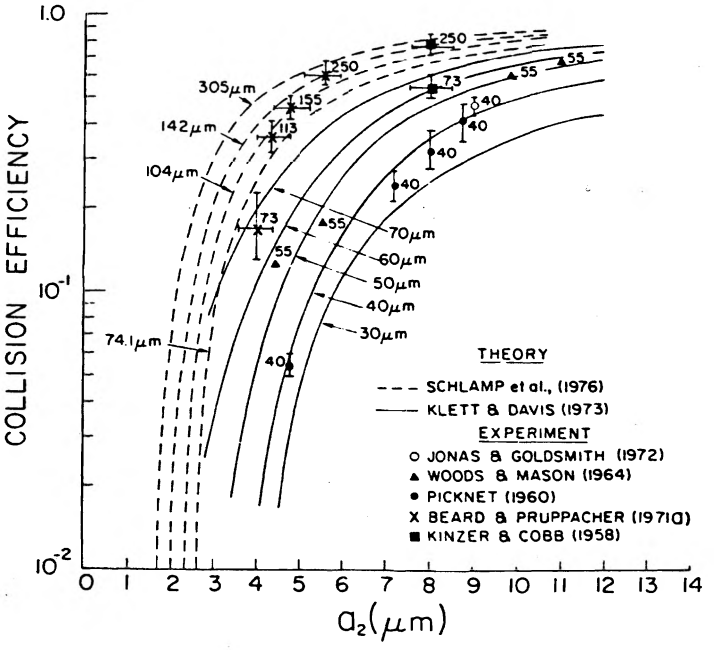

Fig. 5.49 Comparison of theoretical collision efficiencies with experimentally determined collection efficiencies, for water drop pairs of small p-ratio. Label of each curve and data point gives large drop radius in μm (Pruppacher and Klett, 1978).

tional force, the fall velocity attains a constant value or terminal velocity. Then,

GRAVITATIONAL FORCE = RESISTANCE FORCE (f_R)

The nature of the resistance force changes from viscous (frictional) to turbulent via an extensive intermediate region as the drop size and, therefore, Re increase (see Table 5.8).

The resistance force is defined as the product of dynamic pressure, horizontal cross-sectional area A and the drag coefficient C_D:

$$f_R = \tfrac{1}{2}\rho_a w^2 A C_D, \tag{5.107}$$

where $\tfrac{1}{2}\rho_a w^2$ is the dynamic pressure. Using the definition of Re ($= \rho_a w(2r)/\eta$) in Eq. (5.107), we have

$$f_R = 6\pi\eta w r(\mathrm{Re}C_D/24). \quad \text{(spherical case)} \tag{5.108}$$

Since f_R is equal to the gravitational force for a falling sphere,

Table 5.8 Variation of drop fall behavior.

Resistance Force	Flow	Terminal Velocity (Rigid Body)	Water Drops
Molecular hitting (random) $\propto \frac{\eta w r}{\left(1+\frac{A\ell}{r}\right)}$ Viscous (slip)	Free-molecular Slip	Stokes law with Cunningham's correction $\propto \frac{(\rho_p-\rho_a)r^2}{\eta}\left(1+\frac{A\ell}{r}\right)$	A varies (small size) (i)′ 0 -10 μm
Viscous (frictional & continuous) $\propto \eta w r$	Stream line	Stokes law $\propto \frac{(\rho_p-\rho_a)}{\eta} r^2$	(i) 1 - 100 μm
Intermediate $\propto \rho_a^{1/2}\eta^{1/2}w^{3/2}r^{3/2}$	Intermediate	$\propto \left[\frac{(\rho_p-\rho_a)^2}{\eta}\right]^{1/3}\frac{r}{\rho_a}$	(ii) 100-500 μm
Turbulent (inertial) $\propto \rho_a w^2 r^2$	Turbulent	Newton's parabolic law $\propto \left[\frac{\rho_p-\rho_a}{\rho_a}\right]^{1/2} r^{1/2}$	(iii) > 500 μm Drop deforms w_{max}
Turbulent	Turbulent	No terminal velocity Continuous increase	———

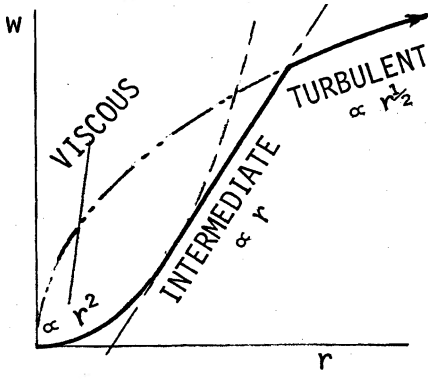

Fig. 5.50 Laws that apply to free falling, spherical particles.

$$f_G = \frac{4}{3}\pi r^3(\rho_w - \rho_a)g,$$

and since $\rho_w \gg \rho_a$, Eq. (5.108) becomes

$$w = \frac{2}{9}\frac{g\rho_w r^2}{\eta(ReC_D/24)}. \qquad (5.109)$$

For very small Reynolds numbers, the Stokes solution to the flow field around a sphere gives $(ReC_D/24) = 1$, or

$$w_S = \frac{2}{9}\frac{g\rho_w r^2}{\eta}, \qquad (3.11)$$

which is independent of ρ_a, and the subscript s stands for Stokes.

For high Reynolds numbers or turbulent regime of hard spheres, C_D becomes independent of Re and $C_D \simeq 0.45$. Then,

$$w \propto r^{1/2}$$

(see Table 5.8) and w depends on ρ_a.

For C_D of spherical particles, an empirical expression proposed by White (1974) agrees well with experimental data for $Re < 5 \times 10^3$;

$$C_D = 0.25 + \frac{24}{Re} + \frac{6}{1 + \sqrt{Re}}, \tag{5.110}$$

(see Fig. 5.51).

The turbulence alters the vertical movement of particles: If the particles are small, the average vertical velocity becomes smaller than the terminal velocity in the still air but when the velocity scale of the turbulent air approaches the terminal velocity, the average fall velocity becomes larger than that of the still air (see Fig. 5.52).

For <u>water drops in the atmosphere</u>:

(i) <u>Regime $0.5 \leq r < 10$ μm ($10^{-6} \leq Re \leq 10^{-2}$)</u>

$$w = (1 + 1.26\ell/r)w_S, \text{ (Stokes-Cunningham Equation)} \tag{5.111}$$

where w_S is the Stokes terminal velocity, Eq. (3.11).

(ii) <u>Regime $10 \leq r \leq 535$ μm ($10^{-2} \leq Re \leq 3 \cdot 10^2$)</u>

As r increases from 10 μm, r dependence of w begins to shift from the quadratic to linear. For the range $100 < r < 500$ μm, <u>w increases almost linearly with r</u> (see Table 5.8).

(iii) <u>Regime 535 μm $\leq r \leq 3.5$ mm ($3 \cdot 10^2 \leq Re \leq 4 \cdot 10^3$)</u>

The drops are <u>no longer spherical</u>. Velocity of large drops increases markedly with altitude (decreasing pressure) in the atmosphere (r = 3.5 mm, 9 m/s at sea level to a value in excess of 12 m/s at 500 mb). The w value becomes eventually independent of size for <u>$r \geq 2.5$ mm</u> due to a flattening effect. This flattening is often followed by sudden development of a concave depression and becomes a bag and bursts. The maximum fall velocity corresponding to the maximum stable size is

$$w_m \simeq \left(\frac{4\pi b}{3aC_D}\right)^{1/2} \left(\frac{\rho_w g \sigma}{\rho_a^2}\right)^{1/4}, \tag{5.112}$$

where a and b are the minor and major axis of oblate drop, σ the surface tension, and it is <u>no longer a function of size</u>. For $Re \geq 300$, drops tend to <u>shed vortices and vibrate</u>.

Pruppacher and Klett (1978) provide some empirical expressions for the last two regimes.

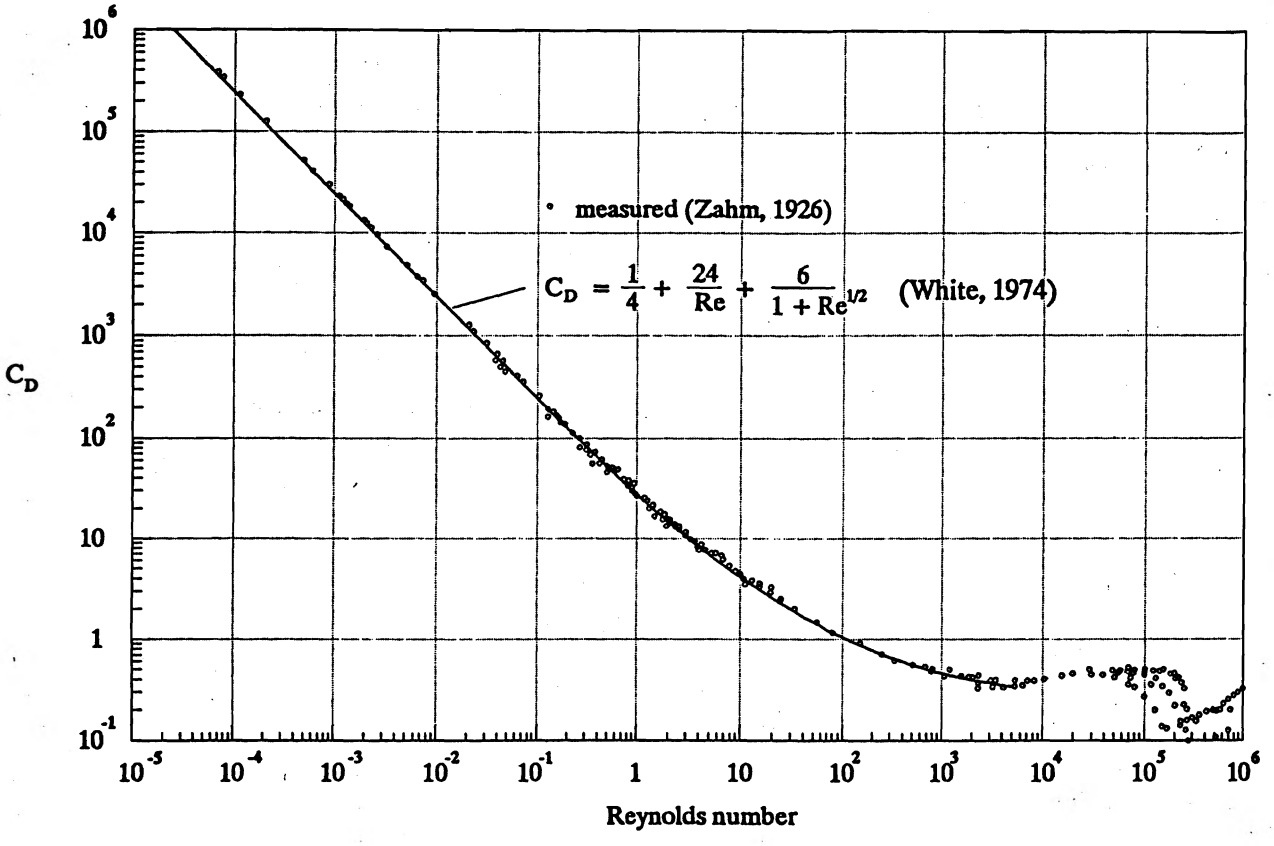

Fig. 5.51 Comparison between experimental data of drag coefficient compiled by Zahm (1926) and the empirical equation proposed by White (1974).

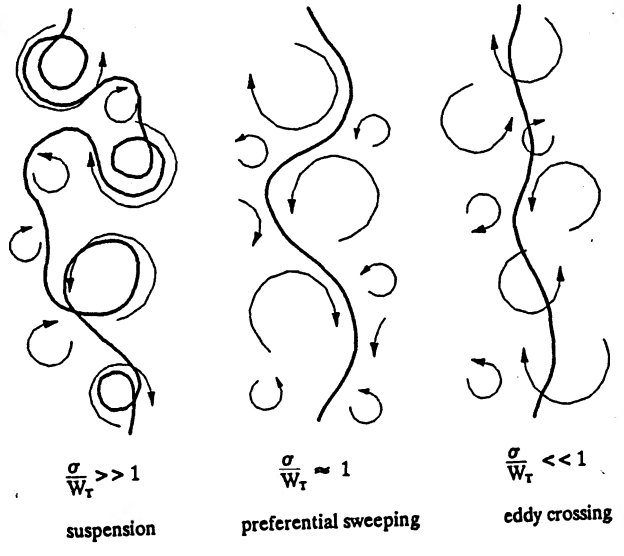

Fig. 5.52 Three regimes of heavy particle motion (after Stout et al., 1995). σ; the velocity scale of the fluid and W_r the terminal velocity of the particle.

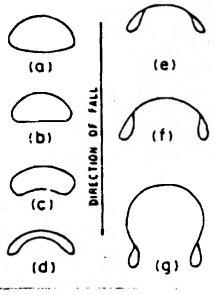

Fig. 5.53 Drop break-up stages (Pruppacher and Klett, 1978).

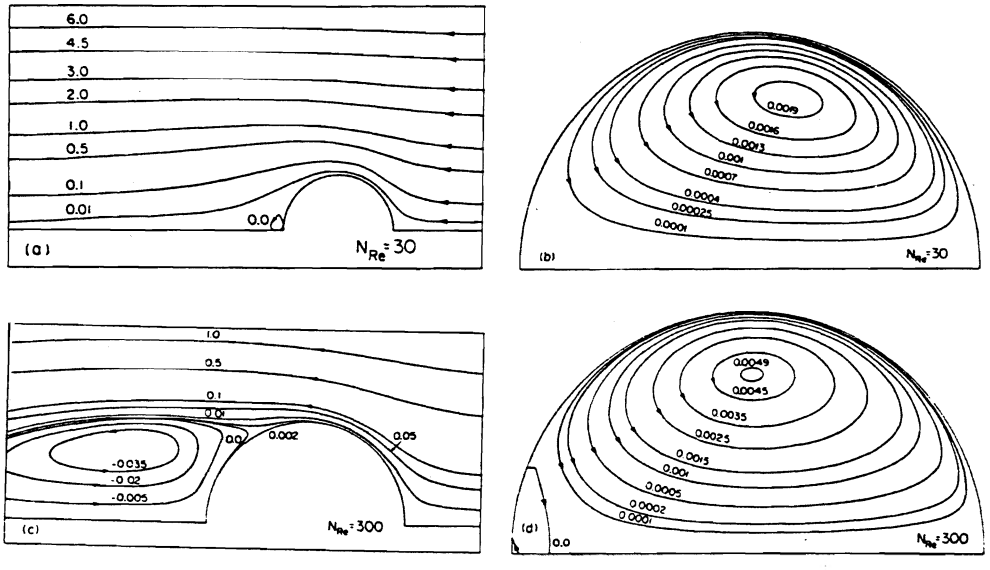

Fig. 5.54a, b, c, d Numerically computed distribution of stream function and vorticity inside and outside a circulating spherical water drop in air at Re = 30(a,b) and at Re = 300(c,d) (Pruppacher and Klett, 1978).

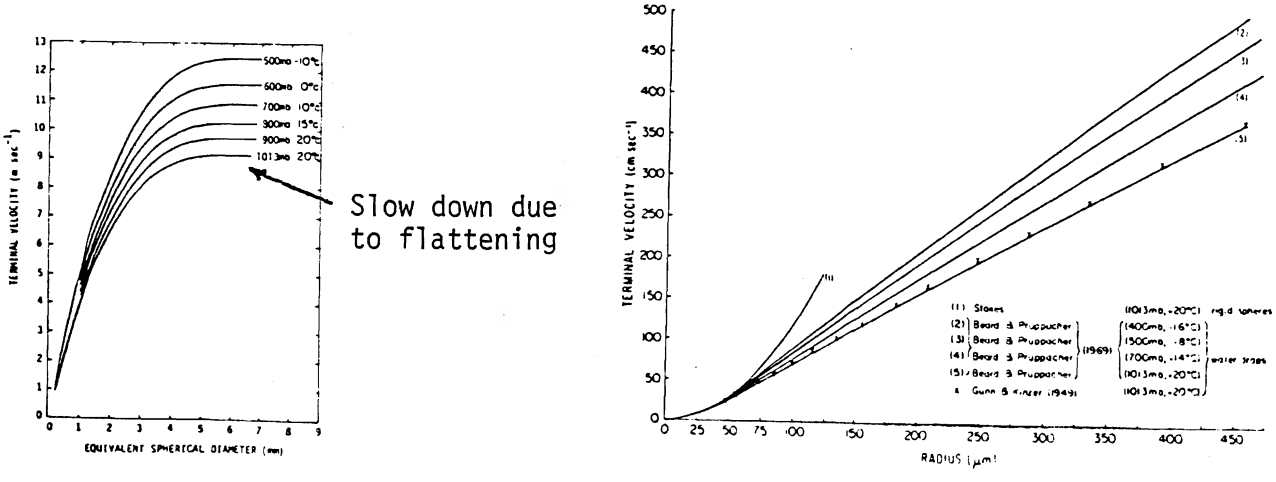

Fig. 5.55 Terminal velocity of water drops (Pruppacher and Klett, 1978).

5.4.4 Drop growth by collision and coalescence (Rogers, 1976)

Suppose a drop of radius R is falling at a terminal velocity w(R) through a population of smaller droplets. The sweep-out volume during the fall of a unit distance is

$$\pi(R + r)^2 \left[1 - \frac{w(r)}{w(R)}\right], \tag{5.114}$$

where r is the radius of smaller droplets and w(r) their terminal velocity. The average number of droplets with radii between r and r + dr collected in a unit distance of fall is

$$\pi(R + r)^2 \left[1 - \frac{w(r)}{w(R)}\right] n(r)E(R,r)dr, \tag{5.115}$$

where E is the product of E′ and the coalescence efficiency. When R < 100 μm, the coalescence efficiency is often assumed to be unity (no rebound or disruption). The total increase in volume of the collector drop within the unit distance of fall is

$$-\frac{dV}{dz} = \int_0^R \pi(R + r)^2 \frac{4}{3}\pi r^3 E(R,r)n(r) \left[1 - \frac{w(r)}{w(R)}\right] dr, \tag{5.116}$$

or

$$-\frac{dR}{dz} = \frac{\pi}{3} \int_0^R \left[\frac{R + r}{R}\right]^2 \left[1 - \frac{w(r)}{w(R)}\right] n(r)r^3 E(R,r)dr, \tag{5.117}$$

where V is the volume of large drop.

Table 5.9 Characteristics of typical clouds (Rogers, 1976).

Cloud type	Droplet number density (cm^{-3})	Median droplet radius (μm)	Liquid water content* (g/m^3)	Thickness for 20% precip. probability (km)
Hawaiian Orographic	10	20	0.5	†
Maritime Cumulus	50	15	0.5	2.5
Continental Cumulus	200	5	0.3-3.0	6

*These figures are quite variable, depending upon extent of cloud development
†Although probability estimates are not available, clouds of this type no thicker than 2 km frequently produce light rain.

If the cloud droplets are much smaller than the collector drop, or

$$|w(r)| \ll |w(R)| \quad \text{and} \quad r + R \simeq R,$$

then Eq. (5.117) becomes

$$\frac{dR}{dz} = -\frac{\bar{E}W_L}{4\rho_w}, \quad \text{(Lagrangian system)} \qquad (5.118)$$

where $\bar{E}$ is the effective average collection efficiency for the population of the droplets. From Eq. (5.118), we have

$$\frac{dR}{dt} = -\frac{\bar{E}W_L}{4\rho_w} w(R). \qquad (5.119)$$

Under an updraft velocity, w_u, Eq. (5.119) has to be expressed by the Eulerian velocity, $dz/dt = w_u + w(R)$. Then, Eq. (5.119) becomes

$$\frac{dR}{dz} = -\frac{\bar{E}W_L}{4\rho_w} \frac{w(R)}{w_u + w(R)}, \quad \text{(Eulerian system)} \qquad (5.120)$$

which is called the Bowen equation.

5.4.5 The Bowen model: Eq. (5.120) (Continuous model)

In Eq. (5.120), important parameters are w_u and W_L. Under a slow updraft, premature fallout occurs. Although droplets are smaller under a fast updraft for a given altitude, they tend to experience greater sweep out and result in larger droplet size at a given height at their return.

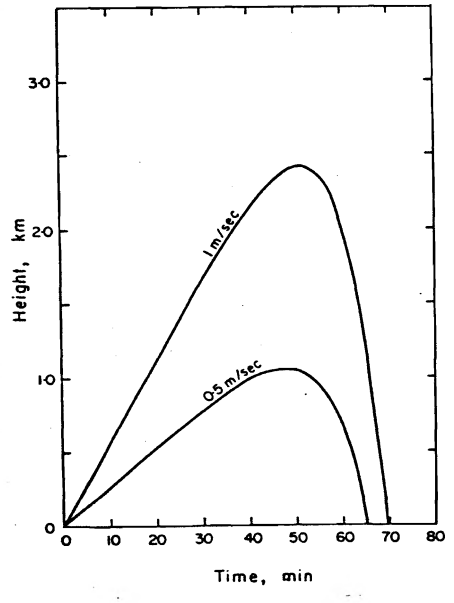

Fig. 5.56 Drop trajectories calculated assuming a coalescence efficiency of unity. Initial drop radius 20 μm. Cloud water content 1 g/m³; all cloud droplets of 10 μm radius (Rogers, 1976).

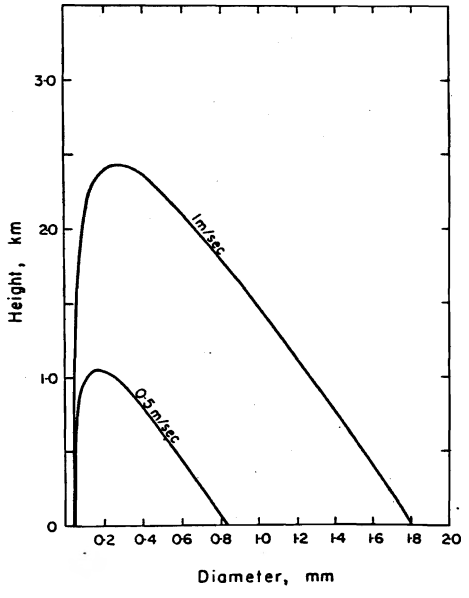

Fig. 5.57 Drop diameters for the trajectories of Fig. 5.57 (Rogers, 1976).

5.4.6 The stochastic coalescence process

Equation (5.120) shows only an average growth rate. Rain development depends on statistical fluctuation for a small number of special drops. If one out of 10^5 or 10^6 ($r = 10\ \mu m \rightarrow 1$ mm) happens to be such a fortunate drop, rain can develop from it. Although the treatment in Eq. (5.120) is continuous, in reality, particularly at the beginning, the growth is discrete. However, the discrete treatment is important only for the first 20 collisions. Thereafter, there is little difference between discrete and continuous treatments.

We now treat evolution of droplet size distribution based on the probability of collision (and coalescence) with others.

(a) Collection kernel

Similar to the coagulation constant Eq. (3.17), we can define the collection kernel as

$$K(R,r) = \pi(R + r)^2 E(R,r)\left|w(R) - w(r)\right|, \tag{5.121}$$

which is the effective sweep-out volume per second per drop. It is equivalent to $4\pi(r + r)^2 D(dn/dr)$ of aerosol particle coagulation in Section 3.2. Diffusion moves the particles toward coagulation, and here the difference of w moves the droplets toward coalescence. K also represents the probability of drop with radius R collides with a droplet of radius r in unit time, provided that both exist with unit concentration.

Instead of K(R,r), a volume function may be used as

$$H(V_R,V_r) = K(R,r) = K\left[\left(\frac{3V_R}{4\pi}\right)^{1/3}, \left(\frac{3V_r}{4\pi}\right)^{1/3}\right]. \tag{5.122}$$

Since the number of droplets per unit volume of space between V_r and $V_r + dV_r$ is

$$n(V_r)dV_r,$$

the total number of coalescence per unit time experienced by drops with droplets of this size range is

$$n(V_r)dV_r \int_0^\infty H(V_R,V_r)n(V_R)dV_R. \tag{5.123}$$

This accounts for all possible capture of the droplets in dV_r by larger drops ($V_r < V_R \leq \infty$) as well as smaller droplets by the droplets in dV_r ($0 < V_R \leq V_r$).

By replacing V_r with V_1 and V_R with V_2, the rate of increase of droplets with volume $V_r = V_1 + V_2$ (a droplet of volume V_1 collides with that of volume V_2) is

$$\tfrac{1}{2}\int_0^{V_r} H(V_1,V_2)n(V_1)n(V_2)dV_1dV_2. \tag{5.124}$$

½ is the factor to avoid double counting of the event. Then, the total rate of change of droplet concentration in the size interval dV_r is

$$\frac{\partial}{\partial t} n(V_r)dV_r = \tfrac{1}{2} \int_0^{V_r} H(V_1,V_2)n(V_1)n(V_2)dV_1dV_2$$
(rate to create droplets in dV_r interval from smaller droplets)
$$- n(V_r)dV_r \int_0^{\infty} H(V_R,V_r)n(V_R)dV_R.$$
(rate to lose the droplets by growing bigger due to coalescence)
(5.125)

Equation (5.125) is called the STOCHASTIC COALESCENCE EQUATION. Examples of computations are given in Figs. 5.58-5.60.

5.4.7 Condensation and stochastic coalescence

After nucleation, initial growth of droplets takes place by a vapor diffusion mechanism; and there is a general tendency for the droplet population towards monodispersity (Problem 2 on p. 5.44). The coalescence process is very slow at the beginning. However, once it starts, it becomes very fast.

It is known that rain development takes as short a time as 15 min after start of condensation in some cumuliform clouds. At this moment, theory takes longer than the observation. For initiation of the coalescence process, broadening of spectrum is important to satisfy the fall velocity difference requirement.

5.5 Scavenging of Aerosol Particles by Precipitation Elements

Aerosol particles larger than about 1 μm in diameter can be easily collected by falling precipitation elements. On the other hand, those smaller than about 0.1 μm coagulate well with the elements by Brownian motion. Aerosol particles in between 0.1 and 1 μm are too small for aerodynamical impaction and too large for effective Brownian coagulation, leaving a gap in collision efficiency (Greenfield, 1957). In the Greenfield gap, phoretic (Section 3.6) and Brownian capture on cloud droplets and their formation on nucleus particles help the aerosol removal from this zone to some extent.

5.6 Evaporation of Rain Drops

Evaporation of an isolated rain drop is basically the same as that of a cloud droplet, except that because of the larger size, the temperature and vapor fields are distorted due to the air ventilation around it. The ventilation makes the evaporation considerably faster than the theory in quiescent air predicts. We shall next treat this ventilation effect of evaporating rain drop.

At around a falling rain drop, there exists an air flow. The flow brings about an advective transportation of the vapor and heat (see Appendix F) so that, for the case of vapor transportation (see Section 2.4),

$$\frac{\partial \rho}{\partial t} = -w\nabla\rho + D\nabla^2\rho. \qquad (F.1)$$

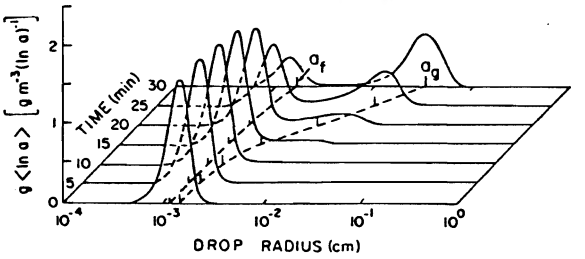

Fig. 5.58 Time evolution of the liquid water spectrum; $a_f(0)=12$ μm, var x=1 (Berry and Reinhardt, 1974).

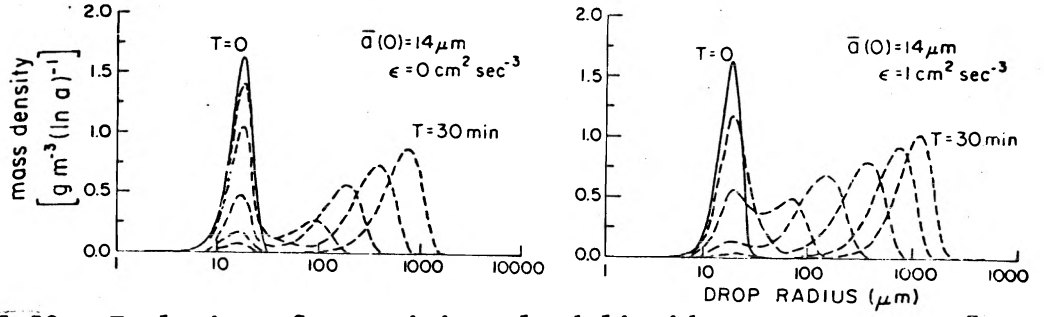

Fig. 5.59 Evolution of a maritime cloud liquid water spectrum for different levels of turbulence (de Almeida, 1975).

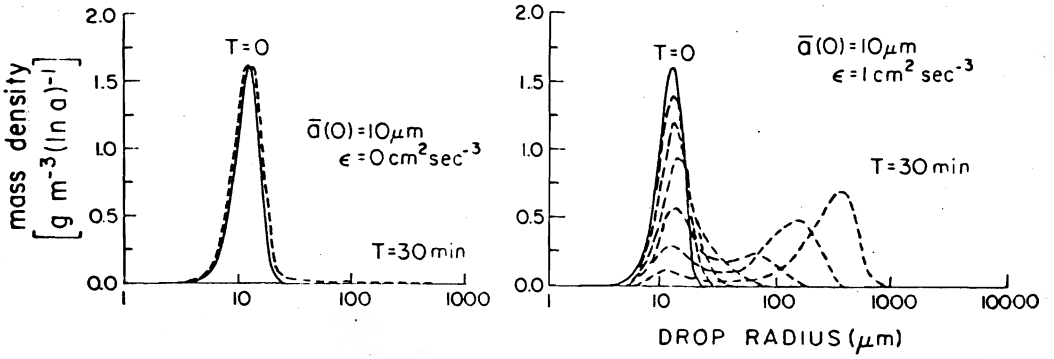

Fig. 5.60 Evolution of a continental cloud liquid water spectrum for different levels of turbulence (de Almeida, 1975).

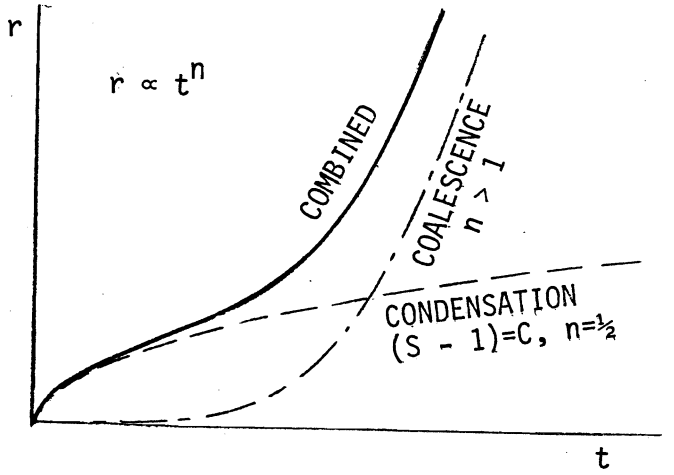

Fig. 5.61 Condensation growth of droplets vs. coalescence.

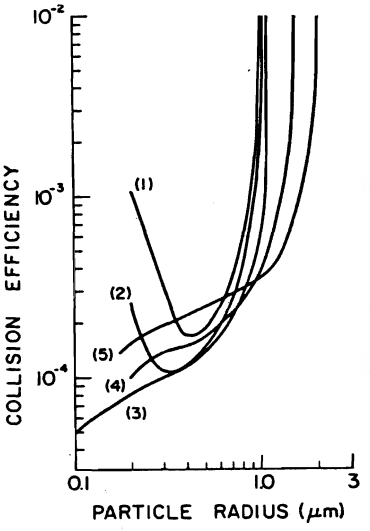

Fig. 5.62 Numerically computed efficiency with which water drops collide by inertial impaction with aerosol particles in air of 10°C and 900 mb; (1) Re=200 (a=438 μm), (2) Re=100 (a=310 μm), (3) Re =30 (a=173 μm), (4) Re=10 (a=106 μm), (5) Re=4 (a=72 μm) (Grover, 1978).

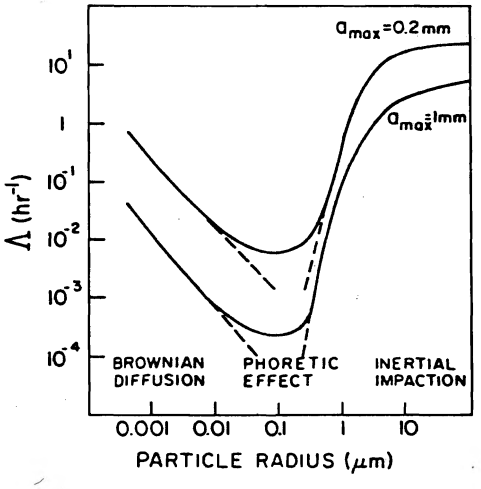

Fig. 5.63 Scavenging coefficient as a function of aerosol particle size for Brownian diffusion, inertial capture, and thermo- and diffusiophoresis; $\Delta T=T_\infty-T=3°C$, precipitation rate R=10 mm h^{-1}; raindrop size distribution $n(a)da=(10^{-4}R/6\ \pi a_{max}^7)a^2\exp(-2a/a_{max})da$, with R in cm s^{-1}; drop terminal velocity $V_\infty=8000a$ (s^{-1}) with a in cm, collision efficiency for inertial impaction based on values of Zimin (1964) (Slinn and Hales, 1971).

The air flow creates specific boundary layers depending on the quantities transported. Considering the conditions at the top of the boundary layers where the advectional [1st term on the right-hand side of Eq. (F.1)] and the diffusional terms become about the same in their magnitude and by introducing corresponding non-dimensional numbers, one can estimate the extent of the field deformation. The resultant evaporation equation for a falling rain drop is

$$\frac{dm}{dt} = \left(\frac{dm}{dt}\right)_M f_v, \quad (f_v \simeq f_h) \tag{F.14}$$

where

$$f_v = 1 + C_2 Re^{1/2} Sc^{1/3}, \tag{F.10'}$$

where C_2 is a constant. Since $Sc = \nu/D = 0.6$ at 0°C, 1000 mb, $C_2\, Sc^{1/3} \simeq 0.23$ is often taken under the condition. Then $Re = 18.4$ gives $f_v = 2$. It is clear that f_v becomes a large factor for large drop.

Falling rain drops cool the air by evaporation. The rate of cooling by individual drop can be determined by Eq. (F.14), but the total cooling depends on the thermodynamic treatment (see Section 1.5). The lowering of the cooled layer will be discussed later. Because of $f_v \simeq f_h$, the temperature of the ventilated drop remains essentially the same as that of the Maxwellian drop in quiescent air [cf. Section 5.3.2(d)]. The air cooled by evaporation of falling drops causes downward air motion such as micro and macro bursts of clouds.

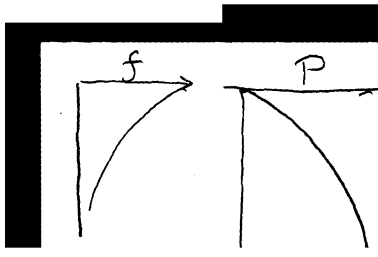
f
P

APPENDIX A

Velocities of Gas Molecules

The number of gas molecules, dn, whose momenta are lying between the limits p_x and p_x+dp_x, p_y and p_y+dp_y, and p_z and p_z+dp_z may be expressed as,

$$\frac{dn}{N} = \frac{e^{-\epsilon/kT}dp_x dp_y dp_z}{\iiint_{-\infty}^{\infty} e^{-\epsilon/kT}dp_x dp_y dp_z}. \tag{A.1}$$

Since

$$2m\epsilon = p_x^2 + p_y^2 + p_z^2 = r^2, \tag{A.2}$$

$dp_x do_y dp_z$, the volume element in phase space, may be expressed by the volume element in polar coordinates,

$$dp_x dp_y dp_z = 4\pi r^2 dr. \tag{A.3}$$

Then, from Eq. (A.2),

$$dr = (2m\epsilon)^{-1/2}\, m d\epsilon. \tag{A.4}$$

Replacing Eq. (A.4) into Eq. (A.3), we have

$$dp_x dp_y dp_z = 2\pi(2m)^{3/2}\epsilon^{1/2}d\epsilon. \tag{A.5}$$

Then, using Eq. (A.5), the denominator of Eq. (A.1) becomes

$$2\pi(2m)^{3/2}\int_0^{\infty} e^{-\epsilon/kT}\epsilon^{1/2}d\epsilon,$$

where the integral is the form

$$\int_0^{\infty} e^{-ax}\, x^n\, dx = n!/a^{n+1}, \tag{A.6}$$

and in this case, $x = \epsilon$, $a = 1/kT$, $n = ½$, and $(½)! = \sqrt{\pi}/2$. Hence,

$$\iiint_{-\infty}^{\infty} e^{-\epsilon/kT}\, dp_x dp_y dp_z = (2\pi mkT)^{3/2}. \tag{A.7}$$

Applying Eqs. (A.5) and (A.7) into Eq. (A.1), we obtain

$$\frac{dn}{N} = \frac{2\epsilon^{1/2}}{\sqrt{\pi}\,(kT)^{3/2}} e^{-\epsilon/kT} d\epsilon. \tag{A.8}$$

which is Maxwell-Boltzmann's distribution of energy.

Since

$$\bar{\epsilon} = \int_0^\infty \epsilon \frac{dn}{N}, \tag{A.9}$$

and introducing Eq. (A.8), we have

$$\bar{\epsilon} = \frac{2}{\sqrt{\pi}\,(kT)^{3/2}} \int_0^\infty e^{-\epsilon/kT}\, \epsilon^{3/2}\, d\epsilon, \tag{A.10}$$

which, again, using Eq. (A.6), leads to

$$\bar{\epsilon} = \tfrac{3}{2}kT, \tag{A.11}$$

as we have seen on p. 2.15.

The velocity distribution of gas molecules may be obtained by observing

$$\epsilon = \tfrac{1}{2} mv^2 \qquad v^2 = v_x^2 + v_y^2 + v_z^2,$$

where v_x, v_y, and v_z are velocity components in x, y, and z directions, respectively, and replacing

$$d\epsilon = mvdv$$

in Eq. (A.8) results in

$$\frac{dn}{N} = \left(\frac{2}{\pi}\right)^{1/2} \left(\frac{m}{kT}\right)^{3/2} e^{-\frac{1}{2}\frac{mv^2}{kT}} v^2\, dv. \tag{A.12}$$

Similar to Eq. (A.9), using

$$\bar{v} = \int_0^\infty v \frac{dn}{N} \tag{A.13}$$

in Eq. (A.12) results in

$$\bar{v} = \left(\frac{2}{\pi}\right)^{1/2} \left(\frac{m}{kT}\right)^{3/2} \int_0^\infty e^{-\frac{1}{2}\frac{mv^2}{kT}} v^3\, dv. \tag{A.14}$$

The integral is in the form

$$\int_0^\infty e^{-ax^2} x^3 \, dx = \frac{1}{2a^2}. \tag{A.15}$$

Hence,

$$\bar{v} = \left(\frac{8kT}{\pi m}\right)^{1/2}, \tag{A.16}$$

which is the accurate expression for the average velocity of an ideal gas molecule, with mass m under temperature T.

We now try to obtain the average value of the component of the velocity. Rewriting Eq. (A.1) by introducing Eq. (A.7) results in

$$dp_x = mdv_x, \; dp_y = mdv_y, \text{ and } dp_z = mdv_z,$$

$$\frac{dn_x}{N} = \left(\frac{m}{2\pi kT}\right)^{3/2} e^{-\frac{1}{2}\frac{mv_x^2}{kT}} dv_x \int_{-\infty}^{\infty} e^{-\frac{1}{2}\frac{mv_y^2}{kT}} dv_y \int_{-\infty}^{\infty} e^{-\frac{1}{2}\frac{mv_z^2}{kT}} dv_z. \tag{A.17}$$

Since

$$\int_{-\infty}^{\infty} e^{-ax^2} dx = \left(\frac{\pi}{a}\right)^{1/2}, \tag{A.18}$$

Eq. (A.17) writes

$$\frac{dn_x}{N} = \left(\frac{m}{2\pi kT}\right)^{1/2} e^{-\frac{1}{2}\frac{mv_x^2}{kT}} dv_x. \tag{A.19}$$

As before

$$\bar{v}_x = \int_{-\infty}^{\infty} \frac{v_x dn_x}{N}$$

$$= \left(\frac{m}{2\pi kT}\right)^{1/2} \int_{-\infty}^{\infty} e^{-\frac{mv_x^2}{2kT}} |v_x| dv_x. \tag{A.20}$$

Applying the relation

$$\int_{-\infty}^{\infty} e^{-ax^2} |x| dx = \frac{1}{a}, \tag{A.21}$$

we have

$$\bar{v}_x = \left(\frac{2kT}{\pi m}\right)^{1/2}. \tag{A.22}$$

For positive component of v_x, as opposed to negative component,

$$\vec{v}_x = \int_0^\infty \frac{v_x dn_x}{N} = \left(\frac{kT}{2\pi m}\right)^{1/2}. \tag{A.23}$$

Comparison of Eqs. (A.16), (A.22), and (A.23) yields

$$\bar{v} = 2\bar{v}_x = 4\vec{v}_x. \tag{A.24}$$

APPENDIX B

Heat Transfer in the Spherical Coordinate System

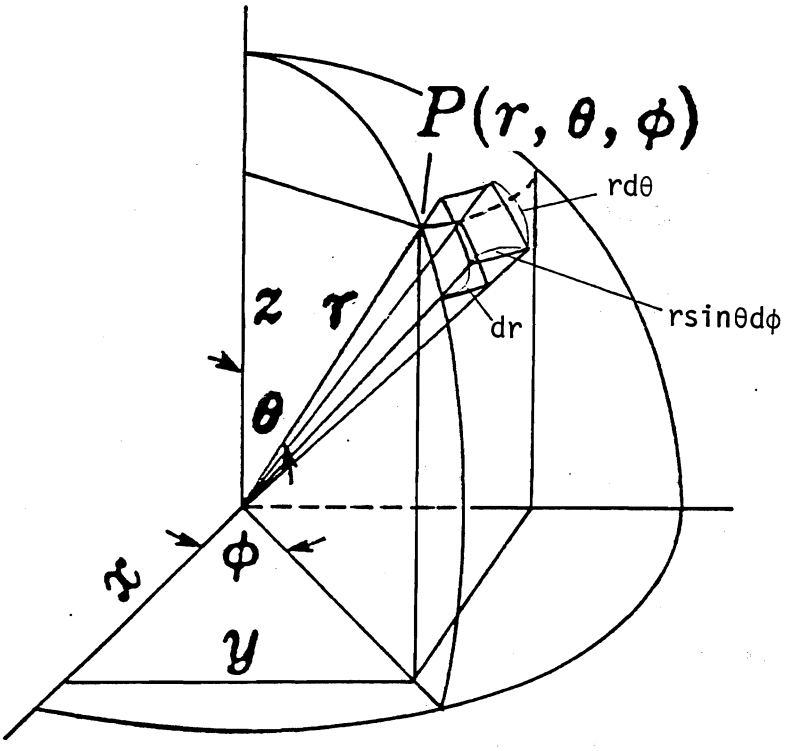

The temperature change in the elementary volume in ∂t time is

$$c_p\rho(dr\cdot rd\theta\cdot rsin\theta d\phi)\frac{\partial T}{\partial t} = (rd\theta\cdot rsin\theta d\phi)\frac{\partial}{\partial r}F_r dr + (dr\cdot rsin\theta d\phi)\frac{\partial}{\partial \theta}F_\theta d\theta$$

elementary volume — area $\perp$ r — area $\perp$ $d\theta$

$$+ (dr\cdot rd\theta)\frac{\partial}{\partial \phi}F_\phi d\phi, \qquad (B.1)$$

area $\perp$ $d\phi$

where

$$F_r = K_r\frac{\partial T}{\partial r}, \qquad F_\theta = K_\theta\frac{\partial T}{r\partial \theta}, \qquad F_\theta = \frac{K_\theta}{rsin\theta}\cdot\frac{\partial T}{\partial \theta}. \qquad (B.2)$$

For an isotropic space,

$$K_r = K_\theta = K_\phi = K, \quad \text{and } \kappa = K/c_p\rho, \qquad (B.3)$$

$$\frac{\partial T}{\partial t} = \frac{\kappa}{r^2}\left[\frac{\partial}{\partial r}\left(r^2\frac{\partial T}{\partial r}\right) + \frac{1}{\sin\theta}\frac{\partial}{\partial\theta}\left(\sin\theta\frac{\partial T}{\partial\theta}\right) + \frac{1}{\sin^2\theta}\left(\frac{\partial^2 T}{\partial\phi^2}\right)\right]. \tag{B.4}$$

The Laplacian of T for the spherical coordinate from Eq. (2.30) is

$$\nabla^2 T = \frac{1}{r^2}\left[\frac{\partial}{\partial r}\left(r^2\frac{\partial T}{\partial r}\right) + \frac{1}{\sin\theta}\frac{\partial}{\partial\theta}\left(\sin\theta\frac{\partial T}{\partial\theta}\right) + \frac{1}{\sin^2\theta}\left(\frac{\partial^2 T}{\partial\phi^2}\right)\right]. \tag{B.5}$$

Other orthogonal systems can be treated the same.

APPENDIX C

Steady Flow Past a Rigid Sphere - Stokes Drag

In the two-dimensional motion of incompressible fluid, stream function ψ is defined to represent the flux by the difference between ψ_{2A} at Point A and ψ_{2B} at Point B. $\psi_{2A} - \psi_{2B} = 0$ or $\psi_2 =$ const gives the streamline.

If ds is an arc of a curve and the direction of the fluid motion is perpendicular to the arc, it becomes clear that

$$\partial\psi_2 / \partial s = v_2, \tag{C.1}$$

where v_2 is the fluid velocity.

On the x-z plane of the cartesian coordinate,

$$w = -\frac{\partial\psi_2}{\partial x}, \quad u = \frac{\partial\psi_2}{\partial z}, \tag{C.2}$$

where w and u are velocity components in z- and x-directions, respectively.

When a solid of revolution moves in the direction of its axis of rotation in a fluid, or vice versa, and the motion is irrotional, similarly Stokes' stream function (sometimes known as the current function), $2\pi\psi$, may be defined in relation with the axisymmetric flux. $\psi =$ const also gives the streamline. For ds element of a curve with a radial distance from the axis, $\bar{w}$, to which the fluid motion is perpendicular with the velocity, v_n, similarly to Eq. (C.1), the flux connects to the stream function as

$$2\pi\bar{w}(ds)v_n = 2\pi\, d\psi, \tag{C.3}$$

where $d\psi$ is the difference of ψ on ds, or

$$v_n = \frac{1}{\bar{w}} \frac{\partial\psi}{\partial s}. \tag{C.4}$$

In the spherical coordinate with z as the axis of rotation, $\bar{w} = r \sin\theta$, r being the radial distance, and Eq. (C.4) becomes

$$v_r = -\frac{1}{r\sin\theta} \frac{\partial\psi}{r\partial\theta}, \quad v_\theta = \frac{1}{r\sin\theta} \frac{\partial\psi}{\partial r}. \tag{C.5}$$

The Stokes stream function far away from the sphere can be obtained by integration of Eq. (C.5) and setting $v_\theta = w_\infty \sin\theta$ at $r = \infty$, as

$$\psi = \frac{1}{2} w_\infty r^2 \sin^2\theta, \tag{C.6}$$

where w_∞ is w of the uniform stream.

For steady, creeping flow around the sphere, it was shown (Milne-Thomson, 1955) that, by neglecting the quadratic terms in the equation of motion,

$$E^4\psi = 0, \tag{C.7}$$

holds, where, in the spherical coordinates,

$$E^2 = \frac{\partial^2}{\partial r^2} + \frac{\sin\theta}{r^2}\frac{\partial}{\partial\theta}\left[\frac{1}{\sin\theta}\frac{\partial}{\partial\theta}\right]. \tag{C.8}$$

Equation (C.7) has to be solved with 3 boundary conditions;

(1) $v_r = 0$ at $r = r$ r:radius of the sphere (C.9)

(2) $v_\theta = 0$ at $r = r$ (C.10)

(3) $\psi = -\frac{1}{2}w_\infty r^2\sin^2\theta$ as $r \to \infty$ (C.6)

Condition (3) suggests that $\psi(r,\theta)$ is of the form

$$\psi = f(r)\ \sin^2\theta. \tag{C.11}$$

Substitution of Eq. (C.11) in Eq. (C.7) with Eq. (C.8) gives

$$\left[\frac{d^2}{dr^2} - \frac{2}{r^2}\right]\left[\frac{d^2}{dr^2} - \frac{2}{r^2}\right] f(r) = 0. \tag{C.12}$$

A trial solution of the form $f(r) = C_1 r^n$ may be applied to Eq. (C.12);

$$[(n-2)(n-3) - 2]\ C_1 r^{n-3}\ [n(n-1) - 2] = 0,$$

or

$$[(n-4)(n-1)]\ [(n-2)(n+1)] = 0. \tag{C.13}$$

$n = -1$, 1, 2 and 4 satisfy Eq. (C.13). This is to say that $f(r)$ is a linear combination of these terms, i.e.,

$$f(r) = \frac{C_2}{r} + C_3 r + C_4 r^2 + C_5 r^4. \tag{C.14}$$

In order for Condition (3) to be satisfied, $C_5 = 0$, and $C_4 = -\frac{1}{2}w_\infty$. Then Eq. (C.11) becomes

$$\psi(r,\theta) = \left[\frac{C_2}{r} + C_3 r - \frac{1}{2}w_\infty r^2\right]\sin^2\theta. \tag{C.15}$$

Replacing Eq. (C.15) into Eq. (C.5), we have

$$v_r = \left[w_\infty - \frac{2C_2}{r^3} - \frac{2C_3}{r}\right]\cos\theta, \tag{C.16}$$

and

$$v_\theta = \left(-w_\infty - \frac{C_2}{r^3} + \frac{C_3}{r}\right)\sin\theta. \tag{C.17}$$

Equations (C.16) and (C.17) under Conditions (1) and (2) yield $C_2 = -\frac{w_\infty r^3}{4}$ and $C_3 = \frac{3w_\infty r}{4}$, so that

$$\frac{v_r}{w_\infty} = \left[1 - \frac{3}{2}\left(\frac{r}{r}\right) + \frac{1}{2}\left(\frac{r}{r}\right)^3\right]\cos\theta, \tag{C.18}$$

and

$$\frac{v_\theta}{w_\infty} = -\left[1 - \frac{3}{4}\left(\frac{r}{r}\right) - \frac{1}{4}\left(\frac{r}{r}\right)^3\right]\sin\theta, \tag{C.19}$$

and

$$\psi = -\frac{w_\infty}{2}\left(r^2 - \frac{3}{2}rr + \frac{r^3}{2r}\right)\sin^2\theta, \tag{C.20}$$

(Bird, et al., 1960).

The viscous stress tensor tangential to the spherical surface on the meridian plane may be obtained applying Eq. (2.16) to Eq. (C.20), with $r \simeq r$, as

$$\tau_t = \eta\frac{\partial v_\theta}{\partial r} = -\frac{3}{2}\frac{\eta w_\infty}{r}\left(\frac{r}{r}\right)^4\sin\theta. \tag{C.21}$$

Under the present slow flow condition or small R_e, $u\nabla u$ term in Eq. (3.4) etc. can be ignored compared with $\nu\nabla^2 u$ term etc. Then, the Navier-Stokes equation condenses into the form

$$\frac{\partial p}{\partial x} = \eta\nabla^2 u, \quad \frac{\partial p}{\partial y} = \eta\nabla^2 v, \quad \frac{\partial p}{\partial z} = \eta\nabla^2 w, \tag{C.22}$$

where v is the velocity component in the y-direction. By differentiation of the continuity equation for incompressible fluid,

$$\frac{\partial u}{\partial x} + \frac{\partial v}{\partial y} + \frac{\partial w}{\partial z} = 0, \tag{C.23}$$

and comparing it with Eq. (C.22), we have

$$\nabla^2 p = 0. \tag{C.24}$$

Considering that the pressure is higher on the upwind surface (lower side) of the sphere, the simplest solution of Eq. (C.24) or the pressure field takes the form

$$p - p_\infty = -\frac{C_4 z}{r^3}, \tag{C.25}$$

where

$$z = r \cos \theta, \tag{C.26}$$

and

$$r = \sqrt{x^2 + y^2 + z^2}. \tag{C.27}$$

Equation (C.25) may readily be shown to satisfy Eq. (C.24) in the spherical coordinate with $\partial p/\partial \phi = 0$, where ϕ is the longitudinal angle, with the axisymmetry of the flow. C_4 may thus be determined from Eqs. (C.18) and (C.22) as

$$C_4 = \frac{3}{2} \eta w_\infty r, \tag{C.28}$$

or Eq. (C.25) becomes

$$p - p_\infty = -\frac{3}{2} \frac{\eta w_\infty}{r} \left(\frac{r}{r}\right)^2 \cos \theta. \tag{C.29}$$

The pressure force acts normal to the spherical surface and the z-component of this force is $-(p - p_\infty) \cos \theta$ per unit area of the surface, and the surface area element is $r d\theta \cdot r \sin \theta \, d\phi$. Then the drag force due to this pressure force may be integrated over the spherical surface:

$$D_n = \int_0^{2\pi} \int_0^{\pi} \left[-(p - p_\infty)\big|_{r=r} \cos \theta\right] r^2 \sin \theta \, d\theta \, d\phi. \tag{C.30}$$

$$= 2\pi \eta w_\infty r, \tag{C.30'}$$

which is called "form drag."

The z-component of viscous stress tensor $\tau \sin \theta$ may be similarly integrated over the surface of the sphere to yield "frictional drag"

$$D_f = 4\pi\eta \, w_\infty \, r. \tag{C.31}$$

The Stokes drag is therefore obtained as

$$D = D_n + D_f = 6\pi\eta \, w_\infty \, r. \tag{C.32}$$

APPENDIX D

Diffusion of Aerosol Particles

To describe the diffusion of small particles by Brownian motion, we shall follow the treatment of Einstein and Smoluchowski:

Let Δ denote the molecule (aerosol particle) displacement on either side of the plane of transit in a horizontal cylinder of unit cross- sectional area. On both sides of the plane, compartments of depth Δ exist.

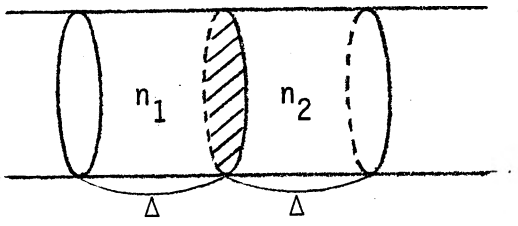

The average rate of displacement of molecules in either compartment is Δ/t; but, as both forward and backward directions of motion are equally probable, the number of molecules crossing the plane of transit per unit time from the left compartment is only $(1/2)\ n_1(\Delta/t)$, where n_1 is the concentration of molecules in that compartment. Similarly, the number crossing the boundary per unit time from the right-hand side to the left is only $(1/2)\ n_2(\Delta/t)$. Hence, the number flux from the left to the right is

$$F_n = \frac{1}{2}\frac{\Delta(n_1 - n_2)}{t}. \tag{D.1}$$

However, the gradient of number concentration is

$$\frac{dn}{dx} = \frac{n_2 - n_1}{\Delta}. \tag{D.2}$$

On substituting these expressions into Fick's first law of diffusion, Eq. (2.19), with nm = ρ,

$$D = \frac{\Delta^2}{2t}, \tag{3.13}$$

which is the <u>diffusion law of Einstein and Smoluchowski</u>. Equation (3.13) is also applicable to aerosol particles.

Next, let us describe D for aerosol particles, again following Einstein. Suppose diffusion aerosol particles move across the boundary with the steady velocity u, so that we have, with viscous resistance force of Eq. (3.6),

$$F_n = nu = \frac{nD}{6\pi\eta r}. \tag{D.3}$$

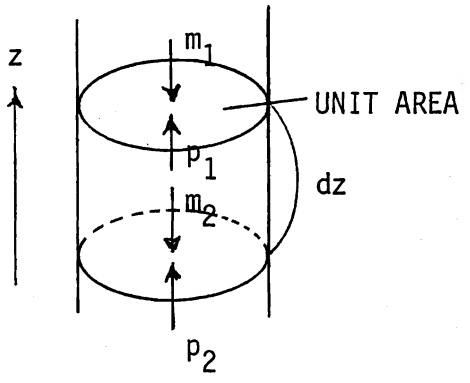

In the atmosphere, the concentration gradient of air molecules is supported by the gravitational force. Then, the force acting on the boundary of unit area is

$$dp = R_a T d\rho_a = \rho_a dz g = f. \tag{D.4}$$

Since the number of molecules in the volume in question is $\rho_a dz/m$, Eq. (D.4) can be written for a single molecule as

$$f_m = R_a T d\rho_a / (\rho_a dz/m) = \frac{mR_a T}{n}\frac{dn}{dz}. \tag{D.5}$$

The same concept is applicable to the aerosol particles in their number concentration gradient. Substitution of Eqs. (D.3) and (D.5) expressed in the x-direction into Fick's first law of the form

$$F_n = D\frac{dn}{dx} \tag{D.6}$$

yields

$$D = kT/6\pi\eta r. \tag{D.7}$$

For small particle size or large K_n, with Cunningham's correction factor to account for the slip flow, Eq. (D.7) becomes

$$D = kT\left[1 + \frac{A\ell}{r}\right]/6\pi\eta r. \tag{3.14}$$

APPENDIX E

Classical Theory of Homogeneous Nucleation of Water Vapor Condensation

(cf. Appendix E′)

Distribution of molecules in phase equilibrium

In thermodynamic equilibrium of two phases, the number concentration of molecules, n, takes the forms for species A and B;

$$n_A = C \exp(-E_A/kT), \tag{E.1}$$

and

$$n_B = C \exp(-E_B/kT), \tag{E.2}$$

where E_A and E_B are free energies of the respective states and C a constant.

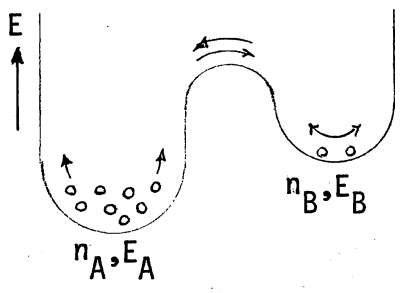

Fig. E.1 Thermodynamic relationship beween the number concentration of molecules, n, and the energy level, E.

If $E_A < E_B$,

for low T, $n_A >> n_B$

for high T, $n_A \simeq n_B$.

Under the equilibrium, the molecular fluxes from State A and those from State B are matching. Thus, for the given temperature, the lower the energy level is, the more abundant the molecules are. A similar relationship was assumed between the number concentration of clusters and their free energy level.[1] Under equilibrium, the larger clusters carry more energy, and they are scarce. Growth of a new phase or nucleation is thought to start from the larger and more scarce critical clusters, as the thermodynamic condition becomes favorable for the change. To examine the problematic contemporary or classical nucleation theory, we shall look into the homogeneous nucleation of water vapor condensation.

---

[1] Strictly speaking, this relationship applies only to number concentration of molecules in the equilibrium of two phases divided by a flat surface. As shown in Section 5.1, the equilibrium distribution of clusters is decided by the rate balance between the formation and disintegration of clusters. The critical embryo of classical theory is merely the Kelvin particle of the nucleation environment which does not possess a critical nature, the vapor pressure maximum. As explained in Section 4.4, the cluster of the true vapor pressure maximum plays the role of critical embryo.

Equilibrium distribution of molecular clusters (Cluster Ensemble)[2]

In the cluster ensemble, the forming and disintegrating molecular clusters are said to be under equilibrium according to their number concentration and energy level as shown above.

$A_1 + A_1 \rightleftharpoons A_2$ (A_1: a single molecule)
$A_2 + A_1 \rightleftharpoons A_3$

$A_{i-1} + A_1 \rightleftharpoons A_i$ (A_i: a cluster consisting of i molecules)

There are other routes for forming the cluster distribution, such as

$A_{i-2} + A_2 \rightleftharpoons A_i$, etc.;

but they are much less probable compared with the single molecule steps.

Using the assummed feature of the ensemble,

$$n_i/n_1 = \exp\left[-(G_i - G_1)/kT\right], \tag{E.3}$$

where $G_i - G_1 = \Delta G$ is the Gibbs free energy for formation of a cluster consisting of i molecules (i-cluster). According to Abraham, the Helmholtz free energy should be used instead of the Gibbs, but the amounts of their variations are the same when $\Delta T = 0$. Therefore, we proceed with Gibbs free energy. Equation (E.3) is used to describe the equilibrium distribution of clusters as mentioned above. As can be seen from Eq. (E.3), the number concentration of single molecules (monomers) is by far the largest; and as the size of the clusters increases, the concentration rapidly decreases. In order to accurately estimate the cluster concentration, the free energy of formation must be evaluated.

Free energy of embryo formation

When a molecular cluster forms, there are two kinds of energy involved, one associated with the bulk volume and the other with the surface. The free energy of embryo formation may be expressed as

$$\Delta G = n_L(\mu_L - \mu_V)V + \sigma_{LV}A, \tag{E.4}[3]$$

where n_L is the number of molecules per unit volume of liquid water, μ_L the Gibbs' free energy per molecule in liquid of flat surface, μ_V G per molecule in the vapor (supersaturated), and σ_{LV} the surface free energy per unit area at the liquid (L)-vapor (V) interface. Using Eq. (4.12) with e_∞ for liquid water of flat surface, the free energy difference may be given as

---

[2] A controversy exists over the replacement free energy (Lothe and Pound, 1962) in argument between thermodynamic and statistical-mechanical theories. In addition, the equlibrium distribution of clusters appears impossible even in statistical mechanics violating the laws governing it (cf. Appendix E′).

[3] Note $\sigma_{LV} = f(r)$, although it is treated as $\sigma = \sigma_\infty$ = constant here.

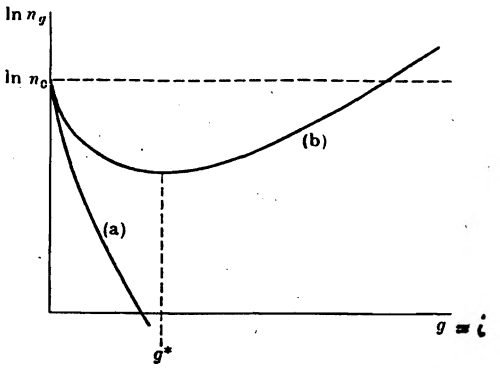

Fig. E.2 The equilibrium distribution of droplets: curve (a) in a saturated system; curve (b) in a supersaturated system. n_g is the number of droplets that contain g molecules, n_0 is the total number of molecules in the system, g^* is the critical size (From Farley, 1952).[4]

$$(\mu_L - \mu_V) = \frac{M}{N}(g_L - g_V) = -kT\ln(e/e_\infty). \tag{E.5}$$

Inserting Eq. (E.5) into Eq. (E.4), and using spherical expressions for V and A,

$$\Delta G = -\frac{4\pi}{3}r^3 n_L kT\ln(e/e_\infty) + 4\pi r^2\sigma_{LV}. \tag{E.6}$$

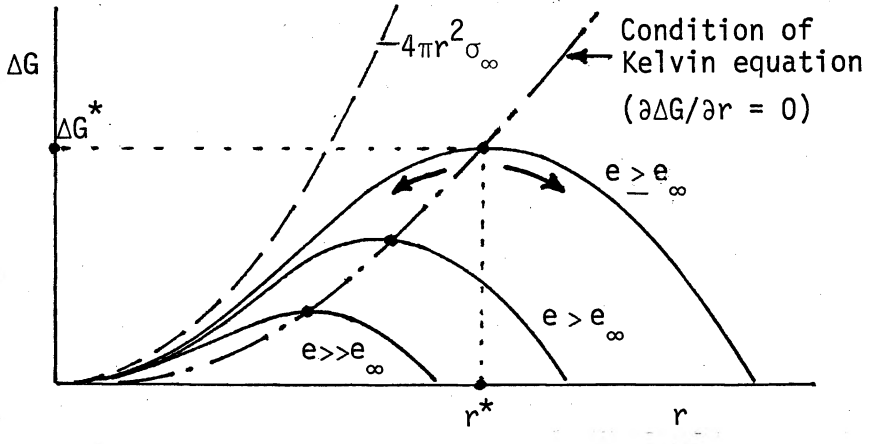

Fig. E.3 The free energy of embryo formation, ΔG, as a function of the radius, r.

Nucleation

From Eq. (E.6), it is immediately apparent that ΔG is a cubic function of r, passing the coordinate origin with a maximum in the zone where r is positive. If there is a maximum in the r-positive zone, G decreases beyond the point indicating the possibility of automatic growth or nucleation. To find the

[4] This relationship does not satisfy the steady state current requirement.

critical condition for nucleation, assuming σ to remain constant, by differentiating Eq. (E.6) with r and setting it to be zero or $\partial(\Delta G)/\partial r = 0$,

$$r^* = \frac{2\sigma_{LV}}{n_L kT \ln(e/e_\infty)}, \qquad (E.7)^5$$

where r^* is the critical radius of the embryo. Equation (E.7) is also the Kelvin equation. Replacement of Eq. (E.7) into Eq. (E.6) yields

$$\Delta G^* = \frac{16\pi\sigma_{LV}^3}{3\left[n_L kT \ln(e/e_\infty)\right]^2} = \tfrac{4}{3}\pi r^{*2}\sigma_{LV}, \qquad (E.8)$$

where ΔG^* is the free energy of critical embryo formation.

Nucleation rate (see Appendix E′)

When nucleation happens in the ensemble, through the subsequent growth, the embryo is removed and molecular clusters redistribute to establish the original status. Thus, a current of critical embryos appears.

For the nucleation, the critical embryo has to acquire molecules so that the growth becomes thermodynamically possible. This rate of molecular acquisition by the embryo is proportional to the arrival rate of molecules at the surface. Since the number of molecules hitting per unit area per unit time is given as,[6]

$$n\vec{v}_x = e/\sqrt{2\pi mkT}, \qquad (E.9)$$

the forward nucleation rate $\vec{J}$ = (the rate of molecular acquisition over the entire embryo surface) x (the number of critical embryos per unit volume), or

$$\vec{J} = B \cdot n_1 \exp(-\Delta G^*/kT), \qquad (E.10)$$

$$n_i^* = n(r^*)$$

where

$$B = (e/\sqrt{2\pi mkT}) \cdot 4\pi r^{*2} \cdot \beta, \qquad (E.11)$$

---

[5] In the zone of $r < r^*$, ΔG decreases (the direction of natural change) with r decrease, i.e., evaporation of the critical embryo has to be thermodynamically enforced. It has been assumed that the nucleation current (formation of clusters through the route starting from monomers to dimers to trimers and so on with each cluster interacting with the monomers, as shown on p. E.3), is supplied by "fluctuation" against this thermodynamic barrier. However, such a statistical-mechanical fluctuation is also virtually impossible (see Appendix E′).

[6] $n\vec{v}_x = n\sqrt{\frac{kT}{2\pi m}}$ $\qquad e = \rho R_v T = nm \cdot \frac{NkT}{M} = nkT$ $\qquad n\vec{v}_x = e/\sqrt{2\pi mkT}$

β being the condensation coefficient. Considering the backward rate, the net nucleation rate is

$$J = \underbrace{[\ln(e/e_\infty)/8r^{*3}n_L]^{1/2}\cdot\vec{J}}_{\simeq\ 0.1\ \text{(Zeldovitch factor)}} \cdot (s\ m^3)^{-1} \qquad (E.12)$$

Computation of homogeneous nucleation rate

Using Eqs. (E.7), (E.8), (E.10), and (E.12),

$$J = \frac{0.1e\beta 4\pi r^{*2}n_1}{\sqrt{2\pi mkT}} \exp\left\{-\frac{16\pi\sigma^3}{3[n_L kT\ln(e/e_\infty)]^2}\cdot\frac{1}{kT}\right\}. \qquad (E.13)$$

Setting $[\ln(e/e_\infty)]^2 = X$ and taking the logarithmic form,

$$\ln J = \underbrace{\ln\left[\frac{0.1e\beta 4\pi\cdot 4\sigma^2\cdot n_1}{\sqrt{2\pi mkT}\cdot(n_L kT)^2}\right]}_{a} - \ln X - \underbrace{\frac{16\pi\sigma^3}{3(n_L kT)^2 kT}}_{b}\cdot\frac{1}{X}.$$

Conditions: $T=273,2$ K, $e_\infty=6.1\times10^3$ dyne cm^{-2}, $\beta=1$, $\sigma=75.7$ dyne cm^{-1}
$k=1.38\times10^{-16}$ erg K^{-1} (assume $e = e_\infty$ in a)

$$a = \ln\left[\frac{0.1\times6.1\times10^3\times1\times4\times3.14\times4\times75.7^2\times\left[6.02\times10^{23}\times\frac{1}{22400}\times\frac{6.1}{1013}\right]}{\left[2\times3.14\times\frac{18\times1.38\times10^{-16}}{6.02\times10^{23}}\times273.2\right]^{1/2}\times\left[\frac{6.02\times10^{23}}{18}\times1.38\times10^{-16}\times273.2\right]^2}\right]$$

$$= \ln(6.7185\times10^{24}) = 1.905 + 55.262 = 57.167$$

$\ln x = \underline{2.302585}\ \log_{10}x$, $\log_{10}x = \underline{0.4342945}\ \ln x$

$$b = \frac{16\times3.14\times75.7^3}{3\left[\frac{6.02\times10^{23}}{18}\times1.38\times10^{-16}\times273.2\right]^2\times1.38\times10^{-16}\times273.2} = 121.2$$

$$\ln J = 57.167 - \ln x - \frac{121.2}{x}$$

x	1.0	1.5	2.0	2.5	3.0
e/e_∞	2.718	3.403	4.113	4.861	5.652
ln J	-64.03	-24.04	-4.126	7.77	15.668
J	1.55×10^{-28}	3.63×10^{-11}	1.61×10^{-2}	2.37×10^{3}	6.38×10^{6}

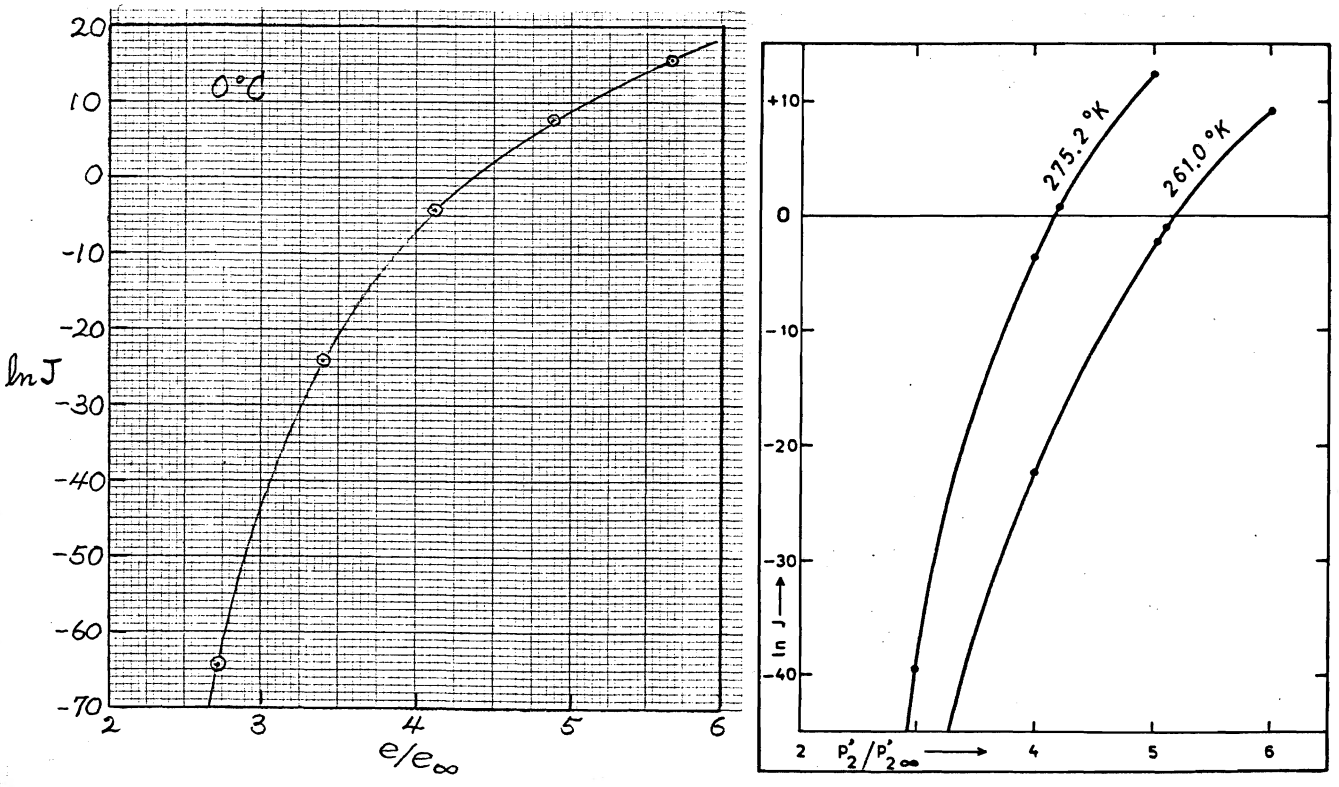

Fig. E.4 Homogeneous nucleation of water vapor in air. Calculated values of natural logarithm of nucleation rate J as a function of saturation ratio (J is the number of germs formed per second in 1 cm^3 of air calculated for $\beta = 1$) (Dufour and Defay, 1963).

Dimensions

Using Eq. (E.13),

$$J = \frac{0.1e\beta 4\pi r^{*2} n_1}{\sqrt{2\pi mkT}} \exp(\text{number})$$

$$= \frac{\text{kg m}}{\text{s}^2} \frac{\text{m}^2}{\text{m}^2\ \text{m}^3} \left(\frac{\text{s}^2}{\text{kg} \cdot \text{kg} \cdot \text{m}^2} \right)^{1/2} = \frac{1}{\text{s} \cdot \text{m}^3}.$$

APPENDIX E′

Problems and Controversies Associated with Theories of Homogeneous Nucleation

(a) Cluster distribution in the nucleation current

The cluster distribution expressed by Eq. (5.3) was thought to have been originally derived by Becker and Döring (1935) by a thermodynamic method with considerable approximations, but the method contains a serious contradiction. Thermodynamics deals only with average and equilibrium values. The relationship between number concentration of particles and free energy holds for the exchange of molecules in phase equilibrium, and the free energy difference describes the distribution of the molecules among the phases without involving surface free energy change (see Section 1.4). Application of the mass action law for description of number concentration of clusters faces the same restriction. The vapor pressure or the number concentration of molecules (not the clusters) (cf. $p = nkT$) only indirectly contributes formation of clusters and their concentration during nucleation, so as to satisfy the steady-state requirements of the current. Thus, the a priori distribution of clusters like Eq. (5.3) regardless of nucleation current in the classical nucleation theory is a violation for the condition of the current, the steady state.

(b) Replacement free energy controversy

Conventional statistical mechanics states that the partition function (p.f.) describes the probability or the number of state. If so, the number of state or clusters in Eq. (5.3) could be obtained by p.f. as was pointed out by Frenkel (1946). Later, Lothe and Pound (1962) actually carried out the computation, which resulted in a large discrepancy with the thermodynamic (classical) theory of Becker and Döring (the replacement free energy controversy). Two books (Abraham, 1974; Zettlemoyer, 1977), as well as numerous papers, have been published regarding this controversy. Experimental evidence appears in general to favor the classical theory, while Abraham takes a totally conventional statistical mechanical view; and the matter has remained unsettled for a long time.

Although the statistical mechanical probability is restricted to phase equilibrium where no surface area change is involved in molecular exchange or with the flat surface only. For cluster formation, surface free energy change is involved being associated with the surface area change, and the conventional statistical-mechanical method does not apply. Furthermore, misconception in the fundamental structure of statistical mechanics has recently been found. Its restructuring is currently underway, together with the refinement of thermodynamics.

(c) The nucleation current leading to the so-called "critical embryo"

Experimental results are said to be in favor of the classical theory, but a close examination of the theory has revealed another fundamental misconception. The classical theory of nucleation relies on the concept of critical embryo formation which is a function of the environmental condition (supersaturation). Nonetheless, the clusters that are smaller than the critical one must carry a current from the monomers. As their vapor pressures are higher than that of critical embryos (see Fig. 4.7), the latter being approximately the vapor pressure of the nucleating environment in question, such small clusters face extreme difficulty for their growth from the environmental vapor. For the dimer formation in the environment, the vapor molecules must flow from the saturation ratio $S \simeq 5$ to the dimer surface with $S \simeq 140$. It is normally stated that the statistical mechanical fluctuation would provide such a current towards the critical embryo by growing smaller clusters, but the current cannot be sustained because there always exists another and far larger fluctuation current towards subcritical clusters in the reverse direction and the net nucleation current is given by the difference of these two fluctuations.

(d) The "critical embryo"

In the classical nucleation theory, a concept of "critical embryo" was included, apparently influenced by the "activated complex" in chemical reaction at the time of the theoretical development. An activated complex shows both energy and vapor pressure maxima, and clearing of the energy maximum permits the change to proceed further. In the classical theory, a cluster which has vapor pressure the same as the nucleating environment, or the Kelvin particle under the condition, is called the critical embryo. The embryo does show a maximum in the free energy of its formation but it does not for the vapor pressure. Therefore, the embryo does not possess the critical nature, or in the classical theory of homogeneous nucleation, the "critical embryo" does not exist. In this regard, the classical theory is inconsistent with the theory of solution droplet nucleation or Köhler equation (see Section 5.1.6).

This contradiction is due to the use of $\sigma = \sigma_\infty$, and it has been recently resolved by the use of the new generalized Kelvin equation (4.12) with the help of the new relationship for $\sigma = f(r)$ (see Figs. 4.3 and 4.7). The cluster with the new vapor pressure maximum must be the true critical embryo (heptamer for nearest neighbor interaction model and the larger for long range interactions). The true critical embryo does not change size according to environmental supersaturation and is a property of the chemical substance facing the nucleation.

The new theory also explains the appearance of opalescence, the dependence of rate on carrier gas pressure, and time lag phenomenon near but slightly below the supersaturation of homogeneous nucleation.

(e) Temperature of clusters

Growing droplets sustain higher temperatures under steady state in order to allow the generated heat of condensation to escape from the surface so that vapor arrival or condensation can continue (see Section 5.3). This heating amounts to about 0.1°C per 1% supersaturation at an environmental temperature of

10°C, pressure 1 atm, droplet radius 10 μm, $\alpha' = 1.0$, $\beta' = 0.0415$. While existence of the condition, $\alpha' < 1$ and $\beta' < 1$, reduces the surface temperature to some extent, the heating reaches as much as 40°C if $S \simeq 5$ occurs for homogeneous nucleation. Nevertheless, small clusters cool down to a temperature close to that of the environment under the steady state as shown in Section 5.3.3. On the other hand, they receive shocks of heating and cooling whenever a molecule is received or lost. Since the classical nucleation theory assumes an isothermal condition in the system, this heating may bring some error.

(f) The empirical nature of classical nucleation theory

The classical theory takes the condition of $\sigma = \sigma_\infty$, which holds approximately for large clusters. Since the problematic critical embryo of the theory places itself somewhat close to the real one, the former behavior is reasonably close to the latter. With the accidental coincidence in the rate, the classical theory is usable as an approximation.

APPENDIX F

The Effects of Air Ventilation Around a Falling Rain Drop

Suppose a rain drop falls and evaporates in air which is assumed to be incompressible. The vapor transportation away from the surface is carried out by diffusion as well as advection. By placing the coordinate origin at the center of the drop, the time rate of change of vapor density at an arbitrarily fixed space point in the flowing air is expressed by two terms, one by advective transportation and the other by diffusion (see Section 2.4);

$$\frac{\partial \rho}{\partial t} = -w\nabla\rho + D\nabla^2\rho. \tag{F.1}$$

Under the steady state or $\partial\rho/\partial t = 0$, (F.1) becomes

$$w\nabla\rho = D\nabla^2\rho. \tag{F.1'}$$

Now, as we have done in Sections 3.2 and 3.3, we try to estimate the relative magnitude of the molecular diffusion and advective transport processes by introducing the dimensionless Péclét number, expressing the ratio of the terms involved in Eq. (F.1');

$$\left|\frac{w\nabla\rho}{D\nabla^2\rho}\right| \propto \frac{w_\infty(\rho_\infty - \rho_{sr})/d}{D(\rho_\infty - \rho_{sr}/d^2} = \frac{w_\infty d}{D} \equiv Pe, \tag{F.2}$$[1]

where $d = 2r$ is the diameter of the rain drop.

Since the dimensionless Schmidt number is defined as

$$Sc \equiv \frac{\nu}{D}, \tag{F.3}$$

from Eqs. (3.5), (F.2), and (F.3), we have

$$Pe = \frac{\nu}{D} \cdot \frac{w_\infty d}{\nu} = ScRe. \tag{F.4}$$

For the momentum transportation, Eq. (F.1) can be modified, by replacing ρ with w and D with ν,

$$\frac{\partial w}{\partial t} = -w\nabla w + \nu\nabla^2 w, \tag{F.5}$$

---

[1] Using (5.46) at $r = 2r$, we have

$$\rho = \tfrac{1}{2}(\rho_\infty - \rho_{sr}),$$

which is the average of vapor density at the environment and that at the surface. Knowing at the surface $\rho = \rho_{sr}$ and the distance from that point is r, the average gradient is $|\rho_\infty - \rho_{sr}|/2r$.

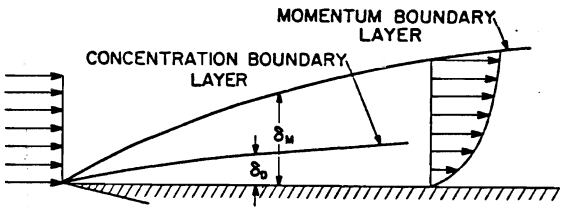

Fig. F.1 Schematic diagram of the development of momentum and concentration boundary layers over a flat plate at high values of the Péclét number.

which under steady state, reduces to [cf. Eq. (3.4)]

$$w\nabla w = \nu\nabla^2 w. \tag{F.5'}$$

In Eq. (F.5'), the left-hand term represents the inertia effect and the right-hand one the viscous effect. When $Re \geq 1$, a momentum boundary layer exists; and both terms are considered to be in the same magnitude:

$$\left| \frac{w\nabla w}{\nu\nabla^2 w} \right| \simeq \frac{w_\infty^2}{d} \frac{\delta_{mv}^2}{\nu w_\infty} = \frac{Re\,\delta_{mv}^2}{d^2} \simeq 1, \tag{F.6}$$

or

$$\frac{\delta_{mv}}{d} \simeq Re^{-1/2}, \tag{F.6'}$$

where δ_{mv} is the thickness of the momentum boundary layer.

For vapor diffusion, a boundary layer also exists, with a thickness δ_D within δ_{mv}. Inside the boundary, the diffusion process dominates, and outside, the advection process controls the vapor transport. At the boundary layer, both processes have comparable magnitudes, so that for $Re \ll 1$,

$$\left| \frac{w\nabla\rho}{D\nabla^2\rho} \right| \simeq 1 \simeq \frac{(w_\infty \delta_D/d)\left[(\rho_\infty - \rho_{sr})/d\right]}{D(\rho_\infty - \rho_{sr})/\delta_D^2} = Pe\frac{\delta_D^3}{d^3}, \tag{F.7}$$

or

$$\frac{\delta_D}{d} \simeq Pe^{-1/3}. \tag{F.7'}$$

Equation (F.7') suggests that since the vapor density gradient at the surface of the rain drop is inversely proportional to δ_D, the steady state vapor flux in the quiescent air F_{vo} is enhanced by a factor proportional to $Pe^{1/3}$ or

$$F_v = F_{vo}(1 + C_1 Pe^{1/3}), \tag{F.8}$$

where C_1 is a constant. C_1 has been experimentally estimated to be about 0.5.

For larger drops with Re > 1, Eq. (F.7) becomes

$$\left|\frac{w\nabla\rho}{D\nabla^2\rho}\right| \simeq 1 \simeq \frac{(w_\infty\delta_D/\delta_{mv})\left[(\rho_\infty - \rho_{sr})/d\right]}{D(\rho_\infty - \rho_{sr})/\delta_D^2}, \tag{F.9}$$

or using Eqs. (F.2), (F.4), and (F.6′), we have

$$\frac{\delta D}{d} \simeq Sc^{-1/3}Re^{-1/2}. \tag{F.10}$$

Then Eq. (F.8) may be modified to

$$F_v = F_{vo}(1 + C_2Sc^{1/3}Re^{1/2}) + F_{vo}f_v, \tag{F.11}$$

where C_2 is a constant and f_v the ventilation factor for vapor transport. Experimentally, it was determined that $0.25 \leq C_2 \leq 0.5$. $C_2 = 0.276$ is used in Green and Lane (1964).

For the heat conduction process, $\kappa = K/c_p\rho_a$ corresponds to D in the vapor diffusion. So, similar to Sc, we can define the non-dimensional Prandtl number as

$$Pr = \frac{\nu}{\kappa}. \tag{F.12}$$

Then, the corresponding correction for the heat flux due to the drop fall, for Re > 1, is

$$F_Q = F_{Qo}(1 + C_3Pr^{1/3}Re^{1/2}) = F_{Qo}f_h, \tag{F.13}$$

where C_3 is a constant and f_h the ventilation factor for heat conduction.

The corrections for F_{vo} and F_{Qo}, i.e., f_v and f_h, can be attached to D and κ (or K), since D and $d\rho/dr$ are mathematically equivalent and f_v modifies $d\rho/dr$. Similarly, f_h can be combined to K to yield, from Eq. (5.53),

$$-\frac{T_r - T_\infty}{\rho_{sr} - \rho_\infty} = \frac{DL_c(1 + C_2Re^{1/2}Sc^{1/3})}{K(1 + C_3Re^{1/2}Sc^{1/3})}. \tag{F.14}$$

Since $D \simeq \kappa$, $Pr \simeq Sc$. Then, $f_v \simeq f_h$. Hence, the two bracketed terms on the right-hand side of Eq. (F.13) can be set to unity, which is the normal practice. This is to say that the deformations to the vapor and temperature fields around the falling rain drop are about the same. Thus, for the falling rain drop

$$\frac{dm}{dt} = \left(\frac{dm}{dt}\right)_M \cdot f_v, \tag{F.15}$$

where $(dm/dt)_M$ is the Maxwellian evaporation rate of rain drop in the quiescent air.